UNIVERSITE PIERRE ET MARIE CURIE
et
INSTITUT DE PHYSIQUE THEORIQUE - CEA/SACLAY

# Thèse de doctorat

Spécialité: **Physique Théorique**

présentée par

**Andrea Puhm**

pour obtenir le grade de

**Docteur de l'Université Pierre et Marie Curie**

Sujet de la thèse:

# Black Holes in String Theory: Guides to Quantum Gravity

soutenue le 4 juillet 2013 devant le jury composé de:

| | |
|---|---|
| Iosif Bena | Directeur du Thèse |
| Mirjam Cvetič | Rapporteur |
| Stefano Giusto | Examinateur |
| Boris Pioline | Président du Jury |
| Herman Verlinde | Rapporteur |

*à maximilien*

# *Acknowledgments*

I am deeply grateful to my PhD advisor Iosif Bena for his guidance, for sharing his insight and for the constant challenge to keep up with his speed of thought and speech which altogether gave me the chance to grow in the field. His highly contagious enthusiasm boosted my curiosity and passion for theoretical physics, and for string theory and black holes in particular. I am also much obliged to him for giving me the leeway to explore directions of my own interest and for his support and guidance in non-scientific matters.

I am grateful to Boris Pioline and Stefano Giusto for agreeing to be members of the Jury of my PhD defense and to Mirjam Cvetič and Herman Verlinde, in particular, for also agreeing to be rapporteur for this Thesis.

I would like to express my gratitude to my collaborators. My particular thanks belong to Bert Vercnocke for his carefulness and patience in answering my many questions and for all the tools and tricks I learned from him over the past years. I am also thankful to him for his comments on a draft of this Thesis. Special thanks belong to Borun Chowdhury and Sheer El-Showk for many intense and challenging discussions and their valuable advice. I am grateful to Nick Warner for his sharp questions and for enlightening discussions. Many thanks to Steven Avery, Gregory Giecold, Monica Guica, Lucien Heurtier, Francesco Orsi and Orestis Vasilakis, for many interesting conversations and calculations.

I am grateful for many enjoyable seminar and coffee break discussions with the members of the String Theory group at the IPhT: Ibrahim Bah, Oscar Dias, Maxime Gabella, Enrico Goi, Mariana Graña, Hagen Triendl, Stefanos Katmadas, Stanislav Kuperstein, Ruben Minasian, Piotr Tourkine, Pierre Vanhove and Thomas Van Riet. Special thanks to my colleague and office mate Stefano Massai for many valuable and challenging discussions.

I am also thankful for enlightening discussions with Nicolay Bobev, Stefano Giusto, Finn Larsen, Samir Mathur, David Turton, Clément Ruef, Eric Verlinde and Amitabh Virmani. I am grateful to Ralph Blumenhagen and Andrés Collinucci for their advice and support.

I would like to acknowledge with much appreciation the CEA/Saclay for a fruitful working environment and for the financial funding over these three years. In particular, I would like to express my gratitude to the IPhT secretaries Catherine Cataldi, Laure Sauboy and Sylvie Zaffanella for help with administrative matters and to Anne Capdepon and the CEA for their support.

On a personal note, my particular gratitude belongs to my father for all his help and kindness. I would like to thank my grandmothers for their kind support over the past years and I am grateful to my late grandfather for always encouraging me to pursue my interests. Hearty thanks to my sisters for many shared moments. My special thanks belong to Maximilian for his constant support, his understanding and for his love.

**Abstract**

In this Thesis, we study black holes and their microscopic properties in extensions of General Relativity that arise as low-energy limits of String Theory. The first question we want to address is how information is released from black holes during evaporation. We make use of quantum information techniques and study information release from qubit systems. We then introduce a general framework to capture the Hawking evaporation process and deduce the constraints unitarity puts on the evolution. This makes the statement of information loss in black hole evaporation more precise and supports the claim that the horizon has to be replaced by a structure, or *fuzzball*, that carries information about the black hole microstates. This immediately raises the question of what this horizon-scale structure is? We address this question in the context of Supergravity. We systematically construct a family of microstates of near-extremal black holes, by placing metastable supertubes inside certain scaling supersymmetric smooth microstate geometries. These non-extremal fuzzballs differ from the classical black hole solution macroscopically at the horizon scale, and for certain probes the fluctuations between various fuzzballs will be visible as thermal noise far away from the horizon. If the black hole horizon is replaced by a horizon-scale structure one can ask what the experience of an observer falling into such a structure is? A recent, much debated, Gedankenexperiment suggests that an infalling observer will burn at a firewall at the horizon. We rephrase this Gedankenexperiment in the decoherence picture of quantum mechanics and ask about the fate of an infalling wave packet. While wave packets of the size of outgoing Hawking quanta can indeed not freely fall through the horizon-scale structure there is a possibility that the experience of macroscopic infalling observers that strongly interact with the structure can have an alternate description of free fall through the horizon of a black hole. We discuss this recently proposed picture of fuzzball complementarity in detail and test it using our newly constructed near-extremal microstates. A key feature of supersymmetric multi-center solutions, used to construct these near-extremal microstates, is that when brane probes are placed in this background in a supersymmetric way they capture the same information as the fully backreacted Supergravity solution. We investigate whether this non-renormalization property also holds for extremal 'almost-BPS' solutions where supersymmetry is broken in a controllable way. We find that despite the lack of supersymmetry, the probe action reproduces exactly the equations underlying the fully back-reacted solution indicating that these equations also do not receive quantum corrections.

**Résumé**

Dans cette thèse, nous étudions les trous noirs et leurs propriétés microscopiques dans les extensions de la relativité générale qui se posent en tant que limites à basse énergie de la théorie des cordes. La première question que nous allons traiter est de savoir comment les trous noirs libèrent l'information lors de l'évaporation. Nous utilisons des techniques de l'information quantique et étudions la libération de l'information de systèmes qubits. Nous présentons ensuite un modèle de cadre général pour capturer le processus d'évaporation Hawking et déduisons les contraintes sur l'évolution dictés par la condition de l'unitarité. Cela rend la conclusion de perte d'information dans le processus d'évaporation des trous noirs plus précise et soutient la thèse selon laquelle l'horizon doit être remplacé par une structure, ainsi appelé *fuzzball*, qui transporte des informations sur les micro-états des trous noirs. Cela pose immédiatement la question de ce qu'est cette structure à échelle d'horizon? Nous poursuivons cette question dans le contexte de Supergravity. Nous construisons systématiquement une famille de micro-états des trous noirs non-extrémaux en plaçant des supertubes métastables dans certaines géométries supersymétriques qui sont complètement lisses et possède la propriété 'scaling'. Ces fuzzballs non-extrémaux diffèrent de la solution du trou noir classique à l'échelle macroscopique de l'horizon, et pour certaines sondes les fluctuations entre les différents fuzzballs seront visibles que le bruit thermique loin de l'horizon. Si l'horizon du trou noir est remplacé par une structure à échelle de l'horizon on peut se demander ce que l'expérience d'un observateur tombant dans une telle structure est? Un récent Gedankenexperiment très controversé suggère qu'un tel observateur brûlera dans un 'firewall' à l'horizon. Nous reformulons ce Gedankenexperiment dans le langage de la décohérence de la mécanique quantique et étudions le sort d'un paquet d'ondes tombant dans un trou noir. Alors que des paquets d'ondes de la taille de quanta de Hawking sortant du trou noir peuvent en effet ne pas tomber librement à travers la structure à l'echelle de l'horizon, il y a la possibilité que l'expérience des observateurs macroscopiques interagissement fortement avec la structure peut avoir une autre description de chute libre à travers l'horizon d'un trou noir. Nous discutons en détail cette image de complémentarité de fuzzball, récemment proposée, et la testons en utilisant nos micro-états non-extrémaux nouvellement construits. Leur construction utilise des solutions multi-centres supersymétriques. Lorsque les sondes membranaires sont placées dans ces géométries d'une façon supersymétrique ils capturent les mêmes informations que la solution de Supergravité - ceci est une caractéristique clé des solutions multi-centres supersymétriques. Nous examinons si cette propriété de non-renormalisation s'applique aussi bien pour des solutions extremaux 'almost-BPS' où la supersymétrie est brisée de manière contrôlable. Nous constatons que malgré l'absence de supersymétrie, l'action de la sonde reproduit exactement les équations qui sous-tendent la solution de Supergravité en indiquant que ces équations ne reçoivent pas de corrections quantiques.

# Publications and Preprints

**P1 Metastable Supertubes and non-extremal Black Hole Microstates,**
I. Bena, A. Puhm and B. Vercnocke,
JHEP **1204** (2012) 100 [arXiv:1109.5180 [hep-th]].

**P2 Decoherence and the fate of an infalling wave packet: Is Alice burning or fuzzing?,**
B. D. Chowdhury and A. Puhm,
submitted to Phys.Rev.D, arXiv:1208.2026 [hep-th].

**P3 Non-extremal Black Hole Microstates: Fuzzballs of Fire or Fuzzballs of Fuzz ?,**
I. Bena, A. Puhm and B. Vercnocke,
JHEP **1212** (2012) 014 [arXiv:1208.3468 [hep-th]].

**P4 Unitarity and fuzzball complementarity: 'Alice fuzzes but may not even know it!',**
S. G. Avery, B. D. Chowdhury and A. Puhm,
submitted to JHEP, arXiv:1210.6996 [hep-th].

**P5 Almost-BPS but still not renormalized,**
I. Bena, A. Puhm, O. Vasilakis and N. Warner,
arXiv:1303.0841 [hep-th].

**P6 Insane Anti-Membrane ?,**
G. Giecold, F. Orsi and A. Puhm,
arXiv:1303.1809 [hep-th].

# Contents

# Introduction

## Black holes as playgrounds for Quantum Gravity

Quantum Mechanics and General Relativity provide extremely good descriptions of our world at respectively small and large scales and have been experimentally tested to great accuracy. Yet, from a theoretical perspective, these theories are incompatible and the attempts to unify them in a more fundamental framework presents one of the major challenges in the physics of our times. While Quantum Mechanics and General Relativity describe physics very well in a regime where the other theory is negligible, the clash between them becomes dramatic when we cannot neglect effects from either. This happens for black holes which thus present an ideal playground to forge a theory of Quantum Gravity. Black holes are solution to Einstein's equations with peculiar properties:

- Black holes have a curvature *singularity* where the laws of General Relativity stop making sense.
- The singularity is 'cloaked' by a *horizon* which separates the exterior space time from the black hole interior in that any infalling matter that has crossed the horizon will be trapped inside.
- The laws of black hole mechanics bear a striking resemblance with the laws of thermodynamics. In particular, the area of the black hole horizon can be ascribed an *entropy*. While 'no-hair' theorem tells us that black holes are uniquely characterized by very few asymptotic parameters, its entropy implies an exponential number of microscopic degrees of freedom and understanding their origin has been a great puzzle in the history of black hole physics.
- Black holes also have a *temperature* and thus radiate. Semiclassical considerations suggest that the final radiation state after complete evaporation of the black hole is thermal. This implies that the information of the original matter that formed the black hole and any matter that has fallen in and stayed trapped inside will be washed out once the black hole has evaporated. This loss of unitarity in the black hole evolution presents a deep conflict with the laws of Quantum Mechanics.

Black holes are interesting objects in their own right and there is observational evidence for their existence in nature. A theory of Quantum Gravity has to explain their peculiar properties and resolve the puzzles. On the other hand, by studying black holes we can learn a lot about the general structure and properties of Quantum Gravity. But to do so we need a precise framework which incorporates General Relativity and Quantum Mechanics as certain limits but which contains new degrees of freedom that allow to formulate sharp questions about the above properties whose answers lie in the scope of the new theory. String Theory provides this framework. In this Thesis we will study black holes and their microscopic properties in String Theory/M-theory and their low-energy limits.

## The problems with black holes and conjectured resolutions

The characterizing properties of black holes: singularity, horizon, entropy and temperature lead to deep conceptual problems that have puzzled the black hole physics community over decades and are a topic of intense research until today. Interesting developments have taken place over the last years and a recent wave of passionate debate has put black holes again in the center of scientific attention. In recent years these questions have been sharpened and promising resolutions have been conjectured. In this Introduction we intend to give the general idea of the problems and proposed resolutions and discuss them further in the main part of this Thesis. In each Chapter we will come back to one or more of the below phrased questions and present our contributions to the attempt to answer them.

### 1. The information paradox

Black holes have a temperature and so they radiate, gradually lose their mass and eventually evaporate completely. In a famous paper [1] Hawking studied the semiclassical evolution of vacuum modes of quantum fields on the curved space around the black hole horizon and found that unitarity is not preserved in the evaporation process. Quantum effects lead to creation of pairs of quanta out of the vacuum at the horizon; the negative energy quanta fall into the black hole while the positive energy quanta escape as radiation to infinity. Hawking showed that after complete evaporation of the black hole through this process, the final radiation state is thermal. Since the initial state that formed the black hole could have been in a pure state, he concluded that black hole evaporation leads to information loss. This result depicts the deep conflict between General Relativity and Quantum Mechanics which becomes sharp in the context of black holes. Hawking's calculation suggests that Quantum Mechanics fails for black holes. To lose the fundamental principle of unitarity would indeed be drastic and we should therefore critically investigate the assumptions Hawking made to arrive at this result.

Since Hawking's calculation uses quantum fields on curved space, where matter is quantized but gravity is treated classically, one might think that one can add small corrections [1] to the Hawking process which accumulate over time to eventually restore unitarity. In [2] Mathur has turned Hawking's argument into a theorem and, as we will review briefly in Section 2.2, has shown that small corrections to the Hawking process cannot restore unitarity. Instead a drastic

[1] These corrections should be suppressed by the order parameter (mass) of the black hole such that General Relativity remains a good approximation at the horizon. In that sense the corrections should be 'small'.

departure from the black hole geometry is required if unitarity is to be preserved. More concretely, the (information-free) horizon must be replaced by some structure, from which radiation is emitted unitarily, and which has been dubbed *fuzzball*. Mathur's argument was based on the requirement of purity of the final radiation state which is a necessary condition for unitarity. It is however not sufficient to guarantee unitarity of the evolution. In Chapter 2 we will go beyond the condition of purity and study the question:

*Q1: When and how does the information of the original state come out?*

We will argue that purity of the final radiation state does not guarantee that the information of the matter that formed the black hole ever comes out. More concretely, we will argue that information has to leave the black hole with every quantum that is emitted and the traditional black hole horizon is thus inconsistent with unitarity at every step of the evaporation process. This statement and the assumptions on which it is based will be discussed in detail in Chapter 2.

**2. The entropy puzzle**

The Bekenstein-Hawking entropy-area law [2]

$$S_{BH} \;=\; \frac{k_B c^3}{\hbar G_N}\frac{A}{4}\,, \tag{1}$$

relates a geometric quantity proportional to the area $A$ of the black hole horizon, to a quantity $S_{BH}$ that satisfies the analog of the first and second law of thermodynamics, and which is interpreted as the entropy of the black hole. Boltzmann's law then associates to it

$$N_{MS} \;=\; e^{S_{BH}} \tag{2}$$

microstates. While for thermodynamics we know that there *is* an underlying microscopic description which can be related to the macroscopic description via statistical (quantum) mechanics, for black holes any microscopic interpretation of $S_{BH}$ within General Relativity has eluded us. In fact, the 'no-hair' theorem of General Relativity says that a black hole is uniquely characterized by its asymptotic parameters: mass, charge, and angular momentum. If in General Relativity there is only one state, the black hole, then 'where' are its $e^{S_{BH}}$ microstates? Clearly, an answer to this question lies beyond the scope of General Relativity.

A powerful framework in addressing questions relevant for understanding the nature of black holes is provided by String Theory. In particular, it provides an understanding of the microscopic degrees of freedom of black holes in terms of bound states of strings and branes when the effective string coupling is weak. [3] This insight paved the road for the discovery of the Anti de Sitter/Conformal Field Theory (AdS/CFT) correspondence [4, 5] which is a very useful tool to study certain microscopic properties of supersymmetric black holes. Those have a near-horizon $AdS$ throat and their entropy can be reproduced exactly by counting bound states in the conjectured dual CFT on the boundary of this $AdS$ space.

[2] In this Thesis we set $c = \hbar = k_B = 1$. The Bekenstein-Hawking entropy is then $S_{BH} = \frac{A}{4G_N}$.

**Microstates at weak coupling.** This has first been shown for the supersymmetric two-charge system. In the F1-P duality frame, the states of the supersymmetric two-charge system can be described by momentum modes (P) on a fundamental string (F1). At zero effective string coupling, these can be analyzed within the underlying conformal field theory where one can use Cardy's formula [6] to compute the degeneracy of states. The two-charge black hole at large effective string coupling has a classically vanishing horizon area which Sen [7] argued to be rendered finite by stringy corrections. Under this assumption, he found the black hole entropy to have same scaling in terms of the charges as the CFT entropy computed from Cardy's formula. The correct numerical factor was found by Dabholkar [8] by computing all higher curvature corrections to the Supergravity action and using the generalization of the Bekenstein-Hawking entropy due to Wald [9]. The degeneracy of supersymmetric states of the two-charge system at weak effective string coupling thus exactly matches the entropy of the two-charge black hole.

While this matching was striking, it was not clear whether this feature carried over to black holes with a classical horizon. However, in a by now famous paper [3], Strominger and Vafa showed that the Bekenstein-Hawking entropy of the five dimensional supersymmetric three-charge black hole with macroscopically large horizon area is exactly reproduced by the degeneracy of CFT states of the supersymmetric three-charge system at weak effective string coupling.

The reason why this remarkable matching works are non-renormalization theorems for supersymmetric systems that protect the number of bound states as one goes from weak to strong effective coupling. The AdS/CFT correspondence thus allows us to identify microscopic degrees of freedom of *supersymmetric* black holes but it remains unclear how to treat non-supersymmetric black holes. Moreover, the statistical interpretation of the entropy of a supersymmetric black hole via the AdS/CFT correspondence is only understood in a regime where gravity is turned off! A satisfactory understanding of the microscopic degrees of freedom of any black hole must answer the question:

*Q2: What are the black hole microstates at strong effective coupling?*

Naively, all objects, other than black holes, become smaller as gravity gets stronger. One would therefore expect that all possible bound states of strings and branes will collapse to a black hole upon backreaction. [10] Surprisingly, this turns out not to be true.

**Microstates at strong coupling.** The above question has first been addressed by Mathur, Lunin, Maldacena, Maoz and others [11, 12, 13, 14, 15, 16] in the context of the two-charge system. See [17, 18] for earlier work in this direction and [19] for a review of that work. In Supergravity, the string source (F1) with momentum waves (P) can be represented semiclassically by an arbitrary shape profile for the string source. In addition to the F1 and P electric charges, there is a dipolar F1 charge, which cannot be measured by a flux integral at infinity, and angular momentum along the string profile. One can transform this system to a frame where the electric charges correspond to D1 and D5 branes and the dipole charge becomes a Kaluza-Klein monopole (KKm). The Supergravity solution in the D1-D5 frame encodes the same semiclassical data as in the F1-P frame, but is now completely *smooth* in six dimensions: there is no singularity or horizon. In yet a different duality frame the two-charge configuration takes the shape of a

supersymmetric tube – a *supertube*. The entropy coming from the arbitrariness of the shape of the closed curve the Kaluza-Klein monopole (or the supertube) is wrapping has been shown [11, 20] to exactly reproduce the entropy of the D1-D5 CFT. The degeneracy of states in the supersymmetric two-charge system at weak coupling can thus be understood by the number of possible *smooth* Supergravity solutions whose asymptotic charges match that of the two-charge black hole.

Since the two-charge black hole only has a 'stretched' horizon at the Planck or string scale, the smooth classical configurations accounting for the entropy of the two-charge system are at, or near, the limit of the Supergravity approximation. To have confidence in the Supergravity approximation it is very important to find explicit microstate geometries for the three-charge system. An intense research program has developed to achieve this task and many supersymmetric and non-supersymmetric three-charge solutions have been constructed so far. An incomplete list of the relevant references includes [21, 22, 23, 24, 25, 26, 27, 28, 29, 30, 31, 32, 33, 34, 35, 36, 37, 38, 39, 40, 41, 42, 43, 44, 45]. For reviews on work on the three-charge system see [46, 47, 48]. While for the two-charge system the entropy is accounted for by the arbitrary shape of the curve the supertube is wrapping – a 'wiggly supertube', it was argued [49] that the entropy of the three-charge system would come from 'superstrata' which have a non-trivial profile that depends on two variables rather than one. This conjecture was developed further in [50, 51, 52].

The perhaps simplest class of microstate geometries are asymptotically flat solutions of five-dimensional Supergravity. They form a class of smooth, geodesically complete, asymptotically flat, stable spacetimes without horizons. Their existence is surprising as no such solutions are known in four-dimensional Supergravity and there even exist 'no-go' theorems that exclude completely non-singular soliton solutions that are regular in four spacetime dimensions. In [53] it was, however, shown that five-dimensional Supergravity evades this 'no-go' theorem. The extra ingredients present in five-dimensional Supergravity were already used in the construction of smooth five-dimensional solutions but the recent result establishes in retrospect why they can exist in five spacetime dimensions while they cannot in four.

Although at this point not enough smooth three-charge solutions have yet been found to account for the full entropy of the three-charge system, the examples that have been constructed so far are quite suggestive: String Theory seems to tell us that a black hole should not be viewed as a fundamental object but rather as an effective coarse-grained description of an ensemble of smooth horizonless configurations with the same asymptotic properties. This is the essence of the *fuzzball proposal* which plays a central role in this Thesis. [3] The focus so far has been on constructing supersymmetric and non-supersymmetric *extremal* microstate geometries. These smooth Supergravity solutions look like the extremal black hole geometry asymptotically but differ from it at the location where the horizon would be. Since these bulk microstates do not radiate, they do not directly address the information paradox. In Chapter 3 we will go beyond extremality and ask what the microstates of non-extremal black holes could look like. Tightly connected to this is the question of how the black hole singularity is resolved in Quantum Gravity.

[3] Note, that we do not mean that all bulk microstates can be described within Supergravity. In fact, to describe a generic fuzzball will most likely require full String Theory/Quantum Gravity. The concept of a horizon may then become ill-defined. To emphasize the departure from General Relativity we will, however, continue to talk about 'horizonless' bulk microstates.

## 3. The singularity

The appearance of a singularity usually signals the limitation of a theory to properly address the problem. A theory of Quantum Gravity must resolve the black hole singularity and the interesting question is:

*Q3. What is the scale of the singularity resolution?*

Since the length scale one can construct from the fundamental constants $c, G_N, \hbar$ by dimensional analysis is the Planck length $l_P = \sqrt{\hbar G_N/c^3}$ one would naturally expect Quantum Gravity effects to become important at this scale. However, if General Relativity was indeed a good approximation all the way up to a Planck length from the singularity then, by arguments given above, it would be very hard, or impossible, to resolve the information paradox. Since the number of microscopic degrees of freedom of a black hole is exponential in its entropy there is, however, another possibility. The large number of microstates might give rise to a second natural length scale $R \sim N^\alpha l_P$, where $\alpha$ is a positive constant that has to be determined by the theory. This length scale is much larger than the Planck scale and can be of the order the horizon scale. Evidence for this new length scale was provided by the above listed references in constructing regular solutions where the singularity is resolved at scales much larger than the Planck length. For example, for the supersymmetric F1-P two-charge solution in five-dimensions one finds [19] $R \sim (N_{F1}N_P)^{1/6} l_P^{(5)}$, where $N_{F1}$ and $N_P$ are the number of F1 strings and units of momentum P and $l_P^{(5)}$ is the five-dimensional Planck length.

If physics were different from that of the black hole at the scale of the horizon, then this would imply a dramatic shift in our understanding of black holes and a profound insight into the nature of Quantum Gravity. A breakdown of the thermodynamic description of black holes would signal that new physics were to appear at the horizon scale that was beyond the grasp of General Relativity: *Quantum gravity effects are not confined to within a Planck length from the singularity but extend to macroscopic distances of the order the black hole horizon!* The three-charge geometries discussed above that have been constructed so far do indeed have a mechanism that prevents the collapse to a black hole: the local dipole charges which are dissolved in flux keep the geometry from shrinking. Since these solutions do not have a singularity but instead smoothly end in a 'cap' at the horizon scale the singularity is resolved at a macroscopic scale. This might at first seem surprising, but there are many known examples in String Theory, like the LLM geometries [54], Klebanov-Strassler [55], the enhançon [56] and Polchinski-Strassler [10] where time-like singularities are resolved at large scales. This picture is also supported by analyzing the physics of instabilities [57, 58, 59, 60, 61] inside the horizon of extremal black holes.

While there is by now good evidence that the singularity of extremal black holes is resolved at the horizon scale, it is not immediately clear what happens for non-extremal black holes which have two horizons. If one is to simply extrapolate the extended evidence for extremal black hole microstates to non-extremal ones, it is well-possible that the timelike singularity of non-extremal black holes is only resolved to the scale of the inner horizon, and that the region between the inner and the outer horizon is still described by the classical black hole solution. The fuzzball proposal and the yearning to solve the black hole information paradox would have the black hole

singularity resolved all the way to the outer horizon,'backwards in time' [4] from the singularity.

To address the question at which scale the singularity resolution happens, one needs to attack the formidable task of constructing non-extremal black hole microstate geometries, which is highly nontrivial. Only two very non-generic non-extremal solutions are known [62, 63, 64, 65, 40] and their generalization is nowhere in sight. In Chapter 3 we will argue for a way to bypass these limitations by adding probes to extremal BPS geometries in such a way that they render the configuration non-extremal. This procedure allows to systematically construct microstates of near-extremal black holes. We will then compute the size of these configurations to determine the singularity resolution scale.

### 4. The infall question

This question is often discussed at the same level as the problems (1)-(3) above. The singularity resolution scale and the microscopic description of black holes at strong effective coupling are questions about the Quantum Gravity solution itself and the resolution of the information paradox involves radiation quanta with typical Killing energy of the order the Hawking temperature at infinity. Infall into a black hole is a *dynamical* process and we are usually interested in macroscopic objects rather than typical quanta. We therefore seek to answer the question of what a macroscopic observer falling into a black hole experiences? General Relativity tells us that the black hole metric is smooth across the horizon and curvatures are low. Applying the equivalence principle then implies that an infalling observer will freely fall through horizon and not experience anything special until she approaches the singularity. However, to resolve the issues (1)-(3) a departure from the traditional black hole picture is required. Since the infall question depends on the interaction of the infalling observer with whatever she falls into, this question can only be phrased in a meaningful way once the above issues have been addressed. If there is no smooth horizon but the Quantum Gravity description of a black hole requires drastic changes at the horizon scale and some information about its microscopic description at strong effective coupling, then the question about infall into a black hole has to be replaced by

*Q4. What does an observer falling into the (quantum) black hole microstate experience?*

Recently, a very passionate debate has formed around this question. In [66] it has been argued that horizon-scale structure causes an infalling observer to burn in a firewall at the horizon. In [67, 68, 69, 70, 71], on the other hand, the possibility of an approximate description of free infall for macroscopic observers is presented in the context of fuzzballs. We will elaborate on these proposals in detail when discussing the above question in Chapter 4.

[4] By this, we do not mean that the singularity is resolved by a fuzzball *after* the black hole has formed; instead the black hole geometry should always be understood as an approximation and a collapsing star never forms a singularity.

**5. Towards a microscopic understanding of non-supersymmetric black holes**

Most of the work so far has focused on studying the microscopic properties of supersymmetric black holes since they are more tractable. Eventually, however, we would like to understand Schwarzschild black holes which are non-supersymmetric. In order to gain some insight on non-supersymmetric black holes we can try to address the question:

*Q5. What properties of supersymmetric solutions carry over to non-supersymmetric solutions?*

For the supersymmetric multi-center solutions constructed so far, a non-renormalization property allows to study their physics either at weak effective string coupling where the configuration is described by a supersymmetric quiver Quantum Mechanics or in the strongly coupled regime where all the centers are backreacted. Interestingly, the Dirac-Born-Infeld probe action where one of the centers is treated as a probe in the background of the other centers also captures the full physics of the solution. To understand the physics of more realistic black holes we need to break supersymmetry and eventually extremality. A first step into this direction is the study of non-supersymmetric but extremal configurations which break supersymmetry in a very mild and controlled way and which are therefore called 'almost-BPS' solutions. In Chapter 5 we study whether the non-renormalization property of supersymmetric multi-center configurations carries over to almost-BPS configurations.

# Organization of the Thesis

This Thesis is organized in five Chapters and additional Appendices.

In Chapter 1 we review black holes in General Relativity and discuss their embedding in String Theory/M-Theory as three-charge solutions. This class of solutions also encompasses geometries that are smooth everywhere and have no horizon. In the context of the fuzzball proposal these can be viewed as black hole microstate geometries. An important ingredient in the study of these microstates are supertubes. We give the derivation for the Hamiltonian for probe supertubes placed in three-charge backgrounds which was first found in **P1**. This provides the basis for the discussions of Chapter 3 and 5.

In Chapter 2 we discuss black hole evaporation and the question of how information is released from black holes. We review the argument, based on the requirement of purity of the final radiation state, that the black hole horizon must be replaced by horizon-scale structure for unitarity to be preserved during the evaporation process. We will then go beyond the requirement of purity and make the statement of information loss more precise. This part is based on **P4**. Using quantum information techniques, the implications of unitarity can be made sharp when modeling black hole evaporation via qubit systems. Our analysis makes the requirement of horizon-scale structure even stronger.

In Chapter 3 we study the potential of supertubes in three-charge backgrounds as derived in Chapter 1. We find that the potential can have supersymmetric and non-supersymmetric minima as well as metastable minima. When the background has the same asymptotics as a BPS three-charge black hole but is regular and smooth everywhere, we argue that metastable

minima of a probe supertube in such a background give rise to microstate geometries of non-extremal black holes after backreaction. The computation of the size of these microstates shows that the singularity of the black hole is resolved at the scale of the horizon and the horizon is in fact replaced by this horizon-scale structure. We also discuss how Hawking radiation can be understood from the dynamics of the supertube via brane-flux annihilation. This Chapter is based on **P1** and **P3**.

In Chapter 4 we ask about the experience of an observer falling into (microstates of) black holes. We discuss the recent firewall argument and rephrase it in the decoherence language of Quantum Mechanics which is based on **P2**. We then elaborate on the recently conjectured possibility of an approximate complementarity picture for infall into fuzzballs. This discussion is based on **P4**. Finally, we attempt to test these ideas using the near-extremal microstates constructed in Chapter 3. This was carried out in **P3**.

A key feature of BPS multi-center solutions, used in our construction of near-extremal fuzzballs is that the equations controlling the positions of these centers are not renormalized as one goes from weak to strong coupling. In Chapter 5 we study this non-renormalization property for a special class of non-supersymmetric extremal, 'almost-BPS', solutions. This is the content of **P5**.

In Appendix A we list Conventions and Appendices B, C and D provide supplementary material for the Chapters 1, 3 and 5 respectively.

The work **P6** it is rather technical and only slightly related to the other topics presented in this Thesis. We will therefore not discuss it here in detail but give a summary of the main result: In Chapter 3 we will present a systematic construction of near-extremal microstates from metastable supertubes in bubbling geometries and one may hope to take these configurations further away from extremality by increasing the mass while keeping the mass to charge ratio fixed. The important question in this context is the backreaction of these metastable supertubes. The backreaction of antibranes in backgrounds with charge dissolved in flux is in general a very complicated topic and at this point there is some uncertainty about the fate of metatstable antibrane configurations when full backreaction is taken into account. The antibrane backreaction studies in the literature [72, 73, 74, 75, 76, 77, 78, 79] suffer from unphysical singularities that appear in directions not related to the worldvolume of the antibrane. In **P6** we asked whether the AdS-like UV boundary in these studies could be responsible for the unphysical singularities and studied the backreaction of antibranes in backgrounds with different UV asymptotics. We considered the first-order backreaction of anti-M2 branes in the $\mathbb{A}_8$ Supergravity solution [80], an asymptotically flat background on which the anti-M2 branes are fully localized. Yet again we find that the backreacted solution has unphysically looking singularities. One may wonder whether the backreaction of the metastable supertubes will suffer from the same problems? It is assuredly not clear whether a naive extrapolation can be done for arguments we will discuss in Chapter 3. The first-order backreaction for this case is also much more difficult and is not feasible with the current technology. On the other hand, if it turns out that the backreacted solution does exhibit singularities that do not obviously stem from the metastable supertubes, this does not necessarily imply that the solution has to be discarded. Indeed, in [81], it was suggested that singularities in fluxes may arise from forcing time-independence on what is inherently a time-dependent process. It is clearly important to investigate this further and we hope to return to it in the future.

**Note.** In order to avoid confusion, we will note here two different uses of the words 'microstate' and 'typical'. When discussing physics at weak effective string coupling, 'microstate' denotes a certain bound state of strings and branes. If this context is not explicitly stated, 'microstate' will always refer to smooth Supergravity solutions. Although these configurations are actually classical, and only become 'microstates' after quantization of the geometry we will, in slight abuse of language, already call them 'microstates'. To make a clear distinction between physics at weak and strong effective coupling we will talk about *CFT microstates* versus *bulk microstates*. The other important distinction must be made when talking about 'typical' microstates. In Chapter 1 we will discuss 'typical' bulk microstates, which in this context are defined to be dual to states in the CFT sector that contains 'typical' CFT states which contribute most to the entropy of the black hole. In Chapters 2 and 4 we will discuss states which are 'typical' in Page's sense. These are states for which all subsystems are almost maximally entangled.

# Chapter 1

# Black holes and their microstates

The purpose of this Chapter is to review black holes in General Relativity and String Theory and introduce the tools used in this Thesis for the study of their microscopic properties. We start in Section 1.1 with a brief review of black hole solutions in General Relativity, discuss their thermodynamic properties and show how they can be embedded in String Theory. In Section 1.2 we introduce the Supergravity framework. This will provide the starting point for the discussion of three-charge solutions in Section 1.4 which encompass black holes as well as the singularity-free and horizonless smooth microstate geometries. In Section 1.5 we introduce the central object of this Thesis: supertubes. We review the probe brane formalism and apply it to supertubes in flat space. We then derive the Hamiltonian for supertubes placed in three-charge backgrounds which will provide the basis for subsequent Chapters.

## 1.1 Black holes in General Relativity

In Subsection 1.1.1 we review the four-dimensional black hole solutions of General Relativity that are completely characterized by their mass, charge and angular momentum. In Subsection 1.1.2 we briefly discuss black hole thermodynamics. This review material can be found, for example, in [82, 83].

### 1.1.1 Black holes in four dimensions

Black holes are solutions to Einstein's equations [1]

$$R_{\mu\nu} - \frac{1}{2} g_{\mu\nu} R = 8\pi G_N^{(4)} T_{\mu\nu} \,, \tag{1.1}$$

where $R_{\mu\nu}$ and $R = g^{\mu\nu} R_{\mu\nu}$ are respectively the Ricci tensor and Ricci scalar of the spacetime metric $g_{\mu\nu}$ and $T_{\mu\nu}$ is the energy-momentum tensor of the matter fields under consideration. In the following we will work in four spacetime dimensions and discuss vacuum solutions ($T_{\mu\nu} = 0$) and General Relativity coupled to electro-magnetism ($T_{\mu\nu} = F_{\mu\rho} F^{\rho}_{\nu} - \frac{1}{4} F_{\rho\sigma} F^{\rho\sigma}$ where $F_{\mu\nu}$ is the electromagnetic field strength.). Black hole uniqueness theorems limit the number of admissible

[1] We will work in conventions where the four-dimensional Newton constant $G_N^{(4)} = 1$.

solutions to Einstein's equations. In the following we review the possible solutions which are characterized by three parameters: mass $M$, charge $Q$ and angular momentum $J$. [2] They are summarized in Table 1.1.

| M | $J = 0$ | $J \neq 0$ |
|---|---|---|
| $Q = 0$ | Schwarzschild | Kerr |
| $Q \neq 0$ | Reissner-Nordström | Kerr-Newman |

Table 1.1: Types of black holes in General Relativity.

### Schwarzschild

The simplest vacuum solution to Einstein's equations that is not Minkowski space is the Schwarzschild solution: a spherically symmetric black hole in vacuum which, due to Birkhoff's theorem, has to be static. The metric of the Schwarzschild black hole is given by

$$ds^2 = -\Big(1 - \frac{2M}{r}\Big)dt^2 + \Big(1 - \frac{2M}{r}\Big)^{-1} dr^2 + r^2 d\Omega_2^2\,, \tag{1.2}$$

where $d\Omega_2^2 = d\theta^2 + \sin^2\theta d\phi^2$ is the line element of the 2-sphere. A striking feature of the Schwarzschild solution is that the metric components become singular at $r_H = 2M$ and $r_S = 0$. While the singularity at $r_S$ is a true curvature singularity that signals the breakdown of General Relativity, the singularity at $r_H$ is just a coordinate singularity as is revealed by a coordinate transformation from Schwarzschild to Kruskal–Szekeres coordinates which cover the entire spacetime of the extended Schwarzschild black hole. What is however special about $r = r_H$ is that surfaces of fixed $r, \theta, \phi$ and varying $t$ change from spacelike to timelike while surfaces of fixed $t, \theta, \phi$ and varying $r$ change from timelike to spacelike. The Schwarzschild radial and temporal coordinates thus exchange their roles when continued to the interior of the black hole. The surface defined by $r_H = 2M$ is called *event horizon*. The Killing vector $\xi^a = (\partial/\partial t)^a$ is timelike outside the horizon, becomes null at the horizon and is spacelike inside the horizon. As a consequence, any matter that crosses the event horizon is trapped inside since a velocity greater than the speed of light would be required to escape.

### Reissner-Nordström

The spherically symmetric solution with an electromagnetic source $T_{\mu\nu} = F_{\mu\rho}F^{\rho}_{\nu} - \frac{1}{4}F_{\rho\sigma}F^{\rho\sigma}$, where $F_{\mu\nu} = \partial_\mu A_\nu - \partial_\nu A_\mu$ is the electromagnetic field strength, is given by the Reissner-Nordström black hole. It is the unique static electrovacuum black hole. Its metric takes the form

$$ds^2 = -\Big(1 - \frac{2M}{r} + \frac{Q^2}{r^2}\Big)dt^2 + \Big(1 - \frac{2M}{r} + \frac{Q^2}{r^2}\Big)^{-1} dr^2 + r^2 d\Omega_2^2\,, \tag{1.3}$$

[2] In Appendix A we give the general formulae for reading off $M, Q$ and $J$ from the metric and gauge potential including Newton's constant.

where $Q$ is the charge of the solution. For a spherically symmetric electrically charged configuration the only non-vanishing component of the electromagnetic field strength $F = F_{tr}\, dt \wedge dr$ is [3]

$$F_{tr} = \frac{Q}{r^2}\,. \tag{1.4}$$

For vanishing electric charge $Q = 0$ we recover the Schwarzschild solution. As in the Schwarzschild case the Reissner-Nordström black hole has a curvature singularity at $r_S = 0$. The metric component $g_{tt}$ has two zeroes at

$$r_\pm = M \pm \sqrt{M^2 - Q^2}\,. \tag{1.5}$$

There are three cases:

- $M^2 < Q^2$: There are no real zeroes ($r_\pm$ become imaginary) and the curvature singularity at $r_S = 0$ is a 'naked singularity', not cloaked by a horizon. These solutions, being considered unphysical, should be discarded by the *cosmic censorship* hypothesis.
- $M^2 > Q^2$: There are two real zeroes at $r_-$ and $r_+$, with $0 < r_- < r_+$, corresponding respectively to the black hole inner and outer horizon. The outer horizon is the event horizon.
- $M^2 = Q^2$: There is only one zero $r_H = r_+ = r_-$ and the two horizons coincide. The black hole has the maximal amount of charge for a given mass allowed by the cosmic censorship conjecture and is therefore called *extremal* Reissner-Nordström.

**Kerr**

The unique stationary solution to Einstein's equations is the Kerr black hole. Its metric in Boyer-Lindquist coordinates is given by

$$ds^2 = -\frac{\Delta}{\Sigma}\Big(dt - a\sin^2\theta d\phi\Big)^2 + \frac{\Sigma}{\Delta}dr^2 + \frac{\sin^2\theta}{\Sigma}\Big((r^2+a^2)d\phi - a dt\Big)^2 + \Sigma d\theta^2\,, \tag{1.6}$$

where

$$\begin{aligned} \Sigma &= r^2 + a^2\cos^2\theta\,, \\ \Delta &= r^2 + a^2 - 2Mr\,, \end{aligned} \tag{1.7}$$

and $a \equiv J/M$ where $M$ is the mass and $J$ is the angular momentum of the black hole. For vanishing angular momentum $J = 0$ we recover the Schwarzschild metric. For $M \neq 0$ the Kerr solution has a ring singularity at $\Sigma_S \equiv \Sigma(r_s) = 0$. The inner and outer horizons are defined as the two solutions to $\Delta = 0$:

$$r_\pm = M \pm \sqrt{M^2 - a^2}\,. \tag{1.8}$$

As for the Reissner-Nordström black hole there are three cases:

[3] In general there are dyonic black holes which can have electric and magnetic charge with vector potentials $F_{tr} = \frac{q_e}{r^2}$ and $F_{\theta\phi} = q_m \sin\theta$ and total charge $Q = \sqrt{q_e^2 + q_m^2}$. Here we consider $q_m = 0$ so that $Q = |q_e|$ is thus the electric charge of the solution.

- $a > M$ ($J > M^2$): The roots in (1.8) become imaginary and there is a naked ring singularity at $r_S = 0$ violating cosmic censorship. To exclude this possibility the angular momentum of black rings has to be bounded by $J \leq M^2$.
- $a < M$ ($J < M^2$): There are two real zeroes at $r_-$ and $r_+$, with $r_+ > r_- > 0$, that correspond respectively to the black hole inner and outer horizon.
- $a = M = \sqrt{J}$: There is only one zero at $r_\pm = M$ and the two horizons coincide. The extremal Kerr black hole has the maximum amount of angular momentum for a given mass allowed by the cosmic censorship conjecture.

The Kerr black hole has an interesting property that is related to its rotation. Similar to Schwarzschild, the norm of the Killing vector $\xi^a\xi_a = g_{tt} = \frac{a^2\sin^2\theta - \Delta}{\Sigma}$ changes from negative to positive values when crossing the location where $g_{tt} = 0$. While for Schwarzschild this happens as one crosses the horizon, for Kerr the asymptotically timelike Killing vector $\xi^a$ becomes spacelike already *outside* the horizon in a region

$$r_+ < r < M + \sqrt{M^2 - a^2\cos^2\theta}\,, \tag{1.9}$$

called the *ergoregion*. This region has an interesting observable property. An observer in the ergoregion cannot remain stationary: To follow an orbit of $\xi^a = (\partial/\partial t)^a$ she would have to go faster than light even though she is outside the black hole. All observers inside the ergoregion are forced to rotate in the direction of rotation of the black hole - an effect known as *frame dragging*.

### Kerr-Newman

The unique stationary, axisymmetric electrovacuum solution to General Relativity is the Kerr-Newman solution. It forms a three parameter family of solutions with spacetime metric

$$\begin{aligned} ds^2 &= -\Big(\frac{\Delta - a^2\sin^2\theta}{\Sigma}\Big)\,dt^2 - \frac{2a\sin^2\theta(r^2+a^2-\Delta)}{\Sigma}\,dt\,d\phi \\ &\quad + \Big(\frac{(r^2+a^2)^2 - \Delta a^2\sin^2\theta}{\Sigma}\Big)\sin^2\theta\,d\phi^2 + \frac{\Sigma}{\Delta}\,dr^2 + \Sigma\,d\theta^2\,, \end{aligned} \tag{1.10}$$

and electromagnetic vector potential

$$A = \frac{Qr}{\Sigma}(dt - a\sin^2\theta d\phi)\,, \tag{1.11}$$

where

$$\begin{aligned} \Sigma &= r^2 + a^2\cos^2\theta\,, \\ \Delta &= r^2 + a^2 + Q^2 - 2Mr\,, \end{aligned} \tag{1.12}$$

and $M, Q$ and $J \equiv aM$ are the three parameters of the family. At $\Sigma_S \equiv \Sigma(r_s) = 0$ the Kerr-Newman black hole has a ring singularity. As for Kerr and Reissner-Nordström, there are two solutions to $\Delta = 0$ defining the inner and outer horizon:

$$r_\pm = M \pm \sqrt{M^2 - Q^2 - a^2}\,, \tag{1.13}$$

of the Kerr-Newman black hole. All stationary black hole solutions are encompassed by this three parameter family and for special values of $Q$ and $J$ we recover

- Kerr: $Q = 0$,
- Reissner-Nordström: $J = 0$,
- Schwarzschild: $Q = J = 0$.

Black hole uniqueness for stationary solutions to Einstein's equations is stated by the 'no-hair theorem': a black hole in General Relativity is uniquely characterized by the three parameters mass $M$, charge $Q$ and angular momentum $J$.

### 1.1.2 Thermodynamics

In the course of studying the laws of black hole mechanics a profound relationship between black holes, thermodynamics and quantum mechanics was uncovered. In 1971 Hawking proved that the area $A$ of a black hole horizon classically never decreases with time: $\delta A \geq 0$. This bears a strong resemblance with the second law of thermodynamics stating that the entropy of a closed system never decreases: $\delta S \geq 0$. This led Bekenstein [84] to conjecture that the horizon area of a black hole can be ascribed an entropy $S_{BH} = \alpha A$ with proportionality constant $\alpha$. Bardeen, Carter and Hawking put this analogy on firmer grounds by suggesting that also the surface gravity $\kappa$ of a black hole behaves as a temperature $T_H = \frac{\kappa}{8\pi\alpha}$. At a classical level the relation between black hole mechanics and thermodynamics was a mere analogy. In semi-classical considerations of Hawking [1], where matter is treated quantum mechanically while the background is treated classically, he found that black holes can emit radiation and must thus have a temperature. This turned the classical analogy into a real identification that allowed to determine the proportionality parameter to be $\alpha = \frac{1}{4}$. The Hawking temperature and the Bekenstein-Hawking entropy associated to the geometric properties, surface gravity and horizon area, of a black hole are

$$T_H = \frac{\kappa_s}{2\pi}\,, \qquad S_{BH} = \frac{A}{4}\,. \tag{1.14}$$

The comparison between the laws of black hole mechanics and thermodynamics is given in Table 1.2. For the stationary electrovacuum solutions discussed above one finds the following expressions for the Hawking temperature and Bekenstein-Hawking entropy:

- Schwarzschild:

$$T_H = \frac{1}{4\pi r_H}\,, \qquad S_{BH} = \frac{\pi r_H^2}{2}\,. \tag{1.15}$$

  With $r_H = 2M$, we get $T_H = \frac{1}{8\pi M}$ and $S_{BH} = 2\pi M^2$.

- Reissner-Nordström:

$$T_H = \frac{r_+ - r_-}{4\pi r_+^2}\,, \qquad S_{BH} = \pi r_+^2\,. \tag{1.16}$$

  In the extremal case $r_\pm = M = Q$, we get vanishing temperature $T_H = 0$ but finite entropy $S = \pi M^2 = \pi Q^2$.

| | Black Hole Mechanics | Thermodynamics |
|---|---|---|
| 0. | The surface gravity $\kappa_s$ is constant at black hole horizon. | The temperature $T$ is constant for body in equilibrium. |
| 1. | $\delta M = \frac{\kappa_s}{8\pi}\delta A + \Omega\delta J + \Phi\delta Q$ | $\delta M = T\delta S + p\delta V + \mu dN$ |
| 2. | $\delta A \geq 0$ The horizon area never decreases. | $\delta S \geq 0$ The entropy never decreases. |
| 3. | $\kappa_s = 0$ (extremal limit) cannot be reached by physical process in finite time. | $T = 0$ (absolute zero) cannot be reached by physical process in finite time. |

Table 1.2: Comparison between laws black hole mechanics and thermodynamics.

- Kerr:
$$T_H = \frac{r_+ - M}{4\pi M r_+}\,, \qquad S_{BH} = 2\pi M r_+\,. \tag{1.17}$$
In the extremal case $r_\pm = M = a$ the temperature vanishes $T_H = 0$ while the entropy $S_{BH} = 2\pi M^2 = 2\pi J$ is finite.

Thermal objects radiate and lose energy until they have evaporated. As discussed in the Introduction, semi-classical black hole evaporation leads to information loss . Since the horizon is just a coordinate singularity, in General Relativity no new physics is expected at this scale. Hawking's calculation therefore seems to imply that quantum mechanics breaks down for black holes. However, a more detailed study of the semiclassical evaporation process, discussed in Chapter 2, shows [2] that if unitarity is to be preserved there is reason to believe that the traditional black hole geometry breaks down at the scale of the horizon and General Relativity ceases to be a good description.

To study the properties of black holes beyond their thermodynamic description in General Relativity we need a framework that captures statistical properties such as the number of microstates that give rise to the Bekenstein-Hawking entropy. This framework is provided by String Theory/M-Theory and we will review now their low-energy effective descriptions.

## 1.2 Supergravity framework

Supergravity theories are supersymmetric extensions of General Relativity and have a natural embedding in String Theory. In this Thesis we will work in the framework of eleven-dimensional Supergravity, reviewed in Subsection 1.2.2, and ten-dimensional type IIA and type IIB Supergravity, reviewed in Subsection 1.2.1, which are low-energy limits of respectively M-Theory and type IIA and type IIB Superstring Theory. Since we are interested in studying classical black hole solutions we will restrict to the bosonic content of these theories. In Subsection 1.2.3 we discuss how eleven-dimensional supergravity is related to type IIA supergravity via dimensional

reduction and how a solution of type IIA supergravity can be transformed into a solution of type IIB supergravity via T-duality. This Section follows [85, 86, 87].

### 1.2.1 Type IIA and type IIB Supergravity

In General Relativity the bosonic field content comprises the metric which determines the dynamics of spacetime and the gauge potential one-form which couples to point particles. These fields generalize in ten-dimensional Supergravity to the ten-dimensional metric and higher-form gauge fields. In addition there are a scalar field called *dilaton* and an antisymmetric two-from called *B-field*. We will now discuss the full field content and action of ten-dimensional Supergravity.

**Fields.** The bosonic field content of ten-dimensional Supergravity is given by the following Neveu-Schwarz Neveu-Schwarz (NS-NS) fields

- the ten-dimensional metric $g$: a traceless symmetric tensor with components $g_{\mu\nu}$.
- an antisymmetric two-from $B_2 = B_{\mu\nu} dx^\mu \wedge dx^\nu$ with 3-form field strength $H_3 = dB_2$,
- the dilaton $\Phi$: a scalar field whose value at spatial infinity is related to the string coupling via $e^{\Phi_\infty} = g_s$,

and the Ramond-Ramond (R-R) fields

- higher-form gauge fields: $p$-form potentials $C_p$ with $(p+1)$-form field strength $F_{p+1} = dC_p$ where $p$ even (0,2,4,6,8) for type IIB and $p$ odd (1,3,5,7) for type IIA.

The graviton $g$ encodes the dynamics of spacetime, the NS-NS gauge field $B_2$ couples electrically to fundamental strings (F1) and magnetically to NS5-branes. The R-R gauge fields $C_{(p+1)}$ couple electrically to D$p$-branes and magnetically to D$(6-p)$-branes. The couplings that will be important in this Thesis are summarized in Table 1.3. We also have Kaluza-Klein monopoles (KKm) and momentum waves P.

| type | **IIA** | | | **IIB** | | |
|---|---|---|---|---|---|---|
| fields | $B_2$ | $C_1$ | $C_3$ | $B_2$ | $C_2$ | $C_4$ |
| electric | F1 | D0 | D2 | F1 | D1 | D3 |
| magnetic | NS5 | D6 | D4 | NS5 | D5 | D3 |

Table 1.3: Coupling of branes to $p$-form potentials in type IIA and IIB Supergravity.

**Action.** The bosonic part of the ten-dimensional action can be split into separate contributions from field in the Neveu-Schwarz and Ramond sector and a Chern-Simons term that involves both types of fields:

$$S_{10d} = S_{NS} + S_R + S_{CS}\,. \tag{1.18}$$

The contributions from NS-NS fields in the string frame[4] are universal (the same for type IIA and type IIB):

$$S_{NS} = \frac{1}{2\kappa_{10}^2}\int d^{10}x\sqrt{-g}e^{-2\Phi}\Big(R + 4\partial_\mu\Phi\partial^\mu\Phi - \frac{1}{2}|H_3|^2\Big)\,, \tag{1.19}$$

where $|\alpha|^2 = \star_{10}\,\alpha\wedge\,\alpha$. The ten-dimensional gravitational coupling constant $\kappa_{10}$ is related to the ten-dimensional Newton constant $G_N^{(10)}$ and the string length $l_s$ via

$$2\kappa_{10}^2 = 16\pi G_N^{(10)} = \frac{1}{2\pi}(2\pi l_s)^8 g_s^2\,. \tag{1.20}$$

The type IIA and type IIB frame differ in their R-R fields and have therefore different contributions $S_R$ and $S_{CS}$. In type IIA Supergravity we have

$$S_R = -\frac{1}{4\kappa_{10}^2}\int d^{10}x\sqrt{-g}\,\Big(|F_2|^2 + |\tilde{F}_4|^2\Big)\,, \tag{1.21}$$

$$S_{CS} = -\frac{1}{4\kappa_{10}^2}\int B_2\wedge F_4\wedge F_4\,, \tag{1.22}$$

while in type IIB Supergravity we have

$$S_R = -\frac{1}{4\kappa_{10}^2}\int d^{10}x\sqrt{-g}\,\Big(|F_1|^2 + |\tilde{F}_3|^2 + \frac{1}{2}|\tilde{F}_5|^2\Big)\,, \tag{1.23}$$

$$S_{CS} = -\frac{1}{4\kappa_{10}^2}\int C_4\wedge H_3\wedge F_3\,, \tag{1.24}$$

where

$$\tilde{F}_3 = F_3 - C_0\wedge H_3\,,\qquad \tilde{F}_4 = F_4 - C_1\wedge H_3\,, \tag{1.25}$$

$$\tilde{F}_5 = F_5 - \frac{1}{2}C_2\wedge H_3 + \frac{1}{2}B_2\wedge F_3\,. \tag{1.26}$$

In type IIB Supergravity one has to impose, in addition to the equations of motion, the selfduality of the 5-from field strength:

$$\tilde{F}_5 = \star_{10}\tilde{F}_5\,. \tag{1.27}$$

### 1.2.2 Eleven-dimensional Supergravity

In eleven dimensions the zoo of fields and extended objects reduces significantly and physics is described in a more symmetric way. In this Thesis we will mostly work in the M-Theory language.

[4]The action can be brought into the Einstein frame, where the kinetic term takes the more conventional form $\int\sqrt{-g}R$, by the redefinition $g^E_{\mu\nu} = e^{-\Phi/2}g_{\mu\nu}$ .

**Fields.** The bosonic fields of eleven-dimensional Supergravity are

- the eleven-dimensional metric $G$: a symmetric traceless tensor with components $G_{MN}$,
- an antisymmetric 3-from $A_3 = A_{MNP}\, dx^M \wedge dx^N \wedge dx^P$ with field strength $F_4 = dA_3$.

The graviton $G$ encodes the dynamics of the eleven-dimensional spacetime and the gauge potential $A_3$ couples electrically to M2 branes and magnetically to M5 branes. There are also massless gravitational waves P and the Kaluza-Klein monopole (KKm) which carries the magnetic charge of a $U(1)$ Kaluza-Klein gauge symmetry and which we will encounter later as the smooth Taub-NUT spacetime.

**Action.** The bosonic part of the action is given by

$$2\kappa_{11}^2 S_{11d} = \int d^{11}x\sqrt{-G}R - \frac{1}{2}\int \star_{11}F_4 \wedge F_4 - \frac{1}{6}\int A_3 \wedge F_4 \wedge F_4\,. \tag{1.28}$$

The eleven-dimensional gravitational coupling constant $\kappa_{11}$ is related to the eleven-dimensional Newton constant $G_N^{(11)}$ and the eleven-dimensional Planck length $l_P^{(11)}$ via

$$2\kappa_{11}^2 = 16\pi G_N^{(11)} = \frac{1}{2\pi}(2\pi l_P^{(11)})^9\,. \tag{1.29}$$

Eleven-dimensional Supergravity is related to type IIA and IIB Supergravity by dimensional reduction on a circle direction. Of relevance for this Thesis is also the reduction to five-dimensional Supergravity obtained, in a similar way as the Kaluza-Klein reduction on a circle, by compactification on a six-dimensional torus. We will give its action and field content when discussing the five-dimensional three-charge solution in Section 1.4.

### 1.2.3 Dimensional reduction and dualities

#### Kaluza-Klein reduction

To get from Supergravity in eleven dimensions down to ten dimensions we dimensionally reduce over the M-Theory circle with radius $R_\# = g_s l_s$. The eleven-dimensional metric can be written in terms of a ten-dimensional metric $g$, a gauge field $C_1$ and a scalar $\Phi$ as

$$G_{MN}dx^M dx^N = e^{-2\Phi/3}g_{\mu\nu}dx^\mu dx^\nu + e^{4\Phi/3}(dx^\# + C_1)^2\,, \tag{1.30}$$

with $M, N = 0, ..., 10$ and $\mu, \nu = 0, ..., 9$ and the 1-form $C_1$ has no legs along $x^\# = x^{10}$. The eleven-dimensional gauge field can be decomposed into a rank-3 gauge field $C_3$ and a rank-two gauge field $B_2$ as

$$A_3 = C_3 + B_2 \wedge dx^\#\,. \tag{1.31}$$

This defines the dilaton $\Phi$, the ten-dimensional metric $g_{\mu\nu}$, the NS-NS field $B_2$ and the type IIA R-R fields $C_1$ and $C_3$. The eleven-dimensional Newton constant is related to the ten-dimensional one by

$$G_N^{(11)} = 2\pi R_\# G_N^{(10)}\,, \qquad \text{with} \qquad R_\# = g_s l_s \quad \text{and} \quad l_s = g_s^3 l_P^{(11)}\,. \tag{1.32}$$

Upon reduction, the M-Theory objects turn into type IIA objects:

$$\begin{array}{cccccccccc} & \text{KKm} & & & \text{M5} & & & \text{M2} & & \text{P} \\ \swarrow & \downarrow & & \swarrow & \downarrow & & \swarrow & \downarrow & \swarrow & \downarrow \\ \text{D6} & \text{KKm} & & \text{D4} & \text{NS5} & & \text{F1} & \text{D2} & \text{D0} & \text{P} \end{array} \quad , \tag{1.33}$$

where the arrows denote whether the M-Theory objects point in the M-Theory direction $x^{\#}$ upon which we reduce ($\swarrow$) or not ($\downarrow$). If there is an isometry along a compact direction, type IIB Supergravity can be obtained from type IIA Supergravity by a duality transformation, called *T-duality*, which maps the type IIA objects into the type IIB objects.

### T-duality

T-duality is a duality in String Theory that leaves the coupling constant invariant up to a radius-dependent rescaling and holds at each order of string perturbation theory. In particular, the spectrum of type IIA with a circle of radius $R$ is equivalent to the spectrum of type IIB with circle of radius $R' = \alpha'/R$ and the dimensionless radii and coupling constants are related as

$$\frac{R'}{l'_s} = \frac{l_s}{R}, \qquad \frac{g'_s}{\sqrt{R'/l'_s}} = \frac{g_s}{\sqrt{R/l_s}}, \quad \text{and} \quad l'_s = l_s = \sqrt{\alpha'}\,. \tag{1.34}$$

The bosonic fields of type IIA Supergravity can be transformed into the fields of type IIB Supergravity (and *vice versa*) by applying Buscher's rules [88] and generalizations thereof [89]. To T-dualize along the isometry direction $y$ is convenient to rewrite the system we want to T-dualize in the following way:

$$\begin{aligned} ds^2 &= g_{yy}(dy + A_\mu dx^\mu)^2 + \hat{g}_{\mu\nu} dx^\mu dx^\nu\,, \\ B_2 &= B_{\mu y} dx^\mu \wedge (dy + A_\mu dx^\mu) + \hat{B}_2\,, \\ C_p &= C_{p-1} \wedge (dy + A_\mu dx^\mu) + \hat{C}_p\,, \end{aligned} \tag{1.35}$$

where hatted quantities do not have any legs along $y$. The T-duality transformed fields are then [5]

$$\begin{aligned} ds'^2 &= g_{yy}^{-1}(dy + B_{\mu y} dx^\mu)^2 + \hat{g}_{\mu\nu} dx^\mu dx^\nu\,, \\ e^{2\phi'} &= g_{yy}^{-1} e^{2\phi}\,, \\ B'_2 &= A_\mu dx^\mu \wedge dy + \hat{B}_2\,, \\ C'_p &= \hat{C}_{p-1} \wedge (dy + B_{\mu y} dx^\mu) + C_p\,. \end{aligned} \tag{1.36}$$

Alternatively to the R-R potentials we can work with the field strengths (which is convenient if $dA_\mu = dB_{\mu y} = 0$) for which the transformations are:

$$F_{p+1} = F_p \wedge (dy + A_\mu dx^\mu) + (-1)^{p-1} C_{p-1}\Big|_y \wedge dA_\mu dx^\mu + \hat{F}_{p+1}\,, \tag{1.37}$$

$$F'_{p+1} = \hat{F}_p \wedge (dy + B_{\mu y} dx^\mu) + (-1)^{p-1} \hat{C}_{p-1} \wedge dB_{\mu y} dx^\mu + F_{p+1}\,. \tag{1.38}$$

[5] We adopt the conventions of [90].

These transformations have a clear physical interpretation. The shift of the dilaton corresponds to a rescaling of the string coupling (1.34) so that the low-energy effective action stays invariant under $R \to R' = \alpha'/R$. The exchange of the NS-NS fields $g_{\mu y}$ and $B_{\mu y}$ under T-duality corresponds to the transformation of the string winding number (F1) with momentum (P) along the string in the T-duality direction. From the transformation of the R-R fields $C_p$ we see that the dimension of D$p$-branes changes under T-duality depending on whether the transformation is performed on a circle parallel ($||$) or perpendicular ($\perp$) to the brane worldvolume. T-duality along the isometry direction of the Kaluza-Klein monopole transforms it into an NS5 brane. In summary:

$$\text{F1} \longleftrightarrow \text{P}\,, \qquad \text{D}p \begin{array}{c} \xrightarrow{||} \\ \xrightarrow{\perp} \end{array} \begin{array}{c} \text{D}(p-1) \\ \text{D}(p+1) \end{array}, \qquad \text{KKm} \longleftrightarrow \text{NS5}\,. \tag{1.39}$$

**S-duality**

S-duality is a duality under which the coupling of the theory changes non-trivially. The weak-strong duality maps states and vacua with coupling constant $g$ in one theory to states and vacua with coupling constant $1/g$ in the dual theory. An example is the $SL(2,\mathbb{Z})$ selfduality of IIB String Theory. In type IIB Supergravity, which possesses a $SL(2,\mathbb{R})$ symmetry (broken to $SL(2,\mathbb{Z})$ in the full String Theory), S-duality flips the sign of the dilaton $\Phi$ and exchanges $B_2$ and $C_2$ while leaving $\tilde{F}_5$ unaltered. Since the dilaton is related to the string coupling the change in sign translates to

$$\tilde{g}_s \;=\; \frac{1}{g_s}\,, \tag{1.40}$$

which exhibits the weak-strong coupling relation. The transformations of these fields imply for the objects of type IIB Supergravity:

$$\text{F1} \longleftrightarrow \text{D1}\,, \qquad \text{NS5} \longleftrightarrow \text{D5}\,, \qquad \text{D3} \longleftrightarrow \text{D3}\,, \tag{1.41}$$

while KKm and P are unaffected. Note that due to the selfduality of the 5-form potential the D3-brane is a dyon.

With this discussion of the general Supergravity framework in ten and eleven dimensions and their duality relations we are now ready to study black holes in String Theory/Supergravity.

## 1.3 Black holes in String Theory

The purpose of this Section is to introduce the necessary ingredients in a step-by-step recipe to embed black holes in String Theory and M-Theory. We will follow [86, 87, 91, 92, 46].

Charged black holes play a special role here because saturation of the extremality bound often coincides with saturation of the Bogomol'nyi–Prasad–Sommerfield (BPS) bound. When this bound is saturated, the system has minimal energy for a given set of parameters. The BPS bound became a very important characterizing property in supersymmetric theories where it relates the

mass $M$ to the central charge $\mathcal{Z}$ of the extended supersymmetry algebra as $M \geq |\mathcal{Z}|$. [6] When this bound is saturated the extremal solution has unbroken supersymmetry. This is the case for the extremal Reissner-Nordström black hole so that its mass becomes equal to its charge. [7] In the following we will focus on the electrically charged extremal Reissner-Nordström black hole and its embedding and generalization in String Theory/Supergravity. [8] Attempts to understand the (extremal) Kerr black hole from a string theoretic perspective have led to the conjectured Kerr/CFT correspondence which is similar in spirit to the AdS/CFT correspondence for (extremal) charged black holes but is far less understood. [93] Recently there has been some progress on embedding the extremal Kerr and Kerr-Newman black hole in String Theory via Supergravity transformations of known extremal non-supersymmetric charged black hole solutions. [94] The Schwarzschild black hole does not possess an extremal limit which makes it extremely difficult to study its microscopic properties.

### 1.3.1 Extremal Reissner-Nordström

The extremal Reissner-Nordström metric

$$ds^2 = -\Big(1 - \frac{r_0}{\tilde{r}}\Big)^2 dt^2 + \Big(1 - \frac{r_0}{\tilde{r}}\Big)^{-2} d\tilde{r}^2 + \tilde{r}^2 d\Omega_2^2 \,, \tag{1.42}$$

can be brought into a convenient form by the coordinate transformation $r = \tilde{r} - r_0$:

$$ds^2 = -H^{-2} dt^2 + H^2 \Big(dr^2 + r^2 d\Omega_2^2\Big) \,, \tag{1.43}$$

with $H = 1 + \frac{r_0}{r}$. In these isotropic coordinates the spatial part of the metric is conformally flat. The warp factor is a harmonic function whose pole is the asymptotic electric charge $r_0 = Q$ and the horizon is located at $r = 0$. The ADM mass of the extremal Reissner-Nordström black hole as read off from the coefficient of $1/r$ in $-g_{tt} = 1 - \frac{2M}{r} + \mathcal{O}(r^{-2})$ is $M = Q$ which saturates the BPS bound $M \geq Q$.

The electric potential one-form is related to the warp factor as

$$A = -H^{-1} dt \,. \tag{1.44}$$

This relation is an important feature of supersymmetric solutions which guarantees that an electrically charged point particle will not feel a force: the gravitational attraction (sourced by the metric) is balanced by the electric repulsion (sourced by the electric potential) independent of the location of the probe:

$$V = \sqrt{-g_{tt}} + A_t = 0 \,. \tag{1.45}$$

In Section 1.5 we will encounter the generalization of this probe action to extended objects; the spirit of the 'no-force' Ansatz (1.44) which we will then call 'floating brane' Ansatz remains the same.

[6] We will use the epithet 'BPS' for solutions that preserve part of the supersymmetry.

[7] The extremal Reissner-Nordström black hole with $M = \sqrt{q_e^2 + q_m^2}$ can be seen as a BPS state in $\mathcal{N} = 2$ Supergravity where the central charge $\mathcal{Z} = q_e - i q_m$ so that the BPS bound is saturated $M = |\mathcal{Z}|$. For $q_m = 0$ the BPS bound becomes $M \geq Q$ which we know from Subsection 1.1.1 to be saturated for the extremal case.

[8] Note that one can easily reinstate magnetic charge by performing electric-magnetic duality transformations on the electrically charged solution.

**Spacetime dimension: from four to five.** In Section 1.4 we will see that the microscopic understanding of black holes at strong coupling and the construction of their bulk microstates requires the existence of extra dimension. In particular, we need at least five spacetime dimensions for the mechanism that can prevent the collapse of matter to a black hole to work. We will therefore focus on studying five-dimensional black holes which are, however, easily related to four-dimensional black holes. It will be convenient to work in conventions where the five-dimensional Newton constant is $G_N^{(5)} = \frac{\pi}{4}$.

We can straightforwardly generalize the Reissner-Nordström metric (1.42) to five spacetime dimensions:

$$ds^2 = -\Big(1 - \frac{\rho_0^2}{\tilde{\rho}^2}\Big)^2 dt^2 + \Big(1 - \frac{\rho_0^2}{\tilde{\rho}^2}\Big)^{-2} d\tilde{\rho}^2 + \tilde{\rho}^2 d\Omega_3^2\,, \tag{1.46}$$

where $d\Omega_3^2$ is the metric on the $S^3$. Defining $\rho^2 = \tilde{\rho}^2 - \rho_0^2$ we obtain a form analogous to (1.43):

$$ds^2 = -Z^{-2} dt^2 + Z\Big(d\rho^2 + \rho^2 d\Omega_3^2\Big)\,, \tag{1.47}$$

with the harmonic function $Z = 1 + \frac{\rho_0^2}{\rho^2}$ and $\rho_0^2 = Q$. The five-dimensional Reissner-Nordström black hole can easily be embedded in String Theory/M-Theory by wrapping branes on various cycles of an internal (five/six dimensional) manifold. For now we focus on the generalization of the metric and gauge potential and postpone the detailed brane interpretation until Section 1.4.

**Electric charge: from one to three.** A generic five-dimensional black hole with a macroscopic horizon has three types of electric charges $Q_I$ coming from three branes wrapping different cycles in the internal compactification manifold. The five-dimensional solution is given by the metric

$$ds^2 = -(Z_1 Z_2 Z_3)^{-2/3} dt^2 + (Z_1 Z_2 Z_3)^{1/3}\Big(d\rho^2 + \rho^2 d\Omega_3^2\Big)\,, \tag{1.48}$$

and the vector potentials

$$A^{(I)} = -Z_I^{-1} dt\,, \tag{1.49}$$

with the harmonic functions

$$Z_I = 1 + \frac{Q_I}{\rho^2}\,, \qquad I = 1, 2, 3\,, \tag{1.50}$$

solving the four-dimensional Laplace equation. Each warp factor is sourced by one of the three branes. This solution describes a spherically symmetric black hole with three electric charges in five dimensions. If all the charges are equal, $Q_1 = Q_2 = Q_3 = \rho_0^2$, the metric (1.48) reduces to (1.47). The ADM mass of the five-dimensional three-charge black hole can be read off from the coefficient of $\rho^{-2}$ in $-g_{tt} = 1 - \frac{2}{3}\frac{M}{\rho^2} + \mathcal{O}(\rho^{-4})$ (in five dimensions there is an extra factor of $1/3$ as compared to (1.3)). For the metric (1.48) we have

$$-g_{tt} = (Z_1 Z_2 Z_3)^{-2/3} = 1 - \frac{2}{3}\sum_{I=1}^{3}\frac{Q_I}{\rho^2} + \mathcal{O}(\rho^{-4})\,, \tag{1.51}$$

with the ADM mass

$$M = Q_1 + Q_2 + Q_3\,. \tag{1.52}$$

saturating the BPS bound $M \geq Q_1 + Q_2 + Q_3$.

**Thermodynamics: cold but entropic.** In Subsection 1.1.2 we found the four-dimensional extremal Reissner-Nordström black hole to have zero temperature but finite entropy. For its five-dimensional supersymmetric cousin we again have $T_H = 0$. The Bekenstein-Hawking entropy is computed from the area of the $S^3$ at the horizon, $A_H = 2\pi^2\sqrt{Q_1Q_2Q_3}$, to be

$$S_{BH} = \frac{A_H}{4G_N^{(5)}} = 2\pi\sqrt{Q_1Q_2Q_3}\,, \tag{1.53}$$

where we used $G_N^{(5)} = \frac{\pi}{4}$. In these conventions the brane charges $Q_I$ correspond to the numbers $N_I$ of branes. In general, the $Q_I$ are charge *densities* and are related to the numbers of branes $N_I$ by a dimensionful factor. The entropy, however, is always given by the dimensionless quantity

$$S_{BH} = 2\pi\sqrt{N_1N_2N_3}\,. \tag{1.54}$$

**Statistics via AdS/CFT: weakly-coupled microscopics.** Black holes in five dimensions with three kinds of electric charges have an interpretation in terms of bound states of strings and branes at weak effective string coupling. The above metric (1.48) can be transformed via a set of T-dualities to a frame where it corresponds to the D1-D5-P bound state in the toroidally compactified type IIB String Theory. The configuration has $N_1$ D1 branes and $N_5$ D5 branes wrapping a circle that carries $N_P$ units of Kaluza-Klein momentum $P$ and the D5 branes additionally wrap the remaining internal torus directions. The near-horizon limit of the D1-D5-P metric is $AdS_3 \times S^3$. This $AdS_3$ spacetime is conjectured to be dual to a two-dimensional conformal field theory (without gravity) formed by the common circle of the D1 and D5 brane and the time direction. The different ways the momentum charge P can be partitioned on this *effective* D1-D5 string gives rise to the number of microscopic configurations of the D1-D5-P system. The entropy of this CFT is given by Cardy's formula [6]

$$S \sim \sqrt{cL_0}\,, \tag{1.55}$$

where $L_0$ is the momentum along the circle and $c$ is the central charge of the CFT. For the D1-D5 system we have $c = N_1N_5$ and, after taking care of all numerical and dimensionful factors, the entropy is given by

$$S_{CFT} = 2\pi\sqrt{N_1N_5N_P}\,. \tag{1.56}$$

This is exactly the Bekenstein-Hawking entropy (1.54)! For this miraculous matching between the entropy of a black hole and the number of configurations of an effective string where gravity is turned off to work, it is crucial that the central charge (and thus the Cardy formula) is independent of the coupling. This non-renormalization property is guaranteed by supersymmetry.

### 1.3.2 General extremal charged black holes in five dimensions

We now proceed to build more complicated supersymmetric black holes in Supergravity that have multiple centers, angular momentum, magnetic flux and a non-trivial four-dimensional base space. These additional ingredients play an important role in the construction of black hole microstate geometries.

### Multiple centers

Since the four-dimensional Laplace equation for the $Z_I$ is linear we can generalize the single-center black hole configuration to multi-center black hole configurations with electric sources at multiple locations $a_i$

$$Z_I = 1 + \sum_{i=1}^{N} \frac{Q_{I,i}}{\rho_i^2}\,, \quad \text{where} \quad \rho_i = |\vec{\rho} - \vec{a_i}|\,, \tag{1.57}$$

with total charges $Q_I = \sum_{i=1}^{N} Q_{I,i}$.

### Adding angular momentum

In five dimensions we can also add angular momentum while preserving supersymmetry [9] by replacing $dt$ in the metric and the gauge field with $dt + k$ where $k = k_i dx^i$ is a one-form in the four-dimensional base space:

$$ds^2 = -(Z_1 Z_2 Z_3)^{-2/3}(dt + k)^2 + (Z_1 Z_2 Z_3)^{1/3} ds_4^2\,, \tag{1.58}$$

$$A^{(I)} = -Z_I^{-1}(dt + k)\,. \tag{1.59}$$

This leads to a non-vanishing $g_{ti}$ cross term in the metric implying that the spacetime itself carries angular momentum. We obtain the five-dimensional spinning three-charge black hole, also known as BMPV black hole [95]. The black hole solution, being still time-independent, is now stationary rather than static ($g_{ti} = 0$). Writing the angular part of $\mathbb{R}^4$ as

$$d\Omega_3^2 = d\vartheta^2 + \sin^2\vartheta\, d\varphi_1^2 + \cos^2\vartheta\, d\varphi_2^2\,, \tag{1.60}$$

the asymptotic angular momentum $J$ can be read off from the $\rho^{-2}$ coefficient in the asymptotic expansion of the angular momentum one-form:

$$k = \frac{J}{\rho^2}\Big(\sin^2\vartheta\, d\varphi_1 - \cos^2\vartheta\, d\varphi_2\Big) + \cdots\,. \tag{1.61}$$

Actually there are two angular momenta in five dimensions but supersymmetry requires them to be equal.[10] This can be written as a selfduality condition on $k$:

$$(1 + \star_4) dk = 0\,, \tag{1.62}$$

where $\star_4$ is the Hodge star defined on $\mathbb{R}^4$.

Turning on asymptotic angular momentum modifies the entropy formula (1.54) to

$$S_{BH} = 2\pi\sqrt{Q_1 Q_2 Q_3 - J^2}\,. \tag{1.63}$$

Angular momentum therefore decreases the entropy of a black hole. For $J^2 > Q_1 Q_2 Q_3$ the solution has closed time-like curves and is thus unphysical.

[9] In contrast, in four dimensions rotating black holes such as the Kerr black hole are non-supersymmetric.

[10] In Chapter 3 we will study non-extremal black holes for which supersymmetry is broken and which consequently have two different angular momenta in five dimensions (see Appendix C.1). For now, we restrict to supersymmetric black holes.

### Adding magnetic flux

Adding angular momentum to an electrically charged black hole sources magnetic components of the field strength in a similar way as a spinning electron induces a magnetic field. If we want explicit magnetic flux we have to add a (locally) closed but not exact form $\Theta^{(I)} = dB^{(I)}$ to the field strength $F^{(I)} = dA^{(I)}$:

$$F^{(I)} = d\Big( - \frac{dt + k}{Z_I} \Big) + \Theta^{(I)} \,, \tag{1.64}$$

where $\Theta^{(I)} = \Theta^{(I)}_{ij} dx^i \wedge dx^j$. Supersymmetry requires the magnetic 2-form field field strength to be selfdual:

$$\Theta^{(I)} = \star_4 \Theta^{(I)} \,. \tag{1.65}$$

In the absence of magnetic flux the warp factors $Z_I$ satisfy a four-dimensional Laplace equation with a delta-function source at the location of a charge $Q_I$. This corresponds to an electric field with action

$$\int \star F \wedge F \,, \tag{1.66}$$

satisfying

$$d \star F = 0 \,, \qquad dF = 0 \,. \tag{1.67}$$

As was discussed in Section 1.2, in addition to the Einstein-Maxwell term (1.66) the (five- and eleven-dimensional) Supergravity action contains also Chern-Simons terms of the form

$$\int A \wedge F \wedge F \,, \tag{1.68}$$

where the magnetic part of the field strength couples to the gauge potential like a source. Hence, electric charge can arise from magnetic flux through the equation

$$d \star F = F \wedge F \,. \tag{1.69}$$

In such a theory the warp factors can be sourced not only by delta-functions but also by magnetic-magnetic interactions [11]

$$\nabla^2 Z_I = \frac{|\epsilon_{IJK}|}{2} \star_4 \Big( \Theta^{(J)} \wedge \Theta^{(K)} \Big) \,. \tag{1.70}$$

Asymptotic electric charge can thus either arise from explicit electric sources or from charge dissolved in magnetic flux. It is then possible to have asymptotically charged objects without explicit sources for the charges! As we will see in Section 1.4 this is the key ingredient for the construction of smooth Supergravity solutions with the same asymptotic electric charges as a black hole but which have no singularities and no horizon.

In the presence of magnetic flux also the equation for the angular momentum one-form gets modified:

$$(1 + \star_4)\, dk = Z_I \Theta^{(I)} \,. \tag{1.71}$$

[11] It should be understood that the equations for the warp factors $Z_I$ also contain delta-function sources with charges $Q_I$ which we omitted here.

This is analogous to the Poynting vector of electromagnetism

$$\vec{J} = \vec{E} \times \vec{B}\,, \tag{1.72}$$

where angular momentum arises from crossed electric and magnetic fields.

### Replacing the flat base by Taub-NUT

So far we considered flat base metrics, but supersymmetry only requires the base to be hyper-Kähler. An interesting class are the Taub-NUT (TN) or Gibbons-Hawking (GH) metrics which take the form of a U(1) fiber over a flat three-dimensional space

$$ds_4^2 = V^{-1}(d\psi + A)^2 + V ds_{\mathbb{R}^3}^2\,. \tag{1.73}$$

The function $V$ is harmonic on the flat $\mathbb{R}^3$ and the connection one-form $A$ on the base is determined by

$$\vec{\nabla} \times A = \vec{\nabla} V\,, \tag{1.74}$$

where $\nabla$ denotes the flat derivative in $\mathbb{R}^3$. For single-center Taub-NUT, the harmonic function $V$ is sourced by geometric charge $v$ at the origin:

$$V = v_0 + \frac{v}{r}\,, \tag{1.75}$$

where $r$ is the radial distance in $\mathbb{R}^3$. The constant $v_0$ is a modulus that determines the asymptotic behavior of the Gibbons-Hawking metric. For $v_0 = 1$ we get get asymptotically Taub-NUT space which is $\mathbb{R}^3 \times S^1$ while for $V = \frac{1}{r}$ the four-dimensional metric (1.73) reduces to the trivial flat metric on $\mathbb{R}^4$.

In general, there can be multiple geometric sources so that $V = v_0 + \sum_i \frac{v_i}{r_i}$. Multi-center Gibbons-Hawking metrics are yet another crucial ingredient in the construction of black hole microstate geometries and we will give a detailed discussion in Section 1.4. Another interesting feature of the Taub-NUT base space is that we can relate five-dimensional to four-dimensional solutions.

### The 4d/5d connection

The embedding of five-dimensional solutions in Taub-NUT allows to interpolate between effectively four-dimensional and five-dimensional solutions by varying the size of the Taub-NUT circle. In the standard spherical coordinates $(r, \theta, \phi)$ of $\mathbb{R}^3$ the Gibbons-Hawking metric is

$$ds_4^2 = V^{-1}(r)(d\psi + A)^2 + V(r)(dr^2 + r^2 d\Omega_2^2)\,, \tag{1.76}$$

with $d\Omega_2^2 = d\theta^2 + \sin^2\theta d\phi^2$. The harmonic function $V$ is as in (1.75) and the one-form on the base is determined by (1.74) to be $A = v\cos\theta d\phi$. The radius of the Taub-NUT circle is given by $R(r) = V^{-1/2}(r)$. At $r = 0$ there appear to be singularities in the GH metric. To reveal that the space is actually smooth at the origin we change to coordinates centered at $r = 0$ with radial coordinate $\rho^2 = 4r$. Near the origin $\rho = 0$, the GH metric then becomes

$$ds_4^2 \overset{\rho \to 0}{\longrightarrow} d\rho^2 + \frac{\rho^2}{4}\Big[d\Omega_2^2 + \Big(\cos\theta d\phi + \frac{d\psi}{v}\Big)^2\Big]\,, \tag{1.77}$$

where we redefined $\rho \to \sqrt{v}\rho$. For $v \neq 1$ there is a deficit angle with identification $\psi \to \psi + \frac{4\pi}{v}$ and we must have $v \in \mathbb{Z}$. If $|v| \neq 1$ the metric on $S^3/\mathbb{Z}_{|v|}$ has an orbifold singularity which is very well under control in String Theory. If $|v| = 1$ we can write

$$ds_4^2 \overset{\rho \to 0}{\longrightarrow} d\rho^2 + \rho^2 d\Omega_3^2 \,, \tag{1.78}$$

where $d\Omega_3^2$ is the standard metric on $S^3$. The space near the origin looks locally like $\mathbb{R}^4$ and the Taub-NUT circle smoothly shrinks to zero size .

In the limit $r \to \infty$ the GH metric (1.76) becomes $\mathbb{R}^3 \times S^1$:

$$ds_4^2 \overset{r \to \infty}{\longrightarrow} (dr^2 + r^2 d\Omega_2^2) + \frac{1}{v_0}(d\psi + \cos\theta d\phi)^2 \,, \tag{1.79}$$

where we have redefined $r \to \sqrt{v_0} r$. At spatial infinity the radius of the Taub-NUT fiber is $R(\infty) = 1/\sqrt{v_0}$. The Taub-NUT metric thus interpolates between $\mathbb{R}^4$ near the origin and $\mathbb{R}^3 \times S^1$ at infinity, as depicted in Figure 1.1. By varying the size of the Taub-NUT circle one can thus

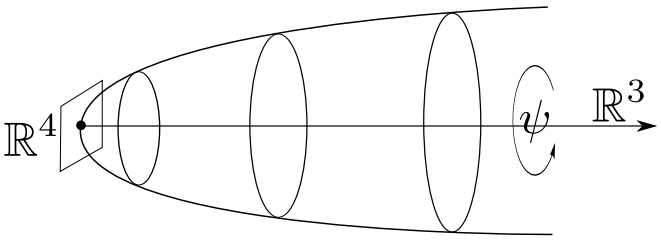


Figure 1.1: Taub-NUT space.

interpolate between effectively four-dimensional and five-dimensional configurations. For small $v_0$ the Taub-NUT circle is very large and the solution behaves five-dimensionally, while for large $v_0$ the Taub-NUT circle is very small and the solution is effectively compactified. Varying the modulus of the solution thus results in a '4d/5d connection' [96, 97, 98, 99, 100, 101].

**In a nutshell.**

To summarize this Subsection, we have replaced the four-dimensional flat base by the (multi-center) Gibbons-Hawking metric and derived a system of equations that describe five-dimensional Supergravity solutions with three electric charges, three magnetic fluxes and angular momentum:

$$\Theta^{(I)} = *_4 \Theta^{(I)} \,, \tag{1.80}$$

$$\nabla^2 Z_I = \frac{|\epsilon_{IJK}|}{2} *_4 \left(\Theta^{(J)} \wedge \Theta^{(K)}\right) \,, \tag{1.81}$$

$$(1 + *_4)\, dk = Z_I \Theta_I \,, \tag{1.82}$$

where the Hodge star $\star_4$ is now with respect to the Gibbons-Hawking metric. In the next Section we review the solutions to these equations in the framework of eleven-dimensional and five-dimensional Supergravity and discuss their brane interpretation.

## 1.4 Three-charge solutions

We present Supergravity solutions that have three electric charges, three magnetic dipole charges and angular momentum describing black holes, black rings and their microstate geometries. For reviews on the work on three-charge solutions see [46, 47, 48]. In [102] it has been revealed that the system of differential equations describing these configurations is governed by a linear structure if solved in a particular order. Large classes of BPS Supergravity solutions have then been constructed [26, 27, 32, 31, 35, 46, 41, 51]. A special class of non-supersymmetric solutions where supersymmetry is broken in a very mild manner has been found from the same system of equations. The brane configurations underlying these extremal 'almost-BPS' solutions [36, 39, 37] preserve four supersymmetries but these are broken by the holonomy of the background. The scale of the supersymmetry breaking is set by the curvature scale of the metric on the four-dimensional base. Requiring the base to be merely Ricci-flat led to the construction of more general non-supersymmetric solutions [38, 65, 40] which reduce to the BPS and almost-BPS class in certain limits. These families of non-supersymmetric solutions include the known extremal, non-BPS black holes and black rings and generalizations of these solutions by including more charges and completely new non-BPS, multi-centered black ring solutions. For the purpose of these Thesis we will focus on BPS solutions and a particular example of almost-BPS solutions.

This Section is organized as follows. In Subsection 1.4.1 we present the M-Theory equations and Ansatz in a form that captures BPS as well as almost-BPS solutions, and discuss their brane interpretation. In Subsection 1.4.2 we derive the general multi-center solution to the BPS equations and in Subsection 1.4.3 we discuss the difficulty of obtaining a general solution to the almost-BPS equations. Upon compactification on an internal six-dimensional torus the eleven-dimensional BPS solutions correspond to supersymmetric and non-supersymmetric solutions of five dimensional $U(1)^3$ ungauged Supergravity summarized in Subsection 1.4.4. When compactified to four dimensions they correspond to solutions of the STU model. The eleven-dimensional (or five-dimensional) BPS solutions encompass, in particular, *smooth* solutions which are completely regular everywhere and have no horizons. We will discuss these solutions in Subsection 1.4.5.

### 1.4.1 M-Theory frame

We begin by reviewing three-charge solutions in the eleven-dimensional M-Theory duality frame which treats the three asymptotic charges of the solutions on equal footing: they are M2 branes wrapped on three orthogonal $T^2$'s inside an internal $T^6$ [102, 103]. [12] The solution also has local magnetic dipole charges corresponding to M5 branes that wrap two of the three orthogonal $T^2$'s and an arbitrary closed curve $\zeta^\mu$ in the four-dimensional base transverse to the $T^6$. This is illustrated in Table 1.4. Additionally the solution admits Kaluza-Klein monopoles and possesses angular momentum.

[12] For more generic solutions, the six-torus should be replaced by a compact Calabi-Yau three-fold.

| | 0 | 1 | 2 | 3 | 4 | 5 | 6 | 7 | 8 | 9 | 10 |
|---|---|---|---|---|---|---|---|---|---|---|---|
| M2 | $\updownarrow$ | • | • | • | • | $\updownarrow$ | $\updownarrow$ | $\leftrightarrow$ | $\leftrightarrow$ | $\leftrightarrow$ | $\leftrightarrow$ |
| M2 | $\updownarrow$ | • | • | • | • | $\leftrightarrow$ | $\leftrightarrow$ | $\updownarrow$ | $\updownarrow$ | $\leftrightarrow$ | $\leftrightarrow$ |
| M2 | $\updownarrow$ | • | • | • | • | $\leftrightarrow$ | $\leftrightarrow$ | $\leftrightarrow$ | $\leftrightarrow$ | $\updownarrow$ | $\updownarrow$ |
| M5 | $\updownarrow$ | | | $\zeta^\mu$ | | $\updownarrow$ | $\updownarrow$ | $\updownarrow$ | $\updownarrow$ | $\leftrightarrow$ | $\leftrightarrow$ |
| M5 | $\updownarrow$ | | | $\zeta^\mu$ | | $\updownarrow$ | $\updownarrow$ | $\leftrightarrow$ | $\leftrightarrow$ | $\updownarrow$ | $\updownarrow$ |
| M5 | $\updownarrow$ | | | $\zeta^\mu$ | | $\leftrightarrow$ | $\leftrightarrow$ | $\updownarrow$ | $\updownarrow$ | $\updownarrow$ | $\updownarrow$ |

Table 1.4: Three-charge solution in the M2-M2-M2 duality frame. The vertical arrows ($\updownarrow$) denote the direction along which the branes are extended, the horizontal arrows ($\leftrightarrow$) represent the smearing directions, the curve wrapped by an M5 brane defines a profile $\zeta^\mu$ in $\mathbb{R}^4$ and the dots (•) indicate that an M2 brane is smeared along the profile and localized in the other three directions.

### BPS and almost-BPS Ansatz

The Ansatz for the metric is:

$$ds_{11}^2 = -Z^{-2}(dt+k)^2 + Z\, ds_4^2 + Z\sum_{I=1}^{3}\frac{ds_I^2}{Z_I}\,, \qquad Z = (Z_1 Z_2 Z_3)^{1/3}\,, \tag{1.83}$$

where $ds_4^2$ is the metric on the four-dimensional base and $ds_I^2$ are unit metrics on the $T_I^2$. The warp factors $Z_I$ and the angular momentum one-form $k$ are functions of the four-dimensional base. The Ansatz for the Maxwell three-form potential is:

$$A_3 = \sum_{I=1}^{3} A^{(I)} \wedge \omega_I\,, \qquad F_4 = dA_3 \tag{1.84}$$

where $\omega_I$ are unit volume forms on the $T_I^2$. The gauge potentials $A^{(I)}$ are sourced by M2 branes electrically and by M5 branes magnetically. To have families of 'floating M2 branes'[38] – M2 branes that do not feel a force – the gauge potentials $A^{(I)}$ are related to the warp factors $Z_I$ as

$$A^{(I)} \;=\; -\,\varepsilon\, Z_I^{-1}\,(dt+k) + B^{(I)} \quad \text{with} \quad \varepsilon \;= \pm 1\,. \tag{1.85}$$

The asymptotic electric charges of the M2 branes are thus encoded in the warp factors $Z_I$. The $B^{(I)}$ are magnetic vector potentials on the four-dimensional base which encode the local magnetic dipole charges of the M5 branes. We define the magnetic two-form field strengths:

$$\Theta^{(I)} \;\equiv\; dB^{(I)}\,. \tag{1.86}$$

### BPS and almost-BPS equations

It was shown in [38] that one obtains solutions to the complete equations of motion of M-Theory if the base is Ricci-flat and solves the linear system of equations (for a fixed choice of $\varepsilon = \pm 1$):

$$\Theta^{(I)} \overset{\text{I.}}{=} \varepsilon *_4 \Theta^{(I)}\,, \tag{1.87}$$

$$\nabla^2 Z_I \overset{\text{II.}}{=} \varepsilon \frac{C_{IJK}}{2} *_4 \left[\Theta^{(J)} \wedge \Theta^{(K)}\right], \tag{1.88}$$

$$(1 \,+\, \varepsilon *_4)\, dk \overset{\text{III.}}{=} \varepsilon\, Z_I \Theta_I\,, \tag{1.89}$$

where $C_{IJK} = |\epsilon_{IJK}|$, $\nabla^2$ is the four-dimensional Laplacian and $*_4$ is the Hodge star on the four-dimensional base. With fixed $\varepsilon = \pm 1$ the first equation fixes the duality structure of the $\Theta^{(I)}$. The magnetic-magnetic interactions $\Theta^{(J)} \wedge \Theta^{(K)}$ then act as sources for the electric potentials $Z_I$ in the second equation. The electric-magnetic interactions $Z_I \Theta^{(I)}$ then source angular momentum in the third equation which can thus be seen as a generalization of the Poynting vector of electromagnetism. The essential feature of this system of equations is that is it *linear* if the equations are solved in the above order: the non-linear terms can be seen as sources in linear equations.

### Duality structure of base metric and magnetic fields

Another remarkable feature of the system of equations (1.87)-(1.89) is that it admits supersymmetric as well as non-supersymmetric solutions depending on the (mis)matching of the duality structure of the magnetic two-form field strengths with the Riemann tensor of the base. If the base is hyper-Kähler one obtains a BPS solution [104, 103, 102] by requiring that the duality structure of the $\Theta^{(I)}$ matches that of the Riemann tensor of the base. That is, one obtains BPS solutions by taking $\varepsilon = +1$ and choosing the base metric to be selfdual hyper-Kähler, or by taking $\varepsilon = -1$ and choosing the base metric to be anti-selfdual hyper-Kähler. In either case the holonomy of the base metric respects the supersymmetries of the family of M2 branes and the solution is $\frac{1}{8}$ BPS. Almost-BPS solutions [36, 37, 39] are also obtained by using hyper-Kähler base metrics but supersymmetry is broken by mismatching the duality structure of the $\Theta^{(I)}$ and that of the Riemann tensor of the base. The almost-BPS solutions were then generalized to bases that are just Ricci-flat [38] and large families of new solutions have been constructed [38, 40, 65]. This is a very mild form of supersymmetry breaking (hence the name 'almost'-BPS): the underlying brane configurations locally preserve four supersymmetries as in the BPS case but supersymmetry is globally broken by the holonomy of the background. The scale of supersymmetry breaking is thus set by the curvature scale of the metric on the four-dimensional base. For a flat base space supersymmetry is fully restored and one recovers a BPS solution from an almost-BPS solution. See [45] for the relation between BPS and almost-BPS solutions for scaling geometries.

**Base metric.** The base space we will henceforth be working with is multi-center Gibbons-Hawking or Taub-NUT:

$$ds_4^2 \;=\; V^{-1}(d\psi + A)^2 \;+\; V\, ds_3^2\,, \tag{1.90}$$

where $ds_3^2 \equiv \delta_{ab}\, dy^a dy^b$ with $a, b = 1, 2, 3$ is the flat metric in $\mathbb{R}^3$ and $A = \vec{A} \cdot d\vec{y}$ is the Kaluza-Klein $U(1)$ gauge field along the $\psi$ circle. To avoid orbifold singularities at singular points of $V$, the range of the coordinate $\psi$ has to be $0 \leq \psi \leq 4\pi$. The metric (1.90) is hyper-Kähler if

$$\vec{\nabla} V \;=\; \pm\, \vec{\nabla} \times \vec{A}\,, \tag{1.91}$$

where $\nabla$ denotes the flat derivative in $\mathbb{R}^3$. The Taub-NUT potential $V$ is thus harmonic on $\mathbb{R}^3$. Let us introduce the frames on the four-dimensional base

$$\hat{e}^1 = V^{-\frac{1}{2}}(d\psi + A)\,, \qquad \hat{e}^{a+1} = V^{\frac{1}{2}} dy^a\,, a = 1, 2, 3\,, \tag{1.92}$$

and define duality using these frames in canonical order: We use the orientation with $\epsilon_{1234} = +1$ and then choosing the positive sign in (1.91) results in a Riemann tensor that is selfdual while choosing the negative sign makes the Riemann tensor anti-selfdual. Henceforth, we will follow the conventions of [45] and take

$$\varepsilon \;=\; +1\,, \tag{1.93}$$

and then the BPS solutions and almost-BPS solutions correspond to choosing the $+$ or $-$ sign, respectively, in (1.91).

**Magnetic fields.** To define the magnetic field strengths on the background, it is convenient to introduce selfdual and anti-selfdual two-forms using the frames:

$$\Omega_{\pm}^{(a)} \equiv \hat{e}^1 \wedge \hat{e}^{a+1} \pm \frac{1}{2}\epsilon_{abc}\hat{e}^{b+1} \wedge e^{c+1}\,, \quad a = 1, 2, 3\,. \tag{1.94}$$

We can then write the magnetic two-form field strengths as

$$\Theta_{\pm}^{(I)} \equiv -\sum_{a=1}^{3} (\partial_a P_{\pm}^{(I)})\, \Omega_{\pm}^{(a)}\,, \tag{1.95}$$

with some functions $P_{\pm}^{(I)}$ and where the subscript $\pm$ corresponds to the choice in (1.91) and hence to BPS or almost-BPS respectively. We can now start to solve the system of equations (1.87)-(1.89) in the given order.

### 1.4.2 BPS solutions

**I. Solving for $\Theta^{(I)}$.** We start by solving (1.87). The magnetic two-form field strengths $\Theta_{+}^{(I)}$ in (1.95) are harmonic if and only if

$$P_{+}^{(I)} = \frac{K^I}{V}\,, \tag{1.96}$$

and the functions $K^I$ are harmonic in $\mathbb{R}^3$:

$$\nabla^2 K^I = 0\,. \tag{1.97}$$

One can find the magnetic vector potentials, $B_+^{(I)}$ with $\Theta_+ = dB_+$ locally:

$$B_+^{(I)} \;=\; P_+^{(I)}(d\psi + A) \;+\; \xi_+^{(I)}\,, \tag{1.98}$$

where $\xi_+^{(I)} = \vec{\xi}_+^{(I)} \cdot d\vec{y}$ and the functions $\vec{\xi}_+^{(I)}$ satisfy

$$\vec{\nabla} \times \vec{\xi}_+^{(I)} \;=\; -\,\vec{\nabla} K^I\,. \tag{1.99}$$

The $\vec{\xi}_+^{(I)}$ are vector potentials for magnetic monopoles located at the poles of the $K^I$.

Such $B_+^{(I)}$ provide the general solution to (1.87) for the BPS case. The corresponding $\Theta_+^{(I)}$ then give rise to sources on the RHS of (1.88). Additionally one can add homogeneous solutions of the equations which are singular sources in the base coming from $\delta(\vec{y})$ functions not displayed in (1.88). The asymptotic electric charges can thus have contributions from 'bare' M2 branes or from charged dissolved in magnetic flux.

**II. Solving for $Z_I$.** Plugging the above $B_+^{(I)}$ into (1.88) we find that the warp factors $Z_I$ have to satisfy:

$$\nabla^2 Z_I = \frac{C_{IJK}}{2}\nabla^2\Big(\frac{K^J K^K}{V}\Big)\,. \tag{1.100}$$

In the BPS case (1.100) can thus be solved in closed form:

$$Z_I = L_I + \frac{C_{IJK}}{2}\frac{K^J K^K}{V}\,, \tag{1.101}$$

where $L_I$ is a harmonic function on $\mathbb{R}^3$ whose poles encode the 'bare' M2 brane charge while the second term yields electric M2 charge from magnetic-magnetic interactions. Plugging this solution for the warp factor $Z_I$ and the magnetic field strength $\Theta_+^{(I)}$ in (1.89) we can solve for the angular momentum one-form $k$ in the BPS case.

**III. Solving for $k$.** Expanding along the fiber $\psi$ of the GH base as

$$k \;=\; \mu\,(d\psi + A) \;+\; \omega\,, \tag{1.102}$$

where $\omega = \vec{\omega} \cdot d\vec{y}$ is a one-form on $\mathbb{R}^3$, (1.89) for the BPS case is solved by

$$\mu \;=\; \frac{C_{IJK}}{6}\frac{K^I K^J K^K}{V^2} + \frac{1}{2}\frac{K^I L_I}{V} + M\,, \tag{1.103}$$

$$\vec{\nabla} \times \vec{\omega} \;=\; V\vec{\nabla}M - M\vec{\nabla}V + \frac{1}{2}\Big(K^I\vec{\nabla}L_I - L_I\vec{\nabla}K^I\Big)\,. \tag{1.104}$$

### The BPS data

The BPS solutions of (1.87)-(1.89) with a hyper-Kähler base space (1.90) that is Gibbons-Hawking or Taub-NUT is thus completely determined by specifying eight harmonic functions

$V, K^I, L_I, M$ in the GH base [105, 106].[13] The harmonic functions can have sources on an arbitrary number of positions in $\mathbb{R}^3$:

$$V = v_0 + \sum_{i=1}^{N} \frac{v_i}{r_i}\,, \qquad M = m_0 + \sum_{i=1}^{N} \frac{m_i}{r_i}\,, \tag{1.105}$$

$$K_I = k_0^I + \sum_{i=1}^{N} \frac{k_i^I}{r_i}\,, \qquad L_I = \ell_{I,0} + \sum_{i=1}^{N} \frac{\ell_{I,i}}{r_i}\,, \tag{1.106}$$

with the $i$th source sitting at position $\vec{r}_i = \vec{y} - \vec{y}_i$. In M-Theory, the $v_i$ correspond to Kaluza-Klein monopole charges, $k_i^I$ to magnetic M5 brane charges, $\ell_{I,i}$ to electric M2 charges and $m_i$ to angular momentum at centers $\vec{r}_i$. Solutions with a GH base have a natural interpretation upon Kaluza-Klein reduction along the GH fiber $\psi$. For the interpretation of $(v, k^I; l_I, m)$ as IIA brane charges, see Table B.1 of Appendix B.1.

The solutions characterized by the harmonic functions $V, K^I, L_I, M$ are invariant under the shifts:

$$V \;\to\; V\,, \tag{1.107}$$

$$K^I \;\to\; K^I + c^I V\,, \tag{1.108}$$

$$L_I \;\to\; L_I - C_{IJK} c^J K^K - \frac{C_{IJK}}{2} c^J c^K V\,, \tag{1.109}$$

$$M \;\to\; M - \frac{1}{2} c^I L_I + \frac{C_{IJK}}{4} c^I c^J K^K + \frac{C_{IJK}}{12} c^I c^J c^K V\,, \tag{1.110}$$

for arbitrary constants $c^I$. This shifts do not modify the metric and field strengths and should thus be viewed as a gauge transformations.

### 1.4.3 Almost BPS solutions

In the BPS case one can solve the equations in closed form for the general case. This is not possible for the almost-BPS case even though the equations differ from the BPS ones only in a few signs.

Solving (1.87) for the almost-BPS case goes along the same lines as the BPS case. The magnetic two-form field strengths $\Theta_-^{(I)}$ in (1.95) are harmonic if and only if

$$P_-^{(I)} = K^I\,, \tag{1.111}$$

and the functions $K^I$ are harmonic in $\mathbb{R}^3$:

$$\nabla^2 K^I = 0\,. \tag{1.112}$$

[13] More generally, for $U(1)^N$ five-dimensional ungauged Supergravity the solution would be determined by $2N+1$ harmonic functions.

One can find the magnetic vector potentials, $B_-^{(I)}$ with $\Theta_- = dB_-$:

$$B_-^{(I)} \;=\; P_-^{(I)}(d\psi + A) \;+\; \xi_-^{(I)}\,, \tag{1.113}$$

where $\xi_-^{(I)} = \vec{\xi}_-^{(I)} \cdot d\vec{y}$ and the functions $\vec{\xi}_-^{(I)}$ satisfy

$$\vec{\nabla} \times \vec{\xi}_-^{(I)} \;=\; -\left(V\vec{\nabla}K^I - K^I\vec{\nabla}V\right). \tag{1.114}$$

The $\vec{\xi}_-^{(I)}$ are vector potentials for magnetic monopoles located at the poles of the $K^I$.

Such $B_-^{(I)}$ provide the general solution to (1.87) for the almost-BPS case. The corresponding $\Theta_-^{(I)}$ then give rise to sources on the RHS of (1.88). Plugging the above $B_-^{(I)}$ into (1.88) we find that in the almost-BPS case the warp factors $Z_I$ have to satisfy:

$$\nabla^2 Z^I = \frac{C_{IJK}}{2}\, V\, \nabla^2\Big(K^J K^K\Big)\,. \tag{1.115}$$

This equation cannot be solved in closed form and one constructs almost-BPS equations in a case by case manner. In Chapter 5 we will review and study the almost-BPS solution for a set of axisymmetric supertubes in Taub-NUT. For now, we will focus on the BPS solution.

### 1.4.4 Five-dimensional $\mathcal{N} = 2$ Supergravity solutions

The above solutions can also be understood as solutions to $\mathcal{N} = 2$ five-dimensional Supergravity coupled to two vector multiplets. [38] Together with the gravi-photon there are three vector fields and two independent scalars which are conveniently parametrized by the fields $X^I$ with $I = 1, 2, 3$ subject to the constraint $X^1X^2X^3 = 1$. The five-dimensional bosonic action is

$$S = \frac{1}{2\kappa_5^2}\int \sqrt{-g}\, d^5x\Big(R - \frac{1}{2}Q_{IJ}F^I_{\mu\nu}F^{J,\mu\nu} - Q_{IJ}\partial_\mu X^I \partial^\mu X^J - \frac{1}{24}C_{IJK}F^I_{\mu\nu}F^J_{\rho\sigma}A^K_\lambda \varepsilon^{\mu\nu\rho\sigma\lambda}\Big)\,, \tag{1.116}$$

with $I, J, K = 1, 2, 3$ and $2\kappa_5^2 = 16\pi G_N^{(5)}$. The metric for the kinetic term is

$$Q_{IJ} = \frac{1}{2}\mathrm{diag}[(X^1)^{-2}, (X^2)^{-2}, (X^3)^{-2}]\,. \tag{1.117}$$

The Ansatz for the spacetime metric $g$ is given by the five-dimensional part of (1.83):

$$ds_5^2 = -Z^{-2}(dt + k)^2 + Z\, ds_4^2\,, \qquad Z = (Z_1Z_2Z_3)^{1/3}\,. \tag{1.118}$$

For BPS solutions obeying the floating brane Ansatz [38] the warp factors are related to the electric potentials through

$$F^{(I)} = dA^{(I)} = d\Big[-Z_I^{-1}(dt + k)\Big] + \Theta^{(I)}\,, \qquad \Theta^{(I)} \equiv dB^{(I)}\,, \tag{1.119}$$

which is just the five-dimensional reduction of (1.84) and the scalars are related to the warp factors as

$$X^1 = \Big(\frac{Z_2Z_3}{Z_1^2}\Big)^{1/3}, \qquad X^2 = \Big(\frac{Z_1Z_3}{Z_2^2}\Big)^{1/3}, \qquad X^3 = \Big(\frac{Z_1Z_2}{Z_3^2}\Big)^{1/3}. \tag{1.120}$$

Supersymmetry requires the four-dimensional base to be hyper-Kähler and five-dimensional solutions are obtained by solving the BPS equations (1.87)-(1.89). The structure constants $C_{IJK} \equiv |\epsilon_{IJK}|$ determine the structure of the vector multiplet sector and its scalar coset. For the metric (1.118) to be asymptotically flat and the vector kinetic term in (1.116) to be well-behaved at spatial infinity, one requires the warp factors $Z_I$ to go to a non-vanishing constant at infinity. Under rescaling of coordinates and fields one can set

$$Z_I \ \rightarrow \ 1 \,, \tag{1.121}$$

at infinity and the vector kinetic term is then canonically normalized.

### 1.4.5 Smooth solutions

Solutions to 1.87-1.89 with harmonic functions 1.105-1.106 generically have multiple poles and are thus singular four-dimensional multi-center configurations. Moreover, the four-dimensional GH metric 1.90 is allowed to be apparently pathological: the signature can change from $(+,+,+,+)$ to $(-,-,-,-)$ with singular intervening surfaces. This appears to present quite a challenge for the construction of regular, smooth solutions. However, the four-dimensional metric is not a physical quantity. Only the *eleven*-dimensional metric 1.83 has to be regular. It turns out that if one chooses the charges and constants in the harmonic functions in a particular way, all singularities can be canceled such that the final solution is completely regular and free of any horizons. Curvatures remain low so that eleven-dimensional Supergravity is a good approximation to M-Theory and the solution smoothly caps off at some value of the radial coordinate. In the context of the fuzzball proposal these smooth solutions can be viewed as microstates for black holes with the same asymptotics charges. At spatial infinity the smooth solutions are constructed to look like the black hole geometry, but as one approaches the location where the black hole horizon would be, one finds instead some structure in the form of topological 2-cycles threaded by flux. These smooth solutions are therefore called 'bubbling' geometries. We now discuss in detail the ingredients that make these remarkable solutions possible. This Subsection is based on the reviews [46, 53] and we refer to these references for more details.

#### Ambipolar bases

The existence of smooth solutions depend on having a non-trivial homology in spacetime. Supersymmetry requires these geometries to be stationary with a non-spacelike Killing vector and the metric restricted to the directions orthogonal to the Killing vector must be conformal to a hyper-Kähler metric which is necessarily Ricci-flat. This presents a major challenge to the existence of non-trivial smooth solutions: A theorem by Schoen, Yau [107] and Witten [108] states that the only complete, non-singular, Ricci-flat, Riemannian manifold that is asymptotically Euclidean is Euclidean space itself. So how can there be supersymmetric solutions with non-trivial topology? This apparent no-go is evaded by allowing the four-dimensional Gibbons-Hawking metric to have regions of changing signature. To understand this, we need to generalize the analysis of the single-center Gibbons-Hawking metric of Section 1.3 to the multi-center case. In the standard form of the Gibbons-Hawking metric (1.90) the function $V$ is taken to have a finite number of isolated sources at positions $\vec{y}^i$ in $\mathbb{R}^3$. The apparent singularities at $r_i = 0$ can be

removed by changing to polar coordinates centered at $r_i = |\vec{y} - \vec{y}_i| = 0$ with radial coordinate $\rho_i^2 = 4r_i$ so that the metric locally takes the form

$$ds_4^2 \sim d\rho_i^2 + \rho_i^2 d\Omega_3^2 \,, \tag{1.122}$$

where $d\Omega_3^2$ is the standard metric on $S^3/\mathbb{Z}_{|v_i|}$ where we must have $v_i \in \mathbb{Z}$. For $|v_i| = 1$ the space around the $i$th center is locally flat $\mathbb{R}^4$. If the constant in the harmonic function $v_0$ is non-vanishing, then $V \to v_0$ at infinity and the GH metric asymptotes to flat $\mathbb{R}^3 \times S^1$. If $v_0 = 0$, then the GH potential at infinity $V \sim \frac{1}{r}\sum_{i=1}^N v_i$, where $r = |\vec{y}|$. The GH metric then takes again the form (1.122), where $d\Omega_3^2$ now is the standard metric on $S^3/\mathbb{Z}_{|\sum_{i=1}^N v_i|}$. For $\sum_{i=1}^N v_i = 1$ one has the positive definite, flat metric on $\mathbb{R}^4$ at infinity. For the Gibbons-Hawking metric (1.90) to be globally positive definite one would need $v_i \geq 0$. This would imply $V \equiv \frac{1}{r}$ and the GH metric would be globally $\mathbb{R}^4$. Thus, in order to get non-trivial metrics that are asymptotically flat $\mathbb{R}^4$ some of the $v_i \in \mathbb{Z}$ are required to be negative. Such a base with regions of changing signature is called *ambipolar*. The hypersurfaces at which the signature of the GH metric changes sign correspond to the region where the Killing field becomes null. The interesting feature here is that these hypersurfaces are not null (corresponding to a Killing horizon) but timelike and correspond to ergosurfaces with no bulk ergoregions.

While the four-dimensional metric is allowed to be singular, the five-dimensional solution has to be a regular smooth Lorentzian five-manifold and this is miraculously achieved through the warp factors of the time fibration and the angular momentum vector.

### Regularity, smoothness and stability

There are several consistency conditions the BPS solutions of Section 1.4 with ambipolar Gibbons-Hawking base metrics have to satisfy to yield regular smooth solutions. These translate in part to constraints on the eight constants in the harmonic functions. Fixing the asymptotics of the metric and gauge field further constrains those constants. We also require a physical solution to be free of closed timelike curves (CTC's), by demanding that the metric component $g_{\varphi\varphi} \geq 0$ for any periodically identified direction $\varphi$. If we furthermore impose that the solution has to be smooth, this puts severe restrictions on the allowed set of charges and gives an extra no-CTC condition. We summarize these conditions in the following. (See [46] for a complete discussion.)

($i$) Absence of CTC's requires:

$$Z_1 Z_2 Z_3 V - \mu^2 V^2 \geq \omega^2 \,, \qquad V Z_I \geq 0 \,. \tag{1.123}$$

The first condition[14] follows from positivity of $g_{\psi\psi}$ and is a sufficient no-CTC condition, which insures the existence of a time function. [27] The second set of conditions is equivalent to having both the polar angle in the three-dimensional base and the $T^6$ directions not to be timelike.

[14]Note that this condition is often hard to verify in practice and the weaker condition $Z_1 Z_2 Z_3 V - \mu^2 V^2 \geq 0$ is often sufficient to guarantee the absence of CTC's.

(*ii*) To have a *smooth* geometry, the warp factors $Z_I$ and the function $\mu$ appearing in the angular momentum one-form $k$ must be regular as $r_i \to 0$.

This leaves only four out of the eight charges at each center to be independent. In particular, one finds the relations

$$\ell_{I,i} = -\tfrac{1}{2} C_{IJK} \frac{k_i^J k_i^K}{v_i}\,, \qquad m_i = \frac{1}{2}\frac{k_i^1 k_i^2 k_i^3}{v_i^2} \qquad \forall i \text{ (no sum)}\,. \tag{1.124}$$

(*iii*) For such a smooth solution, there is a further restriction to ensure absence of CTC's. From the first condition in (1.123), namely $Z_1 Z_2 Z_3 V - \mu^2 V^2 \geq 0$, one notices that $\mu$ has to vanish at each center, since for $r_i \to 0$ the $Z_I$'s tend to finite values while $V^{-1}$ goes to zero:

$$\mu|_{r_i=0} = 0\,. \tag{1.125}$$

By explicitly performing the expansion around each center $\vec{r}_i$, the latter condition gives $N-1$ so-called *bubble equations* [26, 27, 28, 46]. By writing the charges and constants in the harmonic functions as vectors $\Gamma_i = (v_i, k_i^I, \ell_{I,i}, m_i)$ and $h = (V_\infty, K_\infty^I, L_{I,\infty}, M_\infty)$ these are:[15]

$$\forall i: \qquad \sum_{\substack{j=1\\ j\neq i}}^{N} \frac{\langle \Gamma_i, \Gamma_j\rangle}{r_{ij}} + \langle \Gamma_i, h\rangle = 0\,, \tag{1.126}$$

where $\langle \Gamma_i, \Gamma_j\rangle = v_i m_j - m_i v_j + \frac{1}{2}(k_i^I \ell_{I,j} - \ell_{I,i} k_j^I)$ is the symplectic product and $r_{ij} = |\vec{r}_j - \vec{r}_i|$ are the inter-center distances.

Solutions to (1.87)-(1.89) with harmonic functions (1.105)-(1.106) satisfying the conditions (*i*)-(*iii*) are smooth horizonless Supergravity configurations with three asymptotic electric charges and three local dipole charges. The solutions do not contain any localized sources. The asymptotic electric charges come entirely from the magnetic-magnetic interactions in (1.88). These smooth solutions are 'bubbled' geometries. For $N$ centers, there are $N-1$ non-trivial two-cycles, or bubbles, on the GH base. The cycles are supported by $N-1$ non-trivial fluxes $\Pi_{ij}^{(I)}$:

$$\Pi_{ij}^{(I)} \equiv \frac{K^I}{V}\Big|_{r_j} - \frac{K^I}{V}\Big|_{r_i} = \Big(\frac{k_j^I}{v_j} - \frac{k_i^I}{v_i}\Big). \tag{1.127}$$

We depict such a geometry in Figure 1.2. Smooth bubbling solutions are thus given by a multi-center Taub-NUT function $V$ and magnetic fluxes determined by the ratio of the harmonic functions $K^I$ and $V$. When $V$ diverges at the location of the GH center, the GH fiber shrinks to zero size; $K^I$ diverges at the same locations as $V$ and the magnetic fluxes thus stay finite. Going from one center $i$ to another $j$ the fiber grows and shrinks again to zero size. The GH charges $v_i$ of two such centers have opposite sign and the four-dimensional base of smooth multi-center solutions is thus ambipolar.

[15] In more general solutions [109, 110, 111] these equations come from imposing that $\omega$ should have no Dirac-Misner strings at the centers, but in smooth backgrounds this is equivalent to (1.126).

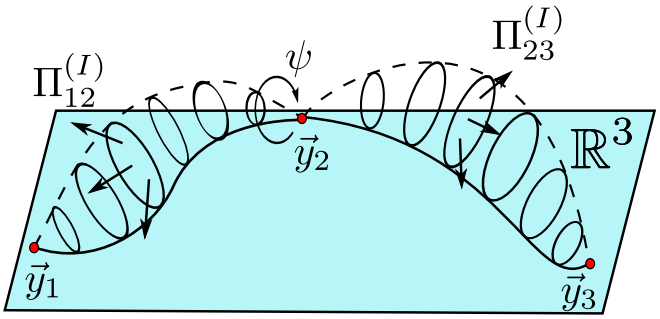


Figure 1.2: Smooth three-charge bubbling geometry.

For smooth solutions, the bubble equations can be written in terms of the magnetic two-form fluxes $\Pi^{(I)}_{ij}$ through the bubbles as:

$$\frac{1}{6}C_{IJK}\sum_{\substack{j=1\\ j\neq i}}^{N}\Pi^{(I)}_{ij}\Pi^{(J)}_{ij}\Pi^{(K)}_{ij}\frac{v_iv_j}{r_{ij}} = -2\Big(m_0v_i + \frac{1}{2}\sum_{I=1}^{3}k^I_i\Big). \tag{1.128}$$

The bubble equations relate the magnetic flux through each bubble to the physical size of each bubble, determined by the inter-center distances $r_{ij}$. The singular sources obeying (1.126) are thus replaced by a non-trivial topology with bubbles threaded by flux obeying (1.128). In terms of the topological fluxes $\Pi^{(I)}_{ij}$ we can write the asymptotic electric charges as

$$Q_I = -C_{IJK}\sum_{i,j=1}^{N}v_iv_j\Pi^{(J)}_{ij}\Pi^{(K)}_{ij}\,. \tag{1.129}$$

In this form the role of the Chern-Simon terms in sourcing the electric charges becomes transparent: the electric charges are quadratic in the topological magnetic fluxes.

### Asymptotic flatness

To specify the asymptotics of a solution, more constraints need to be imposed on the constants $v_0, k^I_0, \ell_{I,0}, m_0$. For example, asymptotically $\mathbb{R}^{4,1}$ solutions have $v_0 = 0$ while asymptotically Taub-NUT solutions have $v_0 \neq 0$. We are mostly interested in smooth solutions that are asymptotic to five-dimensional Minkowski space where we have to impose:

$$v_0 = 0\,,\quad \sum_{i=1}^{N}v_i = 1\,,\quad k^I_0 = 0\,,\quad \ell^I_0 = 1\,,\quad m_0 = -\frac{1}{2}\frac{\sum_{i=1}^{N}\sum_{I=1}^{3}k^I_i}{\sum_{j=1}^{N}v_j} = -\frac{1}{2}\sum_{i=1}^{N}\sum_{I=1}^{3}k^I_i\,. \tag{1.130}$$

The first condition is needed to get asymptotically $\mathbb{R}^4$ from the Gibbons-Hawking metric and the second condition ensures that there are no orbifold singularities. The third condition ensures the absence of non-trivial Wilson lines along the Gibbons-Hawking fiber. The warp factors are required to go to a constant at spatial infinity $Z_I \to \ell^0_I$, and using coordinate rescalings we can

set $\ell_I^0 = 1$. The function $\mu$ related to the angular momentum must vanish at infinity, fixing $m_0$ in terms of the charges $v_i, k_i^I$ which are the only free parameters after imposing absence of closed timelike curves and smoothness.

**Mass.** As for the asymptotically flat three-charge black hole the ADM mass for asymptotically flat smooth three-charge solutions can be read off from the $\rho^{-2}$ term in $-g_{tt} = 1 - \frac{2}{3}\frac{M}{\rho^2} + \mathcal{O}(\rho^{-4})$ of the asymptotic expansion of (1.83):

$$-g_{tt} = (Z_1 Z_2 Z_3)^{-2/3} = 1 - \frac{2}{3}\sum_{I=1}^{3}\frac{Q_I}{\rho^2} + \mathcal{O}(\rho^{-4})\,, \tag{1.131}$$

with $Q_I$ the asymptotic electric charges. The BPS ADM mass is thus given by

$$M = Q_1 + Q_2 + Q_3\,. \tag{1.132}$$

Since we require the solution to be smooth the asymptotic electric charges $Q_I$ do not come from bare brane sources (as for the black hole) but from charge dissolved in flux.

**Charges.** The asymptotic electric charges $Q_I$ can be read off from the $\rho^{-2}$ term in $Z_I = 1 + \frac{Q_I}{\rho^2}$ of the asymptotic expansion of the warp factors (1.101) subject to the smoothness conditions. Since the solution is invariant under gauge transformations $K^I \to K^I + c^I V$ for constant $c^I$, we can define the asymptotic charges in terms of the gauge invariant flux parameters:

$$\tilde{k}_i^I \equiv k_i^I - v_i\Big(\sum_{j=1}^{N} k_j^I\Big)\,. \tag{1.133}$$

The asymptotic electric charges $Q_I$ of a smooth solution are then given by

$$Q_I = -2C_{IJK}\sum_{j=1}^{N}\frac{\tilde{k}_j^J\tilde{k}_j^K}{v_j}\,. \tag{1.134}$$

**Angular momenta.** The five-dimensional angular momenta can be read off from the $\rho^{-2}$ term in $k = \frac{1}{4\rho^2}((J_1+J_2) + (J_1-J_2)\cos\theta)d\psi + \cdots$ of the asymptotic expansion of (1.102) subject to the smoothness conditions. For the angular momentum $J_R \equiv J_1 + J_2$ one finds:

$$J_R = \frac{4}{3}C_{IJK}\sum_{j=1}^{N}\frac{\tilde{k}_j^I\tilde{k}_j^J\tilde{k}_j^K}{v_j^2}\,. \tag{1.135}$$

The angular momentum $J_L \equiv J_1 - J_2$ depends on the details of the geometry. Using the bubble equations, one can associate an angular momentum flux vector $\vec{J}_{L,ij}$ with the $ij^{\text{th}}$ bubble:

$$\vec{J}_L = \sum_{\substack{i,j=1\\ j\neq i}}^{N}\vec{J}_{L,ij}\,, \qquad \vec{J}_{L,ij} \equiv -\frac{4}{3}v_i v_j C_{IJK}\Pi_{ij}^{(I)}\Pi_{ij}^{(J)}\Pi_{ij}^{(K)}\frac{(\vec{r}_i - \vec{r}_j)}{|\vec{r}_i - \vec{r}_j|}. \tag{1.136}$$

Decomposing the charges (1.134) to contributions $Q_{I,ij}$ from individual bubbles:

$$Q_{I,ij} \equiv -\frac{1}{4} C_{IJK} v_i v_j \Pi_{ij}^{(J)} \Pi_{ij}^{(K)} \,, \tag{1.137}$$

one can write the angular momentum flux vector for each bubble as

$$\vec{J}_{L,ij} = -\frac{16}{3} \sum_{I=1}^{3} Q_{I,ij} \Pi_{ij}^{(I)} \frac{(\vec{r}_i - \vec{r}_j)}{|\vec{r}_i - \vec{r}_j|} \,. \tag{1.138}$$

The angular momentum $J_L$ comes from the $\vec{E} \times \vec{B}$ interactions on each of the bubbles and can thus be viewed as a generalized Poynting vector.

### The role of Chern-Simons terms, non-trivial topology and extra dimensions

The constructed five-dimensional microstate geometries [26, 27, 46] form a class of smooth, geodesically complete, stable solutions without horizons. From the perspective of General Relativity these remarkable solutions are surprising as there exist 'no-go' theorems that exclude completely non-singular soliton solutions that are regular in four spacetime dimensions. Five-dimensional Supergravity, however, has structure that is not present in four dimensions. Due to the presence of Chern-Simons terms and non-trivial spacetime topology, which formed the building stones of the so far constructed smooth solutions, five-dimensional Supergravity evades the 'no-go' theorem. This was recently shown in [53] and we summarize now their result.

For a stationary solution in five-dimensional Supergravity with a timelike Killing vector $K$ the conserved mass can be defined via the Komar integral [16]

$$M = -\frac{3}{32\pi G_N^{(5)}} \int_{S^3_\infty} \star_5 dK = -\frac{3}{32\pi G_N^{(5)}} \int_{S^3_\infty} (\partial_\mu K_\nu - \partial_\nu K_\mu) d\Sigma^{\mu\nu} \,, \tag{1.139}$$

where $S^3_\infty$ is a closed spacelike surface at infinity and $d\Sigma^{\mu\nu}$ is the volume form of the $S^3$. Imposing smoothness on a spacelike hypersurface $\Sigma$ whose boundary at infinity is the $S^3$, then the mass can be written as

$$M = -\frac{3}{32\pi G_N^{(5)}} \int_{S^3_\infty} \star_5 dK = -\frac{3}{32\pi G_N^{(5)}} \int_{\Sigma} d \star_5 dK = -\frac{3}{16\pi G_N^{(5)}} \int_{\Sigma} K^\mu R_{\mu\nu} d\Sigma^\nu \,, \tag{1.140}$$

where in the second equality we used that for a Killing vector $\nabla^2 K^\mu = -R^\mu_\nu K^\nu$ and $d\Sigma^\mu$ is the volume form of $\Sigma$. If one assumes the fields $F^I, X^I$ of Subsection 1.4.4 and additionally the 3-form $G_I$ defined by

$$G_{I\,\rho\mu\nu} \equiv \frac{1}{2} Q_{IJ} F^{J\,\alpha\beta} \epsilon_{\alpha\beta\rho\mu\nu} \,, \tag{1.141}$$

[16] To have the explicit normalization for the mass, we reinstated the five-dimensional Newton constant. We will shortly restrict to $G_N^{(5)} = \frac{\pi}{4}$. In $D$ spacetime dimensions the mass is given by $M = -\frac{1}{16\pi G_N^{(D)}} \frac{D-2}{D-3} \int_{S^{D-2}} \star_D dK$.

with $Q_{IJ}$ as in (1.117), to be invariant under diffeomorphisms generated by the Killing vector $K^\mu$, then Einstein's equations obtained from variation of the five-dimensional Supergravity action 1.116 simplify to

$$K^\mu R_{\mu\nu} = \nabla^\mu(\dots)_{\mu\nu} + \frac{1}{6} Q^{IJ} H_I^{\rho\sigma} G_{J\,\rho\sigma\nu}\,, \tag{1.142}$$

where $H_{I\,\mu\nu}$ is a closed but not exact two-form. The ADM mass is then given by

$$M = \frac{1}{32\pi G_N^{(5)}} \int_\Sigma \Big[ Q^{IJ} H_{I\,\rho\sigma} G_J^{\rho\sigma\nu} \Big] d\Sigma_\nu\,. \tag{1.143}$$

If the solution has interior boundaries, an additional boundary term $\int_{\Sigma_{\rm int}}(\dots)$ contributes to (1.143). In the standard application of the Smarr formula (see for example [112, 113]) $H_I$ is assumed to be zero and the interior boundaries are horizons. The ADM mass is then related to the horizon area, charges and angular momenta. If there are no horizons (and $H_I = 0$), the ADM mass vanishes. However (1.140) can be written as

$$M = \frac{3}{16\pi G_N^{(5)}} \int_\Sigma R_{00}\, d^4x\,. \tag{1.144}$$

Vanishing of the ADM mass then implies $R_{00} = 0$ and one concludes that in the absence of horizons there are no non-trivial solutions. This presents an apparent no-go for smooth supergravity solutions. The loop-hole in the argument, however, is that $H_I$ is not necessarily zero if the five-dimensional base has non-trivial second homology. In fact, for the asymptotically flat BPS three-charge solutions of Subsection 1.4.4 we have

$$H_I = -\sum_{J=1}^{3} \frac{C_{IJK}}{2} F^K\,, \tag{1.145}$$

and, if the smoothness conditions of Subsection 1.4.5 are satisfied, one can show that the mass formula (1.143) is then given by the expression [17]

$$M = -\frac{1}{8\pi G_N^{(5)}} \sum_{I=1}^{3} \int_{S^3_\infty} Q_{IJ} F^J_{\mu\nu} d\Sigma^{\mu\nu}\,. \tag{1.146}$$

With the boundary conditions $Z_I \to 1$ at spatial infinity we have $Q_{IJ} \to \frac{1}{2}\delta_{IJ}$ and the mass formula becomes

$$M = \frac{\pi}{4G_N^{(5)}}(Q_1 + Q_2 + Q_3)\,. \tag{1.147}$$

In conventions where the five-dimensional Planck length $l_P^{(5)} = 1$ and therefore $G_N^{(5)} = \frac{\pi}{4}$, the ADM mass (1.147) takes the standard form:

$$M = Q_1 + Q_2 + Q_3\,. \tag{1.148}$$

[17] Note that the term $(\dots)$ of (1.142) contains a one-form that has to be globally well-defined and smooth. Thus, in addition to the presence of Chern-Simons terms in the action and non-trivial second homology, we have to impose the above discussed smoothness conditions on the solution of Subsection 1.4.4.

This result can be obtained directly from the following topological integral:

$$M = -\frac{1}{4\pi^2}\int_\Sigma \frac{C_{IJK}}{2} F^J \wedge F^K \tag{1.149}$$

$$= -2C_{IJK}\sum_{I=1}^{3}\sum_{i=1}^{N}\frac{\tilde{k}_i^J \tilde{k}_i^K}{v_i}\,, \tag{1.150}$$

which upon use of (1.134) yields exactly (1.148).

We thus see that Chern-Simons terms and non-trivial spacetime topology together with extra dimensions (more than four) [18] invalidate the apparent no-go theorems of General Relativity and allow for the existence of horizonless smooth soliton solutions.

### Scaling solutions

The first microstate geometries of three-charge black holes that had been constructed were very special: they typically had maximal angular momentum and carried the quantum numbers of a black hole with zero-horizon area. [29] To look like a black hole from far away, however, an apparent macroscopic throat is required. This is achieved by *scaling solutions*.

We will discuss here the simplest case of a 3-center triangle-scaling solution, which comprises already all the interesting physics. Generalization to multi-center scaling solutions is then straightforward. We denote the symplectic product and vector of constants in the harmonic functions respectively by $\Gamma_{ij} = \langle \Gamma_i, \Gamma_j \rangle$ and $C_i = \langle \Gamma_i, h \rangle$. With $\Gamma_{12} > 0\,,\ \Gamma_{23} > 0\,,\ \Gamma_{31} > 0$ the set of bubble equations is then

$$\frac{\Gamma_{12}}{r_{12}} - \frac{\Gamma_{31}}{r_{31}} + C_1 = 0\,, \qquad + \text{cyclic permutations}\,, \tag{1.151}$$

out of which only two equations are independent. For three centers there is a four-dimensional solutions space: [19] of the nine degrees of freedom (three centers in $\mathbb{R}^3$) three are irrelevant center of mass degrees of freedom and two more get fixed by the bubble equations. The three-center configuration forms a triangle whose sides $r_{ij}$ satisfy the triangle inequalities ($r_{12} + r_{23} \geq r_{31}$ and cyclic permutations). If, in addition, the symplectic products of the charges $\Gamma_{ij}$ satisfy the triangle inequalities

$$\Gamma_{12} + \Gamma_{23} \geq \Gamma_{31}, \qquad + \text{cyclic permutations}\,, \tag{1.152}$$

then

$$r_{ij} = \Gamma_{ij}\epsilon + \mathcal{O}(\epsilon)\,, \qquad j > i\,, \tag{1.153}$$

is a solution to the bubble equations at first order in $\epsilon$ with $\epsilon \to 0$ (in this limit the constants $C_i$ are only relevant at second order in $\epsilon$). In this scaling limit the centers get closer and closer as $\epsilon$ gets smaller and smaller. The clusters of homology cycles in the four-dimensional base shrink while the fluxes on them remain finite. While from the perspective of the spatial base

[18] In four dimensions there is no analogue of $H_I$ and one concludes [114] that there are no soliton solutions without horizons. Note, that the five-dimensional smooth solutions discussed here descend in four dimensions to naked singularities. Extra dimensions are thus important to describe the underlying microstates of black holes.

[19] The bubble equations (1.126) for $N$ centers have a $2(N-1)$ dimensional solution space.

this appears to be a singular limit, in five dimensions this corresponds to the opening of an $AdS$ throat whose length is determined by the scaling parameter $\epsilon$. As $\epsilon \to 0$, the throat gets longer and longer. Since for each $\epsilon$ there is a solution to the bubble equations (at first order), these scaling solutions classically form an infinite family. [32, 115, 35] In the context of the fuzzball proposal scaling black hole microstate geometries would lead to a huge overcount that would be at odds with the finite black hole entropy. However, in [116] it was shown, using geometric quantization of phase space, that scaling geometries that are too deep are wiped out by quantum effects so that a finite, although large, number of scaling solutions survives at the quantum level. Scaling solutions thus have a long $AdS$ throat, just like the black hole, but instead of forming a horizon at the end of the throat they smoothly cap off spacetime, not at the classically infinite depth, but at some finite length of the throat.

**Are smooth scaling BPS solutions typical?**

From the perspective of quantum mechanics, large classical configurations like smooth scaling BPS solutions are very coherent states. The important question, however, is whether they are states in the typical or a very atypical sector of the quantum theory. Since scaling solutions have a very long $AdS$ throat this question can be addressed within the context of AdS/CFT.

To prove or disprove the claim that black holes are a coarse-grained description of an ensemble of black hole-sized configurations without singularities or horizons, one would have to count these configurations or relate them to the states in the boundary CFT. Finding all[20] bulk microstates of a black hole seems a highly non-trivial and ambitious task. What one can hope instead is to be able to identify the bulk description of the CFT states that contribute most to the entropy of the three-charge black hole and which are referred to as *typical* CFT states. The important question is thus whether the above constructed smooth scaling three-charge solutions are dual to typical CFT microstates themselves, or at least lie in the same sector of the CFT as the typical microstates.

To decide whether a bulk microstate is dual to a state in the typical CFT sector one can study the lowest energy fluctuations in the deep throat of the bulk microstates and compare their energy at infinity, using the red-shifts set by the semi-classical quantization of the deep throat geometry, to the mass gap of the CFT. This has been addressed in [46] where it has been shown that the longest wavelength fluctuations that fit inside the $AdS$ throat do indeed have the same energy as the fluctuations in the dual CFT that was used in the original counting. [3] Hence, BPS smooth scaling solutions with a deep throat are dual to states in the typical sector of the CFT.

[20]Since we only consider bosonic modes here, it is clear that counting these solutions cannot give the exact numerical factor. What one can hope to get, however, is the power of charges in the number of bulk microstates to match the entropy $S \sim Q^{3/2}$ of the black hole. Reinstating the fermionic degrees of freedom should then also give the correct numerical factor.

## 1.5 Supertubes

Supertubes play a central role in the study of black hole microstates. They are the simplest example of non-trivial smooth Supergravity solutions and can be described within the class of solutions studied in Section 1.4. A supertube [117, 118, 119] is a brane configuration with two charges, a dipole charge, and angular momentum, that preserves eight supersymmetries. The tube is supported against collapse by a non-zero angular momentum along the longitudinal direction which is generated by the crossed electric an magnetic fields. The crucial property distinguishing the supertube from other examples of 'blow-ups' of branes into higher dimensional configurations [120, 90, 121, 122] is that no external force is needed: the supertube is a fundamental supersymmetric object. While we will focus on 'round' supertubes it has been shown [118, 123] that supersymmetry is preserved for arbitrary shapes. Classically, supertubes thus have an infinite-dimensional moduli space. Upon quantization one reproduces exactly the entropy of the two-charge system[11, 20]. The generalization of these 'wiggly' supertubes to superstrata is suggested to account for the entropy of the supersymmetric three-charge black hole. [49]

A remarkable feature of supertubes in BPS multi-center solutions is that, when treated as a probe, the Born-Infeld Hamiltonian already captures the physical properties of the fully backreacted solution where the supertube becomes an additional Gibbons-Hawking center: the radius relation of the probe supertube essentially becomes the bubble equation for that center. [124] In Chapter 5 we will study whether this non-renormalization property carries over to supertubes placed in non-supersymmetric, 'almost-BPS', extremal solutions.

When a supertube placed in a BPS smooth bubbling solutions forms a supersymmetric bound state with the background, its backreaction will yield again a smooth solution with one additional bubble. However, one can also imagine placing the supertube with the charges oriented opposite to those of the background thus breaking supersymmetry. In Chapter 3 we will use such configurations to construct microstates for non-extremal three-charge black holes.

In Subsection 1.5.1 we review the probe brane formalism (see for example [87]) and apply it in Subsection 1.5.2 to supertubes in flat space. This derivation is more general than the original discussion in [117]. In Subsection 1.5.3 we derive the Hamiltonian for supertubes placed in BPS three-charge backgrounds.

### 1.5.1 Probe brane action

The action of a probe D$p$-brane in the background of NS-NS and R-R fields can be split in two pieces

$$S_{\text{probe}} = S_{\text{DBI}} + S_{\text{WZ}}\,, \tag{1.154}$$

consisting of the Dirac-Born-Infeld action

$$S_{DBI} = -T_{Dp}\int d^{p+1}\sigma e^{-\Phi}\sqrt{-\det \mathbb{P}\Big(g + B_2 + 2\pi\alpha' F_2\Big)}\,, \tag{1.155}$$

and the Wess-Zumino action

$$S_{WZ} = T_{Dp} \int \mathbb{P}\Big(e^{B_2+2\pi\alpha' F_2} \wedge \oplus_n C_n\Big) \,. \tag{1.156}$$

The worldvolume of the D$p$-brane is parametrized by $\sigma$ and $\mathbb{P}$ denotes the pull-back of the bulk fields to the worldvolume. The background NS-NS fields are the dilaton $\Phi$, the metric $g_{\mu\nu}$ and the antisymmetric two-form $B_2$ with pull-backs

$$(\mathbb{P}g)_{ab} = g_{\mu\nu}\frac{\partial x^\mu}{\partial\sigma^a}\frac{\partial x^\nu}{\partial\sigma^b}\,, \qquad (\mathbb{P}B)_{ab} = B_{\mu\nu}\frac{\partial x^\mu}{\partial\sigma^a}\frac{\partial x^\nu}{\partial\sigma^b}\,, \tag{1.157}$$

while $C_n$ denote the background R-R fields with a corresponding expression for the pullback

$$\Big(\mathbb{P}C_n\Big)_{a_0\ldots a_{n-1}} = (C_n)_{\mu_0\ldots\mu_{n-1}}\frac{\partial x^{\mu_0}}{\partial\sigma^{a_0}}\ldots\frac{\partial x^{\mu_{n-1}}}{\partial\sigma^{a_{n-1}}}\,. \tag{1.158}$$

The two-form $F_2 = dA_1(\sigma)$ is the induced abelian field strength on the D$p$-brane worldvolume.

The Dirac-Born-Infeld action is the action of the D$p$-brane in a background created by closed string modes $g, B_2, \Phi$ and thus encodes the dynamics of the D$p$-brane in spacetime. The Wess-Zumino action encodes the coupling to the background R-R fields $C_n$. From (1.156) we see that D$p$-branes can carry charge of lower-dimensional D$p$-branes through the worldvolume field strength $F_2$. The D$p$-brane naturally couples to $C_{p+1}$ through $T_{Dp}\int \mathbb{P}C_{p+1}$ which would be the only term if the induced field strength vanished. With a non-vanishing $F_2$ turned on, there are lower-dimensional form fields $C_{p-1}, C_{p-3}, \ldots$ showing up in the Wess-Zumino action $T_{Dp}\int \Big(C_{p+1} + (B_2 + 2\pi F_2)\wedge C_{p-1} + \ldots\Big)$ which couple, respectively, to D$(p-2)$-branes, D$(p-4)$-branes, ... The appearance of the abelian field strength $F_2$ is thus explained by having lower-dimensional branes dissolved in the probe D$p$-brane. Note that spacetime gauge invariance requires $B_2$ and $F_2$ to show up in the combination $B_2 + 2\pi F_2$ in the action which justifies the appearance of $B_2$ in the probe brane action. Finally, the dilaton $\Phi$ indicates that the dynamics of the D$p$-brane depends on the string coupling $g_s = e^{\Phi_\infty}$.

### 1.5.2 Supertubes in flat space

In its original realization [117, 118, 119] in IIA Supergravity, the electric charges of the supertube correspond to D0 branes and F1 strings dissolved into a tubular D2 brane. The tube is supported against collapse by a non-zero angular momentum along the longitudinal direction which is generated by the crossed electric an magnetic fields associated, respectively, to the F1 and D0 charge through the relation $|J\; d_{D2}| = |q_{D0}\; q_{F1}|$. Because the cycle wrapped by the D2 brane is trivial, $d_{D2}$ does not give an asymptotic contribution and one speaks of a D2 dipole charge. We now study the probe action for the F1–D0 $\rightarrow$ D2 supertube in detail.

In flat space: $\Phi = 0$, $B_2 = 0$, $g_{\mu\nu} = \eta_{\mu\nu}$, and $C_n = 0$ . The Wess-Zumino action vanishes and the only contribution to the Hamiltonian comes from the Dirac-Born-Infeld action:

$$S_{DBI} \;=\; -T_{D2}N_{D2}\int d^3\sigma\sqrt{-\det\mathbb{P}(g + 2\pi\alpha' F)}\,. \tag{1.159}$$

We parametrize the ten-dimensional flat metric $g$ as

$$ds^2_{10} = -dt + dr^2 + r^2 d\varphi^2 + dz^2 + ds^2_{\mathbb{E}^6} \,. \tag{1.160}$$

In this space we embed a cylindrical D2 brane with radius $r$ and with a velocity $v = r\omega$ along the circle $\varphi$. We take the worldvolume coordinates $\sigma$ as:

$$t = \sigma^0 \,, \qquad \varphi = \sigma^1 + v\sigma^0 \,, \qquad z = \sigma^2 \,. \tag{1.161}$$

Then the induced metric on the D2 worldvolume is:

$$ds^2_{D2} = -(d\sigma^0)^2 + r^2(d\sigma^1 + v d\sigma^0)^2 + (d\sigma^2)^2 \,. \tag{1.162}$$

In the conventional treatment of the supertube one takes $v = 0$. The D2 brane has a dipole charge given by $d_3 = T_{D2} N_{D2}$. To introduce the lower dimensional brane charge corresponding to F1 strings and D0 branes, we need the induced abelian two-form field strength on the D2 worldvolume

$$2\pi\alpha' F_2 = \mathcal{E}\, d\sigma^0 \wedge d\sigma^2 + \mathcal{B}\, d\sigma^1 \wedge d\sigma^2 \,, \tag{1.163}$$

whose only non-vanishing components are $\mathcal{E} = 2\pi\alpha' F_{tz}$ and $\mathcal{B} = 2\pi\alpha' F_{\varphi z}$ which, respectively, couple electrically to F1 and magnetically to D0. With this form for the Born-Infeld flux together with the induced metric (1.162) on the supertube worldvolume, the Dirac-Born-Infeld Lagrangian becomes

$$\mathcal{L} = -d_3 \sqrt{\mathcal{B}^2 + r^2(1 - (\mathcal{E} - v\mathcal{B})^2)} \,. \tag{1.164}$$

**Supertube Hamiltonian.** The Hamiltonian density is obtained from the Lagrangian density by a Legendre transformation w.r.t. the electric field $\mathcal{E} = \mathbb{P}\partial_t A_z$ and the velocity $v = \mathbb{P}\partial_t \varphi$ on the D2 worldvolume:

$$\mathcal{H} = \Pi_{\mathcal{E}} \mathcal{E} + \Pi_v v - \mathcal{L} \,, \tag{1.165}$$

where the conjugate momenta are defined as $\Pi_{\mathcal{E}} = \frac{\partial \mathcal{L}}{\partial \mathcal{E}}$ and $\Pi_v = \frac{\partial \mathcal{L}}{\partial v}$. One finds

$$\Pi_{\mathcal{E}} = \frac{\partial \mathcal{L}}{\partial \mathcal{E}} = d_3 \frac{r^2(\mathcal{E} - v\mathcal{B})}{\sqrt{r^2(1 - \mathcal{E}^2) + \mathcal{B}^2}} \,, \qquad \Pi_v = -\mathcal{B}\Pi_{\mathcal{E}} \,. \tag{1.166}$$

The momentum conjugate to the angular velocity is thus not an independent quantity. The Lagrangian depends on the electric field and the angular velocity only through the combination $\mathcal{E} - v\mathcal{B}$. We interpret this as the angular velocity $v$ of the tube giving a contribution to the 'effective' electric field $\mathcal{E} - v\mathcal{B}$. To eliminate $\mathcal{E}$ and $v$ from the expression for the Hamiltonian, we need to use both relations (1.166). This yields

$$\mathcal{H} = \Pi_{\mathcal{E}}(\mathcal{E} - v\mathcal{B}) - \mathcal{L} \tag{1.167}$$

$$= \frac{1}{d_3 r} \sqrt{(\Pi^2_{\mathcal{E}} + d_3^2 r^2)(d_3^2 \mathcal{B}^2 + d_3^2 r^2)} \,. \tag{1.168}$$

Note that the form of the Hamiltonian in terms of the conserved charges is independent of the angular velocity $v$. Reinstating $\Pi_v$ explicitly via (1.166) we obtain

$$\mathcal{H} = \sqrt{\Pi^2_{\mathcal{E}} + d_3^2 \mathcal{B}^2 + d_3^2 r^2 + \frac{\Pi_v^2}{r^2}} \,. \tag{1.169}$$

Choosing convenient units, the D0 and F1 charges and the angular momentum of the tubular configuration are:

$$q_1 = \frac{1}{2\pi}\oint d\varphi\,\Pi_{\mathcal{E}}\,, \qquad q_2 = \frac{1}{2\pi}\oint d\varphi\, d_3\mathcal{B}\,, \qquad J = \frac{1}{2\pi}\oint d\varphi\,\Pi_v\,. \tag{1.170}$$

The Hamilton $H = \frac{1}{2\pi}\oint d\varphi\mathcal{H}$ is then given by

$$H = \frac{1}{d_3 r}\sqrt{(q_1^2 + d_3^2 r^2)(q_2^2 + d_3^2 r^2)}\,, \tag{1.171}$$

or, in a more democratic form,

$$H = \sqrt{q_1^2 + q_2^2 + d_3^2 r^2 + \frac{J^2}{r^2}}\,. \tag{1.172}$$

From this form of the Hamiltonian it becomes clear that the four local charges come in pairs: the global charges $q_1, q_2$ show up in a symmetric way while the dipole charge $d_3$ and angular momentum $J$ are symmetric up to T-duality along the $\varphi$ circle ($r \leftrightarrow 1/r$).

**Supersymmetric minimum and critical effective electric field.** The Hamiltonian is interpreted as a potential for the radius $r$. The minimum is at the radius

$$R^2_{susy} = \frac{|J|}{d_3} = \frac{|q_1\, q_2|}{d_3^2}\,, \tag{1.173}$$

for which the minimum is supersymmetric, hence the name *supertube*. The value of the Hamiltonian at this radius is

$$H_{susy} = q_1 + q_2. \tag{1.174}$$

Note that the energy of the supertube at the supersymmetric minimum only depends on the sum of the electric F1 and D0 charges while the D2 dipole charge $d_3$ and angular momentum $J$ drop out because of (1.173). The supertube energy saturates the BPS bound. At the supersymmetric minimum the effective electric field takes the 'critical' value $\mathcal{E} - v\mathcal{B} = 1$. Note that it is possible to make a supertube without any electric field, by giving it a velocity $v = -1/\mathcal{B}$.

The critical value for the effective electric field drastically symplifies the DBI Lagrangian:

$$\mathcal{L}_{DBI} = -d_3\,\mathcal{B}\,. \tag{1.175}$$

Upon use of (1.166) to replace $\Pi_v$ by its relation to $\Pi_{\mathcal{E}}$ and $\mathcal{B}$, we immediately obtain the supersymmetric Hamiltonian

$$H = \frac{1}{2\pi}\oint\Big(\Pi_{\mathcal{E}} + d_3\,\mathcal{B}\Big) = q_1 + q_2\,. \tag{1.176}$$

Thus, to find the supersymmetric minima of the supertube Hamiltonian we just have to set the effective electric field to its critical value and use the relation between the conjugate momenta. This even applies to non-flat backgrounds.

**Relation to the conventional treatment.** A few comments on the relation to the original derivation of the supertube are in order. In [117], the velocity was set to zero from the beginning and the angular momentum only comes about through the physical motivation as being generated by crossed electric and magnetic fields. The treatment above with $v \neq 0$ shows how the angular momentum comes about directly: through the explicit velocity $v$ in the Lagrangian we see that the associated momentum $J$ is proportional to $q_1 q_2$ immediately. The reason why in the case of $v = 0$, or more generally any $v = \text{const}$, gives the same result is that the momenta conjugate to $\mathcal{E}$ and $v$ are not independent: (1.166) is a *constraint* relation. Therefore, for the computation of the Hamiltonian, we can always set to zero the velocity and only afterwards reinstate $J$ through the constraint.

### 1.5.3 Supertubes in three-charge backgrounds

We now extend the analysis of the previous Subsection to two-charge supertubes in supersymmetric three-charge backgrounds whose Hamiltonian was found in **P1**.. In the M-Theory frame, the three electric charges of the background correspond to M2 branes wrapping three orthogonal two-tori inside an internal six-torus while the three local magnetic dipole charges correspond to M5 branes wrapping two orthogonal two-tori and an arbitrary closed curve in the four-dimensional base which we take to be of Gibbons-Hawking form. The two electric charges of the supertube, $q_1$ and $q_2$, are (anti-)parallel to those of the background and correspond to M2 branes along the first and second two-torus and the dipole charge, $d_3$, corresponds to an M5 brane extended along those two tori and wrapping the fiber of the Gibbons-Hawking base.

Since the M5 brane worldvolume Lagrangian is rather involved [125], we chose to go to a frame that is more amenable to calculations. In particular, we reduce over one of the torus directions, such that the supertube charges are D2 branes and F1 strings that blow up into a D4 brane, hence a D2–F1 $\rightarrow$ D4 supertube. This configuration is analogous (can be seen by two T-dualities) to the original D0–F1 $\rightarrow$ D2 supertube [118, 119] discussed in the previous Subsection: our D2's couple to the magnetic Born-Infeld flux and the F1's to the electric one. For a relation of the supertube charges in the M-Theory frame to that in the IIA frame (reduction over the GH fiber) and the IIA$'$ frame (reduction over a torus direction), see Table 1.5. A similar table of relations for all the charges of the three-charge background in the M-Theory and IIA/IIA$'$ frames is given in Appendix B.1.

| **Charge** | **M theory** | **IIA: M/$S_\psi$** | **IIA$'$: M/$S_6$** |
|---|---|---|---|
| $d_3$ | M5 | D4 | D4 |
| $q_1$ | M2 | D2 | F1 |
| $q_2$ | M2 | D2 | D2 |
| $J$ | $J_\psi$ | D0 | $J_\psi$ |

Table 1.5: Brane interpretation of the two-charge supertube in a three-charge background with Gibbons-Hawking base with fiber $\psi$. The two electric charges of the tube are $q_1$ and $q_2$ and the dipole charge is denoted by $d_3$. The worldvolume angular momentum of the tube, $J$, is related to the other charges by $|J\, d_3| = |q_1\, q_2|$. $J_\psi$ denotes (angular) momentum along the GH circle $S_\psi$.

### Three-charge background in the IIA′ frame

For the computation of the supertube Hamiltonian we work in the IIA′ reduction and reduce over one direction of the first torus. In the string frame, the NS-NS fields are [124]:

$$\begin{aligned} ds^2_{IIA,st} &= -\frac{1}{Z_1\sqrt{Z_2Z_3}}(dt+k)^2+\sqrt{Z_2Z_3}ds^2_4 && (1.177)\\ &\quad +\frac{\sqrt{Z_2Z_3}}{Z_1}dz^2+\sqrt{\frac{Z_2}{Z_3}}ds^2_2+\sqrt{\frac{Z_3}{Z_2}}ds^2_3\,, && (1.178)\\ B_2 &= -A^{(1)}\wedge dz\,, && (1.179)\\ e^{\Phi} &= \Big(\frac{Z_2Z_3}{Z_1^2}\Big)^{1/4}\,, && (1.180) \end{aligned}$$

where $z$ is the remaining direction of the first torus and $ds^2_2$ and $ds^2_3$ are, respectively, the line elements on the second and third torus. The NS-NS fields give rise to the Dirac-Born-Infeld Lagrangian. In the RR sector, the non-trivial fields are $C_3$ and $C_5$. We only list the components we need for computing the supertube Lagrangian:

$$\begin{aligned} C_3 &= \Big[-\Big(\frac{1}{Z_3}-1\Big)dt+\Big(\frac{K^3}{V}-\frac{\mu}{Z_3}\Big)d\psi\Big]\wedge\omega_2\,,\\ C_5 &= \Big[\frac{K^3}{VZ_1}+\Big(\frac{K^1}{V}-\frac{\mu}{Z_1}\Big)\Big]\,dt\wedge d\psi\wedge dz\wedge\omega_2\,, && (1.181) \end{aligned}$$

where $\omega_2$ is the volume form of the second torus. Unlike supertubes in flat space, the non-vanishing R-R fields in this background will give rise to a non-vanishing Wess-Zumino Lagrangian.

### Gibbons-Hawking Hamiltonian

We consider a F1–D2 $\to$ D4 supertube with the D4 worldvolume embedding given as

$$t=\sigma^0,\qquad \psi=\sigma^1,\qquad z=\sigma^2\,, \tag{1.182}$$

and $\sigma^3,\sigma^4$ along the second torus. The Lagrangian is

$$L=-N_{D4}T_{D4}\int d^5\sigma e^{-\Phi}\sqrt{-\det\mathbb{P}\left(g+B_2+\mathcal{F}_2\right)}\quad+N_{D4}T_{D4}\int\left(C_5+(B_2+\mathcal{F}_2)\wedge C_3\right), \tag{1.183}$$

where $\mathcal{F}_2=2\pi\alpha' F_2$ and $F_2$ is the induced abelian 2-form field strength on the D4 worldvolume. The lower-dimensional brane charges are introduced by the worldvolume flux

$$\mathcal{F}_2=\mathcal{E}d\sigma^0\wedge d\sigma^2+\mathcal{B}d\sigma^1\wedge d\sigma^2\,. \tag{1.184}$$

The electric field $\mathcal{E}$ sources IIA string charge along $z$, while the magnetic field $\mathcal{B}$ induces D2 brane charge along the torus $T^2$. The supertube Lagrangian (density) in the IIA′ background is

$$\begin{aligned} \mathcal{L} &= -\frac{d_3}{Z_3V}\sqrt{\left[K^1+V(\mathcal{B}-\mu(1-\mathcal{E}))\right]^2+VZ_2Z_3(1-\mathcal{E})(2-Z_1(1-\mathcal{E}))}\\ &\quad -(\frac{1}{Z_3}-1)d_3\mathcal{B}+\frac{d_3K^1}{VZ_3}+d_3(\frac{K^3}{V}-\frac{\mu}{Z_3})(1-\mathcal{E})\,, \end{aligned} \tag{1.185}$$

with the D4 dipole charge $d_3 = N_{D4}T_{D4}$. This Lagrangian was obtained in a different duality frame in [124] for $d_3 = 1$. The Hamiltonian is obtained by the Legendre transform of $\mathcal{L}$ with respect to the electric field $\mathcal{E}$,

$$\mathcal{H} = \Pi_{\mathcal{E}}\mathcal{E} - \mathcal{L}, \tag{1.186}$$

where $\Pi_{\mathcal{E}} = \frac{\delta\mathcal{L}}{\delta\mathcal{E}}$ is the momentum conjugate to $\mathcal{E}$. After quite some algebra, one finds the Hamiltonian in terms of the F1 and D2 charges, $q_1 = \Pi_{\mathcal{E}}$ and $q_2 = d_3\mathcal{B}$, and D4 dipole charge, $d_3$, to be

$$\mathcal{H} = \frac{\sqrt{Z_1Z_2Z_3/V}}{d_3R^2}\sqrt{\left(\tilde{q}_1^2 + d_3^2\frac{R^2}{Z_2^2}\right)\left(\tilde{q}_2^2 + d_3^2\frac{R^2}{Z_1^2}\right)} + \frac{\mu V^2}{d_3R^2}\tilde{q}_1\tilde{q}_2 - \frac{\tilde{q}_1}{Z_1} - \frac{\tilde{q}_2}{Z_2} - \frac{d_3\mu}{Z_1Z_2} + q_1 + q_2\,, \tag{1.187}$$

where we have introduced

$$\tilde{q}_1 \equiv q_1 + d_3(K^2/V - \mu/Z_2)\,, \quad \tilde{q}_2 \equiv q_2 + d_3(K^1/V - \mu/Z_1)\,, \tag{1.188}$$

and $R$ is proportional to the size of the Gibbons-Hawking fiber

$$R^2 \equiv Z_1Z_2Z_3/V - \mu^2\,, \tag{1.189}$$

and the harmonic functions $K^1$ and $K^2$ encode two of the three dipole moments of the background.

Although the calculation yielding this result treats the two charges of the supertube differently, the final Hamiltonian is symmetric under interchange of indices $(1 \leftrightarrow 2)$, which is a non-trivial check. In flat space, the Hamiltonian (1.187) reduces to (1.171): the first term becomes the flat-space Hamiltonian and the terms in the second line vanish. An important difference between the flat space (1.171) and the GH supertube Hamiltonian (1.187) is that the charges appearing in the latter are shifted from the actual brane charges by a term proportional to the background magnetic fluxes. [21]

The combination $Z_1Z_2Z_3V - \mu^2V^2$ gives the square of the radius of the GH fiber $\psi$ and hence the square of the radius of the tube. In a regular background, free of closed timelike curves (CTC's), this combination is always positive, and hence the Hamiltonian is well-defined throughout the space. Furthermore, one can show that this Hamiltonian is always larger than or equal to the sum of the supertube charges $q_1$ and $q_2$; for supersymmetric minima the equality comes about after a few non-trivial cancellations.

The Hamiltonian (1.187) describes tubes in the most general three-charge background. We expect this Hamiltonian to have both supersymmetric and non-supersymmetric minima. The minima of the potential determine the position on the GH base of (meta)stable supertubes in a given three-charge background. Depending on the relative orientation of the M2 charges of supertube and the background, the minima of the potential will be supersymmetric or non-supersymmetric. The structure of the supertube potential and its dynamics will be studied in detail in Chapter 3.

[21] This shift is the crucial ingredient in the supertube entropy enhancement mechanism. [126]

# Chapter 2

# Information release from black holes

In the Introduction we alluded that when a black hole evaporates through the Hawking pair production process, the final radiation state is thermal and the information about the original state is lost. The effort to restore purity of the final radiation state has led to the surprising argument that Quantum Gravity effects kick in at the scale of the black hole horizon and General Relativity thus ceases to be a good description at this scale. [2] In this Chapter we want to go beyond purity of the final radiation state and include other conditions necessary for a unitary evolution to make the statement of information loss more precise. We thus want to ask the question:

*Q1. When and how does the information of the original state come out?*

To address this question we will make use of quantum information techniques and extend the quantum mechanical qubit model framework to incorporate the non-unitary Hawking evaporation process.

## 2.1 Motivation and summary

General relativity predicts that for a sufficiently large amount of matter in a fixed spatial region, gravitational interactions dominate over all others and the matter inevitably collapses to form a black hole, cf. [127]. Regardless of the matter's initial configuration, the black hole that finally results is essentially unique with only a few independent parameters. Furthermore, if one considers quantum fields in the background of the classical black hole solution, one finds that unlike for an ordinary star, a black hole's 'surface', the event horizon, is in a unique state independent of the collapsing matter. This state, the Unruh vacuum, allows an infalling observer to fall freely through it. On much longer time scales, the black hole evaporates away as pairs of particles are pulled out of the Unruh vacuum at the horizon. Since the horizon contains no information of the original matter, the created pairs are in a special state independent of the matter's initial state. Hawking's calculation [1] implies that the resulting radiation is in a mixed state and therefore the evaporation process is manifestly non-unitary. This presents a foundational conflict between general relativity and quantum mechanics that any complete theory of quantum gravity must resolve.

To resolve the information paradox Mathur argued that the traditional black hole horizon has to be replaced by some information-carrying structure which was dubbed 'fuzzball'. According to the proposal the true microstates accounting for the Bekenstein-Hawking entropy are horizonless but have a macroscopic size of order the horizon-scale. The radiation emanates locally from the fuzzballs, instead of emanating from an information-free horizon, and hence there is no information loss. For reviews of the fuzzball proposal see [19, 102, 47, 48, 128]. For information-carrying radiation originating from fuzzballs see [129, 130].

The fuzzball proposal is a huge departure from the conventional black hole picture in that it basically states that a black hole is a complicated quantum object of horizon-scale size. Many have held the view that giving up the traditional horizon is not necessary to save unitarity and (erroneously) believe that, since the number of emitted quanta is very large, small corrections, such that semi-classical physics can still be trusted with the horizon being approximately the vacuum state, to the leading order Hawking process can accumulate over time and restore unitarity.

This hope is based on Page's argument [131] that information of complex evaporating systems is encoded in delicate correlations between radiation quanta. Concretely, Page has shown that for a macroscopically large evaporating system in a typical state where all subsystems are almost maximally entangled, very little information can be read off unless one can access more than half of the system. From this one concludes that the von Neumann entropy of the radiation emitted from the burning system grows linearly, then turns around at the 'Page time' where half of the system has evaporated and then falls linearly to zero as shown in Figure 2.1a [132]. If black hole evaporation were unitary, then a black hole in a typical state would evaporate according to Figure 2.1a. In a recent series of papers [2, 67, 68, 133, 134], however, Mathur showed that

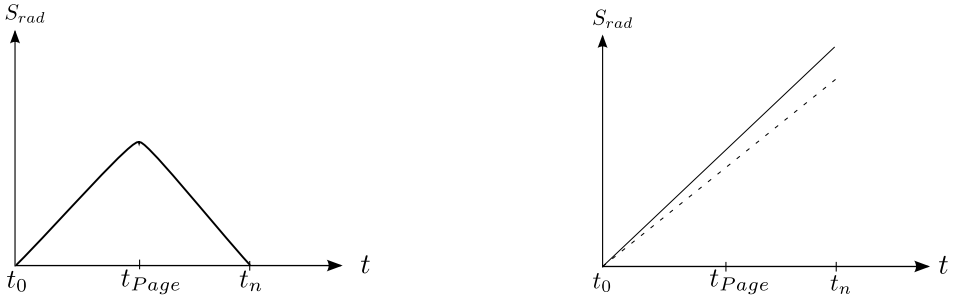


Figure 2.1: Entanglement entropy of radiation from (a) a normal body and (b) a traditional black hole with (information-free) horizon. In normal burning bodies, assuming them to be in a typical state to begin with, the entropy initially goes up and then goes down while for traditional black holes that evaporate via Hawking-pair creation the entropy monotonically increases. Allowing small correction to the leading order process (solid line) decreases the slope (dashed line) but the entropy curve keeps rising.

for black hole evaporation with only *small* corrections to the leading-order Hawking process the von Neumann entropy of radiation keeps monotonically increasing in time with no turnover, as shown in Figure 2.1b. To get an evolution as in Figure 2.1a, he therefore argues that the

small correction have to be made large and we can no longer trust effective field theory at the horizon scale. In other words purity of the final radiation state requires order one corrections (not suppressed in the inverse mass of the black hole) to the Unruh vacuum. Thus, unitarity demands the black hole to have non-trivial horizon-scale structure in accord with the fuzzball program.

While this argument shows that small corrections to the leading order Hawking process cannot restore *purity* of the final state, modifying the process to ensure purity of the final state *does not imply unitarity*. In other words, purity of the final state is a necessary but not a sufficient condition for unitary evaporation. In addition to purity of the final radiation state, unitarity requires linearity, norm preservation and invertibility of evolution. The goal of this Chapter, which is based on **P4**, is to make the statement of information loss in black hole evaporation more precise by imposing these extra conditions. We will work under the assumption that the dimension of the Hilbert space does not drastically change during the evaporation process, that the evaporation process can be described in a local framework and we will not allow for any form of state-dependency in the transformations acting on the system. Under these assumptions, we argue that information has to come out at every step during the evaporation process for unitarity to be preserved. A discussion and possible concerns regarding these assumptions will be given in Section 2.5.

At this point, it is important to note the distinction between information *decoding* and information *release*. In ordinary evaporating systems there are correlations between successively emitted quanta that encode information of the structure of the surface they have been emitted from. While this information can only be read off after the radiation composes more than half of the total system, what is read off depends on what has been emitted previously. In that sense information must have been released with the emitted quanta.

In the context of black hole evaporation using qubit models, this means that for evaporation to be unitary *every quantum coming out of the black hole, before and after Page time, has to carry information of the black hole state*. This will be made more precise in Section 2.3. Thus the state at the horizon [1] cannot be in the Unruh vacuum even before Page time. This result supports the fuzzball conjecture.

This Chapter is organized as follows. In Section 2.2 we review the role of purity in the discussion of the Hawking process and the departure from the traditional black hole picture. We then discuss additional requirements for unitarity in Section 2.3 and use qubit models to study black hole evaporation. We show that for unitarity to be conserved information must be released with each quantum emitted from a black hole in a typical state. There is thus no difference in the process and rate of information release before and after Page time. This is used to argue that if unitarity is to be preserved, the configuration resulting from infalling matter can never be the traditional black hole geometry with Unruh vacuum at the horizon. In Section 2.4 we apply standard quantum information techniques to 'follow the information' in a system by entangling it with a reference system. This language allows to quantify how much information is lost if the state at the horizon is a predetermined state at any point. Finally, in Section 2.5 we summarize

[1] We do not attempt go give a precise definition here; we think the concept of a state at the *horizon* as a classical location is ill-defined, and disappears in a full theory of quantum gravity.

our result and discuss the assumptions.

## 2.2 What it takes to be pure

We start by reviewing the traditional (non-unitary) picture of black hole evaporation in Subsection 2.2.1 via Hawking pair production at the horizon. We then summarize in Subsection 2.2.2 Mathur's theorem that order unity corrections to this process are required to restore unitarity and discuss its consequences.

### 2.2.1 The traditional picture

One can understand the Hawking evaporation process in the following way. Consider a foliation of spacetime by 'nice' slices [2] as depicted in the Penrose diagram in Figure 2.2(a). Such a slicing avoids strong curvature regions and yet smoothly intersects the early radiation, the pair creation site at the horizon and the initial matter that had formed the black hole. [137] The evaporation time scale of a black hole of mass $M$ is of order $M^3$ which is parametrically larger than the time gap between successive quanta coming out which is of order $M$. So, for the purpose of a few emission, we can use the nice slices in Figure 2.2(a). The initial matter, labeled '$D$', that formed the black hole is in the deep interior while any earlier emitted radiation, labeled '$A$', has moved far away from its place of creation at the horizon. The evolution of a slice results in a stretching of the connector region straddling the horizon and this creates the Hawking-pair which is schematically depicted on slice $S_1$ in Figure 2.2(b). In the further evolution the negative energy partner labeled '$C_1$' falls into the black hole, thus reducing its mass, while the positive energy partner labeled '$B_1$' escapes to infinity and becomes part of the radiation detected by an asymptotic observer. On slice $S_2$ the pair $B_1C_1$ has moved away from the horizon in opposite directions and a new pair '$B_2$' and '$C_2$' is created. For details of this process see [142, 2]. We use the letters $B$ and $C$ to denote outside and inside Hawking quanta respectively. When not needed, we omit the subscripts which indicate the slice on which they were created.

The pair created at the horizon is like an EPR pair. While the infalling member of the pair might be 'caught' by the initial matter, it is well known that the EPR pair cannot be used to communicate information. In a similar vein, the information of the initial matter $D$ cannot be carried away by the outgoing member of the Hawking-pair. We give a more technical account of this phenomenon when rephrasing the Hawking process in the language of qubit models.

### 2.2.2 A paradigm change

Mathur [2] has turned Hawking's argument, that information will be lost in the evaporation process of a black hole via pair creation from a horizon, into the following theorem.

[2] There are some arguments against the validity of local quantum field theory on the nice slices in [135, 136, 137, 138, 139]. Indeed outgoing quanta may carry information of the infalling matter if one assumes some non-local effects between the location of the initial matter and the pair creation site. However, there are also some results that claim that semi-classical evolution on such nice slices is consistent [140, 141]. While we use nice slices here to illustrate the Hawking process, they will not be relevant for the discussion in Section 2.3.

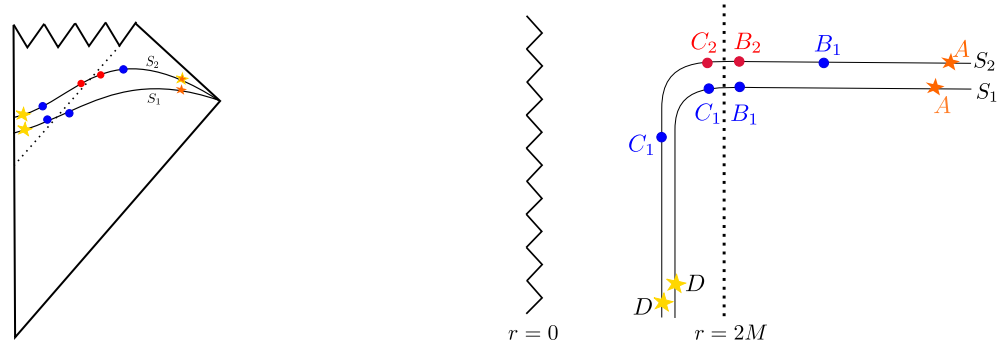


(a) (b)

Figure 2.2: (a) Two subsequent 'nice slices' that smoothly intersect initial infalling matter (yellow), newly created Hawking-pairs (blue and red) at the horizon and early Hawking radiation (orange). (b) Hawking-pair creation at the horizon (dashed line) on two subsequent nice slices sufficiently far away from the singularity (zigzag line) in order to avoid large curvatures.

If we assume that

(a) quantum gravity effects are confined to within a bounded length (like the Planck length $l_P$ or the string length $l_s$)

(b) the vacuum state is unique

then there will be information loss.

To invalidate Hawking's conclusion one must show that one of the assumptions in his calculation is wrong. The argument for information loss is based on the result that the final radiation is in a mixed state. A way to characterize purity (and the lack thereof) of a state of a system $\mathcal{S}$ is to study its von Neumann entropy

$$S_{\mathcal{S}} = -\mathrm{Tr}\Big(\rho_{\mathcal{S}} \log \rho_{\mathcal{S}}\Big)\,, \tag{2.1}$$

where $\rho_{\mathcal{S}}$ is the density matrix of the system. If $S_{\mathcal{S}} = 0$ the system $\mathcal{S}$ is in a *pure* state. If the system $\mathcal{S}$ consists of two subsystems $x$ and $y$, the von Neumann entropy of $x$ is defined as

$$S_x \;=\; -\,\mathrm{Tr}\Big(\rho_x \log \rho_x\Big)\,, \tag{2.2}$$

where

$$\rho_x \;=\; \mathrm{Tr}_y\Big(\rho_{\mathcal{S}}\Big) \tag{2.3}$$

is the reduced density matrix of the subsystem $x$ of $\mathcal{S}$ after tracing out the other subsystem $y$. The subsystem $x$ is pure if its von Neumann entropy vanishes: $S_x = 0$. Starting with system $\mathcal{S}$ in a pure state, vanishing von Neumann entropy of one of the two subsystems implies vanishing

von Neumann entropy of the other subsystem. This means that their respective reduced density matrices are idempotent. In that case the system $\mathcal{S}$ is said to be *separable*. Conversely, $\mathcal{S}$ is called *entangled* if it is not separable. If $\mathcal{S}$ is *maximally entangled* then the reduced density matrices $\rho_x$ and $\rho_y$ are proportional to the identity matrix and the respective von Neumann entropies of the two subsystems are maximal. Neither of the two mutually maximally entangled subsystems $x$ and $y$ can be entangled with any other distinct system, which is the statement of 'monogamy of entanglement', and the state of the combined system $\mathcal{S}$ is thus pure. The above mentioned EPR pair is an example of a maximally entangled quantum state consisting of two qubits:

$$|\psi\rangle = \frac{1}{\sqrt{2}}\Big(|\hat{0}0\rangle + |\hat{1}1\rangle\Big)\,. \tag{2.4}$$

The condition of purity of the final radiation state was emphasized by Page in [132] where he argued that if the black hole is in a typical pure state and *one assumes unitary evaporation*, then the entropy of the radiation at first increases and then decreases to zero again, as for any normal body (depicted in Figure 2.1(a)), so that the final state is indeed pure. This can be roughly understood as follows. In a typical state each small subsystem is almost maximally entangled with the remaining (larger) subsystem [131]. If we assume the state of the entire system to be pure, then measuring the entropy of the radiation is like tracing over the remaining black hole system. As long as the radiation is the smaller part of the system its entropy increases. However, after half the system has evaporated, the black hole is the smaller system and the entropy of the radiation starts decreasing until it becomes zero again.

While this is the case for normal evaporating systems in a typical state, Mathur has argued in a series of recent papers [2, 67, 68, 133, 134] that a Hawking-*like* evaporation process *cannot* bend the entropy curve to go down at any point in time. The Hawking process corresponds to the creation of a pair at the horizon which, for the purpose of the argument, can be assumed to take the simple form (2.4) where the hatted qubit denotes the infalling partner $C$ of the pair while the unhatted qubit $B$ will leave the black hole and become part of the final radiation. Purity of the final radiation state is then characterized by the von Neumann entropy of the radiation

$$S_{rad} \;=\; -\,\mathrm{Tr}\Big(\rho_{rad}\,\log\,\rho_{rad}\Big)\,, \qquad \rho_{rad} \;=\; \mathrm{Tr}_{BH}\Big(\rho\Big)\,, \tag{2.5}$$

where $\rho$ is the density matrix of the full system containing the radiation and the remaining black hole degrees of freedom while $\rho_{rad}$ denotes the reduced density matrix of the radiation at an intermediate step during the evaporation after tracing out the remaining black hole degrees of freedom. Since the Hawking state (2.4) is maximally entangled the von Neumann entropy of the first emitted (unhatted) radiation qubit after tracing over the remaining (hatted) qubit takes its maximal value $S = \log 2$. In the further evolution more pairs are created with the unhatted qubits being emitted as radiation. When the black hole has evaporated after $n$ such steps the von Neumann entropy of the final radiation state is $S_{rad} = n\,\log 2$. A non-vanishing von Neumann entropy implies that the final radiation state is not pure and black hole evaporation via Hawking pairs is non-unitary. For a detailed discussion of this see [2].

We can rephrase this result in the language of the last section where we separate the full system $(ABC)$ at each step of the evaporation process into the early radiation $A$, a newly created

outgoing quantum $B$, and its ingoing partner $C$. The system $ABC$ satisfies *strong subadditivity* [143]

$$S_{AB} + S_{BC} \geq S_B + S_{ABC}\,. \tag{2.6}$$

If the evaporation happens via Hawking-pair production, the state at the horizon, $BC$, is the Unruh vacuum. In other words $B$ and $C$ are maximally entangled, like the EPR pair above, and $S_{BC} = 0$. With this, $S_{ABC} = S_A$ and the above relation becomes

$$S_{AB} \geq S_B + S_A\,. \tag{2.7}$$

On the other hand, the system $AB$ satisfies the subadditivity inequality [144]:

$$S_{AB} \leq S_A + S_B\,. \tag{2.8}$$

Putting (2.7) and (2.8) together yields

$$S_{AB} = S_A + S_B\,. \tag{2.9}$$

The systems $A$ and $B$ are thus not correlated and this implies $S_{AB} \geq S_A$ and the entropy of radiation outside never decreases. Evaporation via the Hawking pair process therefore leads to a monotonically increasing entropy of the radiation and a thermal spectrum of the final radiation.

Before giving up quantum mechanics for black hole we should ask how purity of the final radiation state can be restored? It is sometimes believed that while the leading order Hawking process may violate unitarity there may be subtle correlations that accumulate over the evaporation time scale of the black hole and eventually restore unitarity. For general relativity to be a good approximation at the horizon these corrections need to be small, suppressed by the mass of the black hole such that the horizon is the vacuum state for an infalling observer. Including such corrections to the leading order Hawking process, Mathur [2] showed that if these corrections are small (vanish when $M \to \infty$) then the von Neumann entropy will only change by a very small number

$$\frac{\delta S_n}{S_n} < 2\epsilon\,, \qquad \epsilon \ll 1\,. \tag{2.10}$$

While these corrections may decrease the slope of the entropy curve, they cannot bend it down to go to zero. This is shown in Figure 2.1(b). Hence, small corrections to the Hawking process *cannot* restore purity of the final radiation state. Instead the corrections to (2.4) have to be made *large*. This implies that we cannot have the vacuum state at the horizon and general relativity is no longer a good effective description at this scale. [3]

This result shows that unitarity can be preserved at the expense of giving up Hawking's original assumptions: If no information is to be lost, neither can there be the vacuum state at the horizon nor can quantum gravity effects be confined to the Planck (or string) scale. To

[3]Note that Mathur [2] only explicitly considers one type of correction, which even when made arbitrarily large cannot turn the entropy curve around [145]. The quantitative part of Mathur's argument is therefore unconvincing. However, Avery [146] generalized the result for all corrections, and explicitly considered a family of models that smoothly deforms the Hawking process into unitary evolution if corrections are made large. The specific unitary model that is deformed to was introduced in [147], and further discussed in [148]. This thus demonstrates the correctness of the basic approach in [2].

preserve unitarity Mathur argues that the horizon must be replaced in quantum gravity by some structure dubbed *fuzzball*.

In order to test this proposal one must construct such structure and verify that its size is of the order the horizon scale. This will be the content of Chapter 3. While large corrections at the horizon scale are needed to carry away the information by the radiation quanta, this does not necessarily imply that the motion of objects much heavier than these quanta get significantly distorted at the horizon scale. We will discuss this point in Chapter 4. For now we will continue to discuss the conditions for unitarity out of which Mathur's theorem required only one. We will discuss how the other necessary conditions make the requirement of giving up the horizon even stronger.

## 2.3 Beyond purity

The above arguments around the black hole evaporation process were based on purity of the final radiation state. While this is a necessary condition for a unitary evolution it is not sufficient. Regardless of the details of evaporation, there are at least four necessary conditions for unitarity of black hole evaporation:

1. Purity: Pure states evolve into pure state.

2. Linearity: The map between initial and final states is linear.

3. Preservation of norm: Evolution of states preserves norm.

4. Invertibility: The map of black hole initial state to the radiation is invertible.

While condition 1 has been the focus on many recent works (see [2, 66] and reactions), the other conditions have largely not been discussed to the best of our knowledge. The main goal of this Section is to discuss the implications of the latter three, especially of condition 4.

The discussion of the conditions for unitary evolution of evaporating systems in the subsequent Sections will not rely on nice slice foliations introduced in the previous Section to illustrate the Hawking process. In fact we will carry out a general study of quantum mechanical evaporation via qubit models and the conditions of unitarity without referring to a horizon. However, in order to make contact to the Hawking process, we will continue to use the notation of the previous Section for early radiation ($A$), for a newly emitted radiation quantum ($B$) and the remaining evaporating system which is divided into two subsystems ($C$ and $D$). We will introduce fictitious 'pairs' $BC$ that allow us to deform the unitary evaporation process into the Hawking process and phrase the exact statement for the break-down of unitarity in the qubit framework. We will argue that for evaporation to be unitary, $B$ has to carry away information of $D$ at every step of the evaporation. For typical states (defined as states where each small subsystem is almost maximally entangled with the remaining larger subsystem) at no point can the $BC$ system be in a pure state. For atypical states, while the $BC$ system may be in a pure state, it cannot be in a predetermined state independent of $D$. In the context of black holes this means that the state at the horizon can never be the Unruh vacuum state.

In the discussion below we assume that the dimensionality of the Hilbert space is preserved during evaporation and that the Bekenstein-Hawking entropy is a measure of the number of pre-collapse configurations [149]. We will work in a local framework of qubit evaporation and will not allow for any form of state-dependency in the transformations acting on the system. A discussion and possible concerns regarding these assumptions will be given in Section 2.5.

### 2.3.1 A 'moving-bit' model for evaporation

Following [68, 133, 67, 2, 147, 145, 148, 70, 150] we model the black hole evaporation process through the evolution of qubits. We start with a simple intuitive model before discussing the qubit formalism more generally in Subsection 2.3.2.

Consider simple unitary evolution of a system that moves, qubit by qubit, from location $x$ to location $y$. We start with a system of $n$ qubits at position $x$,

$$|\psi_0\rangle = |D_n^x\rangle \otimes \cdots \otimes |D_1^x\rangle = \bigotimes_{j=n}^{1} |D_j^x\rangle\,, \tag{2.11}$$

where each $|D_j\rangle$ is a qubit and the superscript $x$ denotes the location of a bit. Each $|D_j\rangle$ factor thus actually represents 2 qubits worth of information: 0 or 1, and $x$ or $y$. One could imagine this as the Hilbert space of $n$ spin-$\frac{1}{2}$ distinguishable particles on a 2-site lattice with all particles starting on one site. For illustrative purposes, we have taken a direct product of qubits; the evolution of arbitrary superpositions, including typical states, is determined by the evolution of this basis of states. At the first step of the evolution the first bit gets moved from location $x$ to location $y$, $|D_1^x\rangle \xrightarrow{\mathcal{U}_1} |D_1^y\rangle$. We can write $\mathcal{U}_1$ explicitly as

$$\mathcal{U}_1 = I \otimes (|1_1^y\rangle\langle 1_1^x| + |0_1^y\rangle\langle 0_1^x| + |1_1^x\rangle\langle 1_1^y| + |0_1^x\rangle\langle 0_1^y|)\,, \tag{2.12}$$

where $I$ is the identity which acts on all the other qubits. In later expressions, the identity should be assumed to act on any subspaces not shown. Subsequent evolution operators $\mathcal{U}_2$ through $\mathcal{U}_n$ have the above action on qubits 2 through $n$, respectively. By the $i$th step, the above initial state has evolved to

$$|\psi_i\rangle = \prod_{j=i}^{1} \mathcal{U}_j |\psi_0\rangle = \bigotimes_{j=n}^{i+1} |D_j^x\rangle \otimes \bigotimes_{k=i}^{1} |D_k^y\rangle \qquad i \geq 1. \tag{2.13}$$

The final state after $n$ steps,

$$|\psi_n\rangle = \prod_{j=n}^{1} \mathcal{U}_j |\psi_0\rangle = \bigotimes_{j=n}^{1} |D_j^y\rangle\,, \tag{2.14}$$

is thus just a relocation of the original state.

In this way we can view the 'moving bit' model as a simple evaporation process. Having demonstrated how the basis vectors in (2.11) evolve; the evolution of superpositions of the states of that form follow from the above.

This kind of evaporation looks qualitatively different than black hole evaporation, where it seems that at each step two extra qubits are created. However, since the infalling member of

the Hawking-pair has negative energy it is supposed to somehow cancel with a quantum of the original matter. In order to put unitary models like the 'moving bit' model and potentially non-unitary pair creation models on the same footing, Avery [146] introduced a general model space in which at each time step two extra qubits are created, just like one might model Hawking-pair creation, but one also must define two internal black hole qubits to be auxiliary [146]. By tracing out the auxiliary degrees of freedom one gets a description of the physical, fixed-dimensional Hilbert space. Thus, the auxiliary degrees of freedom are simply a convenient way of parameterizing potentially non-unitary evolution, such as occurs in models of Hawking-pair creation. By the end of the evolution, all of the physical degrees of freedom are radiation, and therefore by definition the remaining black hole degrees of freedom are all auxiliary. More details can be found in Subsection 2.3.2.

We would now like to illustrate how one can reinterpret the above model as a pair creation process using the ideas from [146]. Since the model we give below is simply a rewriting of the above model, it is manifestly unitary. In the 'moving bit' model we are considering, two auxiliary qubits are introduced at each step as follows. The first step of the 'evaporation' process of (2.11) is given by

$$\mathcal{I}_1|\psi_0\rangle = \bigotimes_{j=n}^{2} |D_j^x\rangle \otimes |d_1^x\rangle \otimes |c_1^x\rangle \otimes |B_1^x\rangle\,, \tag{2.15}$$

where $|B_1^x\rangle$ and $|c_1^x\rangle$ are the created pair. The two lower-case qubits, $|d_1^x\rangle$ and $|c_1^x\rangle$, are the auxiliary qubits. To match our 'moving bit' model we have $B_1 = D_1$. Since we are introducing new degrees of freedom, $\mathcal{I}_1$ is not unitary; however, conservation of probability demands that it be isometric, that is to say it must satisfy $\mathcal{I}_1^\dagger \mathcal{I}_1 = I$. This constraint along with $B_1 = D_1$ ensures that the states $|d_1^x\rangle$ and $|c_1^x\rangle$ must be independent of the initial state $|\psi_0\rangle$. (If this point is not clear, it is elaborated on in Subsection 2.3.3.) When this is true, we say that the auxiliary qubits are in fiducial form, 'bleached', or 'zeroed'. Let us comment that the fiducial form can be any predetermined state, so long as it is totally independent of the initial conditions. It should be clear, then, that this step is a trivial rewriting of the state $|\psi_0\rangle$.

This is followed by the unitary transformation $\mathcal{U}_1'$ relocating the qubit $|B_1^x\rangle$ to location $y$ via $|B_1^x\rangle \xrightarrow{\mathcal{U}_1'} |B_1^y\rangle$. Hence, the state after emission of one qubit is

$$|\psi_1\rangle = \mathcal{U}_1'\mathcal{I}_1|\psi_0\rangle = \bigotimes_{j=n}^{2} |D_j^x\rangle \otimes |d_1^x\rangle \otimes |c_1^x\rangle \otimes |B_1^y\rangle\,. \tag{2.16}$$

Similarly, the state at the $i$th step is

$$|\psi_i\rangle = \bigotimes_{j=n}^{i+1} |D_j^x\rangle \otimes \bigotimes_{k=i}^{1} \Big(|d_k^x\rangle \otimes |c_k^x\rangle\Big) \otimes \bigotimes_{m=1}^{i} |B_m^y\rangle\,, \tag{2.17}$$

and the final state is

$$|\psi_n\rangle = \bigotimes_{j=n}^{1} \Big(|d_j^x\rangle \otimes |c_j^x\rangle\Big) \otimes \bigotimes_{m=1}^{n} |B_m^y\rangle. \tag{2.18}$$

Since the auxiliary qubits must all be in fiducial form given by some state $|\phi\rangle$, we can write them as [4]

$$|d_i^x\rangle \otimes |c_i^x\rangle = |\phi\rangle \otimes |\phi\rangle \quad \forall\ i \tag{2.19}$$

so the final step may be written

$$|\psi_n\rangle = \bigotimes_{j=1}^{2n} |\phi\rangle \otimes \bigotimes_{m=1}^{n} |B_m^y\rangle. \tag{2.20}$$

After tracing out the auxiliary degrees of freedom in (2.20) and recalling that for our simple model $|B_i^y\rangle = |D_i^y\rangle$, we see that the final state is just the relocated initial state (2.11). In this simple model of evaporation using auxiliary qubits one can easily see that information leaves the system in every step of the evaporation process.

Let us note that for the specific evolution shown above, the entanglement $S_{B_i c_i}$ is zero at every step; however, the evolution is for a very special basis of states of the form (2.11). A generic state will be a superposition of states of that form. Since the $c_i$ are always in fiducial form, they are direct-producted into the state. Therefore $S_{B_i c_i} = S_{B_i}$, but since we are just moving qubits this is equivalent to computing $S_{D_i}$ in the initial state. We can then appeal to Page [131] to argue that generically for large $n$, $D_i$ is maximally entangled with the rest of the degrees of freedom. Thus, in this model, for typical initial states $S_{B_i c_i}$ is nonzero *at every step*. For atypical initial states, even though $S_{B_i c_i}$ may be zero at some steps, the $B_i c_i$ system is not in a predetermined state which is independent of the initial state.

The important technical lesson here is that unitarity requires the newly emerging $B_i$ quantum (that leaves the system) to carry information of the remaining $D_i$ quantum (that is part of the interior of the system) and avoiding quantum cloning means that the $D_i$ quantum has to be bleached. Unitarity also requires the auxiliary quanta $c_i$ to be bleached. We give a more detailed account of this in Subsections 2.3.2 and 2.3.3.

### 2.3.2 Qubit models of evaporation

The simple model in the previous section serves as an example of unitary evolution that demonstrates for typical states $S_{BC} \neq 0$ at every step of the evolution. For atypical states while $S_{BC}$ may be zero for some steps, the $BC$ system is not in a predetermined state independent of the initial state. Thus in all cases the $BC$ system cannot be in a predetermined state which is independent of the state of the evaporating system during any step of the evaporation. We buttress the above model with a second example. The model below explores what happens if the $BC$ system is in the Hawking-state (and thus has $S_{BC} = 0$) until Page time, at which point one allows for a more general (unitary) evolution.

[4] Note that the fiducial state could take step dependent values, so that the $d$'s and $c$'s have different values at different steps. However, the algorithm assigning the values must be independent of the initial state. For simplicity we take them to be given by the same state $|\phi\rangle$ for all steps.

### General qubit model structure

We start by reviewing the general structure of these qubit models. For more details and more models the reader is referred to [146] (see [68, 133, 67, 2, 147, 145, 148, 70, 150] for related models). The initial matter is modeled as a set of $n$ 'matter qubits':

$$\rho_0 = |\psi_0\rangle\langle\psi_0| \qquad |\psi_0\rangle \in \text{span}\{|\hat{q}_1 \cdots \hat{q}_n\rangle\} \tag{2.21}$$

where each $\hat{q}$ is a qubit. After a sequence of intermediate steps the final state consists entirely of radiation, modeled as a (possibly mixed) density matrix, $\rho_f$, acting on $n$ radiation qubits. Throughout the evolution we keep the dimension of the physical Hilbert space fixed.

Following [147], we use hats to distinguish the internal black hole qubits from the external radiation qubits. The hatted qubits represent all degrees of freedom that are inaccessible outside the black hole; unlike [2], we do not distinguish between degrees of freedom from the initial matter, from gravitational interactions, or any that arise during the evaporation process. One could model general (not necessarily unitary) discrete time evolution on the $n$-qubit Hilbert space in two ways [146, 151]: as a sequence of mappings [5] on $n$-qubit density matrices, or alternatively as unitary transformations on pure states in an enlarged Hilbert space. In typical applications, one imagines that the additional degrees of freedom in the enlarged Hilbert space represent environmental degrees of freedom; however, since we are considering potentially fundamental non-unitarity, the additional degrees of freedom are just 'auxiliary' degrees of freedom. Motivated by the latter and typical discussions of the pair creation process, we model the dynamics as a sequence of isometric mappings in an enlarging Hilbert space. The extra degrees of freedom are auxiliary variables that provide a convenient language to discuss a more general evolution. While we keep the dimension of the *physical* Hilbert space fixed, at each step of emission we introduce two auxiliary qubits. Thus on the $i$th step of the evolution, the total state is described by a $n+2i$ qubit state $|\psi_i\rangle$ with $2i$ hatted auxiliary qubits and $i$ radiation qubits. At each step $i$, the physical state may be recovered by tracing over the auxiliary space

$$\rho_i = tr_{aux}\left(|\psi_i\rangle\langle\psi_i|\right) . \tag{2.22}$$

We model the evolution in two steps: a creation step effected by isometric operators $\mathcal{I}_i$; [6] and an internal evolution step effected by unitary $\hat{U}_i$ acting on the hatted qubits and unitary $U_i$ acting on the unhatted radiation qubits. Basis vectors at each step look like

$$\text{span}\left\{|\hat{q}_1\hat{q}_2\cdots\hat{q}_{n+i}\rangle|q_i q_{i-1}\cdots q_1\rangle\right\} \xrightarrow{\mathcal{I}_i} \text{span}\left\{|\hat{q}_1\hat{q}_2\cdots\hat{q}_{n+i}\hat{q}_{n+i+1}\rangle|q_{i+1}q_i q_{i-1}\cdots q_1\rangle\right\} \tag{2.23}$$

$$\xrightarrow{\hat{U}_i\otimes U_i} \text{span}\left\{|\hat{q}_1\hat{q}_2\cdots\hat{q}_{n+i}\hat{q}_{n+i+1}\rangle|q_{i+1}q_i q_{i-1}\cdots q_1\rangle\right\} \tag{2.24}$$

The qubits are arranged in the above order to match with a crude notion of locality expected on the nice slices [2, 147].

For the majority of the discussion, we focus on the $\mathcal{I}_i$ and are content to set $\hat{U}_i = U_i = I$. What properties should the $\mathcal{I}_i$ satisfy? Conservation of probability and the linearity of quantum

[5] Physically reasonable requirements suggest that the mappings should be trace-preserving quantum operations [151]. Thus, the two descriptions correspond to the operator–sum representation and the environmental-coupling representation of quantum operations.

[6] These were called $C_i$ in [146].

mechanics suggest that the $\mathcal{I}_i$ should preserve the norm and be linear, which means that we should require

$$\mathcal{I}_i^\dagger \mathcal{I}_i = I\,, \tag{2.25}$$

where there is no sum on $i$. Note that $\mathcal{I}_i$ is an isometric, but non-unitary mapping. We also assume that, apart from the newly created pair, the $\mathcal{I}_i$ act only on the hatted black hole qubits and not on the unhatted radiation qubits which are far away from the pair creation site.

We can write the $\mathcal{I}_i$ in the following form

$$\mathcal{I}_i = |\varphi_1\rangle \otimes \hat{P}_1 + |\varphi_2\rangle \otimes \hat{P}_2 + |\varphi_3\rangle \otimes \hat{P}_3 + |\varphi_4\rangle \otimes \hat{P}_4\,, \tag{2.26}$$

where $|\varphi_j\rangle$ are an orthonormal basis for the created pair qubits, and the $\hat{P}$'s are linear operators which act on the previous hatted qubits (with implicit $i$ dependence). Since there are no operators acting on the unhatted radiation qubits, the evolution of qubits outside the black hole is local. Following [68, 147], we use the basis

$$\begin{aligned}
|\varphi_1^i\rangle &= \frac{1}{\sqrt{2}}\big(|\hat{0}_{n+i+1}\rangle|0_{i+1}\rangle + |\hat{1}_{n+i+1}\rangle|1_{i+1}\rangle\big)\,,\\
|\varphi_2^i\rangle &= \frac{1}{\sqrt{2}}\big(|\hat{0}_{n+i+1}\rangle|0_{i+1}\rangle - |\hat{1}_{n+i+1}\rangle|1_{i+1}\rangle\big)\,,\\
|\varphi_3^i\rangle &= |\hat{0}_{n+i+1}\rangle|1_{i+1}\rangle\,,\\
|\varphi_4^i\rangle &= |\hat{1}_{n+i+1}\rangle|0_{i+1}\rangle\,,
\end{aligned} \tag{2.27}$$

for the newly created pair. The constraint in Equation (2.25) implies the following condition on the $\hat{P}$s:

$$\mathcal{I}_i^\dagger \mathcal{I}_i = \hat{P}_1^\dagger \hat{P}_1 + \hat{P}_2^\dagger \hat{P}_2 + \hat{P}_3^\dagger \hat{P}_3 + \hat{P}_4^\dagger \hat{P}_4 = \hat{I}\,. \tag{2.28}$$

Note that this defines the $\hat{P}$s as a set of generalized measurement operators acting on the black hole Hilbert space. A fully specified model, then, entails

1. A set of $\hat{P}$s at each step $i$ that satisfy the completeness relation (2.28).
2. The unitary operators $\hat{U}_i$ and $U_i$ for each $i$.
3. A clear delineation of the auxiliary subspace at each step $i$.

This gives a very general model space that makes it easy to compare and contrast different models of evolution. We investigate the conditions for unitarity of the evolution in more detail in Subsection 2.3.3, but let us now give the basic picture. If one wants to acquire the fixed-dimensional Hilbert space description then one must trace out the auxiliary degrees of freedom at each step. Thus, in unitary models the auxiliary degrees of freedom must be direct-producted into the physical state. Since in a unitary model the physical state is by definition a unitary transformation from the previous physical state and since there can be no entanglement with auxiliary degrees of freedom for all previous physical states, the auxiliary degrees of freedom must be put into a fiducial state. That is to say, in unitary models the auxiliary degrees of freedom must be bleached of all information. Regardless of the details of the model, at the end of $n$ steps, when the black hole is supposed to have evaporated away, all of the hatted qubits are auxiliary and should be traced over to recover the physical state of the radiation.

### A pure but non-unitary evaporation

With this brief overview on qubit models we are ready to discuss (non-unitary) models. We consider a model which has $S_{BC} = 0$ for the first half of the evolution (until Page time) and $S_{BC} \neq 0$ in the second half. In this model the entropy of radiation before Page time goes up while after Page time it goes down again. We consider an initial state of $n$ qubits,

$$|\hat{q}_1 \cdots \hat{q}_n\rangle. \tag{2.29}$$

For simplicity, let us take $n$ even. For the first $n/2$ time steps let the pair creation be governed by exactly the Hawking-pair creation process

$$\mathcal{I}_i = |\varphi_1^i\rangle \otimes \hat{I} \quad \text{for} \quad i \leq \frac{n}{2}\,. \tag{2.30}$$

In each subsequent step we want to emit the information of all the earlier ingoing qubits from the black hole; this is achieved by mapping the information of an earlier ingoing qubit to a newly created outgoing qubit while bleaching the former via the operator

$$\begin{aligned} \mathcal{I}_i &= \frac{1}{\sqrt{2}}(|\varphi_1^i\rangle + |\varphi_2^i\rangle) \otimes |\hat{0}\rangle\langle\hat{0}|_{\frac{n}{2}+i} + |\varphi_3^i\rangle \otimes |\hat{0}\rangle\langle\hat{1}|_{\frac{n}{2}+i} \\ &= |\hat{0}0\rangle_{\text{pair}} \otimes |\hat{0}\rangle\langle\hat{0}|_{\frac{n}{2}+i} + |\hat{0}1\rangle_{\text{pair}} \otimes |\hat{0}\rangle\langle\hat{1}|_{\frac{n}{2}+i} \quad \text{for} \quad i > \frac{n}{2}\,. \end{aligned} \tag{2.31}$$

The $\hat{P}_i$ act on the $(\frac{n}{2}+i)$th black hole qubit (which is the infalling member of one of the Hawking-pair states created during the first $\frac{n}{2}$ states). The information of this qubit is mapped to the $i$th outgoing qubit of the newly created pairs while the $(\frac{n}{2}+i)$th black hole qubit has to be set to a fiducial value which we choose to be zero. In addition the new infalling qubit is also bleached to zero. This part of the evolution is equivalent to a model without auxiliary qubits that just emits (removes the hat from) the $(\frac{n}{2}+i)$th qubit; that is to say, it is equivalent to the 'moving bit' model introduced in Subsection 2.3.1. Let us work through a 4 qubit example of the evolution to illustrate the dynamics:

$$|\hat{q}_1\hat{q}_2\hat{q}_3\hat{q}_4\rangle \xrightarrow{i=1} \frac{1}{\sqrt{2}}\,|\hat{q}_1\hat{q}_2\hat{q}_3\hat{q}_4\rangle(|\hat{0}0\rangle + |\hat{1}1\rangle) \tag{2.32}$$

$$\xrightarrow{i=2} \frac{1}{2}\;|\hat{q}_1\hat{q}_2\hat{q}_3\hat{q}_4\rangle(|\hat{0}\hat{0}00\rangle + |\hat{0}\hat{1}10\rangle + |\hat{1}\hat{0}01\rangle + |1\hat{1}11\rangle) \tag{2.33}$$

$$\xrightarrow{i=3} \frac{1}{2}\;|\hat{q}_1\hat{q}_2\hat{q}_3\hat{q}_4\hat{0}\rangle(|\hat{0}\hat{0}000\rangle + |\hat{1}\hat{0}010\rangle + |\hat{0}\hat{0}101\rangle + |\hat{1}\hat{0}111\rangle) \tag{2.34}$$

$$\xrightarrow{i=4} \frac{1}{2}\;|\hat{q}_1\hat{q}_2\hat{q}_3\hat{q}_4\hat{0}\hat{0}\hat{0}\hat{0}\rangle(|0000\rangle + |1010\rangle + |0101\rangle + |1111\rangle). \tag{2.35}$$

In the first two steps evaporation happens by the Hawking mechanism and in the subsequent two steps the previously created infalling member of the Hawking-pair is spat out. It is easy to verify that the von Neumann entropy of the radiation behaves like Page's prediction in Figure 2.1a. However, it is also easy to see that the final state, obtained by tracing out the hatted black hole qubits, is independent of the initial state. This evolution is not invertible and thus not unitary.

Note that this model has a pure final state. It also allows for the state of the created pair to be the Hawking-pair state for the first half of the evolution thus allowing for free infall of observers through the horizon until Page time. This clearly demonstrates that purity of the final state of radiation does not necessarily ensure unitarity of the evaporation process.

### 2.3.3 Conditions for unitarity

Before going into conditions for unitary evolution of the physical degrees of freedom, let us first discuss isometries in generality for a moment. Consider an isometric operator $\mathcal{I}$ that maps states from one Hilbert space $\mathcal{H}_1$ to another (at least as big) Hilbert space $\mathcal{H}_2$. Let us introduce an orthonormal basis of states for $\mathcal{H}_1$, $\{|\hat{w}_i\rangle\}$, then the most general isometry may be written as

$$\mathcal{I} = \sum_i |v_i\rangle\langle\hat{w}_i|, \tag{2.36}$$

where $|v_i\rangle \in \mathcal{H}_2$. At this point, we have not said anything about the states $|v_i\rangle \in \mathcal{H}_2$; however, the isometry condition is

$$\hat{I} = \mathcal{I}^\dagger\mathcal{I} = \sum_{i,j} |\hat{w}_i\rangle\langle v_i|v_j\rangle\langle\hat{w}_j|. \tag{2.37}$$

Writing $\hat{I} = \sum_i |\hat{w}_i\rangle\langle\hat{w}_i|$, we conclude that the $|v_i\rangle$ must be orthonormal. Let the range of $\mathcal{I}$ be the subspace $\mathcal{V} \subset \mathcal{H}_2$ where $\dim\mathcal{V} = \dim\mathcal{H}_1 \leq \dim\mathcal{H}_2$. We can decompose $\mathcal{H}_2$ as the direct product $\mathcal{H}_2 = \mathcal{V} \oplus \mathcal{V}^\perp$. Moreover, when $\dim\mathcal{H}_1$ divides $\dim\mathcal{H}_2$, as is true for qubits, we may decompose as $\mathcal{H}_2 = \mathcal{V}' \otimes \mathcal{B}$, where $\mathcal{V}'$ is isomorphic to $\mathcal{V}$. The kets $|v_i\rangle$ then decompose as

$$|v_i\rangle = |v_i'\rangle \otimes |b\rangle, \tag{2.38}$$

where all $|v_i\rangle$ have the same $|b\rangle \in \mathcal{B}$. This is all to say that the isometry $\mathcal{I} : \mathcal{H}_1 \to \mathcal{V}' \otimes \mathcal{B}$ must act on $|\hat{w}\rangle \in \mathcal{H}_1$ as

$$\mathcal{I} : |\hat{w}\rangle \mapsto \big(U|\hat{w}\rangle\big) \otimes |b\rangle, \tag{2.39}$$

where $U$ is a unitary transformation and $|b\rangle$ does not depend on the state $|\hat{w}\rangle$. This follows from the no-cloning theorem. Thus every isometry can be given by specifying the bleaching subspace $\mathcal{B}$, its fiducial state $|b\rangle$, and the unitary transformation $U$. Therefore, every isometry that is not unitary necessarily bleaches a bleaching subspace $\mathcal{B}$ with dimension $\dim\mathcal{B} = \dim\mathcal{H}_2/\dim\mathcal{H}_1$ – a unitary isometry would has an empty bleaching space B.

Returning to qubit models of black hole evaporation, recall that to describe the physical $n$-qubit space, we need to trace out the 'auxiliary' subspace. On step $i$, let the $2i$-qubit auxiliary subspace be $\mathcal{A}_i$. Suppose that the evolution of the *physical* degrees of freedom up to step $i$ have been unitary. This means that tracing $\mathcal{A}_i$ out of $|\psi_i\rangle$ gives a pure state:

$$\mathrm{tr}_{\mathcal{A}_i}\left(|\psi_i\rangle\langle\psi_i|\right) = |\Psi_i\rangle\langle\Psi_i|, \tag{2.40}$$

where $|\Psi_i\rangle$ describes the $n$-qubits worth of physical degrees of freedom. Moreover, unitarity means that $|\Psi_i\rangle$ is a unitary transformation of the initial $n$-qubit state $|\psi_0\rangle$:

$$|\Psi_i\rangle = U|\psi_0\rangle. \tag{2.41}$$

The cumulative isometry from the initial state $|\psi_0\rangle$ to the state $|\psi_i\rangle$ given by $\mathcal{I}_i\mathcal{I}_{i-1}\cdots\mathcal{I}_1$ maps an $n$-qubit space into a $(n+2i)$-qubit space, thus the bleaching subspace $\mathcal{B}$ of the cumulative isometry must coincide with the auxiliary subspace $\mathcal{A}_i$. If this were not true, then tracing out $\mathcal{A}_i$ would not give a pure state for all possible initial states $|\psi_0\rangle$. This follows from the general form of an isometry in Equation (2.39) and the no-cloning theorem.

Now, consider the evolution from $|\psi_i\rangle$ to $|\psi_{i+1}\rangle$. The isometry $\mathcal{I}_{i+1}$ maps the $(n+2i)$-qubit space into a $(n+2i+2)$-qubit space and thus has a 2-qubit bleaching space $\mathcal{B}$. By assumption, we know that $\mathcal{I}_{i+1}$ acts as the identity on the $i$ radiation qubits outside the black hole. If $\mathcal{I}_{i+1}$ is going to generate unitary evolution of the physical degrees of freedom, then tracing out $\mathcal{A}_{i+1}$ needs to give a pure state $|\Psi_{i+1}\rangle$, which is also a unitary transformation of $|\Psi_i\rangle$. One can then see that the 2-qubit bleaching space of $\mathcal{I}_{i+1}$ must coincide with the 2-qubit space added to $\mathcal{A}_i$ to form $\mathcal{A}_{i+1}$.

By contrast, evolution for which the von Neumann entropy of the created pair ($S_{BC} = 0$) vanishes for all possible 'input states', $|\psi_i\rangle$, is necessarily non-unitary. If the created pair is not entangled with the rest of the system for all $|\psi_i\rangle$, then the creation operator must be of the form

$$\mathcal{I} = |\psi_{\text{pair}}\rangle \otimes \hat{P}\,. \tag{2.42}$$

Thus, the pair state space corresponds to the bleaching space $\mathcal{B}$ and $\hat{P}$ must be unitary in order to satisfy (2.25) so that probability is conserved. On the other hand, we know that at each time step two new qubits must become part of the auxiliary space. If the physical evolution is going to be unitary, then that auxiliary space must be part of the bleaching space, projected into a fiducial form. As discussed in [146], there are two slightly different ways to do this: either both new auxiliary qubits can be chosen from the old hatted qubits, or the new black hole qubit in the pair state can be put in fiducial form along with one old hatted qubit. Let us note that the second possibility already implies that the pair is not in the Hawking-state $|\varphi_1^i\rangle$. Regardless, unitarity of the physical evolution demands that $\mathcal{I}$ projects at least one qubit's worth subspace of the old black hole qubits into fiducial form; however, it is not simultaneously possible for $\hat{P}$ to be unitary and to project out a two-dimensional subspace. Hence the Hawking-pair production always leads to a non-unitary evolution.

If one does not take the above conditions for unitarity at intermediate steps seriously and only wishes to discuss unitarity in terms of the initial and final states, then one may be tempted to circumvent the above argument in the following way. One might suggest that the evolution does not bleach qubits on some early steps in the evolution, and then make up for it at the end of the evolution by bleaching more degrees of freedom; however, this too is not possible. At each step, one only has enough freedom to bleach at most 2 qubits worth of degrees of freedom, and there are only $n$ steps to bleach $2n$ black hole qubits. The freedom to bleach 2 qubits comes precisely from the 4-dimensional pair space. This was exactly why the model in Subsection 2.3.2 failed to be unitary. It should be clear that while our discussion uses qubits, the arguments apply more generally.

Alternatively, one might suggest that demanding that the pair has vanishing entanglement for *all* input states is too restrictive. This is especially true if one subscribes to the argument advanced in [152, 153] that young black holes are 'special.' How special do young black holes need to be? If the 4-dimensional bleaching space is all old black hole qubits (the first possibility mentioned in the previous paragraph), then the $|v_i\rangle$ in Equation (2.39) must span the remaining $2^{n+i}$ dimensional space *including the 4 pair states*. Thus, the subspace which produces the Hawking state has codimension 4 with the total space of input states assuming unitarity *at each step* of the evolution. A model of this kind is proposed in [147], along with the suggestion that the black hole starts in a specific state.

## 2.4 Where is the information?

We can more precisely quantify what happens to the information by using the standard quantum information technique of entangling degrees of freedom with a fictitious reference system [151]. We follow the approach of Giddings and Shi [145], which refers to earlier work in this context [154]. In order to quantify what then happens in the evaporation process to all possible initial states, we can introduce a 'tracking state' that is maximally entangled between the black hole initial state and the reference system:

$$|T\rangle = \frac{1}{2^{\frac{n}{2}}} \sum_{i=1}^{2^n} |\hat{w}_i\rangle |\tilde{r}_i\rangle \,, \tag{2.43}$$

where $\{|\hat{w}_i\rangle\}$ is an orthonormal basis for the $n$-qubit initial state, and $\{|\tilde{r}_i\rangle\}$ is an orthonormal basis for the $n$-qubit reference system. We then evolve the black hole degrees of freedom using the evolution under study, while acting on the reference system by the identity. This allows us to keep track of the fate of each initial state—the location of the initial entanglement with the reference system tells us the fate of the information.

As discussed in [145], using the state $|T\rangle$, the decrease of the von Neumann entropy of the black hole degrees of freedom quantifies how much information has *left* the black hole; whereas the von Neumann entropy of the external radiation quantifies how much information is now in the radiation alone. In general, these two quantities need not be equal, since information may be stored in the correlations between the two subsystems. The amount of extra correlation is given by the mutual information between the two subsystems, which [145] conjectures to be zero for black hole evaporation. When the mutual information vanishes, Giddings and Shi term the evolution 'subsystem transfer' [145]. Perhaps the simplest example of subsystem transfer would be the moving bit model in Subsection 2.3.1.

In fact, as we now show, in our qubit framework one finds that any unitary evolution necessarily has vanishing mutual information between the black hole and the radiation with the tracking state $|T\rangle$. Let the space of black hole qubits at step $i$ be $D_i$, and the space of radiation qubits be $A_i$. Recall from the discussion in the previous section that unitarity demands that at every step of the evolution two qubits of $D_i$ be bleached of information, while only one hatted qubit is created. Thus, at step $i$ the effective dimension of $D_i$ is $2^{n-i}$-dimensional, and therefore

$$S(D_i) \leq (n-i)\log 2. \tag{2.44}$$

On the other hand subadditivity implies that

$$S(D_i) + S(A_i) \geq S(D_i A_i) = n \log 2 \,, \tag{2.45}$$

where the last step follows from the form of the tracking state and the reference degrees of freedom not mixing with the rest of the system. Together (2.44) and (2.45) imply

$$S(A_i) \geq i \log 2 \,. \tag{2.46}$$

Since the space of radiation qubits is $2^i$-dimensional, it follows that

$$S(A_i) = i \log 2 \,, \qquad S(D_i) = (n-i)\log 2 \tag{2.47}$$

for all $i$. Thus, we find that unitary evolution implies that information leaves the black hole at *every step* via 'subsystem transfer'. Let us note that the requirement may be relaxed slightly if one supposes that the dimension of the physical Hilbert space increases in the evaporation process, so that there are more than $n$ steps of evolution for the information to come out; however, one still finds that information comes out from the beginning of the evolution if the extra steps are evenly interspersed. Even if one frontloads the extra steps, according to arguments of [149] one still only anticipates 30% extra steps and information still starts coming out well before Page time. We discuss our assumptions about the size of the Hilbert space more in Section 2.5.

One may be confused by the above statement since Page's result [131] is often colloquially stated as showing that information starts leaving the black hole only after the black hole has evaporated halfway. In fact, Page's result shows that one may start *reconstructing* the original black hole state only after Page time, after the black hole has evaporated halfway. This is actually a different statement. Page's result is further weakened by the observations in [154] that after Page time new information entering the black hole may be recovered in the black hole scrambling time, and black holes have subsequently been conjectured to be the fastest physically achievable scramblers in nature [155].

Using the above tracking state, we may also quantify how much information has been lost in the case of non-unitarity evolution. In particular, the von Neumann entropy of the auxiliary subsystem $\mathcal{A}_i$ measures the entanglement between the reference system and the auxiliary degrees of freedom. In other words, for the tracking state $|T\rangle$, $S(\mathcal{A}_i)$ gives the amount of information lost. Let us illustrate this with an example. Let the initial black hole state with basis $\{|\hat{w}_j\rangle\} \in D_0$ be a 2-qubit system that is maximally entangled with a reference system system with basis $\{|\tilde{r}_j\rangle\} \in R_0$ in a tracking state (2.43) that is initially of the form

$$|T_0\rangle = \frac{1}{2}\Big(|\hat{0}\hat{0}\rangle|\tilde{0}\tilde{0}\rangle + |\hat{0}\hat{1}\rangle|\tilde{0}\tilde{1}\rangle + |\hat{1}\hat{0}\rangle|\tilde{1}\tilde{0}\rangle + |\hat{1}\hat{1}\rangle|\tilde{1}\tilde{1}\rangle\Big). \tag{2.48}$$

Let the evolution be governed by an isometry that mimics the moving bit model of Subsection 2.3.1: [7]

$$\mathcal{I}_i = \Big(|\hat{0}\hat{0}\rangle|0\rangle\langle\hat{0}|_{(3-i)} + |\hat{0}\hat{0}\rangle|1\rangle\langle\hat{1}|_{(3-i)}\Big)_{D_{i-1}} \otimes I_{A_{i-1}} \otimes I_{R_{i-1}} \quad \text{for} \quad i = 1, 2 \tag{2.49}$$

where the subscript $(3-i)$ on the RHS indicates the action on the $(3-i)$th hatted qubit of the black hole system $D_{i-1}$ at the $i$th step and the action on the reference system $R_{i-1}$ and the outside radiation $A_{i-1}$ is the identity. The first step of the evolution yields

$$|T_1\rangle = \mathcal{I}_1|T_0\rangle = |\hat{0}\hat{0}\rangle \otimes \frac{1}{2}\Big(|\hat{0}0\rangle|\tilde{0}\tilde{0}\rangle + |\hat{0}1\rangle|\tilde{0}\tilde{1}\rangle + |\hat{1}0\rangle|\tilde{1}\tilde{0}\rangle + |\hat{1}1\rangle|\tilde{1}\tilde{1}\rangle\Big). \tag{2.50}$$

By comparison with (2.39) we can see that the direct producted state comes from the bleaching space $\mathcal{B}_1$. The unhatted qubits are the radiation qubits in $A_1$; which of the hatted qubits are part of the physical space of black hole qubits $D_1$ after tracing out the auxiliary space $\mathcal{A}_1$ is part of the model. Here we are interested in how much information we loose if we trace over the remaining hatted qubit of the initial state and one of the qubits of the bleaching space. We can easily verify that the thus obtained density matrix $\rho_1 = \mathrm{Tr}_{\mathcal{A}_1}|T_1\rangle\langle T_1|$ has $\mathrm{Tr}\rho_1^2 < 1$ and is

[7] Note that (2.49) is the same evolution operator as (2.31).

thus mixed. How much information we lost by tracing out part of the initial state is encoded in $S(\mathcal{A}_1)$. The density matrix in the auxiliary space is

$$\rho_1^{aux} = |\hat{0}\rangle\langle\hat{0}| \otimes \frac{1}{2}\Big(|\hat{0}\rangle\langle\hat{0}| + |\hat{1}\rangle\langle\hat{1}|\Big)\,, \tag{2.51}$$

with von Neumann entropy

$$S(\mathcal{A}_1) = -\mathrm{Tr}(\rho_1^{aux}\log\rho_1^{aux}) = \log 2\,. \tag{2.52}$$

The auxiliary space thus contains the maximal information of the traced out qubit that has been part of the initial black hole state. After the second evolution step we identify the auxiliary space $\mathcal{A}_2$ with the bleaching space $\mathcal{B}_2$ and the final state of the radiation is given by the density matrix

$$\rho_2^{rad} = \mathrm{Tr}_{\{R_2,\mathcal{A}_2\}}(\mathcal{I}_2\rho_1\mathcal{I}_2^\dagger) = \frac{1}{2}\Big(|00\rangle\langle 00| + |01\rangle\langle 01|\Big)\,. \tag{2.53}$$

While in this simple example we have chosen the initial state to be a 2-qubit system the extension to $n$-qubit systems is straightforward. This example shows that if, at any step $i$ of the evolution, we trace out a qubit that is maximally entangled with the remaining system we lose the maximal amount of information of $\log 2$ on that qubit encoded in the von Neumann entropy $S(\mathcal{A}_i)$ of the auxiliary space at that step. While this simple example results in the maximum amount of information loss on a qubit, more general examples should have $0 < S(\mathcal{A}_i) < \log 2$ for each physical qubit that has erroneously been traced out. That unitary evolution should have no information loss and therefore $S(\mathcal{A}_i) = 0$ for the tracking state, immediately implies that the auxiliary space must coincide with the bleaching space in accord with the discussion in the previous subsection. Let us emphasize that the interpretations of the entanglement entropies discussed in this section only hold when considering the state $|T\rangle$.

## 2.5 Discussion of the results

Since most of the discussion in this section was technical we now recap the main result, mention the assumptions we have made and analyze similarities and differences with ideas of some other works.

In Section 2.3 we used qubit models to show that:

1. Unitary evaporation requires *information of the original state to come out in every step of the evolution.*

2. There is *no difference between before and after Page time as far as information release is concerned.* [8]

We have worked with four main assumptions which we list here explicitly so as to help make the comparison of our results with other models of quantum black holes easier.

[8] As noted before, while *decoding* of information may only be possible when having access to more than half of the evaporating system (after Page time), the *release* of information must start with the very first quantum being emitted.

- *The dimension of physical Hilbert space is constant*
  The first assumption we made in our work is that the dimension of the physical Hilbert space does not change. While one would certainly expect this to be true for any unitary theory, and thus for quantum gravity in particular, one may still be concerned that the qubit model is not able to capture all the Hilbert space when the volume in which the radiation is being emitted is infinite. In particular the irreversibility of free streaming Hawking radiation leads to about 30% extra entropy in the radiation compared to the black hole [149] [9] (at the same time it is also shown in [149] that if the black hole is allowed to evaporate in a reversible manner the entropy of the radiation equals that of the black hole). Thus one may wonder if there is a possible loophole in our argument for free streaming Hawking radiation. While it is indeed true that the qubit model is unable to capture free streaming processes and one may think that some fraction of the created pairs may be in a special state (although for true free streaming they would not be in a special state but a random state), we would expect such events to be interspersed and not to affect our general argument. Furthermore, this cannot get one all the way to Page time.

- *The black hole initial state is not special*
  Another assumption we made is that the black hole formed is itself not in a special state to begin with, otherwise the emitted radiation would also be in a special state. There have been some papers advocating that in a suitably fine-grained description the number of degrees of freedom available to ordinary matter is parametrically smaller than the entropy of the black hole [152, 153]. We find this claim puzzling for two reasons. In a large enough box radiation can have arbitrarily many fine-grained configurations. Adiabatically collapsing the box does not change the number of possible configurations and the final state of the collapse, the black hole, can thus not be in a predetermined state. This idea is supported by Zurek's calculation [149] that a black hole can be allowed to evaporate in a reversible manner. One may object that a black hole is not ordinarily made in such a controlled fashion but rather by collapsing a shell. However, the fundamental properties of black holes should not depend on how they were formed. Secondly, even though black holes formed by 'normal' astrophysical collapse may only occupy a small part of the total initial state space, it seems strange to posit that these states coincide with the states that are treated specially by the *dynamics*, especially in light of the fast scrambling conjecture.

- *The evaporation process can be described within a local framework*
  In our discussion of black hole evaporation via qubit models we did not allow for any form of non-local effects that might somehow map the information to the outside radiation. While one might argue that a theory of quantum gravity will be non-local to some extent, one would have to specify the degree of non-locality outside the horizon and explain how it alters (or why it does not alter) physics in other systems consistent with experiments. For example Giddings, in a series of papers [145, 156, 157], argues that information can be recovered if we give up the notion of *local* quantum field theory as an exact framework. It is however not clear how unitarity can be preserved this way without drastically changing the thermodynamics of the black hole and the evaporation time scale. The purpose of this

[9] We are thankful to Samir Mathur for pointing this out to us.

Chapter was to formulate the black hole evaporation process in a local framework of qubit models and deduce the consequences of unitarity restoration.

- *The definition of the interior spacetime is state-independent*
  In our discussion of infall, we implicitly assume that the modes $B$ and $C$ must be in one particular 'safe state', $|\varphi_1\rangle$ , for the infalling observer to 'see' the Unruh vacuum. Moreover, we assume that the $C$ qubit in the discussion is predetermined. One may imagine trying to evade some of the arguments in AMPS and here by supposing that the interior/horizon spacetime is defined in a state-dependent way. For example, we might say that we take the last emitted $B$ and look for the qubit with which it is maximally entangled, and define that to be 'C', and the entangled state to be the 'safe state' $|\varphi_1\rangle$ . Before the Page time the $C$ one arrives at via this procedure is at least still a black hole degree of freedom, but after the Page time it gives a $C$ from the radiation and is therefore nonlocal. This state-dependence appears to be a kind of nonlinear quantum mechanics, which we do not consider here.

The recent results of Mathur [2] have shown that small corrections to the semi-classical Hawking evaporation cannot ensure purity of final state. This might lead one to think that the evaporation process is described by the usual semi-classical Hawking evaporation before Page time as long as after Page time there are large corrections to it. We found that the traditional picture of the state at the horizon being the vacuum state at *any* time of the evolution is inconsistent with unitarity and so modifying the state only after Page time is not enough. This means that the $BC$ system cannot be in the Unruh vacuum at any point during the evaporation of the system, where $B$ is the outgoing qubit and $C$ is a one qubit worth of the system remaining behind. Not having the vacuum state at the horizon means that there has to be some *structure*. To ensure unitarity, this structure must contain the information of whatever it was formed by and whatever has since then fallen into it, it must contain the information of the microstates of the black hole.

The fuzzball proposal states that black holes are a coarse-grained description of the true microstates accounting for the Bekenstein-Hawking entropy which are horizonless and singularity-free solutions of quantum gravity. Being coarse-grained, black holes cannot be used to study processes that require knowledge of the microscopic structure of the state, in particular we have shown in Section 2.3 that black holes cannot evaporate unitarily. The radiation coming from fuzzballs, however, carries away the information of the state and there is no information paradox.

While it is currently still out of scope of the theory to test these conjectures for Schwarzschild fuzzballs as there are no explicit solutions yet, progress has been made with special charged non-extremal fuzzballs. In [158] it was shown that the JMaRT solution [62] has a classical 'ergoregion instability' and the energy radiated through the unstable modes was shown [129] to be exactly the Hawking radiation for these microstates. This result shows how 'Hawking emission' emerges from the interior and carries information out to infinity. The JMaRT solution is, however, a very special non-extremal solution and while it may be reasonable to argue that in more general solutions there will be a similar type of emission with information leaving the state with the radiation, more generic microstates need to be constructed to test the conjecture. This is the content of Chapter 3 to which we turn next.

# Chapter 3

# Non-extremal black hole microstates

In Chapter 2 of this Thesis we argued that for black hole evaporation to be unitary, information has to leave the black hole with every emitted quantum and there cannot be an information-free horizon. Instead the horizon has to be replaced by horizon-scale structure. While there are many explicit examples of supersymmetric Supergravity solutions with horizon-scale size, to test the fuzzball proposal for black holes that actually evaporate we need to construct non-extremal bulk microstates. This is the purpose of this Chapter. Thus, in the context of non-extremal black holes, we want to address the question:

*Q2: What are the black hole microstates at strong effective coupling?*

The idea is to start with BPS smooth bubbling geometries and place certain probe branes in such a way that supersymmetry is globally broken. If the probes are supertubes, the backreaction of its supersymmetric bound state with the bubbling geometry is known and smooth, and can again be described in the class of BPS three-charge microstates discussed in Section 1.4. Supertubes thus appear to be the natural candidates for the construction of microstates of near-extremal black holes. We will study the structure of the supertube Hamiltonian in a bubbling background, which we derived in Section 1.5, and argue that metastable minima of the potential correspond to non-extremal microstates upon backreaction.

To show that these microstates have indeed horizon-scale size we must address the question:

*Q3. What is the scale of the singularity resolution?*

We will answer this question by explicitly computing the size of the near-extremal configurations and comparing the result to that of the corresponding black hole.

## 3.1 Motivation and summary

### Metastable supertubes

Metastable vacua are an important feature of supersymmetric gauge theories [159], and the construction of such vacua in String Theory has been the subject of much study. The most direct

way to obtain such vacua in Supergravity is to put antibranes in a background that has brane charge dissolved in flux. This has been first done by Kachru, Pearson and Verlinde [160], who argued that probe anti-D3 branes in a smooth Klebanov-Strassler solution [55] are metastable, and can decay by annihilating against the positive D3 brane charge dissolved in flux via a process termed 'brane-flux annihilation'. Similarly, Klebanov and Pufu considered anti-M2 branes in a smooth solution with M2 brane charge dissolved in fluxes [161], and found that in the probe approximation these also give rise to metastable vacua [162]. While there is at this point some uncertainty about the fate of these antibrane constructions when full backreaction is taken into account (see [72, 73, 74, 75, 78] and **P6**), it is clear that placing probe antibranes in flux backgrounds is the most obvious starting point in hunting for metastable vacua. The purpose of this Chapter is to apply this procedure to supersymmetric black hole microstate geometries and to argue that in the probe approximation antibranes give rise to metastable solutions that should be interpreted as microstates of non-extremal black holes.

There exist huge families of supersymmetric solutions that have the same charge, mass and angular-momentum as a black hole with a macroscopically-large horizon area, and have no singularity and no horizon. See Section 1.4 of this Thesis and [46] for a review. The singularity (that can be thought of as coming from the singular brane sources) is resolved by a geometric transition that yields a geometry with many bubbles threaded by fluxes. The charge of these black hole microstate solutions is entirely dissolved in these fluxes. The physics of these solutions strongly suggests that the time-like singularity of extremal black holes is resolved by low-mass modes that correct the geometry on scales comparable to the horizon scale, and completely excise the region between the singularity and the horizon. These resolution channels thus modify the singular geometry to a *large* distance away from the singularity, exactly as it happens in other well-understood string-theoretic resolutions of timelike singularities, like Polchinski-Strassler [10], Klebanov-Strassler [55] or LLM [54, 163]. Moreover, there is recent evidence from numerical relativity studies of extremal and near-extremal black holes that the region inside the horizon is unstable, and the instability yields a final configuration with essentially no spacetime inside the horizon (see [61] for an overview, and [60, 58, 59] for earlier work).

Hence, there appears to be a growing consensus that extremal black hole singularities are not resolved at Planck scale, but at horizon scale. See Figure 3.1. While this fits very well with Mathur's conjecture (see [19, 46, 164, 48, 47, 128] for reviews), it leaves unanswered the question of what happens for non-extremal black holes. Given the resolution mechanism of the extremal black hole singularity it is quite natural to expect that the timelike singularity will be resolved at the scale of the inner horizon, and thus that there will be no more spacetime in the region from the singularity to the inner horizon; this also agrees with other insights coming from numerical relativity [58], and with earlier analytic work about the instability of inner horizons [165, 60, 59].

However, this is not sufficient for the final radiation state to be pure [2] and to have information come out in the evaporation process (see our results of Chapter 2). The requirement that the information paradox be vindicated implies something much stronger: the singularity of non-extremal black holes should be resolved all the way to the outer horizon, 'backwards in time' from the singularity. To understand whether this indeed happens, one must understand what happens to the extremal black hole microstates when one tries to make them near-extremal. If they all collapse behind a horizon, then most likely the singularity resolution scale is that of the

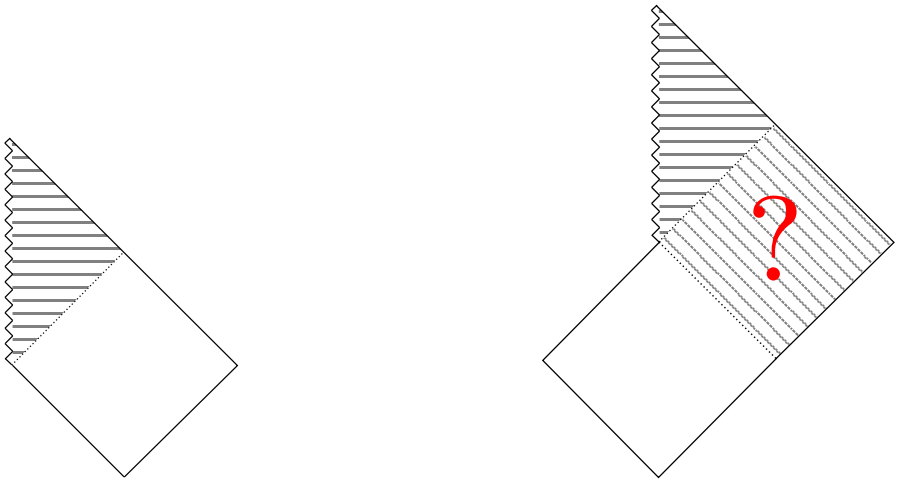


(a) Extremal RN spacetime. (b) Non-extremal RN spacetime.

Figure 3.1: Penrose diagrams for the extremal (left) and non-extremal (right) Reissner-Nordström black hole. At this moment there is a growing consensus that the extremal black hole singularity is resolved at horizon scale. For non-extremal black holes it is unclear whether the singularity resolution extends to the inner horizon, or all the way to the outer horizon, as in Mathur's proposal.

inner horizon, and these microstates do not help too much in solving the information paradox. On the other hand, if these microstates survive the near-extremal deformation and do not collapse behind a horizon, this indicates that the singularity is resolved all the way to the outer horizon, just like the fuzzball proposal says. Note that settling the issue of the near-extremal fate of the microstate geometries is suggestive for arguing that the fuzzball proposal applies to all non-extremal black holes: the Penrose diagram of a large Schwarzschild black hole to which one adds one electron is the same as the one of the near-extremal Reissner-Nordström black hole, and if the singularity-resolution scale of the latter is the outer horizon, it is very implausible that it will be anything else for the former.

To address the question at which scale the singularity resolution happens, one needs to attack the formidable task of constructing non-extremal black hole microstate geometries, which is highly nontrivial. Only two classes of non-extremal microstate solutions are known: the JMaRT [62, 63] and the running-Bolt [65, 40] solutions, and all the arguments so far that the fuzzball proposal applies to non-extremal black holes have been based on the physics of these solutions [158, 129, 130]. Given that these solutions are very special, and due to the technical difficulty involved in finding new ones, it is in rather difficult to take these arguments too far away.

In the first part of this Chapter, based on **P1**, we argue for a way to bypass these limitations, by adding supertube probes to extremal BPS geometries in such a way that the solutions become non-extremal. We find that supertubes placed in generic bubbling solutions can have metastable minima, that can decay into the supersymmetric ones by brane-flux annihilation, exactly as it happens when one places antibranes [160] in the Klebanov-Strassler geometry [55].

To prove the existence of metastable supertubes [1] and to understand their decay mechanism,

[1]We use the word supertube to refer to minima of the supertube Hamiltonian, or from a four-dimensional

it is enough to focus on supertubes in BPS microstate geometries built upon a Gibbons-Hawking base with two centers. From the physics we find, it is quite obvious that metastable supertubes will exist in generic multicenter BPS three-charge geometries, and most likely also in non-BPS extremal multicenter solutions.

### Near-extremal black hole microstates

In the second part of this Chapter, based on **P3**, we take the above described technology one step further, and use metastable supertubes to systematically construct microstates of near-extremal black holes. We start from supersymmetric microstate geometries that have the same mass, charges and angular momentum as a supersymmetric three-charge black hole, and have a very long throat (hence they correspond to a scaling solution from the perspective of four-dimensional Supergravity [32, 35, 111]). We construct near-extremal black hole microstate solutions by placing metastable supertubes in these supersymmetric microstate geometries.

There are two ways to obtain such long-throat supersymmetric solutions. The first is to consider a general scaling multicenter solution and tune the length of the throat by moving the centers near each other [110, 111, 35]. The other is to keep the centers aligned on an axis, and to bring them closer and closer by tuning their charges by hand [32]. [2] The advantage of the second approach is that it produces five-dimensional solutions with $U(1) \times U(1)$ invariance, and in these solutions the physics of metastable supertubes is under much better control than in scaling solutions with less symmetry.

The supersymmetry of solutions with metastable supertubes is broken by the relative orientation of the electric charges of the supertube with respect to the solution. Furthermore, we will consider supertubes whose charges are much smaller than those of the background, so we expect generically that their backreaction will give smooth solutions with long throats, that have more mass than charge, and hence are microstates of *non-extremal* black holes.

Indeed, it was shown in [124] that in the six-dimensional duality frame where the supertube charges correspond to D1 and D5 branes, a supertube in a bubbling solution backreacts into a smooth Supergravity solution. The smoothness is ensured by certain conditions near the supertube, which are identical to those coming from minimizing the DBI probe supertube action; thus we expect that the backreaction of a probe supertube at its minimum, supersymmetric or not, will always give a smooth solution. Another way of seeing this, is to recall that the supertube is an object that locally preserves 16 supersymmetries, and all these objects can be dualized into fluxed D6 branes, whose eleven-dimensional uplift is smooth [31]; for metastable supertubes all these supersymmetries are incompatible with those of the background, but this is not something that is visible in the near-supertube region, and hence does not affect the smoothness.

One can worry that the extra supertube charges, though small, may disturb the delicate balance of charges needed to create a long throat. Indeed, in a long throat the leading contributions to the bubble equations cancel, and the supertube contributions may end up being of the same order or larger than the subleading leftovers. However, this is not a problem; even if a supertube

perspective to a fluxed D4 brane, even when these configurations are not supersymmetric. The reason is that we are dealing with a supersymmetric object that is being placed in a background of the wrong orientation.

[2] This method has also been used to obtain extremal non-supersymmetric scaling solutions [45].

changes significantly the length of a throat, one can always tune the flux between cycles by a tiny amount to change this length back to the original one, and this gives a very small correction to the overall charges of the solution.

Having obtained large classes of microstates of near-extremal black holes, we can go on and attack the much harder problem of figuring out what is the physics of these microstates. Indeed, according to the fuzzball proposal one expects the microstates to have the same size as the black hole, but there are various scenarios of how this can happen. It is possible that microstates extend only microscopically away from the horizon, and hence, as suggested in [66], they could give nothing more than a realization of a stretched horizon. Alternatively, the fuzzballs can differ from the black hole on a scale comparable to that of the horizon, and hence give very different physics.

These questions do not make sense for BPS and extremal black holes, and cannot be answered using the BPS black hole microstates constructed so far. Indeed, the thickness of BPS throats is completely determined by the charges, and hence a fuzzball and a black hole that have the same charges automatically have throats of equal thickness. Furthermore, the length of the throat of the black hole is infinite, while the length of the throat of the fuzzballs is always very large but finite [3], which does not allow for a meaningful size comparison. On the other hand, near-extremal black holes have throats of *finite* length, which one can compare with the throat lengths of the family of fuzzballs we construct. The thicknesses of the throats are still automatically equal, because they are mostly controlled by the charges in the near-extremal limit.

As we will see, we are able to construct microstates whose throat has the same length as that of a non-extremal black hole, but we can also obtain with equal ease microstate geometries that have the same mass and charges as the non-extremal black hole, but whose throats are longer or shorter. This is depicted in Figure 3.2. As far as our construction is concerned, there appears to be no dynamical reason why throats of the same length as the black hole are preferred over longer or shorter ones, and this indicates that the fuzzballs of non-extremal black holes will not differ from the black hole only at microscopic distances from the horizon [4].

The fuzzball geometries we construct can be used to extract other pieces of physics that have been inaccessible until now. For example, one can use a KKLMMT-type argument [167] to find the forces with which our non-extremal fuzzballs attract various D-branes, and compare these forces to those of the corresponding black hole. This will be presented in Chapter 4 in the context of infall into black holes and fuzzballs. One could also compute the tunneling probabilities of the metastable supertube to the supersymmetric minimum, and compare this to the Hawking radiation rate of the near-extremal black hole; this is left for future work.

This Chapter is organized as follows. The purpose of Section 3.2 is to give a systematic method to construct and analyze near-extremal non-supersymmetric microstate solutions. We propose that starting from a generic extremal supersymmetric microstate solution one can build

[3]The only way to Figure out whether a long BPS microstate is typical, is to compare its length to the mass gap of the typical microstate in the dual CFT as discussed in Section 1.4. This comparison indicates that long microstates whose angular momentum is of order one belong indeed the sector where the typical microstates live [32, 35, 166].

[4]Most likely there will be a distribution of fuzzballs of various lengths. The length of the typical ones may come out to be same as the length of a black hole by some entropy enhancement reason [126].

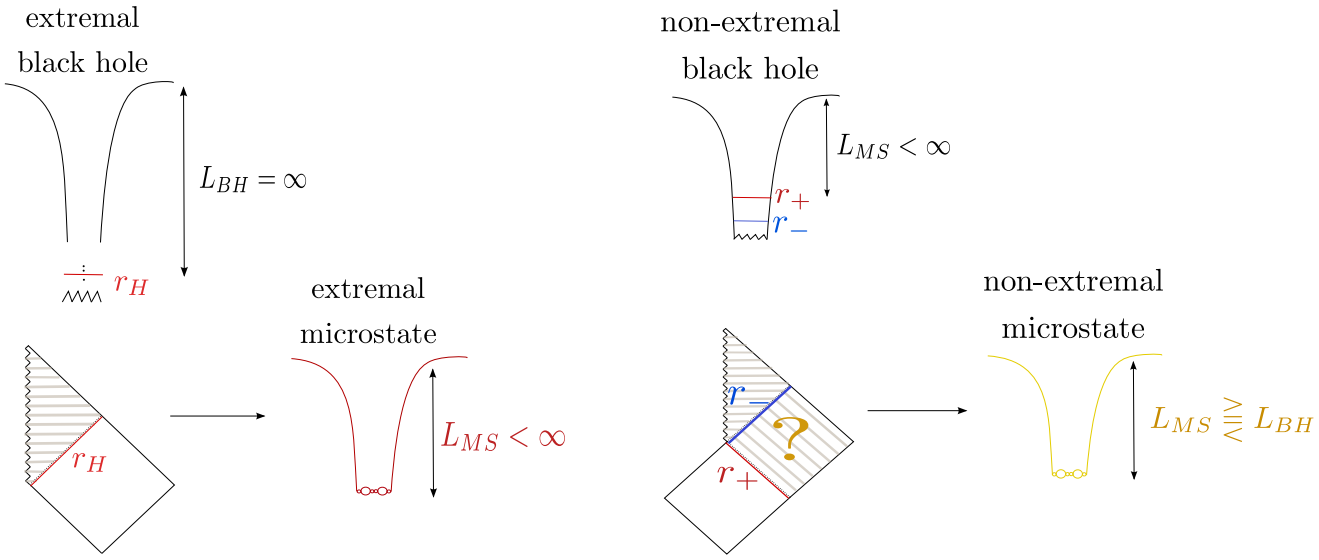


(a) Extremal black holes.

(b) Non-extremal black holes.

Figure 3.2: Singularity resolution scale.

non-extremal microstates by adding certain branes with non-compatible supersymmetries. In particular we focus on two-charge supertubes (which correspond to fluxed D4 branes upon reduction to 4 dimensions). We recall the Hamiltonian for a supertube in an arbitrary three-charge solution with a Gibbons-Hawking base, as derived in Section 1.5, and explore its minima analytically. We then focus on a particular two-center background, and find that, depending on the supertube charges, it can have both supersymmetric and non-supersymmetric minima, as well as metastable minima. We study their structure numerically. In Section 3.3 we explain the mechanism by which the supertube can annihilate against some of the charge dissolved in fluxes, and decay into a supersymmetric solution. In Section 3.4 we then take the probe brane method one step further and study supertubes in smooth scaling solutions whose metastable minima should correspond to near-extremal black hole microstates. We focus on a scaling solution with seven centers and plot the potential of a typical probe supertube in this background. In Section 3.5 we discuss the interpretation of our configurations as microstates (or fuzzballs) of non-extremal black holes, and compare their properties to those of black holes. Finally, we conclude in Section 3.6 with some speculations on the implication of this work for our microscopic understanding of Hawking radiation and the resolution of spacelike singularities in String Theory, and discuss possible future directions. We relegated the geometry of the non-extremal black hole to Appendix C.1, and in Appendix C.2 we present an approximation that allows us to compare very easily the lengths of a black-hole throat and of a fuzzball throat.

## 3.2 Supertubes in smooth three-charge backgrounds

We want to study the dynamics of two-charge supertubes in supersymmetric three-charge backgrounds. In the M-Theory frame, the three electric charges of the background correspond to

M2 branes wrapping three orthogonal two-tori inside an internal six-torus while the three local magnetic dipole charges correspond to M5 branes wrapping two orthogonal two-tori and an arbitrary closed curve in the four-dimensional base which we take to be of Gibbons-Hawking form. The two electric charges of the supertube, $q_1$ and $q_2$, are (anti-)parallel to those of the background and correspond to M2 branes along the first and second two-torus and the dipole charge, $d_3$, corresponds to an M5 brane extended along those two tori and wrap the fiber of the Gibbons-Hawking base. Since we want to study microstate geometries, we focus on BPS bubbling geometries whose M2 and M5 charge is entirely dissolved in flux through topological cycles ('bubbles'). [5] These backgrounds were discussed in detail in Section 1.4. An illustration of supertubes placed in bubbling backgrounds is given in Figure 3.3.

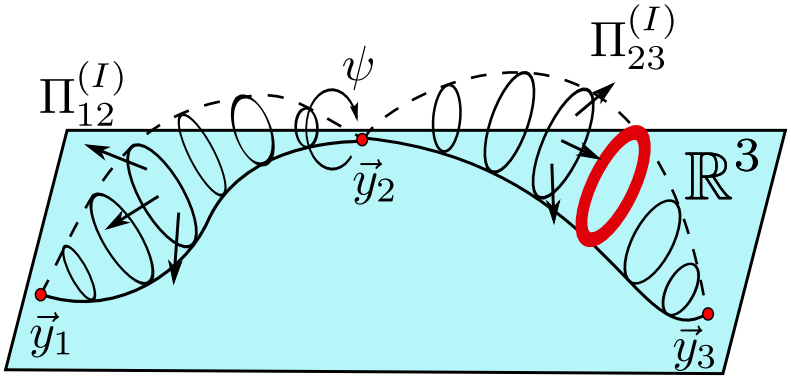


Figure 3.3: A smooth three-charge bubbling geometry with fluxes $\Pi_{ij}^{(I)}$ through the bubbles between the centers $i$ and $j$. A supertube (red) is placed on one of the cycles along the GH fiber $\psi$.

To study the dynamics of supertubes in this background we rely on the Dirac-Born-Infeld – Wess-Zumino probe action reviewed in Section 1.5. If the tube is supersymmetric, then the fully-backreacted solution is again in the class of supersymmetric three-charge solutions and the Born-Infeld description of the supertube captures all the aspects of the backreacted solution [124]. However, since we are trying to study *non-supersymmetric* supertubes, for which no fully-backreacted description has been constructed so far, we will work in a probe approximation, ignoring the backreaction of the supertube.

In Subsection 3.2.1 we summarize for convenience the three-charge background in the M-Theory frame which we discussed in detail in Section 1.4. In Subsection 3.2.2 we then study whether there are tubular configurations where the two sets of M2 branes blow up into an M5 brane along the GH direction $\psi$. We denote this tube as M2–M2 $\rightarrow$ M5. The method is to write down the Lagrangian (consisting of a Born-Infeld and Wess-Zumino contribution) of an M5 brane with the lower-dimensional charges (corresponding to the two M2 branes) and search for stable configurations. This is done by looking for supersymmetric and non-supersymmetric (meta)stable minima in the Hamiltonian which is obtained from the Lagrangian by a Legendre transform and which was derived in Section 1.5.

[5] While we continue to talk about M2 and M5 *branes* to characterize the charge of the background, it should henceforth be understood that all brane charges are dissolved in flux.

### 3.2.1 Three-charge backgrounds

The metric and gauge potential in the M-Theory duality frame in which the three charges correspond to M2 branes wrapping orthogonal $T^2$'s inside $T^6$ is [102, 103]:

$$ds_{11}^2 = (Z_1Z_2Z_3)^{-2/3}(dt+k)^2 + (Z_1Z_2Z_3)^{1/3}ds_4^2 + (Z_1Z_2Z_3)^{1/3}\sum_I \frac{ds_I^2}{Z_I}\,, \tag{3.1}$$

$$A^{(I)} = -Z_I^{-1}(dt+k) + B^{(I)} \tag{3.2}$$

where $ds_I^2$ are unit metrics on the three orthogonal $T^2$'s and $ds_4^2$ is the metric of the hyper-Kähler base space. When the latter metric is Gibbons-Hawking (GH) or Taub-NUT:

$$ds_4^2 = V^{-1}(d\psi + A)^2 + V ds_3^2 \qquad \text{with} \qquad dA = \star_3 dV, \tag{3.3}$$

where $ds_3^2$ is the flat metric on $\mathbb{R}^3$, the solution is completely determined by specifying eight harmonic functions $V, K^I, L_I, M$ in the GH base [105, 106]. In terms of these, the magnetic fields, warp factors and rotation vector are given by

$$B^{(I)} = V^{-1}K^I(d\psi + A) + \xi^I\,, \quad \text{with} \quad d\xi^I = -\star_3 dK^I\,, \tag{3.4}$$

$$Z_I = L_I + \frac{1}{2}C_{IJK}V^{-1}K^JK^K\,, \tag{3.5}$$

$$k = \mu(dt+\omega) + A\,, \quad \text{with} \quad \mu = \frac{1}{6}C_{IJK}V^{-2}K^IK^JK^K + \frac{1}{2}L_IK^I + M\,, \tag{3.6}$$

and $C_{IJK} = |\epsilon_{IJK}|$. For this geometry to be a bubbling solutions where the M2 and M5 brane charge is entirely dissolved in flux, we have to impose the smoothness conditions of Section 1.4. In such a smooth three-charge background we now study the dynamics of supertubes.

### 3.2.2 The supertube potential

The supertube Hamiltonian in terms of the M2 charges, $q_1$ and $q_2$, and M5 dipole charge, $d_3$, as obtained in Section 1.5, is

$$\mathcal{H} = \frac{\sqrt{Z_1Z_2Z_3/V}}{d_3R^2}\sqrt{\left(\tilde{q}_1^2 + d_3^2\frac{R^2}{Z_2^2}\right)\left(\tilde{q}_2^2 + d_3^2\frac{R^2}{Z_1^2}\right)} + \frac{\mu V^2}{d_3R^2}\tilde{q}_1\tilde{q}_2 - \frac{\tilde{q}_1}{Z_1} - \frac{\tilde{q}_2}{Z_2} - \frac{d_3\mu}{Z_1Z_2} + q_1 + q_2\,, \tag{3.7}$$

where we have introduced

$$\tilde{q}_1 \equiv q_1 + d_3(K^2/V - \mu/Z_2)\,, \quad \tilde{q}_2 \equiv q_2 + d_3(K^1/V - \mu/Z_1)\,, \tag{3.8}$$

and $R$ is proportional to the size of the Gibbons-Hawking fiber

$$R^2 \equiv Z_1Z_2Z_3/V - \mu^2\,, \tag{3.9}$$

and the harmonic functions $K^1$ and $K^2$ encode two of the three dipole moments of the background.

The Hamiltonian (3.7) describes tubes in the most general three-charge background. We expect this Hamiltonian to have both supersymmetric and non-supersymmetric minima. The minima of the potential determine the position on the GH base of (meta)stable supertubes in a given three-charge background. Depending on the relative orientation of the M2 charges of supertube and the background, the minima of the potential will be supersymmetric or non-supersymmetric.

**Minima of the Supertube Hamiltonian**

**Supersymmetric minima.** The supersymmetric minima of the Hamiltonian have

$$\mathcal{H}_{BPS} = q_1 + q_2 \,. \tag{3.10}$$

This value is obtained when the supertube radius is related to the supertube charges by

$$d_3^2 \frac{Z_3}{V} = (q_1 + d_3 \frac{K^2}{V})(q_2 + d_3 \frac{K^1}{V}) \tag{3.11}$$

and provided that

$$(q_1 + d_3 \frac{K^2}{V})(q_2 + d_3 \frac{K^1}{V}) \geq 0 \,. \tag{3.12}$$

For this radius the Hamiltonian (3.7) reduces to

$$\mathcal{H} = q_1 + q_2 + \frac{Z_1 Z_2 Z_3 V}{Z_1 Z_2 Z_3 V - \mu^2 V^2} \Big[ \Big| \frac{\tilde{q}_1}{Z_1} + \frac{\tilde{q}_2}{Z_2} \Big| - \Big( \frac{\tilde{q}_1}{Z_1} + \frac{\tilde{q}_2}{Z_2} \Big) \Big] \tag{3.13}$$

which saturates the BPS bound only if

$$\frac{\tilde{q}_1}{Z_1} + \frac{\tilde{q}_2}{Z_2} \geq 0 \,. \tag{3.14}$$

When the conditions (3.12) and (3.14) are not met, the Hamiltonian has no supersymmetric minimum. The first condition (3.12) is needed for the absence of CTC's: $Z_I V \geq 0$ (see Section 1.4 Equation (1.123)) implies that both sides of (3.11) have to be positive, which is equivalent to (3.12). Similarly, if one is to construct the backreaction of the supertube, the warp factors near the supertube center (which we can take at $r = 0$) would diverge [124] as $(Q_{1,2} + d_3 K^{2,1}/V)/r$. These divergences are controlled by the effective, or enhanced M2 charges

$$q_1^{\text{eff}} \equiv q_1 + d_3 \frac{K^2}{V} \qquad \text{and} \qquad q_2^{\text{eff}} \equiv q_2 + d_3 \frac{K^1}{V} \,. \tag{3.15}$$

If these charges do not have the same sign the solution has CTC's.

**Non-supersymmetric minima.** Given the complicated nature of the Hamiltonian (3.7), and given that we are trying to construct metastable black hole microstates, we focus from now on on supertubes in smooth bubbling multi-center solutions. The most generic such solution has a multi-center Taub-NUT or GH four-dimensional base space, with three non-trivial fluxes on the two-cycles stretching between every pair of Taub-NUT or GH centers [26, 27, 28].

In order to study the existence of non-supersymmetric minima, we first expand the Hamiltonian near one of the smooth centers:

$$\mathcal{H}|_{r_i\to 0} = \left|\left(q_1 + d_3\frac{K^2}{V}\right)\left(q_2 + d_3\frac{K^1}{V}\right)\right|\sqrt{\frac{v_i}{Z_1Z_2Z_3}}\ (r_i)^{-1/2}\Big|_{r_i=0} gf + \mathcal{O}[(r_i)^0]\,, \tag{3.16}$$

where $r_i$ is the distance to the $i^{\text{th}}$ center and $v_i$ is the coefficient of the $1/r_i$ pole in $V$.

When both $(q_1+d_3K^2/V)|_{r_i=0}$ and $(q_2+d_3K^1/V)|_{r_i=0}$ are non-zero this Hamiltonian diverges near the centers [6] and hence there is at least one minimum between the centers. If (3.12) is satisfied, the minimum is supersymmetric. To find a non-supersymmetric minimum one simply has to find a set of supertube charges such that at the minimum $(q_1+d_3K^2/V)(q_2+d_3K^1/V) < 0$.

When one of the effective charges vanishes, say $(q_1 + d_3K^2/V)|_{r_i\to 0} = 0$, then the supertube radius is zero. The divergent term of the Hamiltonian vanishes, and the leading term is:

$$\mathcal{H}|_{r_i\to 0} = q_1 + q_2 + \left|\frac{q_2 + d_3K^1/V}{Z_2}\right| - \frac{q_2 + d_3K^1/V}{Z_2}\,. \tag{3.17}$$

One might naively think that a supertube of zero radius is nothing but a collection of branes, and may wonder why the dipole charge $d_3$ still appears in the Hamiltonian. The answer has to do with the existence of Dirac strings for the gauge field $A^{(1)}$ (given by Equations (3.2) and (3.4)). Since the solution has non-trivial fluxes, to completely describe the physics one must use multiple patches. The values of the gauge field $A^{(1)}$ differ from patch to patch, and in a generic patch there will be Dirac strings at generic centers. In particular, as we will discuss in detail in Section 3.3, when $K^1/V$ is non-zero at the center, the zero-sized supertube described by (3.17) wraps a Dirac string, and is not just a collection of parallel branes. When removing the Dirac string, the supertube brane charges shift, and become equal to the effective charges.

It is then the orientation of these effective charges with respect to the background that determines whether supersymmetry is broken or not. In our example, when the effective charge of the supertube, $q_2 + d_3K^1/V$, has the same orientation as the charge of the background (proportional to $Z_2$), the Hamiltonian is equal to the sum of the charges, and the configuration is supersymmetric. When this effective charge has the opposite orientation, the Hamiltonian is strictly larger than $\mathcal{H}_{BPS}$, and the configuration has a non-supersymmetric minimum or maximum (depending on the sign of the next-to-leading order term).

Given that supersymmetric tubes have a critical worldvolume electric field, one may attempt to analytically obtain a non-supersymmetric minimum using a supertube with a critical electric field oriented opposite to the background ($(q_2 + d_3\frac{K^1}{V})/Z_2r_i < 0$). When one of the effective charges is zero, this naive guess yields a non-supersymmetric minimum with energy

$$\mathcal{H}_{non-BPS} = q_1 + q_2 - 2\frac{q_2 + d_3K^1/V}{Z_1}\,. \tag{3.18}$$

which agrees with (3.17)! Thus the naive guess gives the correct energy of the zero-radius non-supersymmetric configuration. The naive guess also gives a radius relation:

$$-\frac{Z_3}{V} = (q_1 + d_3\frac{K^2}{V} - 2d_3\frac{\mu}{Z_2})(q_2 + d_3\frac{K^1}{V})\,, \tag{3.19}$$

[6] From a four-dimensional perspective, these supertubes are fluxed D4 branes with two non-zero fluxes, and hence a non-zero D0 charge; these are repelled by the fluxed D6 centers.

which is satisfied trivially for degenerate supertubes. Unfortunately, non-degenerate supertubes do not have a critical electric field, and the naive minima obtained from (3.19) do not agree with those of the Hamiltonian. It would be interesting to get a deeper understanding of why this naive guess describes correctly the metastable vacua with degenerate supertubes but not the other ones.

To summarize, one can use the Hamiltonian (3.7) to infer analytically the existence and properties of degenerate vacua, as well as the existence of non-degenerate vacua. However, we could not find any easy analytic way to describe non-degenerate non-supersymmetric vacua. Thus, we will now focus on a simple two-center bubbling solution, and analyze the possible minima numerically.

### 3.2.3 Metastable supertubes in a two-center solution

We now evaluate the Hamiltonian in a specific two-center solution. Depending on the values of their charges $q_1, q_2$, the supertubes can have a rich structure of minima and interesting decay patterns. We scan for the candidate charges yielding metastable vacua by first plotting the supertube Hamiltonian on the axis between the centers. We find examples with either one supersymmetric, or one non-supersymmetric, stable minimum. There can also be two minima for a given set of supertube charges $q_1, q_2$. Either they are both supersymmetric or one is stable (supersymmetric or non-supersymmetric) and the other is metastable. We expect this rich minima structure to carry over to other smooth background geometries with *multi*-center Taub-NUT base spaces. When the candidate configuration is metastable, we also plot the Hamiltonian away from the axes to insure that the supertube is not unstable to rolling away from the symmetry axis.

#### Details of the background

The Hamiltonian depends on the spacetime coordinates through the harmonic functions

$$\begin{aligned} V &= v_0 + \frac{v_1}{|\vec{r}-\vec{r}_1|} + \frac{v_2}{|\vec{r}-\vec{r}_2|}\,, \qquad & M &= m_0 + \frac{m_1}{|\vec{r}-\vec{r}_1|} + \frac{m_2}{|\vec{r}-\vec{r}_2|}\,, \\ K^I &= k^I_0 + \frac{k^I_1}{|\vec{r}-\vec{r}_1|} + \frac{k^I_2}{|\vec{r}-\vec{r}_2|}\,, \qquad & L_I &= \ell_{I,0} + \frac{\ell_{I,1}}{|\vec{r}-\vec{r}_1|} + \frac{\ell_{I,2}}{|\vec{r}-\vec{r}_2|}\,. \end{aligned} \tag{3.20}$$

We choose a cylindrical coordinate system $(\rho, z, \theta)$ in three dimensions, where $z$ runs along the axis through the center and $\rho, \theta$ are polar coordinates in the orthogonal plane. Since we have cylindrical symmetry, the solution only depends on the coordinates $z$ and $\rho$.

We consider a two-center background where the inter-center distance is $r_{12} = |\vec{r}_1 - \vec{r}_2| = 120$ and we fix the two centers on the symmetry axis as $z_1 = -60, z_2 = 60$. We choose $K^I = K$ all equal and the following charges and asymptotics in the harmonic functions $V, K$:

$$\begin{aligned} v_0 &= 2\,, \qquad & v_1 &= 10\,, \qquad & v_2 &= -2\,, \\ k_0 &= -3\,, \qquad & k_1 &= 0\,, \qquad & k_2 &= 14\,. \end{aligned} \tag{3.21}$$

Because at spatial infinity $V \to v_0 \neq 0$, the GH space is in fact a two-center Taub-NUT space asymptotic to $\mathbb{R}^3 \times S^1$. Furthermore, $K$ has a non-vanishing constant asymptotic value, and

hence the solution has non-trivial Wilson lines along the Gibbons-Hawking fiber (which descend to axions upon reduction to four dimensions). This choice of charges and asymptotic values is a representative choice that has the generic features of a smooth geometry with a two-center Taub-NUT base space. Furthermore, with the choice $k_1 = 0$, there are no Dirac strings at center '1'.

Note that the harmonic functions $M$ and $L_I$ are completely determined through the regularity conditions on $Z_I$ and $\mu$ and the bubble equations (Equations (1.124) and (1.125) of Section 1.4). Finally, without loss of generality we consider a tube with dipole charge $d_3 = 1$.

### Plots of the potential

We plot the Hamiltonian, shifted to $H = \mathcal{H} - (q_1 + q_2)$ (such that $H = 0$ for supersymmetric tubes), in terms of the coordinate $z$ at $\rho = 0$ (i.e. on the symmetry axis). Varying the supertube charges, a rich structure of different minima arises.

**One minimum** We first choose charges $q_1, q_2$ for which there is one minimum. When $H = 0$ the minimum is supersymmetric, (see Figure 3.4(a)), and the supertube generically sits close to one of the centers. The supersymmetric minimum describes a supertube whose radius can be found from Equation (3.11), and the backreaction of this configuration is a supersymmetric solution with three centers [124].

A minimum with $H \neq 0$ describes a non-supersymmetric supertube (see Figure 3.4(b)). Given that this tube is locally-BPS, we expect its backreaction to yield a solution that in the D1-D5-P duality frame is smooth at the supertube location. This smooth solution should represent a microstate of a non-supersymmetric black hole. It is interesting to ask whether the absolutely-stable non-supersymmetric minimum, which has no obvious decay channel, may correspond to an extremal non-BPS black hole, and hence fit in the recent classification of [44], or whether it will represent a very long-lived microstate of a non-extremal black hole.

As explained analytically in the previous Section, for some choices of charges there also exist supersymmetric and non-supersymmetric stable minima where the supertube has zero size. As expected, this happens when one of the *effective* M2 charges $q_I^{\text{eff}} = q_I + K/V$ is zero (see Figures 3.5(a) and 3.5(b)).

**Two minima.** There is also a wide range of charges for which two minima appear. The first possibility is to have two supersymmetric minima, which is depicted in Figure 3.6.

Figure 3.6(a) illustrates two different positions (each one close to one of the background centers) at which a supertube with fixed charges $q_1, q_2$ can be located. Again, one of these minima can degenerate when one of the effective charges $q_I + K/V$ goes to zero (Figure 3.6(b)).

The most interesting potentials arise when at least one of the two minima is non-supersymmetric, as depicted in Figure 3.7. These describe a metastable tube close to one center that can decay to a stable tube close to the other center. The plots in Figure 3.7 show that the stable tube can be either supersymmetric or non-supersymmetric.

Note that near the metastable minimum the potential looks like a Mexican hat brim that is very slightly tilted. This is hard to see from Figure 3.7, and is shown in Figure 3.8.

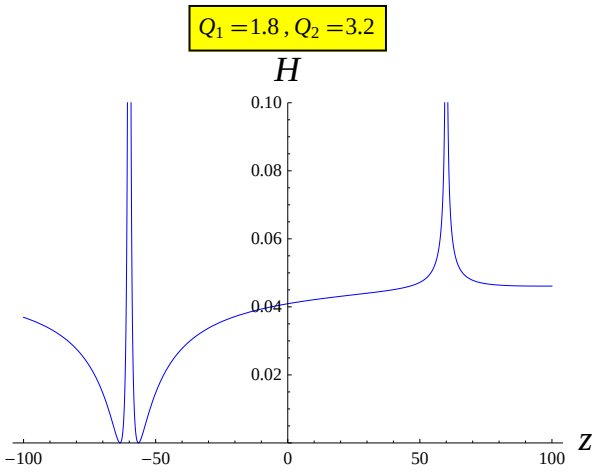


(a) One supersymmetric minimum.

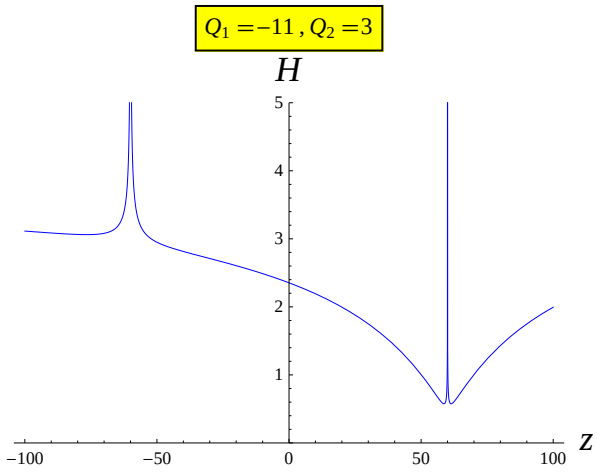


(b) One non-supersymmetric minimum.

Figure 3.4: A single stable minimum between the two centers. When both charges are positive and have the same orientation as the background (which has electric potential $Z > 0$ at the left center), the minimum is supersymmetric. When one of the charges has the wrong orientation, the minimum is non-supersymmetric. Note that the apparent second minimum outside the 2-center range is connected to the one inside by a Mexican-hat-type potential around the center in the $z - \rho$ plane. As we will show below in Figure 3.8, when supersymmetry is broken this Mexican-hat potential is slightly tilted.

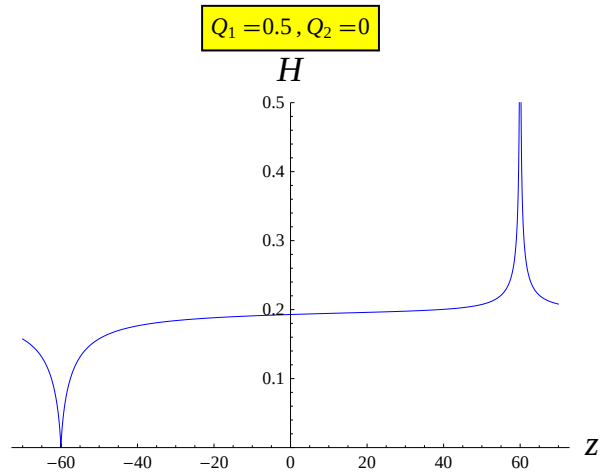


(a) Degenerate supersymmetric minimum.

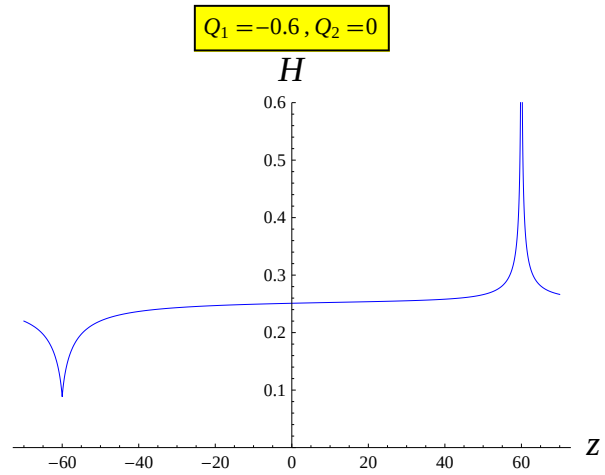


(b) Degenerate non-supersymmetric minimum.

Figure 3.5: When one of the effective charges is zero, the supertube degenerates. In this example, we choose $q_2 + \frac{K}{V}\big|_{r_1} = 0$. (Remember we work in patch '1' where $\frac{K}{V}\big|_{r_1} = 0$.) When the other charge has the same orientation as the background, the minimum is supersymmetric (a), when the orientations are opposite, the minimum is non-supersymmetric (b).

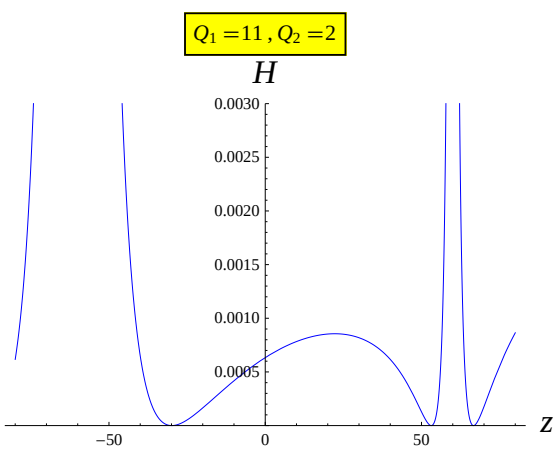


(a) Smooth supersymmetric minima.

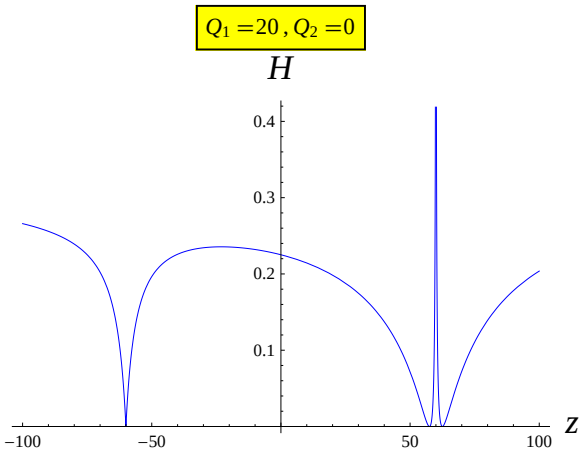


(b) Smooth and degenerate supersymmetric minima.

Figure 3.6: Two supersymmetric minima between the centers. When $q_2 = 0$ in patch '1', the minimum close to the left center degenerates, and the supertube becomes a collection of parallel branes. Again, the additional minima outside the 2-center range are connected to the ones inside by a Mexican-hat-type potential around the respective center in the $z - \rho$ plane.

## 3.3 The decay of metastable supertubes

When the metastable supertube tunnels to the stable minimum, its quantized M2 charges stay the same, but its effective M2 charges

$$q_1^{\text{eff}} = q_1 + d_3 \frac{K^2}{V}\,, \qquad q_2^{\text{eff}} = q_2 + d_3 \frac{K^1}{V}\,, \tag{3.22}$$

change. Much like the decay of antibranes in backgrounds with charge dissolved in flux [160, 162], the decay of the metastable supertube can be understood as brane-flux annihilation. However, since the supertube has multiple charges, and generically has a non-zero radius both before and after the decay, the details are a bit more involved.

Recall that the solution has a non-trivial magnetic flux through the two-cycle between the two GH points, given by

$$\Pi_{12}^{(I)} = \frac{1}{4\pi}\int_{r_1}^{r_2} dB^{(I)} = \frac{K^I}{V}\Big|_{r_2} - \frac{K^I}{V}\Big|_{r_1}\,. \tag{3.23}$$

Since the supertube has a non-trivial $d_3$ dipole charge which couples magnetically to $B^{(3)}$, when the supertube sweeps out the two-cycle from the North Pole to the South Pole, the amount of $\Pi_{12}^{(3)}$ flux on this two-cycle decreases by $d_3$ units.

Imagine now lowering from infinity a supertube to the metastable minimum. If this minimum is, say, near the North Pole, in order to bring the supertube 'into position' we need to work in a patch where there is no Dirac string at this pole. The change of patch in Supergravity is realized

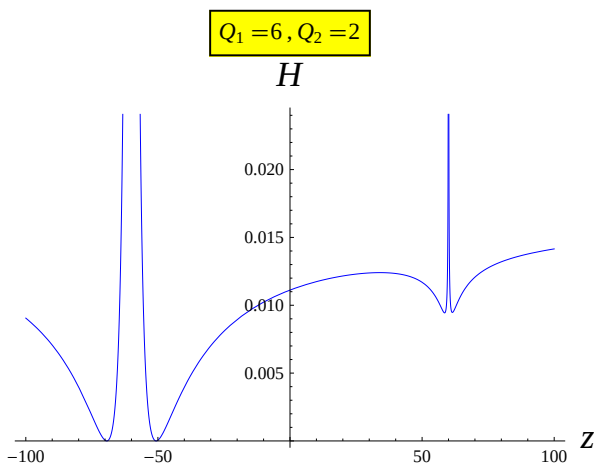


(a) Metastable and supersymmetric stable minima.

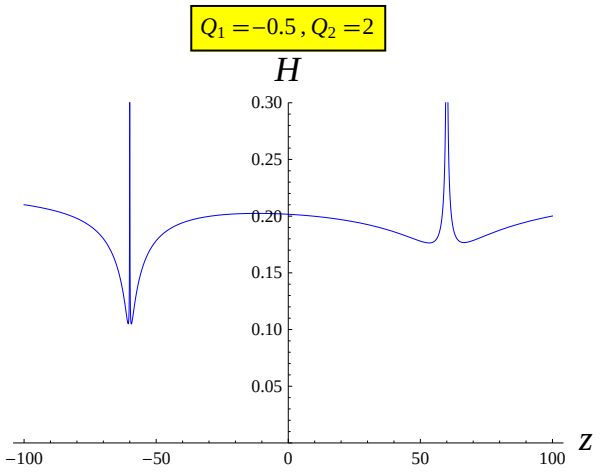


(b) Metastable and non-supersymmetric stable minima.

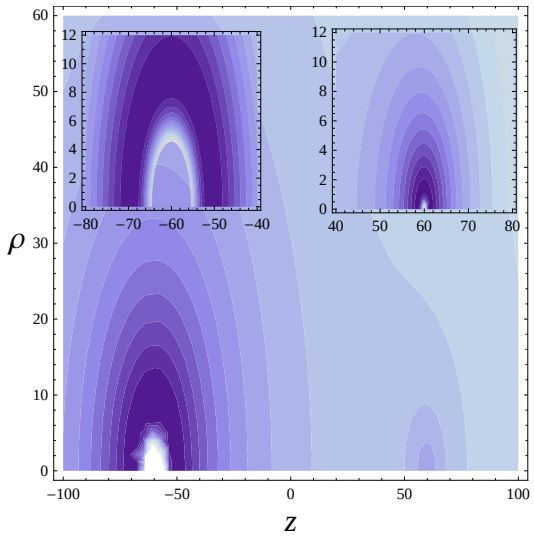


(c) Contour Plot of 3.7(a) in a plane of fixed polar angle around the symmetry axis (the $(z, \rho)$-plane): darker colours mean lower energy, the color scales in the main figure and the insets are not the same.

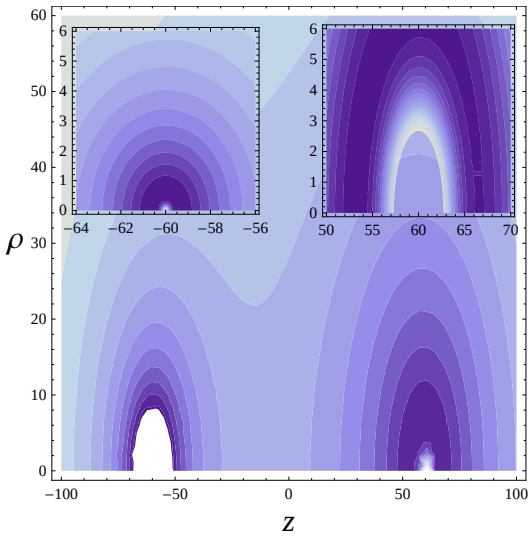


(d) Contour Plot of 3.7(b) in the $(z, \rho)$-plane: darker colors mean lower energy, the color scales in the main figure and the insets are not the same.

Figure 3.7: Metastable configurations. The supertube charges are given in the patch where there are no Dirac strings at the left center (point '1'). At this center, the M2 charge of the background is positive ($Z > 0$). When both charges are aligned with the background (left), the stable minimum is supersymmetric. When at least one of the supertube charges has the wrong orientation, the lowest minimum is non-supersymmetric.

by a gauge transformation [99, 46], which transforms the eight harmonic functions via

$$\begin{aligned} V &\to V\,, & L_I &\to L_I - C_{IJK}\gamma^J K^K - \tfrac{1}{2}C_{IJK}\gamma^J\gamma^K V\,, \\ K^I &\to K^I + \gamma^I V\,, & M &\to M - \tfrac{1}{2}\gamma^I L_I + \tfrac{1}{12}C_{IJK}\left(V\gamma^I\gamma^J\gamma^K + 3\gamma^I\gamma^J K^K\right)\,, \end{aligned} \tag{3.24}$$

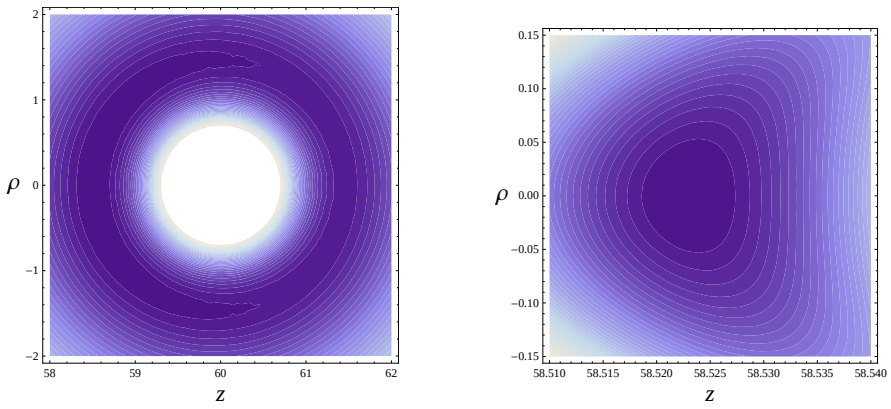


Figure 3.8: Two consecutive zooms on the minimum near $z = 60$ with $q_1 = 6, q_2 = 2$ of Figure 3.7(c), shows the 'Mexican-hat' type potential, which is slightly tilted to the left. (Darker colors mean lower energy.) The actual metastable minimum lies between the two centers on the symmetry axis.

where $\gamma^I$ are constants, but leaves the warp factors, rotation vector and field strengths invariant. To reach a patch where there are no Dirac strings at the point $i$, one has to perform a gauge transformation such that the value of $K^I/V$ at this point is zero, or alternatively $K^I$ has no pole. It is not hard to see that to go from a patch where there are no Dirac strings at point $i$ to a patch where there are no Dirac strings at the point $j$, the gauge transformation parameters $\gamma^I$ have to be equal to the flux between the two centers:

$$\gamma^I_{ij} = \frac{K^I}{V}\Big|_{r_i} - \frac{K^I}{V}\Big|_{r_j} = -\Pi^{(I)}_{ij} \,. \tag{3.25}$$

Thus, when changing patch, in order to make sure that one is describing the same supertube, (with the same radius and energy), the *effective* supertube charges have to stay the same. Hence the quantized charges have to shift by

$$\begin{aligned} q_{1,j} &= q_{1,i} + d_3\, \gamma^2_{ij} = q_{1,i} - d_3 \Pi^{(2)}_{ij} \,, \\ q_{2,j} &= q_{2,i} + d_3\, \gamma^1_{ij} = q_{2,i} - d_3 \Pi^{(1)}_{ij} \,, \end{aligned} \tag{3.26}$$

where we have denoted by $q_{1,i}$ and $q_{2,i}$ the charges of the supertube in the patch where there are no Dirac strings at the point $i$. Note that for supersymmetric minima, the Supergravity 'GH charges' of the backreacted supertubes are equal to the quantized charges [124], and the shift of the quantized charges when one changes patch is the same as the shift of the GH charges under the gauge transformation (3.24).

To summarize this discussion, in order to describe the dynamics and vacuum structure of a supertube, one has to work in a fixed patch (in the examples above we have chosen the one where there are no Dirac strings at the point '1'). However, to understand the physics of a supertube minimum near one of the poles one has to change to a patch where there are no Dirac strings at that pole.

Armed with the understanding of how to change patches, we are now ready to explain how metastable supertubes decay as depicted in Figure 3.9.

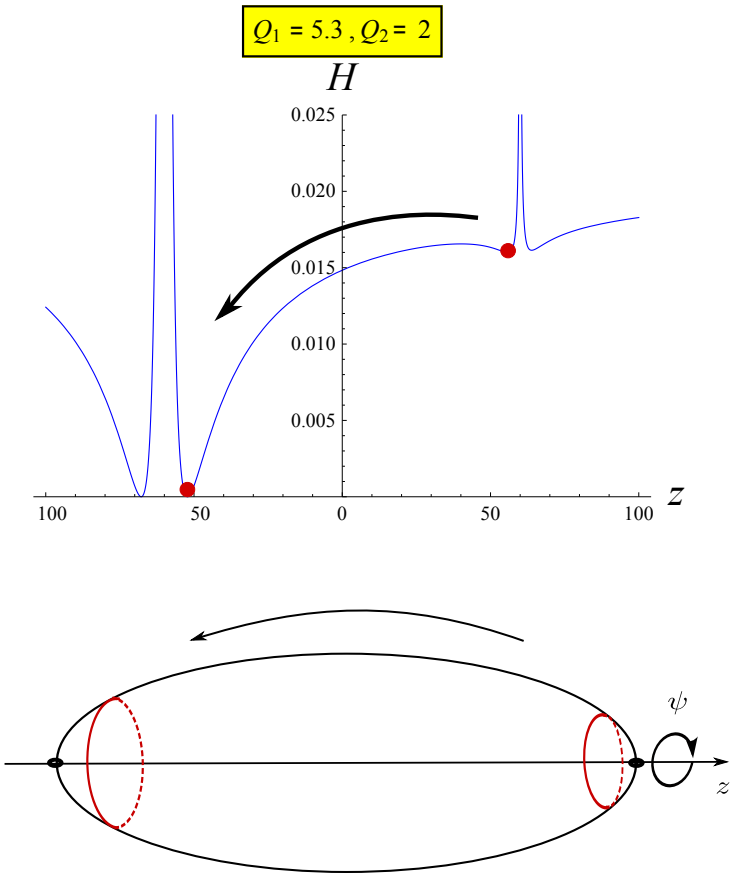


Figure 3.9: Illustration of the tunneling process. Supertubes are depicted as red circles wrapping the Gibbons-Hawking fiber $\psi$. A metastable supertube close to one center can tunnel to a stable supertube close to the other center, reducing in the process the flux on the two-cycle between these two centers.

Let us first discuss the example where the metastable supertube decays to a degenerate supersymmetric minimum, illustrated in Figure (3.10). In the patch with no Dirac strings at the point '2', the zero-radius supertube wraps the Dirac string at point '1'. Hence, this tube is non-contractible (cannot be taken away). In order to reveal that the zero-radius supertube is a bunch of parallel branes, one has to go to the patch with no Dirac strings at point '1', and the charges of the branes will shift as in (3.26). These supersymmetric branes are now parallel to the background, and can be taken away to infinity.

So in the Gedankenexperiment of lowering the supertube into position at the metastable minimum, having it decay to the supersymmetric minimum and taking the decay products back to infinity as, the charge difference between the initial and the final probe branes is

$$\Delta q_1 = -d_3 \Pi_{12}^{(2)}\,, \qquad \Delta q_2 = -d_3 \Pi_{12}^{(1)}\,. \tag{3.27}$$

Furthermore, as we have explained above, when the supertube sweeps out the two-cycle between the points '$i$' and '$j$' it lowers the $\Pi^{(3)}$ flux of the background by $d_3$ units. Hence, the charges of the background, which come entirely from the magnetic fluxes

$$Q_1^{\rm bg} = \Pi_{12}^{(2)} \Pi_{12}^{(3)}\,, \qquad Q_2^{\rm bg} = \Pi_{12}^{(1)} \Pi_{12}^{(3)}\,, \tag{3.28}$$

are lowered by exactly the amount in (3.27). The net result of this process is that the negative charges of the metastable tube have annihilated against the positive charges dissolved in flux.

On can repeat the same Gedankenexperiment with a metastable supertube that decays into a non-degenerate minimum: to take away the decay product one needs again to change patch, and thus shift the charges of the supertube as in (3.27). The change in charges of the tube is again compensated by a change in the fluxes, which reduces the charges of the background by the same amount.

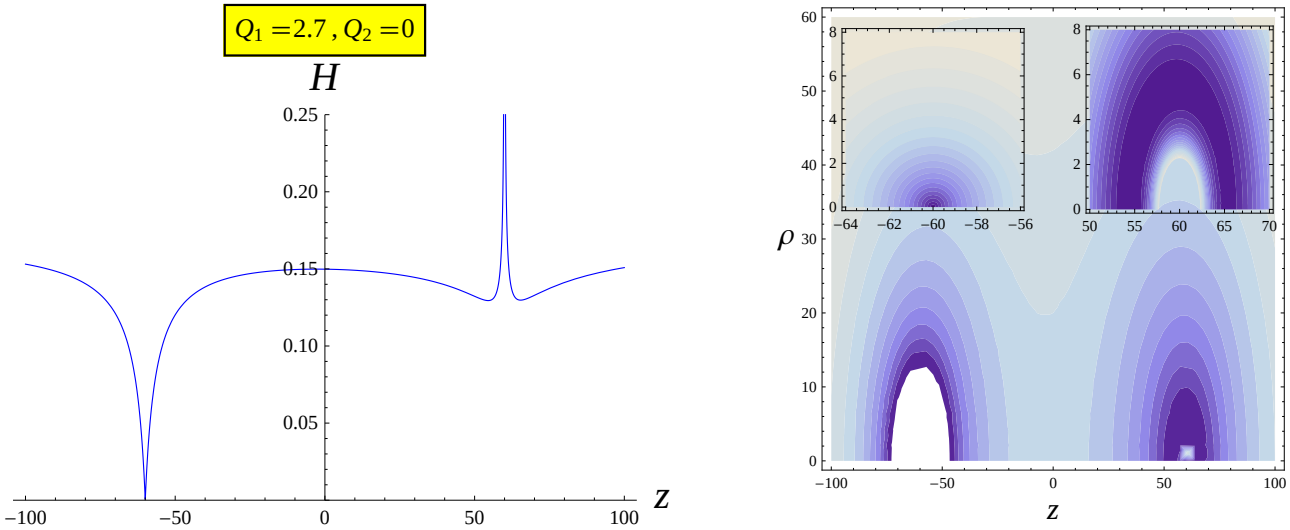


Figure 3.10: A metastable minimum and a degenerate supersymmetric at the center on the left. The white region in the contour plot on the right is an artifact of the choice of range for the contour plot; see the insets for a complete picture. The color scales in the insets and main contour plot are different.

## 3.4 Supertubes in smooth scaling three-charge backgrounds

We now extend the analysis of supertubes in bubbling backgrounds to supertubes placed in *scaling* three-charge backgrounds. The latter are microstate geometries of black holes and black rings as reviewed in Section 1.4. In Subsection 3.4.1 we review the data characterizing smooth scaling three-charge backgrounds and discuss the scaling property of the supertube Hamiltonian. As an example, in Subsection 3.4.2 we study supertubes in a seven-center scaling solution.

### 3.4.1 Smooth scaling backgrounds

Microstate geometries are everywhere smooth and free of horizons, such that each individual geometry carries no entropy. They have the same mass, charges and angular momenta as their black hole or black ring counterpart. Deep microstate geometries have a scaling behavior: the centers can be put arbitrarily close such that the geometry develops a very long throat (see Figure 3.11), while the curvature is small everywhere.

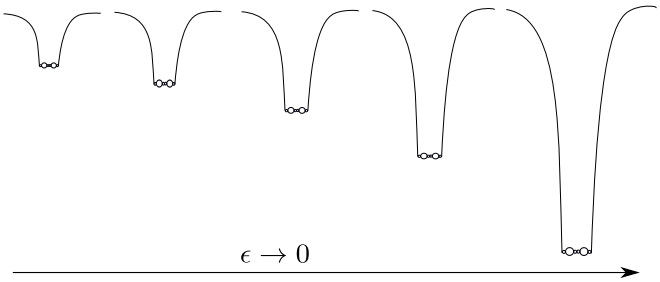


Figure 3.11: Heuristic picture of scaling microstate geometries.

### Smoothness, regularity and asymptotic flatness

The physical requirements for regular smooth three-charge backgrounds have been discussed in detail in Subsection 1.4.5. We summarize here the form of the harmonic functions after imposing regularity, smoothness and asymptotic flatness. We are interested in asymptotically $\mathbb{R}^{4,1}$ solutions for which $v_0 = 0$ and $Z_I \to 1$ at spatial infinity. The harmonic functions $V$ (Taub-NUT charges) and $K^I$ (dipole charges) are fixed as:

$$V = \sum_{j=1}^{N} \frac{v_j}{r_j}\,, \qquad K^I = \sum_{j=1}^{N} \frac{k_j^I}{r_j}\,. \tag{3.29}$$

Regularity requires these harmonic functions to be sourced at the same points and one must take $v_j \in \mathbb{Z}$. For the base metric to be asymptotically $\mathbb{R}^4$ one must impose

$$\sum_{j=1}^{N} v_j = 1. \tag{3.30}$$

Then smoothness determines $L_I$ (M2 charges) and $M$ (momentum along $\psi$) to be

$$L_I = 1 - \frac{1}{2} C_{IJK} \sum_{j=1}^{N} \frac{k_j^J k_j^K}{v_j} \frac{1}{r_j}, \qquad M = m_0 + \frac{1}{12} C_{IJK} \sum_{j=1}^{N} \frac{k_j^I k_j^J k_j^K}{v_j^2} \frac{1}{r_j}, \tag{3.31}$$

with

$$m_0 = -\frac{1}{2} \frac{\sum_{j=1}^{N} \sum_{I=1}^{3} k_j^I}{\sum_{i=1}^{N} v_i} = -\frac{1}{2} \sum_{j=1}^{N} \sum_{I=1}^{3} k_j^I. \tag{3.32}$$

After imposing regularity and smoothness as well as asymptotic flatness there is a residual freedom in choosing $N-1$ Taub-NUT charges and $N$ dipole charges.

### Asymptotic charges and angular momenta

We summarize the charges and angular momenta of the five-dimensional solutions which were discussed in Subsection 1.4.5. Since the solution is invariant under the gauge transformation

$K^I \to K^I + c^I V$, or $k^I_j + c^I v_j$, for any constant $c^I$, we define asymptotic quantities in terms of the gauge invariant flux parameters:

$$\tilde{k}^I_j \equiv k^I_j - v_j \left( \sum_{j=1}^{N} k^I_j \right) . \tag{3.33}$$

The electric charges of the solution as measured at infinity are extracted from the $\rho^{-2}$ term, with $r = \frac{1}{4}\rho^2$ in the expansion of the warp factors $Z_I$: [7]

$$Q_I = -2C_{IJK} \sum_{j=1}^{N} \frac{\tilde{k}^J_j \tilde{k}^K_j}{v_j}. \tag{3.34}$$

In five dimensions there are two angular momenta, which are read off from the asymptotic behavior of $k$ in (3.6) from the terms that have a $\rho^{-2}$ fall-off:

$$k = \frac{1}{4\rho^2}\Big( (J_1 + J_2) + (J_1 - J_2)\cos\theta \Big) d\psi + \dots \tag{3.35}$$

where $\theta$ is the angle between $\vec{r}$ and the dipoles $\vec{D} \equiv \sum_{j=1}^{N} \sum_{I=1}^{3} \tilde{k}^I_j \vec{r}_j$. The two angular momenta are then given by

$$J_R \equiv J_1 + J_2 = \frac{4}{3} C_{IJK} \sum_{j=1}^{N} \frac{\tilde{k}^I_j \tilde{k}^J_j \tilde{d}^K_j}{v_j^2} \quad \text{and} \quad J_L \equiv J_1 - J_2 = 8|\vec{D}|. \tag{3.36}$$

Using the bubble equations, one can associate an angular momentum flux vector with the $ij^{\text{th}}$ bubble:

$$\vec{J}_L = \sum_{i>j} \vec{J}_{L,ij} \,, \qquad \vec{J}_{L,ij} \equiv -\frac{4}{3} v_i v_j C_{IJK} \Pi^{(I)}_{ij} \Pi^{(J)}_{ij} \Pi^{(K)}_{ij} \frac{(\vec{r}_i - \vec{r}_j)}{|\vec{r}_i - \vec{r}_j|}. \tag{3.37}$$

The flux on the left-hand side of the bubble equation (1.128) yields the contribution of the bubble to $J_L$.

### Supertubes in scaling backgrounds

A scaling background is a bubbling configuration that has a set of GH points that can approach each other arbitrarily close. This was discussed in Subsection 1.4.5 for the simple case of three centers. As the points get closer together, the solution develops an ever deeper throat and looks more and more like the black hole with the same asymptotic charges. Deep scaling solutions are dual to states that belong to the same CFT sector as the typical microstates, that give the leading contribution to the black hole entropy [32, 35, 166].

For a given set of charges, a scaling limit exists if we can find a solution to the bubble equations (1.126) or (1.128) for

$$r_{ij} = \epsilon \tilde{r}_{ij} \qquad \text{with} \quad \epsilon \to 0. \tag{3.38}$$

[7] To isolate the charges of the solution one needs to take (3.3) to a standard polar form for $\mathbb{R}^4$ via $r = \frac{1}{4}\rho^2$.

When such a solution can be found, all distances in the GH base scale to zero, but the physical size of the bubbles and ratios between distances are preserved throughout the scaling $\epsilon \to 0$, because the warp factors along the bubbles diverge appropriately.

When we focus on scaling backgrounds we find that the Hamiltonian has a similar scaling. By rescaling the coordinates on the 3d base as $\vec{r} = \epsilon\,\vec{\tilde{r}}$, and taking the limit $\epsilon \to 0$, the Hamiltonian scales as

$$\mathcal{H}\big(\epsilon\,\vec{\tilde{r}}\big) = \epsilon\,\mathcal{H}\big(\vec{\tilde{r}}\big) + \mathcal{O}(\epsilon^2) \tag{3.39}$$

As already mentioned, there exist two ways of obtaining a scaling solution. The first is to consider a set of $N$ centers whose charges allow for scaling behavior; they satisfy $N-1$ bubble equations, and their $2N-2$ dimensional moduli has a region where the points come together, and the fully backreacted solution develops a long throat [111, 35]. The second way is to insist that the centers be collinear – their positions are now parametrized by $N-1$ variables that are completely determined by the $N-1$ bubble equations – and force the centers to scale by tuning by hand some of the flux parameters on the centers or some of the moduli of the solution [32].

We will use the second approach, essentially because it gives much more control on the dynamics of the supertube. If one adds a supertube to a scaling solution whose centers are not collinear, the energy of the supertube depends on the length of the throat, and can change as the centers move in the moduli space. On the other hand, in a $U(1) \times U(1)$ invariant solution the centers are collinear and hence frozen, and if the supertube charges are smaller than those of the other centers, the physics of the metastable supertube is expected to be captured by its probe action in the background.

Thus, in the examples in the next Section, we focus on scaling solutions where all the GH points are collinear and we will 'turn the knob' of the scaling control parameter $\epsilon$ by tuning one of the charges $k_i^I$.

### 3.4.2 Metastable supertubes in a seven-center scaling solution

In this Subsection, we analyze the minima the probe supertubes in a 'pincer' supersymmetric scaling background (inspired from [32]) whose centers are collinear in $\mathbb{R}^3$ and have $J_L = 0$. This pincer solution contains a central 'blob' of total GH charge one, as well as two symmetric satellite blobs of GH charge zero. For computational ease, we take a configuration that is made up out of a total of seven points on the GH base: a central blob made from three points, of GH charges $-n, 2n+1, -n$, and two satellites with two points that have GH charges $-Q$ and $+Q$. The configuration, depicted in Figure 3.12, is $\mathbb{Z}_2$ symmetric, and hence has $J_L = 0$ by construction.

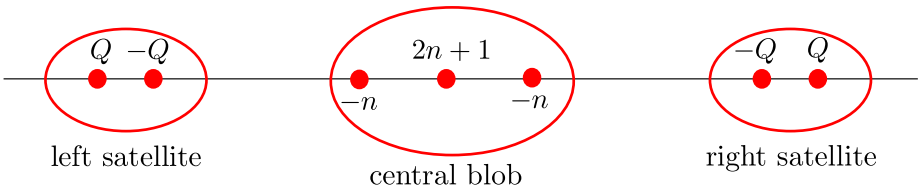


Figure 3.12: Our setup consists of a central blob of three centers and two satellite blobs of two centers each, with the GH charges as given in the figure.

One can then choose fluxes between the various GH centers such that the total configuration has the charges of a BPS black hole with a macroscopically-large horizon area. The particular choice of fluxes that ensures that a five-point solution has no CTC's was obtained in [32] by tediously analyzing blob mergers, and our configuration is simply the $\mathbb{Z}_2$ symmetrization of that choice.

### Background data

We choose a cylindrical coordinate system $(\rho, z, \theta)$ in three dimensions, where $z$ runs along the axis through the centers and $\rho, \theta$ are polar coordinates in the orthogonal plane. Since we have cylindrical symmetry, the solution only depends on the coordinates $z$ and $\rho$. The seven centers are put on the $z$-axis and are numbered $z_1 \dots z_7$ as in Figure 3.13.

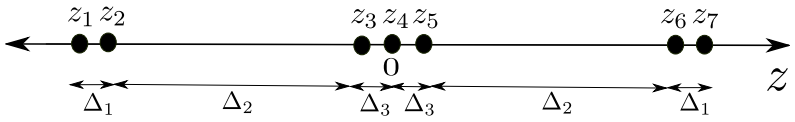


Figure 3.13: Schematic picture of our microstate configuration.

We choose the GH charges to be

$$v_1 = 20,\ v_2 = -20, \qquad v_3 = -12,\ v_4 = 25,\ v_5 = -12, \qquad v_6 = -20,\ v_7 = 20. \tag{3.40}$$

The flux parameters of the central blob are chosen as

$$k_i^1 = \frac{5}{2}|v_i|, \qquad k_i^2 = \hat{k}|v_i|, \qquad k_i^3 = \frac{1}{3}|v_i|\,, \qquad i = 3, 4, 5\,, \tag{3.41}$$

and those of the satellites are

$$\begin{aligned} k_1^1 &= 1375\,, & k_1^2 &= -\frac{1835}{2} + 980\hat{k}\,, & k_1^3 &= -\frac{8360}{3}\,, \\ k_2^1 &= -1325\,, & k_2^2 &= \frac{1965}{2} - 980\hat{k}\,, & k_2^3 &= \frac{8380}{3}\,, \end{aligned} \tag{3.42}$$

and their mirror image $k_7^I = k_1^I$, $k_6^I = k_2^I$.

The charges of the harmonic functions are then a function of $\hat{k}$ only. For every value of $\hat{k}$, the bubble equations (1.128) fix the position of the seven centers. One can approximate the size of the microstate by $z_6 \approx r_0$ as in [32]:

$$r_0 = \frac{\widehat{J}_L}{8\sum_I (k_6^I + k_7^I)}\,, \tag{3.43}$$

where $\widehat{J}_L$ is the angular momentum contained in the centers $z_3, \dots z_7$. In the given background, this is linear in $\hat{k}$ as:

$$r_0 = \frac{56}{31} \times 10^3 |\hat{k} - \hat{k}_\star|\,, \qquad k_\star \approx 3.17975\,. \tag{3.44}$$

We will tune $\hat{k}$ such that $r_0 \to 0$ and the configuration scales down into a deep throat.

In Table 3.1 we list the relevant distances and ratios of distances for various values of the flux parameter $\hat{k}$. Starting from one set of inter-center distances the bubble equations (1.128) successively determine the equilibrium distance for every value of $\hat{k}$ during the scaling.

| Background | $\hat{k}$ | $z_6$ | $\frac{z_6}{r_0}$ | $\frac{\Delta_3}{\Delta_1}$ | $\frac{\Delta_2}{\Delta_1}$ |
|---|---|---|---|---|---|
| 1 | 3.08333 | 176.088 | 1.011 | 1.5464 | 6730.9 |
| 2 | 3.16667 | 23.91 | 1.01166 | 1.61449 | 6664.58 |
| 3 | 3.175 | 8.69039 | 1.01279 | 1.6215 | 6657.94 |
| 4 | 3.1775 | 4.12444 | 1.01474 | 1.62362 | 6655.95 |
| 5 | 3.178 | 3.21125 | 1.0158 | 1.62404 | 6655.55 |
| 6 | 3.17833 | 2.60246 | 1.01693 | 1.62432 | 6655.29 |
| 7 | 3.17867 | 1.99366 | 1.01874 | 1.6246 | 6655.02 |
| 8 | 3.1795 | 0.471667 | 1.04441 | 1.62531 | 6654.36 |
| 9 | 3.17967 | 0.167268 | 1.11114 | 1.62545 | 6654.22 |

Table 3.1: Distances between the points throughout the scaling process. The distances $\Delta_i$ and $z_6$ are as in Figure 3.13. The parameter $\hat{k}$ is tuned for the scaling, all the other charges are kept fixed at their values (3.40) and (3.41). It is clear that the relative distances stay approximately the same during the scaling. Also the total charges $Q_I$ and angular momentum $J_R$ stay approximately the same throughout the scaling.

### Charges and angular momenta

The values of the electric charges and the right-moving angular momentum as defined in (3.34) and (3.36) stay approximately constant throughout the scaling

$$Q_1 \approx 1.476 \times 10^5\,, \quad Q_2 = 1.196 \times 10^5\,, \quad Q_3 \approx 1.76 \times 10^5\,, \quad \text{and} \quad J_R \approx 1.018 \times 10^8\,. \tag{3.45}$$

Note that $Q_2$ is independent of $\hat{k}$. Since the configuration is symmetric (the charges of opposite centers are the same), the left-moving angular momentum is exactly zero throughout the whole merger process. [8] Since the charges and angular momenta all stay nearly constant *throughout the scaling* these microstates have the charges of a black hole of non-zero entropy in all regimes: when they are shallow (before the scaling), when they are very deep (in the scaling limit) and in the whole intermediate regime.

### The supertube potential

We plot the potential for a probe supertube in this background, with supertube charges

$$(q_1, q_2, d_3) = (10, -50, 1)\,. \tag{3.46}$$

The potential is normalized to zero for a supersymmetric minimum:

$$H \equiv \mathcal{H} - (q_1 + q_2)\,. \tag{3.47}$$

[8] For configurations with only one satellite this symmetry is broken and $J_L \neq 0$. Then $J_L$ goes to zero as the solution gets deeper and deeper. The end-point of such a merger is a BMPV black hole microstate with $J_L = 0$. Only in this deep-throat limit the microstates have the charges of a black hole of non-zero entropy, while our background has the charges of a BMPV black hole throughout the scaling.

For illustrative purposes, we plot the potential of the supertube in the background '2' of Table 3.1 as a function of $z$ and perform a Contour plot around the minima in a plane through the $z$-axis, see Figure 3.14. The positions of the seven centers in background 2 are

$$z_1 = -23.9136\,,\;\; z_2 = -23.91\,,\;\; z_3 = -0.00579078\,,$$
$$z_4 = 0\,,\;\; z_5 = |z_3|\,,\;\; z_6 = |z_2|\,,\;\; z_7 = |z_1|\,. \tag{3.48}$$

The potential has several supersymmetric minima: two lie inside the central blob, two lie just outside and there are two more minima in between the central blob and the satellite centers at $z \approx \pm 10$. There are two metastable minima close to the satellites, near $z_2$ and $z_6$. Since the setup is symmetric, we focus on the metastable minimum at $z_{\rm ms} \lesssim z_6$:

$$z_{\rm ms} = 23.8729\,, \qquad z_6 = 23.91\,. \tag{3.49}$$

The supertube in that minimum can tunnel to the supersymmetric minimum at $z \simeq 10$ via brane-flux annihilation as explained in Section 3.3. Note that the additional non-supersymmetric minima near $z = \pm 50$ as seen from Figure 3.14 are in fact saddle points and they have a runaway behavior off the axis.

In order to stay well in the probe approximation one needs to make sure that the charges of the supertube are small compared to the charges of the background (as measured by the poles of $L_I$). In particular, the metastable minimum at $z_{\rm ms}$ sits close to the centers $z_6$ and $z_7$ of the background, and we have to make sure that the charges at that position are large compared to the ones of the supertube. For the charges and flux parameters as fixed in (3.40) and (3.41) the background electric charges at the black ring centers are of the order $3 \times 10^5$ and hence our supertube is well in the probe regime.

As explained before, the supertube potential scales down linearly with the coordinate distance between the background centers, see Equation (3.39). As an illustration, we compare the potential for two scaling backgrounds, 2 and 9 of Table 3.1 in Figure 3.15. One clearly sees the self-similarity of the potentials. Also the supertube position $z_{\rm ms}$ scales down with the throat: its relative position to the other centers stays unchanged.

## 3.5 Non-extremal microstate throats

Upon backreaction, metastable supertubes in scaling backgrounds should become microstates of non-extremal black holes. In this Section we want to compare the size of these microstates to the size of the corresponding black hole, and understand the scale at which non-extremal fuzzballs differ from the black hole.

### 3.5.1 The idea

One can estimate the depth of a black hole or of a fuzzball throat by integrating the radial metric component:

$$L = \int_{r_{\rm bottom}}^{r_{\rm neck}} \sqrt{g_{rr}}\, dr\,, \tag{3.50}$$

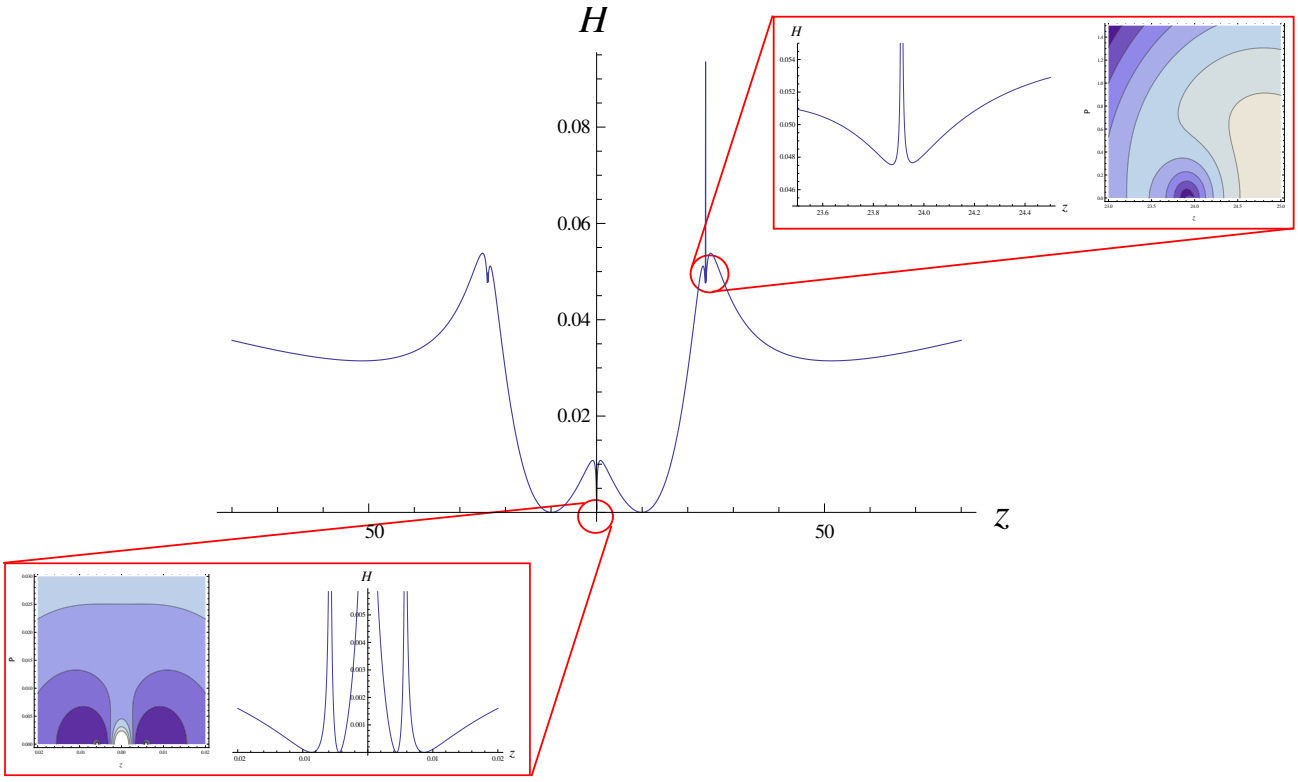


Figure 3.14: Zoom on the supertube potential for charges $(q_1, q_2, d_3) = (10, -50, 1)$ in background 2. Note the metastable minimum near $z_6 = 23.91$ (and its mirror near $z_2 = -23.91$). The contour plot shows that this minimum is of 'Mexican hat – type' in the $z - \rho$ plane around the center $z_6$ ($z_2$); darker colors mean lower energy. On can see that this minimum has no runaway behavior in the $\rho$ direction and hence is truly metastable. The supertube in that minimum can tunnel to a supersymmetric state. Note also that the minima near the central blob are in fact two mirror copies of a Mexican hat-type circular band of minima, as the contour plot in the bottom left corner shows.

between the bottom and the neck of the throat. To get the depth of the non-extremal microstate, we can evaluate this integral in the supersymmetric background geometry since the probe supertube will not affect the geometry too much. We then compare this to the depth of the throat of the non-extremal black hole (a Cvetic-Youm black hole [168], see appendix C.1) that has the same charges.

The main result of **P3** is that we, indeed, find microstates that are of the same depth as the non-extremal black hole, but we also find deeper ones and shallower ones. This is not surprising: Supertube probes placed in deep scaling solutions will not affect the background geometry too much upon backreaction and the resulting non-extremal microstate will, hence, be of the same size as the supersymmetric background. The size of the corresponding non-extremal black hole, however, depends on the extremality parameter which is set by the charges of the supertube. Small supertube charges correspond to deep black holes; increasing the tube charges takes the black hole further away from extremality and thus makes the throat more shallow. Hence, by tuning the supertube charges we can always find the throat of the non-extremal black hole to be

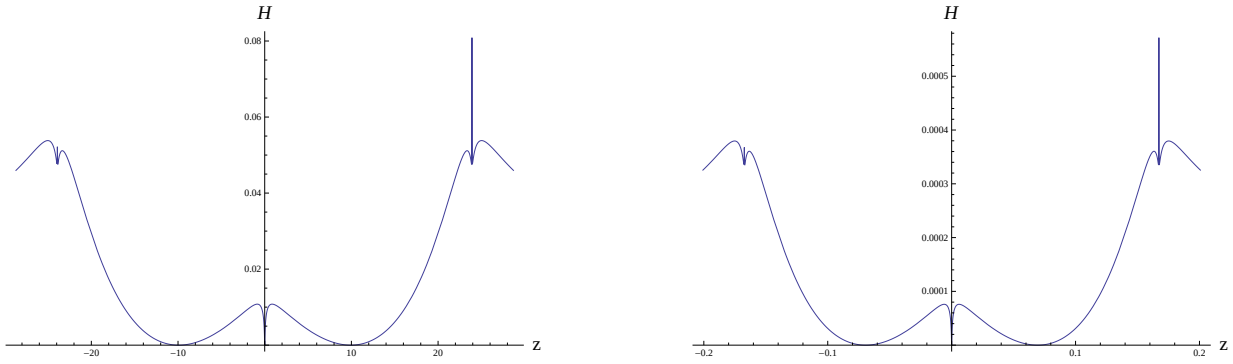


(a) Potential in background 2, $z_6 = 23.91$

(b) Potential in background 9, $z_6 = 0.167268$

Figure 3.15: The supertube potential for charges $(q_1, q_2, d_3) = (10, -50, 1)$ in two scaling backgrounds. The energy scales down linearly with the coordinate size between the centers.

of a size comparable to that of its microstates. This intuition is summarized in Figure 3.16.

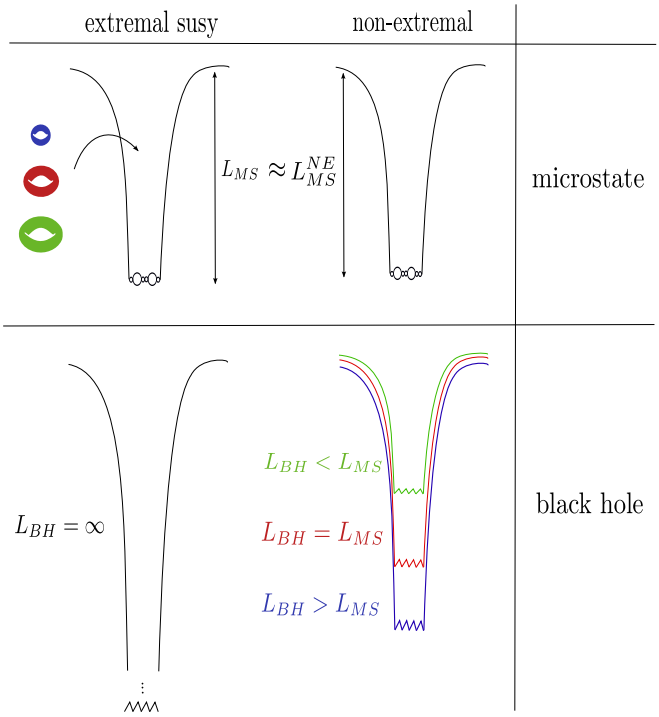


Figure 3.16: The scaling of the background determines the size of the metastable black hole microstates. For a BPS background of a fixed depth, adding heavy supertubes gives a microstate of a black hole that has shorter throat, while adding light supertubes gives a microstate of a black hole with a longer throat.

In the remainder of this Section we make this intuitive picture more precise. First, we determine the data of the non-extremal black hole with the charges of the metastable bound

states in Subsection 3.5.2. We give the depths of the black hole and microstate throats in Subsection 3.5.3. Since the resulting integrals are quite complicated, we make an insightful approximation in appendix C.2.

### 3.5.2 Non-extremal black hole parameters

We begin with a supersymmetric fuzzball solution that has the charges of a supersymmetric rotating BMPV black hole, and its mass is hence

$$M = Q_1 + Q_2 + Q_3 \,. \tag{3.51}$$

Adding a supertube with charges $q_1, q_2$ increases the mass by the value of the supertube potential at the minimum $\mathcal{H}_{\min} = q_1 + q_2 + \Delta M$ (see also Figure 3.17). When the minimum is supersym-

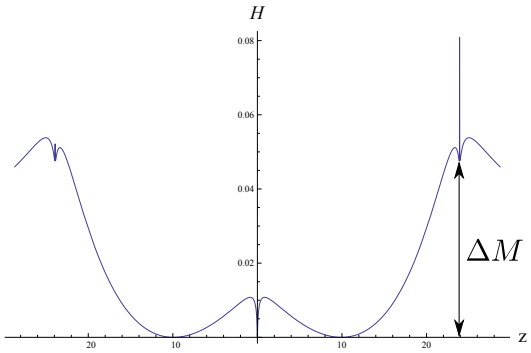


Figure 3.17: The metastable supertube brings in an excess energy $\Delta M = M^{\rm BH}_{ADM} - \sum_I Q^{\rm BH}_I$.

metric $\Delta M = 0$, and the resulting configuration is a BPS microstate. When the supertube minimum is metastable, the mass is:

$$M = Q_1 + Q_2 + Q_3 + q_1 + q_2 + \Delta M \,, \tag{3.52}$$

and the charges are

$$Q_1^{\rm tot} = Q_1 + q_1 \,, \qquad Q_2^{\rm tot} = Q_2 + q_2 \qquad Q_3^{\rm tot} = Q_3 \,. \tag{3.53}$$

Since, $M_{ADM} > \sum_I Q_I$, the configuration with a metastable supertube has the charges and mass of a non-extremal black hole. The energy above extremality is exactly given by $\Delta M$:

$$\Delta M = M - \sum_I Q_I^{\rm tot} \,. \tag{3.54}$$

In appendix C.1, we review the non-extremal rotating M2-M2-M2 black hole geometry. The solution depends on six parameters: a mass parameter $m$, three 'boosts' $\delta_I$ and angular momentum parameters $a_1, a_2$ which are related to the ADM mass, charges and angular momenta

$$M^{\rm BH}_{ADM} = \sum_I \frac{m}{4}(e^{2\delta_I} + e^{-2\delta_I}) \,, \qquad J_1^{\rm BH} = m(a_1 c_1 c_2 c_3 - a_2 s_1 s_2 s_3) \,, \tag{3.55}$$

$$Q^{\rm BH}_I = \frac{m}{4}(e^{2\delta_I} - e^{-2\delta_I}) \,, \qquad J_2^{\rm BH} = -m(a_2 c_1 c_2 c_3 - a_1 s_1 s_2 s_3) \,, \tag{3.56}$$

where $c_I = \cosh\delta_I$ and $s_I = \sinh\delta_I$. We determine the parameters $\delta_I, a_i, m$ of the metastable state. The parameters $\delta_I$ are given by the charges and parameter $m$ as

$$\frac{m}{2}e^{2\delta_I} = Q_I^{\rm BH} + \sqrt{(Q_I^{\rm BH})^2 + \frac{m^2}{4}}\,. \tag{3.57}$$

The parameter $m$ is determined by the energy of the metastable supertube as follows. With (3.56) the energy above extremality (3.54) can be written in terms of $m$ and $\delta_I$ as

$$\Delta M = \sum_I \frac{m}{2}e^{-2\delta_I}\,. \tag{3.58}$$

In the probe approximation, the supertube charges are small compared to those of the background. Then the non-extremal black hole is close to the supersymmetric limit ($m/Q_I^{\rm BH} \ll 1$) and the black hole charges are approximately those of the background and (3.57) becomes

$$\frac{m}{4}e^{2\delta_I} = Q_I\,. \tag{3.59}$$

The non-extremality parameter is then given by the charges and energy of the metastable state

$$m = \sqrt{\frac{8\Delta M}{\sum_I 1/Q_I}}\,. \tag{3.60}$$

In this approximation, the angular momentum parameters $a_1, a_2$ are:

$$\begin{aligned} J_L^{\rm BH} &\equiv J_1^{\rm BH} - J_2^{\rm BH} = \frac{\sqrt{m}}{2}(a_1+a_2)\sqrt{Q_1Q_2Q_3}\left(\frac{1}{Q_1}+\frac{1}{Q_2}+\frac{1}{Q_3}\right)\,, \\ J_R^{\rm BH} &\equiv J_1^{\rm BH} + J_2^{\rm BH} = \frac{2}{\sqrt{m}}(a_1-a_2)\sqrt{Q_1Q_2Q_3}\,. \end{aligned} \tag{3.61}$$

### 3.5.3 Comparing the microstates and the black hole

As explained in Section 3.1, extremal black holes have an infinite throat, and comparing the length of this throat to that of the fuzzballs is meaningless. Comparing the thicknesses of the throats on the other hand gives automatically the same result: the thickness is only controlled by the charges. For near-extremal black holes the thickness is also largely controlled by the charges, so it will automatically be the same for fuzzballs and black holes. On the other hand, non-extremal black holes have a finite throat, and hence comparing the lengths of the throats is now meaningful, and can indicate which fuzzballs are expected to be more typical than the others, and whether fuzzballs differ from the black hole away from the horizon microscopically or macroscopically.

We denote the difference in the length of the non-extremal black hole throat and that of its microstates by

$$\Delta L \equiv L_{BH} - L_{MS}\,. \tag{3.62}$$

Although we have not backreacted the metastable bound state, we have argued above that a small probe supertube will not significantly change the geometry and hence $L_{MS}$ will be the

length of the supersymmetric microstate throat given by (3.1). We can estimate the throat length by integrating along the $z$-axis, from the outermost center $z_{MS} \equiv z_7$ up to a suitable cutoff scale $z_{\rm neck}$. The depth of the black hole throat is the metric distance from the horizon at $\rho = \rho_+$ to the end of the throat at $\rho = \rho_{\rm neck}$ with the metric (C.1). A suitable cutoff is $z_{\rm neck} = \rho_{\rm neck} = (Q_1^{BH} Q_2^{BH} Q_3^{BH})^{1/6}$. The expression for $\Delta L$ is quite complicated, but as we explain in appendix C.2 we can make a very insightful approximation through which we obtain

$$\Delta L \approx \rho_{\rm neck} \ln \left( 2 \frac{\rho_{MS}}{\rho_+} \right) , \tag{3.63}$$

where we replaced the cutoff $z_{MS}$ by $\rho_{MS}$ in a spherically symmetric approximation of the microstate geometry.

Consider the following scaling of the supertube charges and of the coordinates of the GH centers:

$$\begin{aligned} (q_1, q_2, d_3) &\rightarrow e^{\lambda} (q_1, q_2, d_3) , \\ \rho_{MS} &\rightarrow e^{\mu} \rho_{MS} . \end{aligned} \tag{3.64}$$

The approximated difference in depths then goes as

$$\boxed{\frac{\Delta L}{\rho_{\rm neck}} \rightarrow \frac{\Delta L}{\rho_{\rm neck}} - \frac{1}{4}\lambda + \frac{3}{4}\mu} . \tag{3.65}$$

This reveals that the black hole throat can be made deeper than that of the microstate ($\Delta L$ positive) by taking either smaller tubes or deeper background microstates.

To confirm this approximation, we evaluate $\Delta L = L_{BH} - L_{MS}$ numerically. We do this for supertubes of charges

$$(q_1, q_2, d_3) = e^{\lambda} (10, -50, 1) , \tag{3.66}$$

with $\lambda = -10, -9, \ldots, 9, 10$. The supertubes are placed in the nine background scaling geometries of different sizes of Table 3.1. The size of the black hole throat $L_{BH}$ is calculated from (C.11) for the rotating black hole geometry (C.1), and the parameters of the black hole are extracted from the metastable supertube minima as in Subsection 3.5.2. The size of the microstate throat is obtained by integrating (C.9). We replace the background microstate geometry by that of the extremal black hole.

We plot our findings in Figures 3.18(a) and 3.18(b). In Figure 3.18(a) we show the effect of scaling the tube charges. We plot $\Delta L$ for tubes of various sizes ($\lambda = -10, -9, \ldots, 9, 10$), in three scaling solutions of Table 3.1. We find all possibilities: microstates that are deeper, of the same depth, and shallower than the black hole. By making the tubes smaller, the black hole can always be made deeper than the microstate. It is also clear that $\Delta L$ has the scaling behavior anticipated in (3.65).

In Figure 3.18(b) we show the effect of putting the tube in backgrounds of different scaling size and depth. We plot $\Delta L$ for tubes in all nine scaling solutions (2,6 and 9 of Table 3.1), in terms of $\mu \equiv \log z_7$, where $z_7$ is the position of the outermost center of the scaling background. This reveals that the approximately linear scaling (3.65) still holds.

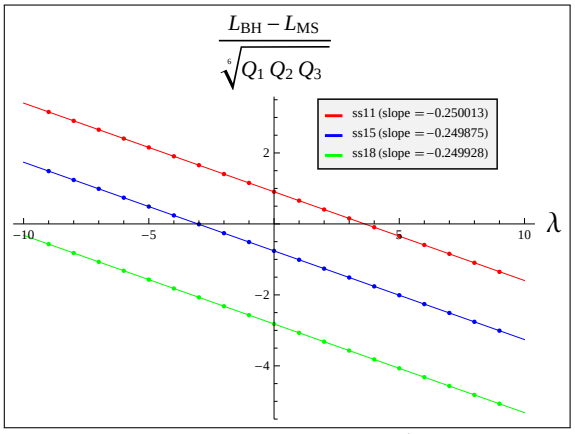


(a) The difference in depths $\frac{\Delta L}{\rho_{\rm neck}}$ in terms of the tube charge scaling sizes $(q_1, q_2, d_3) = e^{\lambda}(10, -50, 1)$ for the backgrounds 2, 6 and 9 of Table 3.1.

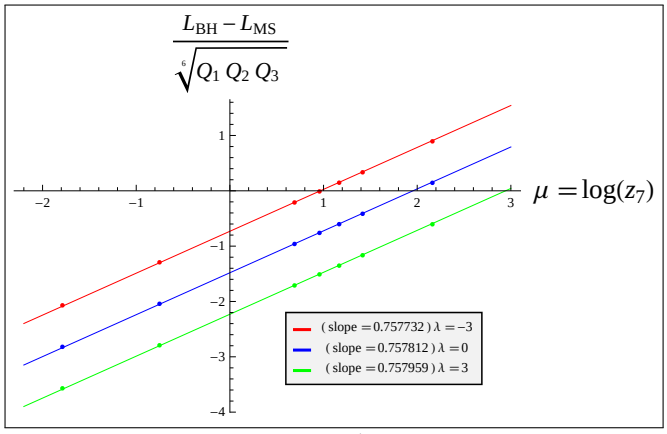


(b) The difference in depths $\frac{\Delta L}{\rho_{\rm neck}}$ in terms of the scaling solution sizes measured by the logarithm of the position of the $7^{\rm th}$ center $z_7$.

Figure 3.18: The difference in depths $\Delta L = L_{BH} - L_{MS}$ for tubes of size $\lambda = -10, -9, \ldots, 9, 10$ in several scaling backgrounds.

### 3.5.4 The range of validity of our construction

Having obtained non-extremal microstates by placing probe supertubes inside long supersymmetric fuzzballs, it is important to study the ranges of charges in which our construction is valid. Clearly, since we have not backreacted the supertube, and treated them as probes, we are automatically assuming that their charges and dipole charges are much smaller than those of the GH centers and we are only describing configurations whose mass above extremality is much smaller than the sum of the charges. These correspond to microstates of near-extremal black holes.

A possible mechanism for invalidating our construction is if the microstates we create will have closed timelike curves. In the absence of backreaction one cannot say precisely when or whether this will happen; however, one can estimate whether the angular momentum of a microstate is larger or smaller than the angular momentum that would cause closed timelike curves in a black hole of identical charges and length.

The non-extremal black hole geometry has closed timelike curves unless $m \geq (a_1 \pm a_2)^2$. This gives two 'cosmic censorship bounds' on the black hole angular momenta. For a near-extremal black hole, the angular momenta (3.61) have to satisfy:

$$\begin{aligned} J_L^{\rm BH} &\leq \frac{m}{2}\sqrt{Q_1Q_2Q_3}\left(\frac{1}{Q_1}+\frac{1}{Q_2}+\frac{1}{Q_3}\right), \\ J_R^{\rm BH} &\leq 2\sqrt{Q_1Q_2Q_3}\,. \end{aligned} \tag{3.67}$$

The second bound is automatically satisfied because we are starting with a BPS microstate of a black hole with a large horizon area, and adding a probe supertube only changes the charges and $J_R$ by very small amounts.

The first bound is more problematic. Since the BPS microstate has $J_L = 0$, the resulting metastable microstate will get its left-moving angular momentum entirely from the $\vec{E} \times \vec{B}$ interactions between the supertube and the background. If we call this contribution $J_L^{\rm tube}$ and express the parameter $m$ in terms of the energy of the metastable supertube $\Delta M$, this bound becomes

$$J_L^{\rm tube} \leq A(Q)\sqrt{\Delta M}\,, \qquad A(Q) = \sqrt{2}\sqrt{Q_1 Q_2 Q_3}\sqrt{\frac{1}{Q_1}+\frac{1}{Q_2}+\frac{1}{Q_3}}\,. \tag{3.68}$$

Since both the angular momentum $J_L^{\rm tube}$ and $\Delta M$ scale linearly with the tube charges, we see that in a solution of fixed length this condition will be violated when the tube charges become very large.

Alternatively, one can consider a supertube with fixed charges in a solution whose length is dialed by hand by bringing the centers together on the GH base. The mass above extremality $\Delta M$ is linear in the inter-center separation, while we expect (from the known supersymmetric solutions) that the $\vec{E} \times \vec{B}$ interactions that give rise to $J_L^{\rm tube}$ will remain constant. Hence, a solution with a single supertube that becomes too deep will start having charges and angular momenta outside of the cosmic censorship bound, and will most likely have closed timelike curves.

Of course, the way to avoid all these complications is to use the fact that the original solution is $\mathbb{Z}_2$-symmetric and place two identical supertubes in metastable minima symmetric around the origin, such that resulting configuration preserves this symmetry. In such a symmetric configuration the contribution to $J_L^{\rm tube}$ from the interaction of the supertubes with the background vanishes, and the cosmic censorship conditions are always satisfied.

## 3.6 Discussion of the results

In the first part of this Chapter we studied the Hamiltonian for supertubes in supersymmetric three-charge solutions with a Gibbons-Hawking base space and found that the potential can have both supersymmetric and non-supersymmetric minima. For non-supersymmetric minima, one or both of the charges of the supertube are oriented opposite to the background charges. For concreteness we focused on a specific two-center smooth solution, and found that a probe supertube can have also metastable minima, which decay into both supersymmetric and non-supersymmetric stable minima. We then discussed tunneling between the metastable and supersymmetric minima and showed that during the decay, the supertube charges are either partially or totally annihilated against the charges dissolved in flux, much like it happens in other antibrane probe constructions [160, 162, 75].

In the second part of this Chapter we have taken the technology one step further and used probe supertubes to construct microstate geometries, or fuzzballs, that have the same mass and charges as three-charge non-extremal black holes. We computed the length of the throats of these solutions, and found that one can easily build microstates whose throats are longer, shorter or have the same length as the throat of the black hole. Since in our construction there is no dynamical mechanism that sets the microstate length to be the same as that of the black hole throat, this indicates that this mechanism might be entropic: there will be many more microstates of black hole throat length than shorter or longer ones. Of course, to produce such

an entropic argument one needs first to make sure that our method for constructing non-extremal microstates can produce at least a subset of the typical ones, and then count these microstates.

However, the absence of a dynamical mechanism for fixing the microstate length indicates that fuzzballs will differ from the black hole at macroscopic distances from the horizon, and not just in its vicinity (as recently mentioned as a possibility in [66]). Of course, this intuition applies to near-extremal fuzzballs, and the extrapolation to more generic black holes may break down. Nevertheless, one can use near-extremal black holes as a testing ground for ideas proposed in relation to Hawking radiation, spacelike singularity resolution and infalling observer physics. We postpone the study of the latter to Chapter 4 and conclude here with a discussion of the former two.

### 3.6.1 Is Hawking radiation coming from brane-flux annihilation ?

The metastable supertubes we use to construct non-extremal fuzzballs decay into supersymmetric vacua via brane-flux annihilation as discussed in Section 3.3, and this decay corresponds to the near-extremal black hole emitting its last Hawking radiation quantum and becoming an extremal black hole. This process is quite difficult to study from the black hole side, essentially because thermodynamics breaks down [169, 170]. A comparison of the fuzzball decay rates (which one can compute rather straightforwardly) to the near-extremal black hole emission rate may shed light on how thermodynamics breaks down, and also on which fuzzballs are more typical than others: the decay rates depend on how big the bubbles of a fuzzball are, and can be used to determine the typical bubble size.

The other important question is what is the backreacted solution corresponding to our metastable supertubes. The JMaRT solution [62], which is one of the two known fully-backreacted non-extremal fuzzballs, has ergoregions, and its instability [158] has been argued [130] to correspond to Hawking radiation. The other fully-backreacted non-extremal fuzzball, the running-Bolt solution [65], is also unstable, but its instability does not come from ergoregions. Our configurations on the other hand are metastable, at least in the probe approximation. It might be possible that the energy of some metastable supertubes will decrease by taking one of the GH centers off the symmetry axis, and if this happens the fully backreacted solution will probably be unstable as well. However, it is also very likely that one will be able to construct metastable supertubes that remain metastable when fully backreacted, and thus will have very different physics from the JMaRT and running-Bolt solutions.

The other issue with the metastable supertube backreaction is that most of the work analyzing the backreaction of antibranes in backgrounds with charge dissolved in fluxes indicates that such backreacted solutions have unphysically-looking singularities, both at first order (see [72, 73, 74, 75, 76, 77] and **P6**), and when looking at the fully-backreacted solutions (see [78, 79]). If one naively extends this result to our work, one might expect that anti-M2 branes in long BPS throats will also give rise to unphysically-looking singularities. However, in our construction we are not using bare antibranes, but supertubes that carry two kinds of antibrane charges, and also have a dipole charge and a nonzero angular momentum. The advantage of supertubes is that if they are solutions of the DBI Hamiltonian they backreact into geometries that are smooth in the D1-D5-P duality frame [124]. Hence we expect the backreaction of our metastable supertubes to give rise to regular solutions; it would be very interesting to confirm this by constructing directly

this challenging non-supersymmetric cohomogeneity-two solution.

### 3.6.2 Are spacelike singularities resolved backwards in time ?

The existence of microstate solutions that have the same mass, charges and throat length as non-extremal black holes indicates that the singularity of these black holes will most likely not only be resolved to the inner horizon (as one may expect by extrapolating the extremal black hole result) but all the way to the outer one, which is backwards in time from where the singularity is, as the Penrose diagrams in Figure 3.2 show. One can now try to see what this intuition may tell us about singularity resolution.

Indeed, since the Penrose diagram of the near-extremal black holes is the same as that of all Reissner-Nordström black holes, one can extrapolate our result and assume that the singularity of all Reissner-Nordström black holes is resolved all the way to the outer horizon. One can then take the small charge limit (in which the inner horizon and the timelike singularity merge to form a spacelike singularity) and infer that the spacelike singularity of the zero-charge Schwarzschild black hole is also resolved backwards in time, all the way to the horizon.

If this is indeed the correct pattern of the resolution of spacelike singularities in String Theory, one can ask two questions:

1. What is the mechanism by which this happens and the corresponding scale?

2. What does this imply for the physics of other spacelike singularities, like the cosmological ones?

To answer Question 1, one can argue that singularities in String Theory have low-mass degrees of freedom, that destroy the spacetime on macroscopic distances. One can also refine the answer, and argue [171] that an incoming shell that will form such a singularity in the future will enter in a region where there are a very large number of fuzzball-like states, and even if the probability of tunneling into any of them is tiny, since there are so many of them, the incoming shell will tunnel in the fuzz with probability one. The size of the region where the singularity is resolved depends on the mass of the singularity, and on the density of fuzzballs.

The answer to Question 2 depends largely on the mechanism for the backwards-in-time resolution. If this mechanism involves tunneling into fuzzball-like configurations that live near, say, a Big Crunch singularity, then the scale for the resolution will probably be given by the typical size of these configurations (which is quite hard to estimate at this point, in the absence of any explicit Big-Crunch-resolving fuzzballs). Furthermore, one can argue that such configurations were also present in the early universe, where they can be thought of as giving a 'forward-in-time' resolution of the Big Bang singularity, and their physics might have cosmological implications [172, 173].

# Chapter 4

# Falling into (microstates of) black holes

In this Chapter we want to study the experience of an observer falling into a black hole. In General Relativity the horizon of a large black hole is a smooth region in spacetime where curvatures are low. By application of the equivalence principle, an infalling observer should not feel anything special until she approaches the singularity. However, in Chapter 2 we argued that for the evaporation process of a black hole to be unitary, the horizon has to be replaced by horizon-scale structure. In Chapter 3 we perturbatively constructed such structure for near-extremal black holes and showed that the size is indeed of the order the black hole horizon. Hence, to study the experience of infalling observers we have to address the question:

*Q4. What does an observer falling into the (quantum) black hole microstate experience?*

In light of the discussion in Chapters 2 and 3 we want to study the above question in the context of the fuzzball proposal. Although no explicit fuzzball solutions for Schwarzschild black holes have been constructed so far [1], it appears to be possible to make general arguments in the context of the AdS/CFT correspondence. One may then hope to extend the general results to black holes in flat space. For Reissner-Nordström black holes, on the other hand, there are many extremal Supergravity fuzzball constructions and in Chapter 3 we argued that such fuzzballs can be made near-extremal. One may hope to gain some insight regarding the question of infall into fuzzballs by studying these near-extremal solutions.

## 4.1 Motivation and summary

In General Relativity a black hole's event horizon is a smooth and structureless 'surface' that divides the black hole into an exterior spacetime accessible to all observers and an interior spacetime only accessible to infalling observers. Considering quantum fields on this classical background the state at the horizon, the Unruh vacuum, allows an infalling observer to fall freely through it. On much longer time scales, the black hole evaporates away as pairs of particles are pulled out of the Unruh vacuum at the horizon. Since the horizon contains no information of the

[1] Recently there is, however, progress being made. [174]

original matter, the created pairs are in a special state independent of the matter's initial state and information seems to be lost once the black hole has evaporated completely.

The principle of black hole complementarity (BHC) [175] was advanced to reconcile the ideas of unitary evaporation of black holes and free fall through the horizon of the black hole. BHC postulates that, as far as an asymptotic observer (one who stays outside the black hole forever) is concerned, the black hole behaves like a hot membrane emitting Hawking-like quanta in a unitary fashion; however, BHC also certifies that an infalling observer does not crash into this membrane but instead experiences the infalling vacuum state (Unruh vacuum) at the horizon and therefore nothing unusual until the singularity is approached.

While this is an interesting picture, BHC does not provide a microscopic description of the membrane and hence no *mechanism* for information retrieval. Moreover, the idea of free infall is in considerable tension with unitarity of the evaporation process. This was made sharp in a recent Gedankenexperiment performed by Almheiri, Marolf, Polchinski and Sully (AMPS) [66] which challenges the whole idea of black hole complementarity (BHC). They argue that preservation of unitarity in the evolution of a black hole implies that an infalling observer can not freely fall through the horizon but instead burns at a firewall. While this claim relies on Mathur's result [2] that large corrections are needed at the horizon scale to preserve unitarity, it is not immediately clear that horizon scale structure implies a violent fate for the infalling observer.

Indeed Mathur has argued, in a recent series of papers [68, 67, 70, 176], for the possibility of an *approximate complementarity* for fuzzballs where the interaction of infalling observers, whose asymptotic Killing energy is much larger than the Hawking temperature at infinity, with the fuzzball has an alternate description as free-fall through the horizon of the black hole. This description is, however, short-lived as the infalling observer will eventually thermalize in the fuzzball and is not applicable to infalling quanta that have an asymptotic energy of the order the Hawking temperature at infinity. Besides fuzzball complementarity, there are other interesting proposals on the experience of an infalling observer [177, 178, 179].

The AMPS Gedankenexperiment has sparked a passionate debate on the fate of an infalling observer. While there seems to be basic agreement on the result of [2] that unitary black hole evaporation is inconsistent with an information-free horizon, proposals differ on what an infalling observer will experience. For fuzzball complementarity there is an inherent separation of energy scales which contrasts the common picture that the infall experience is universal for all kinds of infalling observer.

This Chapter is organized as follows. We start our discussion of the infall question by challenging the view of universal infall in Section 4.2. To study the question of infall into the Schwarzschild black hole, we rephrase the Gedankenexperiment of AMPS in Section 4.3 in the decoherence picture of quantum mechanics and ask about the fate of an infalling wave packet. We then turn to discuss infall into fuzzballs. In Section 4.4 we elaborate on the fuzzball complementarity proposal. To test the fuzzball/firewall ideas, in Section 4.5, we use the non-extremal microstates constructed in Chapter 3 and compare the force on a probe in the near-extremal fuzzball to that in the black hole background. In Section 4.6 we summarize the discussion and argue why fuzzball complementarity can work despite the Gedankenexperiment of AMPS. We also speculate about the interpretation of our result on infall into near-extremal microstates.

## 4.2 Is infall universal?

In Chapter 2 we argued that for unitarity to be preserved in the evaporation process, every quantum coming out of the black hole has to carry information out and the information-free horizon has to be replaced by some information-carrying structure. Keeping this result in mind one can consider the following Gedankenexperiment shown in Figure 4.1. When a quantum

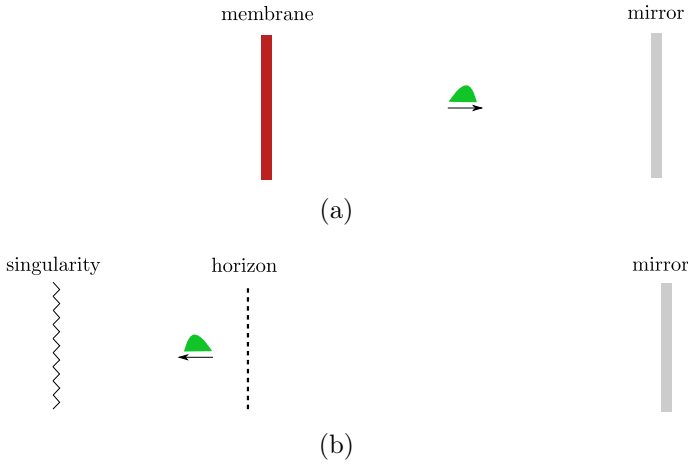


Figure 4.1: (a) A typical quantum comes out of the system. To preserve unitarity it must carry information of the state. According to black hole complementarity it originates from a hot membrane outside the event horizon. (b) According to views held by many if such a quantum is reflected back in it will have a free infall, independent of the details of the state. This seems odd because if there is a microscopic description of the emission process one would expect the microscopic dynamics to be reversible.

comes out of the black hole, a mirror can be placed to throw it back in. While for unitary evaporation of a black hole the spectrum of outgoing radiation cannot be exactly thermal, we still expect information to be mostly carried by the typical quanta which have asymptotic energy $E \sim T_H$, where $T_H$ is the Hawking temperature at infinity. After being reflected from the mirror back towards the black hole it seems unreasonable to think that such a quantum will freely fall through the horizon-scale structure much like falling through a horizon since, when coming out it carried information of the state. Basically, if there is a microscopic description of the emission process, we expect the microscopic dynamics to be reversible. 'Infall' and 'outfall' of information should be a symmetric process.

While this suggests that quanta of energy $E \sim T_H$ notice the horizon-scale structure rather strongly and cannot have free infall, it is not immediately clear whether other infalling observers, in particular observers of energy $E \gg T_H$, have a similarly violent interaction with the structure.

## 4.3 Decoherence and the fate of an infalling wave packet

In Subsection 4.3.1 we summarize the Gedankenexperiment of AMPS. We then rephrase it in Subsection 4.3.2 in the decoherence language of quantum mechanics and ask for the fate of an infalling wave packet in Subsection 4.3.3.

### 4.3.1 The Gedankenexperiment of AMPS

AMPS start with three postulates as put forth in [175] based on the assumption that black hole evolution is consistent with quantum mechanics:

- Postulate 1 (BHC): The process of formation and evaporation of a black hole, as viewed by a distant observer, can be described entirely within the context of standard quantum theory. In particular, there exists a unitary S-matrix which describes the evolution from infalling matter to outgoing *Hawking-like* radiation.
- Postulate 2 (BHC): Outside the stretched horizon of a massive black hole, physics can be described to a good approximation by a set of semi-classical field equations.
- Postulate 3 (BHC): To a distant observer, a black hole appears to be a quantum system with discrete energy levels. The dimension of the subspace of states describing a black hole of mass M is the exponential of the Bekenstein entropy S(M).

and add one more Postulate to this set which states:

- Postulate 4 (AMPS): A freely falling observer experiences nothing out of the ordinary when crossing the horizon [2].

They go on to argue, citing results of [131], that if a body in a pure state is radiating unitarily, the entanglement entropy in the radiation initially rises but at some point has to start decreasing and eventually reaches zero when the body has radiated away completely. Moreover, there is an upper bound, the Page time, when the entropy has to start decreasing: namely when half the entropy has been radiated away. See Figure 2.1(a) and the discussion of this point in Chapter 2.

The firewall argument goes as follows. Imagine a pure state collapsing into a black hole and emitting half its entropy in early Hawking radiation denoted by $A$. Unitary black hole evaporation as measured by an asymptotic observer, Bob, now requires that any further outgoing quantum of radiation $B$ has to be maximally entangled with $A$ so that the entropy of the combined system of early and later Hawking radiation starts decreasing. Let us introduce an infalling observer, Alice, who encounters these outgoing Hawking quanta $B$ close to the stretched horizon. If the horizon were in the vacuum state, Alice would pass through the $B$ quanta and later their partner quanta $C$ behind the horizon without noticing anything. For this to happen, the $B$ quanta would have to be maximally entangled with the $C$ quanta. After Page time, however, the next $B$ quantum has to be maximally entangled with $A$ for unitarity, and so it cannot be entangled with $C$. AMPS

[2] An observer-centric language ('experiences' of observers) may cause confusion. To avoid this, we reformulate the firewall argument in Subsection 4.3.2 in terms of local interactions of wave packets.

then claim that Alice encounters highly blue-shifted $B$ quanta at the horizon and 'burns up', hence the name *firewall*.

In summary, the postulates 1), 2) and 4) - purity of the Hawking radiation, semi-classical behavior outside the horizon and absence of infalling drama, are mutually inconsistent and they decide to give up the last one. That an information-free horizon cannot lead to a unitary evolution of black hole evaporation has already been shown by Mathur [2, 133]. But while he proposes [176, 70] that the interaction of Alice with the information-carrying horizon-size structure may have some interesting dynamics where Alice does not immediately notice any structure, AMPS propose that the black hole is protected by a Planck-scale firewall at which any infalling observer immediately burns up.

### 4.3.2 The rephrased Gedankenexperiment

We now rephrase the 'observer-centric' discussion of the AMPS argument in favor of decoherence [180]. Therefore, we replace the 'observers' Alice and Bob by wave packets. While we will continue to use the names Alice and Bob, they should not be understood as some sentient beings but as wave packets with properties like large density of states to make them classical enough. In this picture, wave packets interact when they overlap via a local, unitary evolution and get entangled. To discuss the AMPS Gedankenexperiment, we first have to understand the fate of a wave packet that is moving towards the black hole horizon in the black hole complementarity picture. We then contrast the result with the firewall argument.

#### Black hole complementarity

Far from the black hole Alice is described by semi-classical evolution (Figure 4.2). When it gets

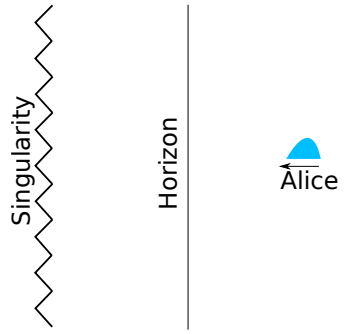


Figure 4.2: A wave packet far away from the horizon evolves semi-classically.

close to the horizon there are two complementary descriptions: one where it passes through and then hits the singularity (Figure 4.3) and another where it hits a 'membrane', scrambles, and with its information being finally re-emitted unitarily, escapes to infinity (Figure 4.4).

While discussing in a non-observer centric language we realize that the crucial feature in black hole complementarity is that when the wave packet reaches the stretched horizon it evolves in two distinct ways. In *some sense*, its state gets mapped onto *two copies* in separate Hilbert


(a) (b)

Figure 4.3: In one of the complementary descriptions the wave packet passes through the horizon and hits a singularity.

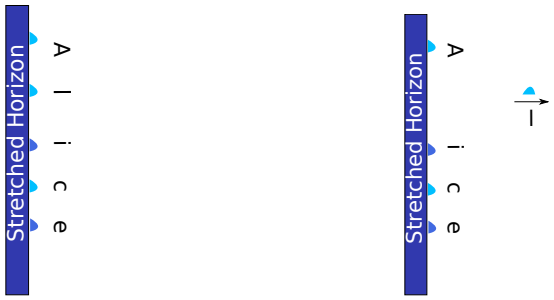


(a) (b)

Figure 4.4: In the other complementary description the wave packet gets mapped onto the degrees of freedom on a membrane. This wave packet is now scrambled, loses any semblance of itself, but the information leaks out of the membrane unitarily.

spaces which then evolve with different Hamiltonians [3]. This remarkable proposal was forwarded in [175, 181] to reconcile a pair of otherwise incompatible statements, that there is nothing from which a wave packet can *bounce off* at the horizon and yet *somehow* information must be recovered. In normal situations such an ad hoc prescription is not allowed as it leads to many inconsistencies and - in trying to fix them - unnecessary postulates. Copying of quantum states, for example, leads to *cloning*. While this does not evoke problems if the copies cannot interact as is in the case of black hole complementarity, one might still ask what it means to have two copies of a state?

This prescription is consistent if the complementary pictures are *dual* descriptions. For example, the state of a closed string heading towards a stack of D-branes gets mapped onto them as open string states in one picture, while in the dual description the closed string continues to move on into an AdS space [4]. For such dual descriptions there is no issue with cloning. However, the Hamiltonian evolutions of the states need to be consistent since, at the end of the day, in

[3]For discussion why this is consistent with no quantum cloning see [181, 154] and our comments below.
[4]We thank Samir Mathur for pointing this out to us.

one description, the closed string emerges out of the AdS as a closed string in flat space and in the other description the open strings leave the D-brane as a closed string. They must be in the *same state*.

However, black hole complementarity is not a duality. This conclusion can be drawn from the completely different outcomes in the two complementary pictures. If it is not a duality then one can ask *what* it is and what is this operation that makes two copies of the states? [5]

### The firewall argument

Now let us look at the AMPS Gedankenexperiment in terms of wave packets. We begin with the unitary evolution process of Alice away from the black hole in the causal future of early radiation $A$. While for clarity we have drawn only one wave packet $A$ in Figure 4.5, when Alice interacts with $A$, it should be understood to interact with many such wave packets successively. How strong the interaction is and how much entanglement will be generated between Alice and

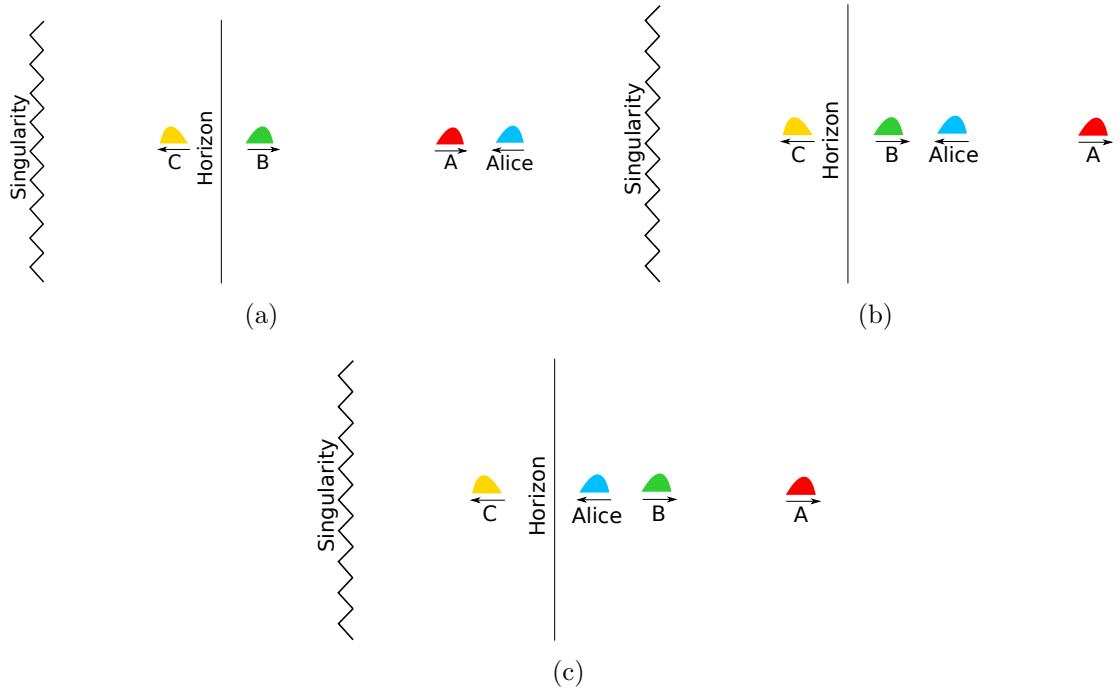


Figure 4.5: Away from the horizon, Postulate 2 tells us that the usual rules of quantum mechanics work. When wave packet 'Alice' crosses the wave packets 'A' and 'B', they will get entangled successively.

$A$ in the process is governed by local unitary dynamics and the properties of the wave packet Alice (like what frequencies it is supported on). In each encounter there is some mixing between Alice and wave packets in $A$. When Alice gets closer to the horizon it interacts and mixes with wave packet $B$. Since $B$ is just a blue shifted version of $A$ and Alice is also blue shifted, this

[5] If one is uncomfortable with the language of making two copies of a state, one can say that there are two descriptions of the same state which evolve differently.

interaction is stronger than any of the Alice-$A$ interactions. At this point, it is worth observing that Alice's interactions with $A$ and $B$ and their mutual entanglement are now encoded in Alice and in the $AB$ system. We have not talked about any measurements or observations yet but we will comment on this in Subsection 4.3.3.

At the (stretched) horizon, black hole complementarity dictates two pictures:
According to one picture, depicted in Figure 4.6, the wave packet Alice (entangled with $AB$) goes through the horizon and encounters wave packet $C$, the infalling Hawking pair of $B$, with which it interacts and mixes. Eventually Alice hits the singularity. [6]

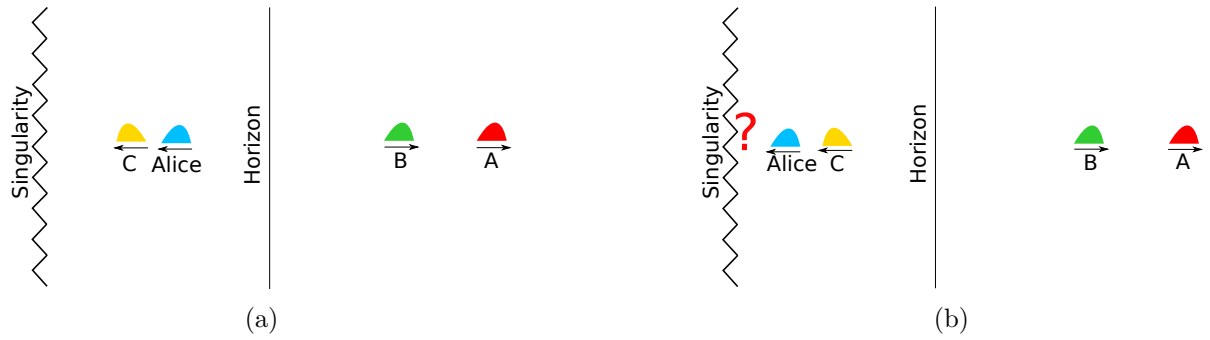


Figure 4.6: In one complementary picture Alice having interacted with $A$ and $B$ falls through the horizon. Its interaction with $C$ will depend on whether $B$ was entangled with $A$ or $C$. It then falls into the singularity.

In the complementary picture Alice's (entangled with $AB$) state gets mapped onto the thermal membrane at the stretched horizon where it gets scrambled and eventually re-emitted unitarily as radiation to infinity (Figure 4.7).

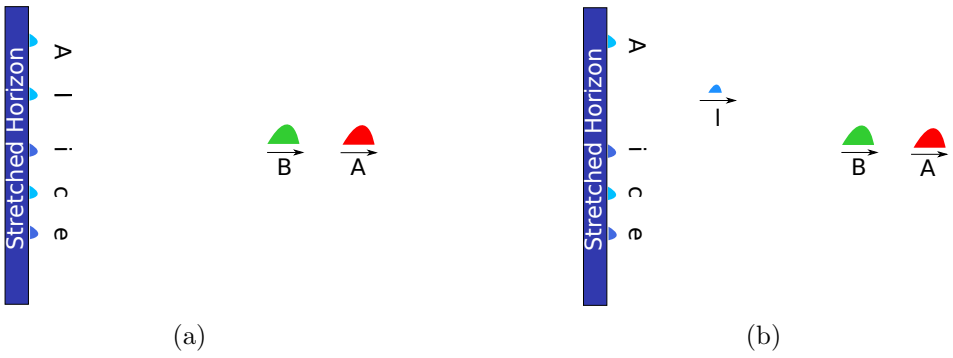


Figure 4.7: In the other complementary picture Alice's state after having interacted with $AB$ is registered on the membrane. It gets scrambled but eventually leaks out unitarily.

[6] While one might argue that the singularity will get resolved at Planck scale it is not clear how this picture can be modified to make black hole complementarity an actual duality.

Alice's interaction with the system $AB$ and subsequently with $C$ will have different evolutions depending on the initial entanglement structure of $B$ with $A$ and $C$. Applying the reasoning of Subsection 4.3.2, unitarity of black hole evaporation requires $B$ to be maximally entangled with $A$ no later than Page time, while free infall requires $B$ to be maximally entangled with $C$. However, a system cannot be maximally entangled with two distinct systems and this leads to the firewall result. Since $B$ is maximally entangled with $A$, AMPS argue that Alice's encounter with $B$ is fatal and hence black hole complementarity has to be given up. In our language, this should be understood as wave packet Alice changing so much that it does no longer resemble its former self. While the AMPS Gedankenexperiment shows that Alice's interaction with the information-carrying structure (or membrane) is different from what one expected from strict application of black hole complementarity, it is not immediately clear by how much. By rephrasing the AMPS Gedankenexperiment in the decoherence language of quantum mechanics, we see that the interaction of wave packet Alice with the $BC$ system may crucially depend on its properties and the Hamiltonian. The AMPS result may not apply to all types of wave packets and there seems to be room for novel dynamics. We will now give some evidence for this.

### 4.3.3 Is Alice burning or fuzzing ?

AMPS claim that since the state of the final Hawking radiation is pure, it can be written as an early and late part

$$|\Psi\rangle = \sum_i |\psi_i\rangle_E \otimes |i\rangle_L \,, \tag{4.1}$$

where $|i\rangle_L$ is an arbitrary complete basis for late radiation and $|\psi_i\rangle_E$ is a state in the early Hawking radiation. After Page time, the Hilbert space of the early radiation is much larger than that of the late radiation and so, for typical states $|\Psi\rangle$, the reduced density matrix describing the late-time radiation is close to the identity. Thus one can construct operators acting on the early radiation whose action on $|\Psi\rangle$ is

$$P_i|\Psi\rangle \propto |\psi_i\rangle_E \otimes |i\rangle_L \,. \tag{4.2}$$

AMPS claim that Alice can make measurements on early radiation tantamount to projection onto the eigenvector of the number operator of late radiation. She can thus know the number of photons in a mode of the late radiation. Through postulate 2, these late radiation modes are related to early radiation modes by large red-shifts. Now, if the state at the horizon is in the eigenstate of the number operator of the late radiation, it cannot simultaneously be the vacuum for an infalling observer whose infalling modes are related to the outgoing radiation modes by Bogoliubov coefficients. Thus an infalling observer encounters high-energy quanta and 'burns'.

In [179] Nomura, Varela and Weinberg raise an objection to this reasoning, and argue that 'the existence of the projection operator for an arbitrary $i$ does not imply that a measurement, in a sense that it leads to a classical world, can occur to pick up the corresponding state'. In other words measurement is a dynamical process dictated by a unitary evolution of the state. They thus claim that AMPS's conclusion that an infalling observer must see a firewall is incorrect.

Translated into our wave packet language this means that when Alice passes through early radiation $A$, it cannot *choose* which basis it projects onto. Instead the interaction of Alice and

$A$ is governed by a local Hamiltonian. Let the typical (asymptotic) energy of quanta in $A$ be of the order the Hawking temperature $T_H$ at infinity. Then there are distinct cases:

- Alice is a wave packet with support on energies $E \sim T_H$ and thus is of the same size as wave packets in $A$. In this case a typical interaction of them will project $A$ onto the number operator basis. When Alice falls in, it will encounter $B$ and will be able to 'predict' the number of quanta in a mode of $B$.

- Alice is a wave packet with support on energies $E \gg T_H$ and is thus smaller than typical wave packets in $A$. In this case Alice's interaction with $A$ does not project onto the number operator basis in any typical interaction and it cannot 'predict' the number of quanta in a mode of B.

The remaining case of $E \ll T_H$ is not so interesting as for such wave packets the wavelength is bigger than the black hole.

As argued for in the previous Subsection, we see that the interaction of the wave packet Alice with the $BC$ system seems to crucially depend on its properties. In particular, there seems to be a separation of energy scales that may give rise to different dynamics:

- AMPS claim that an infalling observer encounters high energy quanta in the number basis near the horizon. This appears to be true for wave packets of asymptotic energy $E \sim T_H$. The above discussion suggests that this should not be true for wave packets with asymptotic energy $E \gg T_H$. [7]

- For quanta of asymptotic energy $E \gg T_H$, Mathur claims that there could be a complementarity picture that approximately describes the dynamics of infall of these quanta into the horizon-scale structure by infall into a black hole. This picture, however, does not apply to wave packets of asymptotic energy $E \sim T_H$.

The above observation is consistent with the argument of Section 4.2, that low-energy wave packets should notice the microscopic horizon-scale structure necessary for unitarity. [8] While this rather violent interaction with the outgoing Hawking-like quanta might justify to call it 'burning' at a 'firewall', this interaction is not confined to within a Planck length from the stretched horizon. On the other hand, it is not clear whether high-energy wave packets that cannot distinguish between different microstates should have an equally violent encounter with the structure. To understand how a complementary picture for these observers as falling through a horizon may emerge, one needs to understand the nature of the interaction of the wave packet with the horizon-scale structure. This is what we turn to next.

[7] It is not immediately clear that a local wave packet Alice cannot sample all of $A$ on the sphere in some coherent way and then fall in and encounter $B$ projected on a number basis. However typical interaction will not have this effect.

[8] This picture is not very different from a wave packet heading towards a burning piece of coal. A wave packet of thermal energy undergoes Brownian motion by being scattered off the outgoing radiation, while a wave packet of energy much greater than the thermal energy manages to travel on a 'classical trajectory' and hit the piece of coal. However, the analogy stops here because there is no nice approximate complementarity picture for a hot piece of coal.

## 4.4 On the possibility of complementarity

The purpose of this Section is to study general properties of non-extremal fuzzballs and to discuss the fuzzball complementarity proposal.

### 4.4.1 Fuzzballs

In Chapter 2 we argued that purity of the final radiation state is not sufficient to guarantee a unitary evolution and showed that additional conditions make the argument for horizon-scale structure considerably stronger. Using qubit models we found that, taking into account linearity, norm preservation and invertibility of the evolution in addition to the requirement of purity, at no point can there be a predetermined pure state (like Unruh vacuum) at the horizon. While Unruh and Hartle-Hawking vacuum have regular stress tensor at the future horizon, a mixed state is expected to have a divergent stress tensor and we thus need to look at the microstates of quantum gravity. To answer the question of what happens to an infalling observer one must therefore understand the nature of these microstates.

**Information release.**

According to the fuzzball proposal the true microstates accounting for the Bekenstein-Hawking entropy have neither a singularity nor a horizon shielding it. A fuzzball is well approximated by a black hole asymptotically and, presumably, all the way to the potential barrier that surrounds the black hole. Beyond the barrier a fuzzball starts differing from a black hole at a location that depends on the particular fuzzball and ends in a, possibly non-geometric, complicated stringy 'fuzz' somewhere between the potential barrier and the location of the would-be horizon. This proposal nicely resolves the information paradox as the radiation now emerges from the surface of these fuzzballs and thus carries information of them, much like the radiation emerging from the surface of a star. Unitary evolution is thus built into fuzzballs by construction. For a review of the proposal see [19, 102, 47, 48, 128] and to see how radiation from fuzzballs carries information see [129, 182].

**Infall experience.**

Replacing the black hole solution by a fuzzball naturally raises the question: What is the experience of an infalling observer? To make contact with the firewall argument we need to study infall into fuzzballs that are typical in Page's sense. [9] The mirror argument of Section 4.2 and the discussion of Section 4.3 suggest that we should further split the infall question according to observers [10] with Killing energy $E \sim T_H$ and those with $E \gg T_H$. Since typical radiation

[9] It was pointed out in [153] that the time for the full system to become generic is the recurrence time $\sim Me^{M^2}$. Note that this is parametrically larger than the evaporation time $\sim M^3$ so the system never becomes generic. However, an infalling observer experiences a small part of the system and thus by typical we mean scrambled. In [155] scrambling time is conjectured to be $\sim M \log M$. After scrambling time we expect to be able to approximate a small part of the system by a thermal density matrix for appropriate coarse-grained operators.

[10] A simple model for an observer is the Unruh-de Witt detector [183].

quanta ($E \sim T_H$) do not come from the evolution of Unruh vacuum but from the surface of the fuzz, it is clear that at least infalling quanta of such energies can not have free infall. The fate of infalling quanta with asymptotic energy $E \gg T_H$ is not so obvious. In the remainder of this Section we elaborate on a recent conjecture of Mathur where he claims that infall of high-energy modes into *typical* fuzzballs can be approximated by infall into black holes.

### 4.4.2 Falling into typical fuzzballs

In this Section we speculate on the structure of typical fuzzballs and their similarities with and differences from black holes. In the traditional black hole picture it is well known that the perfect thermal nature of the emitted radiation is 'spoiled' by gray-body factors. These arise from the potential barrier outside the horizon through which the Hawking quanta have to tunnel to escape to infinity. While the exact form of this barrier is angular momentum dependent it peaks around a distance $\sim \mathcal{O}(M)$ outside the horizon. In the fine-grained version the horizon is not there and the fuzzball ends with a boundary, the fuzz, which is somewhere between the potential barrier and the location of the would-be horizon. The picture expected for a typical fuzzball is illustrated in Figure 4.8 where we denote the location of the barrier by $r_*$. A quantum that leaves the fuzz has a non-vanishing probability of getting reflected by the potential barrier back towards it. Thus after the scrambling time, we expect a gas of quanta filling the region between the fuzz and the barrier in dynamic equilibrium with the fuzz. If this system is embedded in flat space, then any outgoing quantum which manages to escape to the other side of the potential barrier escapes to infinity. We refer to the region between the fuzz and the potential barrier as 'near-fuzz' region in analogy with the 'near-horizon' region.

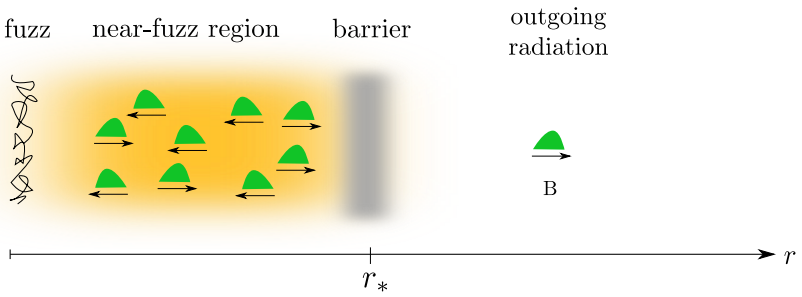


Figure 4.8: To answer the infall question we have to discuss the interaction of the infalling observer with the full system: radiation quanta emitted from the fuzzball either cross the potential barrier at $r_*$ or get reflected back into the fuzz. An infalling observer thus encounters a single radiation quantum outside the barrier but a lot of quanta partially trapped between the barrier and the fuzz. Further they encounter the fuzz itself. We refer to this region as 'near-fuzz' instead of 'near-horizon' to emphasize the lack of a horizon in the fuzzball picture.

AMPS's firewall argument is based on the experience of an infalling observer with a highly blue-shifted quantum $B$ in her own frame. The interaction with a quantum $B$ in isolation is possible outside the potential barrier located at $r_*$. Repeating the argument of AMPS for this case we find that quantum $B$ cannot generically be maximally entangled with a quantum in the

near-fuzz region after Page time and, according to our analysis in Chapter 2, not even before. Since quantum $B$ is not close to the horizon it is not sufficiently blue shifted to argue for a universal firewall for all kinds of infalling observers.

The more interesting case is when the infalling observer crosses the barrier and enters into the near-fuzz region where she now encounters not one but many quanta. To capture the full dynamics of an observer falling into a fuzzball one must deal with the interaction of the observer with all the quanta in the near-fuzz region and more importantly the 'fuzz' itself. [11] Since AMPS analysis relies on effective field theory all the way up to the (stretched) horizon both of these additional interactions are absent. While the finding of a diverging stress tensor is evidence that effective field theory breaks down, it does not automatically imply that the strong dynamics of the microstates of quantum gravity leads to a universally dramatic encounter for all types of infalling observers. To answer what the experience of an infalling observer is, one must understand the nature of the quantum gravity microstates. While the description of the entire dynamics of an infalling observer with a typical fuzzball might seem a daunting task, after scrambling time it seems possible to make an insightful approximation which we discuss next.

### 4.4.3 Fuzzball complementarity

In this Subsection we review the proposal of fuzzball complementarity as developed in [68, 67, 70, 176, 69] and which draws from recent ideas of [184, 185]. While we work in the context of the AdS/CFT correspondence, we expect the lesson that will be drawn from this to hold more generally.

We start with a typical state in a CFT. For *sufficiently coarse-grained operators* probing the system we can *approximate* a typical state by a thermal density matrix $\rho$ by using the standard technique of going from the microcanonical to the canonical ensemble. [12] The temperature of the approximated thermal density matrix is fixed by the dynamics of the system and the energy of the typical state $|\psi\rangle$. The expectation values of coarse-grained operators $\hat{O}$ in the typical state get approximated by a thermal average over the energy eigenstates

$$\langle\psi|\hat{O}|\psi\rangle \approx Tr(\rho\hat{O}) = \frac{1}{\sum_i e^{-\frac{E_i}{T_H}}} \sum_k e^{-\frac{E_k}{T_H}} \ \langle E_k|\hat{O}|E_k\rangle \,. \tag{4.3}$$

Any density matrix may be purified by enlarging the Hilbert space. For example, a density matrix of the form

$$\rho = a|A\rangle\langle A| + b|B\rangle\langle B| \tag{4.4}$$

with orthonormal $\{|A\rangle, |B\rangle\}$ can be purified by introducing an auxiliary set of orthonormal states $\{|\alpha\rangle, |\beta\rangle\}$ and defining

$$|\Psi\rangle = \sqrt{a}|A\rangle \otimes |\alpha\rangle + \sqrt{b}|B\rangle \otimes |\beta\rangle. \tag{4.5}$$

[11] Note that Figure 4.8 should not be taken to mean that there is clear distinction between the fuzz and the high-energy quanta in the near-fuzz region. While we would expect the physics to be well described by classical gravity for $r \gtrsim r_*$, the Figure should be taken to mean a smooth transition from highly quantum-stringy states at the location of the fuzz to a gas of particles on a gravity background at $r \simeq r_*$.

[12] As emphasized in the previous Subsection this approximation cannot be made for fine-grained operators which probe the energy scale of typical quanta of the state.

One recovers $\rho$ as the reduced density matrix by tracing out the newly introduced degrees of freedom. We already used this technique in Chapter 2 to connect the 'moving bit' model to the Hawking pair process.

We can purify the density matrix as defined in (4.3) by addition of states in an auxiliary CFT to obtain the pure state

$$|\Psi\rangle = \frac{1}{\sqrt{\sum_i e^{-\frac{E_i}{T_H}}}} \sum_k e^{-\frac{E_k}{2T_H}} |E_k\rangle_L \otimes |E_k\rangle_R \,, \tag{4.6}$$

where the $|E_k\rangle_R$ denote the energy eigenstates of the original CFT, which we call $CFT_R$, while $|E_k\rangle_L$ are the energy eigenstates of an auxiliary $CFT_L$. With this we can rewrite (4.3) as

$$_R\langle\psi|\hat{O}_R|\psi\rangle_R \approx \langle\Psi|\hat{O}_R|\Psi\rangle \,, \tag{4.7}$$

where we have put a subscript on the operator and the typical state of Equation (4.3) as well.

It should be noted that purification is a formal mathematical operation and *not* a dynamical process. In particular, the new kets $|E_k\rangle_L$ that belong to the new $CFT_L$ do not correspond to any real degrees of freedom. However, based on Israel's description of eternal black holes [186], Maldacena found in [187] that the state (4.6) is dual to the eternal AdS black hole as depicted in Figure 4.9. Note that the $CFT_L$ and $CFT_R$ on either side of the Penrose diagram are *entangled* as a result of the purification process. In [184] Van Raamsdonk has recently taken this notion

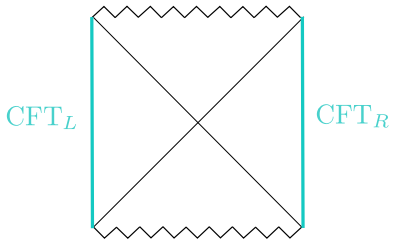


Figure 4.9: Penrose diagram of the extended AdS Schwarzschild black hole. It contains two asymptotically AdS regions that each lie behind the horizon of the other region and contain each a boundary CFT.

of entanglement of states of CFTs further to the *entanglement of asymptotically gravitational solutions*. Each state $|E_k\rangle$ of one of Maldacena's CFTs should be dual to an asymptotically AdS solution $|g_k\rangle$. Thus we should be able to write the eternal AdS black hole geometry as

$$|G\rangle_{eternal} = \frac{1}{\sqrt{\sum_i e^{-\frac{E_i}{T_H}}}} \sum_k e^{-\frac{E_k}{2T_H}} |g_k\rangle_L \otimes |g_k\rangle_R \,. \tag{4.8}$$

While the two CFTs are entangled but not connected, their entanglement results in a description of connected asymptotically *AdS* solutions. Note the similarity of this procedure of getting the eternal AdS black hole as entangled gravitational solutions (4.8) to the procedure to obtain the Minkowski vacuum as an entanglement of Rindler states [183].

Based on the conclusions of Chapter 2 we expect the $|g_k\rangle$ to be true quantum gravity solutions which have no horizon and no singularity and which have structure before the location of the would-be horizon from which radiation is emitted unitarily. We therefore work under the assumption that the $|g_k\rangle$ are fuzzballs.

The Penrose diagram of an eternal AdS black hole can then be understood as an entanglement of fuzzball solutions $|g_k\rangle_L$ and $|g_k\rangle_R$. This is depicted in Figure 4.10. We want to emphasize that

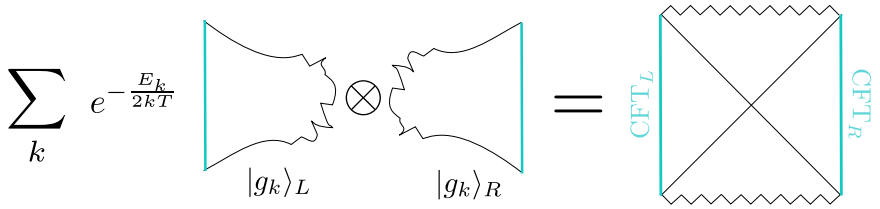


Figure 4.10: The extended AdS Schwarzschild black hole can be understood as the sum over entangled fuzzball solutions $|g_k\rangle_L$ and $|g_k\rangle_R$.

there is only one real set of fuzzball solutions, $\{|g_k\rangle_R\}$, the other one is purely auxiliary and is not associated with any real degrees of freedom. It is merely used as a computational tool to answer questions which are too difficult to address in the typical fuzzball (right wedge alone).

What are the implications of all this for an observable $\hat{O}$ measured in a typical fuzzball $|g\rangle_R$? From the above discussion we see that we can obtain an approximate answer by inserting the operator in the eternal AdS Schwarzschild solution

$$ {}_R\langle\psi_g|\hat{O}_R|\psi_g\rangle_R \approx \langle G|\hat{O}_R|G\rangle. \tag{4.9}$$

This is all very well for a time independent operator which corresponds to an observer who is at a constant radial location in the bulk. But what can we say about the experience of an infalling observer which corresponds to a time dependent operator? According to the proposal the above picture of free infall is still valid as long as the infalling observer corresponds to a sufficiently coarse-grained measurement. This is where the *scale dependence* of fuzzball complementarity comes in. Since outgoing typical quanta have Killing energy $E \sim T_H$, an incoming quantum of such energy will experience the fine-grained structure of the fuzzball and will thus not evolve in a way describable by infall in a black hole geometry. An infalling high-energy quantum with asymptotic energy $E \gg T_H$, on the other hand, is insensitive to the details of the fuzzball and may evolve in a way describable by semi-classical evolution in a black hole geometry.

How should we understand this process? Where did this extra spacetime beyond the fuzz come from? The infall into the black hole should be viewed as an alternate - *auxiliary* - description of the, otherwise complicated, interaction of an infalling observer hitting the fuzz and exciting its collective degrees of freedom. [13] However, this description is short-lived as there is a singularity

[13]This is not an unfamiliar situation. A closed string hits a stack of D-branes and yet has a description of falling into AdS spacetime.

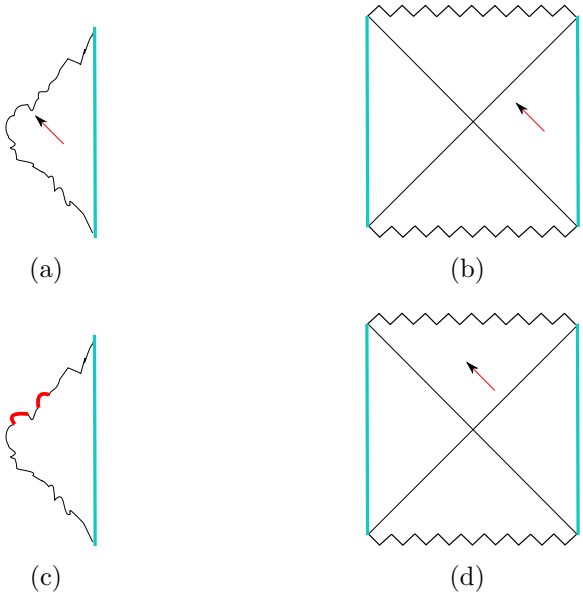


Figure 4.11: In (a) and (c) we show the process of infall into a typical fuzzball. Based on the discussion in the main body we expect that a high-energy quanta hitting such a fuzzball will be absorbed by it and excite its collective modes. This process is expected to have an alternate description of infall into a black hole shown in Figure (b) and (d). Note that this description is short-lived as is evidenced by the presence of a singularity. This feature is related to the limited phase space coming from the finiteness of the Hilbert space of the fuzzball wave function.

which the infalling observer eventually hits. This would probably be related to the energy in the collective modes leaking into the thermal modes because of the finite dimensionality of the Hilbert space of fuzzballs.

### 4.4.4 Alice fuzzes but may not even know it!

We have studied two extreme cases. For typical modes ($E \sim T_H$) we do not expect to have a semi-classical description up to the horizon, otherwise we have again information loss. Hence they cannot even approximately have a free infall description through a horizon. On the other hand high-energy modes ($E \gg T_H$) may not notice the details of the state, and so for them the approximation of microcanonical to canonical ensemble becomes arbitrarily good and the fate of such modes can be described sufficiently well by infall into black holes. For intermediate energies we expect an intermediate picture.

In the discussion we used the AdS/CFT correspondence, but recall that according to the arguments in [188] the CFT captures the physics inside the potential barrier. The decoupling limit is when the potential barrier become infinitely high and for certain solutions this is a consistent limit to take. It is such solutions which have a near-horizon AdS region in the decoupling limit. While for the Schwarzschild black hole there is no decoupling limit, we still expect the general lesson obtained above to hold in the nearly decoupled case. In other words, the arguments of the

preceding Subsection suggest that for sufficiently coarse-grained ($E \gg T_H$) operators we may approximate the region inside the potential barrier in Figure 4.8 by an eternal Schwarzschild black hole in the Hartle-Hawking state as shown in Figure 4.12. A high-energy infalling observer may thus experience a drama-free infall for as long as the auxiliary picture is a good approximation to the full fuzzball dynamics. [14] For fine-grained ($E \sim T_H$) operators on the other hand

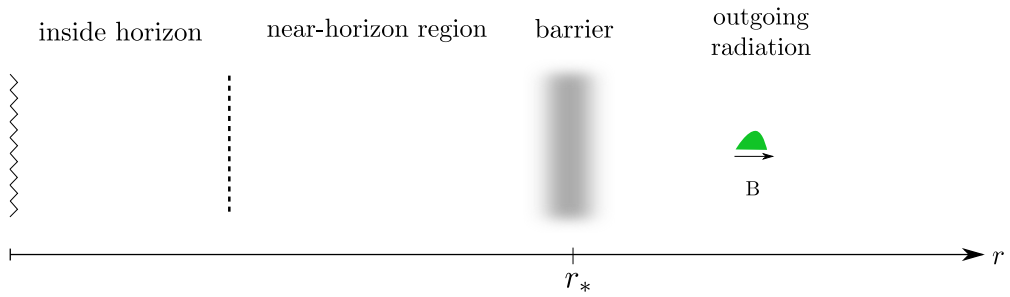


Figure 4.12: The region inside the potential barrier at $r_*$ of Figure 4.8 can be approximated by a black hole geometry in the Hartle-Hawking state. Unitarity requires that such an approximation be valid only for a time scale less that $\sim M$. In other words, it is not consistent to patch such geometries together in time for times larger than $\sim M$. A high-energy ($E \gg T_H$ ) infalling quantum experiences the black hole geometry. Since the time for infall is $\sim M$ it is consistent with the limits on the approximation. However, a low energy quantum ($E \sim T_H$) does not experience a universal infall because it can distinguish between microcanonical and canonical ensemble.

we cannot approximate a typical fuzzball by a black hole. Indeed, this is consistent with the idea that typical quanta which carry away information of the system should not have a universal interaction with the system when reflected back towards it as was alluded to in Section 4.2

A word of caution is necessary here. The central theme of fuzzball complementarity is an approximation of the microcanonical ensemble by the canonical ensemble. For appropriate coarse-grained observables a typical pure state (a typical fuzzball) can be approximated by a thermal state (a black hole). While a 'zeroed-out' Unruh-de Witt detector tuned to high energies being dropped from just outside the potential barrier at $r_*$ qualifies for this, the same detector when it stays in the near fuzz region at a constant radius does not. Such a detector necessarily has access to a larger part of the system. For instance such a detector staying outside for longer than Page time will experience a drop in the outside radiation entropy. Someone making readings on it will thus conclude that the geometry is not that of a black hole and conclude semi-classical physics is violated at the horizon scale as the black hole geometry leads to an ever increasing entropy. This should not come as a surprise because indeed the fuzzball proposal does state that the black hole geometry is an approximation.

[14] Exact details will depend on whether the observer is modeled by a simple Unruh-de Witt detector or something more complicated. This will decide how coarse-grained the operator is.

## 4.5 Testing fuzzball/firewall ideas

In the preceding Sections we studied infall into Schwarzschild black holes and putative Schwarzschild fuzzballs. We now turn to Reissner-Nordström black holes for which we have explicit fuzzball constructions. To test the aforementioned fuzzball complementarity and firewall ideas in this context we compute in Subsection 4.5.1 the force on probes in near-extremal fuzzballs and compare the result to the force in the corresponding black hole background. In Subsection 4.5.2 we speculate on the implications of this result for the infall question.

### 4.5.1 The force on probes in non-extremal fuzzballs

In Section 3.5 of the preceding Chapter we computed the throat length of the newly constructed near-extremal microstates using metastable supertubes. Comparing our result to the throat length of the corresponding near-extremal black hole we found strong evidence that the fuzzball proposal extends to near-extremal black holes. Another quantity that one can compute in both the near-extremal black hole geometry and in the non-extremal fuzzballs we construct, is the force on a probe brane whose charge is carried by the black hole. Of course, this force is identically zero in the BPS black hole and in the BPS fuzzballs, but now we have more mass than charge, and we expect such a probe brane to start feeling a force. We may then use the result to speculate in Section 4.6 on the force (experience) felt by other probes (infalling 'observers').

The potential for an M2 brane wrapping the $I^{\text{th}}$ torus $T^2_I$, in the Cvetic-Youm black hole (appendix C.1) is easy to compute [15]

$$V^{(I)}_{BH} = V_{DBI} + V_{WZ} = \frac{1}{H_I}(\sqrt{H_m} - \coth\delta_I)\,. \tag{4.10}$$

As before, in the near-extremal limit with no rotation $Q^{BH}_I \approx Q_I$ and $m \ll Q_1$. The leading-order contribution to the potential of a probe M2 brane wrapping the torus $T^2_I$ is proportional to what we may define as the mass above extremality in the $I^{\text{th}}$ channel:

$$V^{(I)}_{BH} = \frac{\Delta M_I}{\rho^2}\,, \qquad \text{where} \quad \Delta M_I \equiv \frac{m^2}{8Q_I} \qquad \text{and} \quad \Delta M = \sum_{I=1}^{3}\Delta M_I + \mathcal{O}(m^3)\,. \tag{4.11}$$

Note that probe branes wrapping different tori will correspond upon compactification to five dimensions to point particles with different types of U(1) charges, and feel different forces.

To compute the force on a probe M2 brane in the non-extremal fuzzball one may think naively that one needs to construct the fully backreacted solution corresponding to metastable supertubes, but this is not so. Using the fact that in the absence of a metastable supertube one can add a BPS M2 brane at a large distance away from the throat without breaking supersymmetry, one can calculate the action of a metastable supertube in a microstate geometry both with and without the brane. The difference between the two actions gives then by Newton's third law the potential felt by a far-away M2 brane as a function of its position, which can then be used to determine the force it feels. In the examples where a backreacted solution exists, this method,

[15] The force is $\vec{F}_{BH} = q_{M2}\frac{\partial V_{BH}}{\partial \vec{r}_{M2}}$.

first introduced in KKLMMT [167], reproduces correctly the force computed from Supergravity [189, 76, 74, 190].

Adding an M2 brane with charge $q_{M2}$ far away from the scaling centers introduces another term in the M2 harmonic function

$$L_I = \sum_{i=1}^{7} \frac{\ell_i}{|\vec{r} - \vec{r}_i|} + \frac{q_{M2}}{|\vec{r} - \vec{r}_{M2}|}\,, \tag{4.12}$$

and for small charges this changes the energy of the metastable supertube by

$$V_{MS}^{(I)} = \frac{\partial \mathcal{H}}{\partial L_I}\bigg|_{\min} \frac{1}{|\vec{r}_{\min} - \vec{r}_{M2}|}\,, \tag{4.13}$$

which by Newton's third law gives then the potential felt by the M2 brane in the non-extremal fuzzball.

Given that our non-extremal microstates have the same mass and charges as a non-extremal black hole, we would expect by Birkhoff's theorem that the leading-order term in the potential felt by an M2 brane far away from the region of the throat would be the same. However, the leading-order term in (4.13) is not of the same form as (4.11); in particular the microstate attractive potential (4.13) does not scale properly with the length of the microstate throat:

$$\frac{V_{MS}^{(I)}}{V_{BH}^{(I)}} \sim \frac{1}{L_I}\,. \tag{4.14}$$

Since $1/L_I$ is linear in the inter-center distances of the scaling background, the force with which the microstate attracts the M2 brane vanishes as one considers deeper and deeper microstates with the same mass. Furthermore, another surprise is in store. A microstate with a metastable supertube with electric charges $q_1$ and $q_2$ will attract M2 branes with charges $Q_1$ and $Q_2$, but will repel M2 branes with charge $Q_3$. This can be seen both by investigating (4.13), or by evaluating the potential numerically:

$$\frac{V_{MS}^{(1)}}{V_{BH}^{(1)}} \approx 3.0 \times 10^{-5}\, z_6\,, \qquad \frac{V_{MS}^{(2)}}{V_{BH}^{(2)}} \approx 2.9 \times 10^{-5}\, z_6\,, \qquad \frac{V_{MS}^{(3)}}{V_{BH}^{(3)}} \approx -6.4 \times 10^{-5}\, z_6\,. \tag{4.15}$$

The 'wrong' sign of $V_{MS}^{(3)}$ and the linear dependence of these ratios on $z_6$ implies that one cannot hope to obtain the 'correct' black-hole force on probe M2 branes from microstates constructed this way. One can also imagine constructing other types of black hole microstates, by placing single anti M2-branes or other more complicated objects inside bubbling geometries; however, the 'force problem' persists, and it can be summarized as follows:

Given a background that does not attract M2 branes, the mass above extremality generated by adding a probe that breaks supersymmetry inside a long throat generically goes like the mass of that probe divided by the warp factor at the bottom of the throat. On the other hand, if one computes 'à la KKLMMT' the force on a probe M2 brane, this force scales generically like the mass of the probe divided by the *square* of the warp factor, and hence like the ADM mass of the solution divided by the warp factor at the bottom. If one now makes the throat longer or

shorter keeping the mass fixed, the force in a microstate changes, unlike in a black hole solution where this force is always proportional to the mass above extremality.

This force analysis indicates that the non-extremal microstates obtained by placing single metastable supertubes inside BPS microstates do not attract M2 branes in the way one may naively expect of a typical black hole microstate. The underlying reason for this is that the supertube couples not only to the warp factor and electric fields but also to extra scalars in five dimensions, which come from the volume moduli of the torus. This extra interaction, which is absent for M2 probes in the background of the black hole, leads to the different scaling behavior of the force on a probe M2 in the microstate background and to the repulsive force felt by an M2-brane along the third torus.

Even if the microstates we obtain by placing one metastable supertube do not attract M2 branes the way the black hole does, one can clearly bypass this problem and construct very large numbers of microstates that attract M2 branes typically by placing several species of metastable supertubes, and by fixing the supertube charges such that the length of the microstate is exactly that of the black hole (3.65) and furthermore such that at this length the forces are exactly those of the black hole (4.13). However, this is more a matter of engineering, and can obscure an important piece of physics that the force computation reveals: the fact that the force on a probe M2 branes varies wildly from microstate to microstate, and can be even negative, implies that M2 branes will feel the thermal fluctuations between various fuzzballs as thermal fluctuations in the force even if they are quite far away from the black hole. Thus, these M2 branes will become aware of the existence of fuzzballs and of the breakdown of classical physics further away from the horizon than other probes.

### 4.5.2 What does an in-falling observer see ?

In the most straightforward interpretation of the fuzzball proposal, which one may call a 'fuzzball of fire' interpretation, the classical geometry breaks down at the horizon, and is replaced by an ensemble of fuzzballs [46]. Hence, the horizon is the scale where the 'thermodynamic' description of physics (in terms of a classical spacetime) breaks down, and the 'statistical' description (in terms of fuzzballs) takes over. In a naive analogy with an ideal gas, the scale of the horizon is like that of the mean free path, and hence we might expect the incoming observers to experience large statistical fluctuations in the same way in which a particle of smaller and smaller size in a gas experiences larger and larger fluctuations. Below a certain size of the particle the Brownian motion deviations overtake the classical trajectory, and the notion of 'particle moving in a continuous fluid' breaks down. In the same way, a particle far away from a black hole experiences a classical spacetime, but as the particle approaches the horizon the statistical fluctuations become stronger and stronger, and at the horizon the notion of 'particle moving in a classical spacetime' breaks down.

From the point of view of the incoming particle, the increasing fuzzball fluctuations it feels at the scale of the horizon are not a very pleasant experience, which agrees with the recent proposal of AMPS [66] that an incoming particle must see a firewall at the horizon scale in order for the information paradox to be solved. In Section 4.3 we argued that the pleasantness of the experiences of an in-falling particle depends on its energy; particles with energy of the order of the Hawking temperature should thermalize in the bath of out-going radiation which thus

constitutes a 'firewall' for these in-falling particles, while particles much more higher-energetic than Hawking radiation should pass the bath nearly unaltered.

According to Mathur's recent fuzzball complementarity proposal [68, 67, 70, 176, 69], the scale of fuzzball thermalization/loss of spacetime experience does not only depend on the location of the infalling observer, but also on its energy. High-energy observers will continue experiencing a spacetime even after they have passed the horizon scale and have entered the fuzzball region, and for these observers spacetime will emerge from the quantum superposition of the fuzzballs. On the other hand lighter particles, of order the Hawking radiation energy, stop experiencing a classical spacetime at the horizon – this is necessary in order for the Hawking radiation to be able to carry off the black hole information to infinity and solve the information paradox. The analogy with the ideal gas in the 'fuzzball of fire' argument above is not so straightforward, essentially because in the ideal gas there is only one scale, while when describing an observer falling into a black hole one has two scales: the observer's mass and its location.

It is hard to tell directly whether our non-extremal fuzzballs will be felt by an incoming observer as 'fuzzballs of fire' or as 'fuzzballs of fuzz' (in the sense of fuzzball complementarity). To do this one would have to construct first more generic non-extremal fuzzballs, and then to scatter various particles off them. Such a research program is feasible; one can in particular use the quiver quantum mechanics that describes these fuzzballs in the regime of parameters where gravity is turned off [110], and analyze the scattering of various charged centers, as one does in supergoop studies [191]. One can analyze for example the collision of a multicenter near-extremal fuzzball goop with a center whose charges are much bigger than those of the centers that compose the fuzzball, and see whether such a center gets absorbed by the fuzzball goop as soon as it reaches it or traverses it with impunity, and if so how the trajectory of this center differ s from the trajectory in a single-center black hole geometry.

However, even before such a calculation is done, there are two features of our construction that are relevant in the fuzzballs of fire/fuzz discussion. First, the fact that nothing dramatic happens as the throat of microstate geometries becomes longer or shorter than that of a black hole implies that the difference between fuzzballs and the classical black hole is not strongly suppressed immediately above the horizon scale. Hence, if an observer heavier than Hawking particles continues to experience a spacetime below the horizon scale then, by extension, an observer lighter than the Hawking particles should stop experiencing a spacetime *above* the horizon scale. The physics of this possibility can get quite unpalatable: a spaceship orbiting at say five Schwarzschild radii above the horizon cannot send to another nearby spaceship any photons that have an energy lower than the Hawking radiation energy divided by five to some power; such photons are thermalized by the ensemble of fuzzballs already at that scale and hence cannot propagate.

It seems quite counterintuitive that observers, be they very small, start experiencing large statistical fluctuations of spacetime and dissolve in the fuzz far away from the horizon. This Gedankenexperiment might thus tilt the balance against 'fuzzball complementarity', and towards the 'fuzzball of fire' interpretation. On the other hand, another piece of fuzzball physics in our construction seems to incline the balance backwards: We have computed the force on probe M2 branes (that experience no force when the fuzzball is supersymmetric), and we have found that this force varies wildly, and can even change sign when one goes from one metastable fuzzball to another. It may be that this wild variations in the force are just a feature of the very specific

type of fuzzballs we have succeeded to construct, and some yet-to-be-constructed more typical microstates will not attract M2 branes in such erratic ways. However, it is also possible that we have uncovered a fundamental feature of fuzzballs of near-extremal black holes: they may attract very erratically the components of the extremal black hole with the same charges.

Now, if these very special probes see the thermal noise from the fuzzball and experience statistical fluctuation already at a very large distance, way above the horizon scale, it does not seem so far-fetched that other observers, in particular those with energy below that of Hawking radiation, could also see this thermal noise far away from the horizon, while other (more massive) observers continue experiencing a spacetime well into the fuzzball, as the fuzzball complementarity proposal suggests.

## 4.6 Discussion of the results

In Section 4.2 we argued that infall and outfall of information should be a symmetric process and infalling quanta of energy the Hawing temperature at infinity should thus not be able to freely fall through a black hole horizon. In Section 4.3 we reviewed the firewall argument and rephrased it in the language or wave packets and decoherence. We found that the fate of an infalling wave packet may crucially depend on its properties and the Hamiltonian evolution and one thus has to understand the nature of the interaction of the wave packet with the horizon-scale structure that is required by unitarity. In Section 4.4 we studied general properties of typical fuzzballs and elaborated on the fuzzball complementarity proposal. We discussed how and when the region inside the potential barrier of a typical fuzzball (Figure 4.8) can by approximated by the eternal black hole in the Hartle-Hawking state (Figure 4.12). The procedure discussed is based on the approximation of a typical fuzzball state by a thermal state. While the approximating procedure shows *how* it may be possible to get the black hole as a coarse-grained description of fuzzballs it is essential to keep in mind *when* it is applicable:

- A thermal state can be a good approximation for *typical* states only.
- Infalling quanta of typical energy ($E \sim T_H$) experience the details of the fuzzballs and so their evolution cannot be described by free infall.
- Free infall is only possible for high-energy ($E \gg T_H$) observers represented by *sufficiently coarse-grained operators* probing the typical state.
- While we have only discussed the extreme limits of $E \sim T_H$ and $E \gg T_H$, infalling observers with asymptotic energies in between are expected to experience a continuous variation of dramatic to free infall.

The physical mechanism behind fuzzball complementarity is the strong dynamics of the infalling observer with the typical fuzzball state which results in the excitation of collective modes. While a detailed description of this process is presently not feasible we can attempt to answer the infall question by making the above approximation. This has revealed a crucial feature of fuzzball complementarity: the *separation of energy scales*. While black hole complementarity advances

the idea of a *frame change* such that infalling and asymptotic observers may have different experiences, for fuzzball complementarity an operator probing a system will yield different answers (experiences) according to whether it is coarse-grained or fine-grained. While the experience of high-energy infalling observers that are insensitive to the details of the microstates (coarse-grained) may be described by free infall into a black hole, infalling low-energy observers may be seen as the mirror image of the outgoing radiation quanta (fine-grained) and thus cannot have such a drama-free experience.

In Section 4.5 we attempted to test the fuzzball complementarity and firewall ideas when applied to the the newly constructed near-extremal fuzzballs of Chapter 3 by computing the force on certain probes. While those were very special probes, extrapolation to more general probes suggests that low-energy probes will become aware of the fuzz at the horizon-scale or earlier, while high-energy probes might continue to experience some notion of spacetime beyond the fuzzball surface. However, to establish the fuzzball complementarity proposal for Reissner-Nordstöm black holes, one would have to construct more generic non-extremal fuzzballs and repeat the force calculation for more generic probes.

When approximating the interaction of certain infalling observers with the fuzzball at the would-be horizon by the infalling observer crossing a horizon one must worry, in particular in light of the discussion in Chapter 2, that a smooth horizon requires a particular entanglement structure of the modes around the horizon. Running the AMPS argument again one would expect free infall not to be possible after Page time. [192, 193] This conclusion may, however, be premature: There is a major difference between the black hole setup of AMPS and the auxiliary black hole picture that arises in fuzzball complementarity. While in the former a particular entanglement structure of the modes across the horizon was forced by requiring unitarity of the evaporation process, in the latter unitarity is built into the idea of fuzzballs and the black hole arises only as an approximation to questions regarding infall. [16] In particular, it is only used as a computational tool to describe the otherwise complicated dynamics of infall into an actual fuzzball and it may evade the AMPS result by the following argument. When a mode of Killing energy $E = nT$ impinges on a fuzzball the number of possible states grows exponentially [69]

$$\Delta\mathcal{N} = e^{GM^2} e^n. \tag{4.16}$$

If $n \gg 1$, in other words if the infalling quantum has asymptotic energy $E \gg T$, exponentially more degrees of freedom become available. A strong interaction between the infalling observer and the fuzzball degrees of freedom and assuming fast scrambling dynamics may then 'use' these extra degrees of freedom to create many new (analogues of) $BC$ pairs. This argument applies even after Page time. The new degrees of freedom may account for the entanglement structure in the auxiliary black hole picture needed for free infall. [69, 194]

We would like to emphasize once more that the approximation of infall into the fuzzball by infall into a fictitious black hole is only a computational tool and it remains an open question to identify the appropriate operators/observables in this auxiliary description that accurately describe the full dynamics of the infalling observer with the fuzzball.

[16] Indeed, the approximation of a typical fuzzball state by a thermal state has as consequence that questions about the unitary nature of evaporation are discarded.

# Chapter 5

# Non-renormalization for almost-BPS extremal solutions

Most of the focus on studying black hole microstates in Supergravity has focused on the construction of BPS solutions because supersymmetry yields many interesting and simplifying properties. In this Chapter we want to ask the question:

*Q5. What properties of supersymmetric solutions carry over to non-supersymmetric solutions?*

In Chapter 3 we used supersymmetric multi-center solutions as starting point for the construction of near-extremal black hole microstates from metastable probe supertubes. A key feature of these BPS solutions is the non-renormalization property of the equations that govern the location of the centers. This property allows to study the system at weak or strong effective coupling and at intermediate regimes of the effective coupling where some centers are treated as probes in a fully back-reacted multi-center Supergravity solutions. In this Chapter we want to study whether this non-renormalization property of supersymmetric multi-center configurations carries over to almost-BPS configurations.

## 5.1 Motivation and summary

The physics of multi-center four-dimensional BPS solutions and of their five-dimensional counterparts [109, 110, 111, 105, 26, 27, 28] could be one of the keys that helps unlock longstanding mysteries of black hole physics, such as the information paradox and the microscopic origin of the black hole entropy. These solutions yield the easiest-to-construct black hole microstate geometries [32, 35] and can be used to study the wall-crossing behavior of black hole partition functions [115, 195]. They also provide the best-known examples of entropy enigmas [196, 115, 197].

Another key feature of BPS, multi-center solutions is that the equations controlling the positions of these centers, also known as the bubble equations, are not renormalized as one goes from weak to strong effective coupling. At weak coupling, these configurations are described by a supersymmetric quiver Quantum Mechanics (QQM) [110], and the equations determining the vevs of the QQM Coulomb-branch fields are the same as those determining the inter-center distances of the fully-backreacted Supergravity solution. This remarkable non-renormalization

property has allowed one to compute the symplectic form, quantize the moduli space of Supergravity solutions from the QQM perspective [166] [1] and has given a clear mapping of some of the microscopic black hole degrees of freedom to horizonless solutions that exist in the same regime of the moduli space as the classical black hole [198, 199, 200].

For BPS solutions one can also test this non-renormalization of the bubble equations by considering multi-center solutions in an intermediate region of the effective coupling, where some of the branes have backreacted while others are treated as probes. More precisely, one can place a supertube in a multi-center solution and examine its supersymmetric minima. The equations that determine the positions of these minima can then be shown to be identical to the bubble equations [124]. Hence, one can recover the BPS bubble equations both at small effective coupling from the QQM, at intermediate coupling from the supertube DBI action, and at large effective coupling by asking that the fully backreacted solution has no closed timelike curves.

Since the non-renormalization of the bubble equations is established by invoking quantities protected by supersymmetry, one might naively expect that the beautiful pieces of physics that are protected from renormalization in BPS systems would no longer survive in non-supersymmetric, multi-center solutions or in non-supersymmetric fuzzballs. The purpose here is to demonstrate that, on the contrary, in certain classes of non-supersymmetric multi-center solutions - the so-called almost-BPS solutions [36, 39, 37] - the bubble equations are also protected when one goes from intermediate to strong coupling. This suggests that there are no quantum corrections despite the lack of supersymmetry.

This result is quite surprising because there is neither supersymmetry nor any other underlying symmetry that would prevent the bubble equations from receiving corrections and because the bubble equations of almost-BPS solutions contain complicated cubic combinations of the inter-center distances, whose coefficients do not *a priori* appear to be related to anything one can define in a quiver quantum mechanics. However, in retrospect, this result may not look so surprising: Emparan and Horowitz have shown in [201] that the entropy of certain extremal non-supersymmetric black holes can be calculated at weak effective coupling, and does not change as one increases this coupling. Since a certain subclass of almost-BPS solutions can be dualized to the black hole considered in [201], it seems plausible that whatever principle protects the quantum states calculated at weak coupling from being uplifted and disappearing at strong coupling also protects the bubble equations from receiving quantum corrections [2].

To establish that the almost-BPS bubble equations are not changing with the coupling, we consider an intermediate-coupling configuration where all the centers, except one, have backreacted into an almost-BPS Supergravity solution. One can then probe this solution with a supertube and use the (Dirac-Born-Infeld and Wess-Zumino) action to determine the equilibrium position of the probe. If one considers the backreaction of the probe then the supertube would become another center of the Supergravity solution and its location is fixed by the bubble equations, which arise from requiring that there be no closed time-like curves. The comparison of these two physically distinct conditions, one in field theory on the brane and the other from its

[1] This in turn has confirmed that quantum effects can wipe out macroscopically large regions of certain smooth low-curvature solutions [35, 166].

[2] It is also interesting to note that whatever underlying principle protects the states and bubble equations of almost-BPS system from being uplifted by quantum corrections can be even stronger than supersymmetry, which, for example, does not protect the degeneracy of the D1-D5-P system in the non-Cardy regime [197].

gravity dual, yields the test of non-renormalization between the intermediate and strong coupling regimes. At first glance, the equations look nothing like each other: both differ from the BPS bubble equations by extra cubic terms, but these cubic terms are not the same. However, the story is a bit more complicated: Unlike the BPS solution, the quantized electric charge of the supertube DBI action and the electric charge parameters in the Supergravity harmonic functions are not the same. One can then ask whether there exists a relation between the DBI and the Supergravity electric charges of the supertube that maps one set of bubble equations onto the other. One of the primary results here is to prove that such a relation exists, and write it down for the most general known almost-BPS solution in a single-center Taub-NUT space, involving an arbitrary collection of concentric supertubes and black rings.

The implications of this relation for the physics of almost-BPS solutions are quite significant. First, in a general Supergravity solution that contains several supertubes, the quantized charges of these supertubes are not the obvious coefficients in the Supergravity harmonic functions. The Supergravity parameters are related to the quantized charges by certain shifts that come from dipole-dipole interaction and depend on the location of all the other centers of the solution. An interesting features of these shifts is that they only depend on the dipole charges and positions of the centers that lie between location of the charge in question and the (supersymmetry-breaking) center of the Taub-NUT space.

For almost-BPS black rings the effect of the charge shift is more subtle because the black rings have more than one dipole charge, and hence the formulae that give the dipole-dipole contribution to the charge appear to be degenerate. However one can assemble a black ring by bringing together three supertubes with different kinds of dipole charges, and this will allow us to calculate the shifts between the black-ring Supergravity and the quantized charges.

The second significant implication has to do with charge quantization, and solves a longstanding puzzle of the physics of almost-BPS black rings and of multi-center almost-BPS solutions. As one can see from [37] or from [45], the (quantized) asymptotic charge of such solutions is equal to the sum of the Supergravity charges of the centers plus an extra dipole-dipole term that depends on the positions of the centers and the moduli of the solution. If the Supergravity charges were equal to the quantized ones, this would have implied that the moduli-dependent contribution to the charges are also quantized, and hence multi-center almost-BPS solutions could only exist on special codimension-three slices of the moduli space (where the moduli-dependent contributions are integers). This would have been quite puzzling. The results presented here show that this does not happen. Upon using our formulas that relate the Supergravity and the quantized charges, one finds that the asymptotic charge of the almost-BPS black ring is equal to the sum of the quantized charges of its centers, and hence the almost-BPS black ring as well as other multi-center almost-BPS solutions exists for any values of the moduli. If one keeps the quantized charges fixed and changes the moduli, the quantities that change are simply the Supergravity charge parameters of the centers. Our result also implies that the $E_{7(7)}$ quartic invariant of the almost-BPS black ring of [39] needs to be rewritten in terms of the quantized charges, and also yields the relation between the 'quantized' angular momentum of this black ring and the angular-momentum parameter that appears in the corresponding almost-BPS harmonic function.

A third, perhaps more unexpected consequence of our result is that if one probes a certain Supergravity solution with a supertube and finds, say, two minima, one where the supertube is at the exterior of the other supertubes and one where it is at an intermediate position, these two

minima do not correspond to two vacua in the same vacuum manifold of the bubble equations. Indeed, one can relate both minima of the supertube potential to almost-BPS Supergravity solutions, and then use our recipe to compute the quantized charges of the centers of these two solutions. Since the shifts of the charges of the centers depend on the position of the tube, the quantized charges of the centers of the two resulting solutions will not be the same, and hence these solutions do not describe different arrangements of the same supertubes, and thus cannot be related by moving in the moduli space of solutions of a certain set of bubble equations. Instead they live in different superselection sectors.

This Chapter is organized as follows. In Section 5.2 we review the structure of BPS and almost-BPS Supergravity solutions and in Section 5.3 we calculate and examine the action of supertube probes in these solutions. We show that one can reproduce the Supergravity bubble equation of the outermost supertube by considering this supertube as a probe in the fully backreacted solution formed by the other supertubes and find the equation that relates the Supergravity charge parameters and the quantized charges of the probe. We then give a recipe to read off the quantized supertube charges in a general multi-center almost-BPS solution. In Section 5.4 we then show that one can also recover the bubble equations of all the other supertube centers by examining the minima of probe supertubes and relating their Supergravity charges to their quantized charges. This demonstrates that all the Supergravity data of a multi-center solution can be recovered from the action of supertube probes, and hence this data is not renormalized as one goes from weak to strong effective coupling. We also discuss in more detail the physics behind the shift needed to relate Supergravity and quantized charges. Section 5.5 contains our conclusions and a discussion of further issues arising from this work. Some of the technical details of this chapter have been relegated to Appendix D.

## 5.2 The Supergravity solutions

In Section 1.4 we reviewed the system of almost BPS equations and the Ansatz for the metric and gauge potential. For convenience will summarize in Subsection 5.2.1 the relevant formulas and contrast the almost-BPS with the BPS case. In Subsection 5.2.2 we will present the axisymmetric multi-supertube solution which we study in the following.

### 5.2.1 BPS and almost-BPS equations

The simplest way to describe the solutions of interest is to work in M-theory, with the metric

$$\begin{aligned} ds_{11}^2 = & -(Z_1 Z_2 Z_3)^{-\frac{2}{3}} (dt+k)^2 + (Z_1 Z_2 Z_3)^{\frac{1}{3}}\, ds_4^2 \\ & + \left(Z_2 Z_3 Z_1^{-2}\right)^{\frac{1}{3}} (dx_5^2+dx_6^2) + \left(Z_1 Z_3 Z_2^{-2}\right)^{\frac{1}{3}} (dx_7^2+dx_8^2) + \left(Z_1 Z_2 Z_3^{-2}\right)^{\frac{1}{3}} (dx_9^2+dx_{10}^2)\,, \end{aligned} \quad (5.1)$$

where $ds_4^2$ is a four-dimensional hyper-Káhler metric. The three-form potential is given by:

$$A_3 = A^{(1)} \wedge dx_5 \wedge dx_6 + A^{(2)} \wedge dx_7 \wedge dx_8 + A^{(3)} \wedge dx_9 \wedge dx_{10}\,, \quad (5.2)$$

where the Maxwell fields are required to obey the 'floating brane Ansatz' [38]:

$$A^I \;=\; -\,\varepsilon\, Z_I^{-1}\,(dt+k)+B^{(I)}\,, \tag{5.3}$$

and where $\varepsilon \;=\pm 1$ and $B^{(I)}$ is a 'magnetic' vector potential with field strength $\Theta^{(I)} \;\equiv\; dB^{(I)}$ on the base, $ds_4$. Here we will work with the Taub-NUT metric:

$$ds_4^2 \;=\; V^{-1}(d\psi+A)^2 \;+\; V\,(dx^2+dy^2+dz^2)\,, \tag{5.4}$$

with [3]

$$V \;=\; h \;+\; \frac{q}{r}\,, \tag{5.5}$$

where $r^2\equiv \vec{y}\cdot\vec{y}$ with $\vec{y}\equiv(x,y,z)$. We will also frequently use polar coordinates: $x=r\sin\theta\cos\phi$, $y=r\sin\theta\sin\phi$ and $z=r\cos\theta$. The metric (5.4) is hyper-Káhler if

$$\vec{\nabla}V \;=\; \pm\,\vec{\nabla}\times\vec{A}\,, \tag{5.6}$$

where $\nabla$ denotes the flat derivative of $\mathbb{R}^3$. For (5.5) we get

$$A= \;\pm\, q\,\cos\theta\, d\phi\,, \tag{5.7}$$

where we chose the integration constant to vanish. We use the orientation with $\epsilon_{1234}=+1$ and then choosing the positive sign in (5.6) results in a Riemann tensor that is self-dual while choosing the negative sign makes the Riemann tensor anti-self-dual. We will follow the conventions of [45] and take

$$\varepsilon \;=\; +1\,, \tag{5.8}$$

and then the BPS solutions and almost-BPS solutions correspond to choosing the $+$ or $-$ sign, respectively, in (5.6) and (5.7), as explained in detail in Section 1.4.

### 5.2.2 BPS and almost-BPS solutions with a Taub-NUT base

We now summarize, in some detail, the solutions presented in [45]. [4] On a Gibbons-Hawking (GH) base the vector potentials, $B_\pm^{(I)}$ in (5.3) are given by:

$$B_\pm^{(I)} \;=\; P_\pm^{(I)}(d\psi+A) \;+\; \vec{\xi}_\pm^{(I)}\cdot d\vec{y}\,, \qquad \text{with} \qquad \begin{array}{rcl} P_+^{(I)} &=& K_+^I\,V^{-1}\,,\\ P_-^{(I)} &=& K_-^I\,, \end{array} \tag{5.9}$$

and

$$\nabla^2 K_\pm^I \;=\; 0\,, \qquad \begin{array}{rcl} \vec{\nabla}\times\vec{\xi}_+^{(I)} &=& -\,\vec{\nabla}K_+^I\,,\\ \vec{\nabla}\times\vec{\xi}_-^{(I)} &=& K_-^I\vec{\nabla}V - V\vec{\nabla}K_-^I\,, \end{array} \tag{5.10}$$

[3] Note that in previous Chapters we denoted Taub-NUT charges by $v$ and reserved the letter $q$ for the electric charge of probe branes. For single-center Taub-NUT configurations it is common in the literature to denote the Taub-NUT charge by $q$. We will use this notation here, also because we will be comparing supergravity charges (and dipole charges), which are denoted by $Q_I$ ($k^I$), to quantized probe charges (and dipole charges) which are then more naturally denoted by $\widehat{Q}_I$ ($\widehat{k}^I$).

[4] Since we are using the conventions (5.8), there will be some sign differences compared to [45].

where the $\pm$ corresponds to the choice in (5.6) and hence to BPS or almost-BPS respectively.

A 'type I' supertube, $I = 1, 2, 3$, has a singular magnetic source for $B^{(I)}$ and singular electric sources for $Z_J$ and $Z_K$, where $I, J, K$ are all distinct. As in [45], we study an axisymmetric supertube configuration with one supertube of each type on the positive $z$-axis and thus we take harmonic functions:

$$K^I_\pm \;=\; \frac{k^\pm_I}{r_I}\,, \tag{5.11}$$

where

$$r_J \;\equiv\; \sqrt{x^2+y^2+(z-a_J)^2}\,. \tag{5.12}$$

Without loss of generality we will assume that

$$0 < a_1 \;<\; a_2 \;<\; a_3\,. \tag{5.13}$$

We then have

$$\xi^{(I)}_+ \;=\; -k^+_I\,\frac{(r\cos\theta - a_I)}{r_I}\,d\phi\,, \qquad \xi^{(I)}_- \;=\; -\frac{k^-_I}{a_I\,r_I}\left[\,q\,(r-a_I\cos\theta)+h\,a_I\,(r\cos\theta-a_I)\,\right]d\phi\,, \tag{5.14}$$

and we may then write

$$B^{(I)}_+ \;=\; \frac{K^I_+}{V}\left[\,d\psi + \frac{q\,a_I}{r}\,d\phi - h\,(r\cos\theta - \,a_I)\,d\phi\,\right], \tag{5.15}$$

$$B^{(I)}_- \;=\; \frac{k^-_I}{a_I\,r_I}\left[\,a_I\,d\psi - q\,r\,d\phi - h\,a_I\,(r\cos\theta - a_I)\,d\phi\,\right]. \tag{5.16}$$

One can measure the local dipole strength by taking the integral of $\Theta^{(I)}$ over a small sphere, $S^2_\epsilon \subset \mathbb{R}^3$, around the singular point and one finds:

$$\int_{S^2_\epsilon}\,\Theta^{(I)} \;=\; \begin{cases} -4\,\pi\,k^+_j & \text{for BPS} \\ -4\,\pi\left(h+\frac{q}{a_j}\right)k^-_j & \text{for almost-BPS.}\end{cases} \tag{5.17}$$

Hence, the quantized dipole charges are

$$\widehat{k}_j \;\equiv\; \left(h+\frac{q}{a_j}\right)k^-_j \tag{5.18}$$

in the almost-BPS solutions.

The electrostatic potentials are relatively simple. For BPS supertubes it is straightforward to apply the results of [26, 27]:

$$Z_1 \;=\; L_1 \;+\; \frac{K^2_+\,K^3_+}{V} \;=\; 1 \;+\; \frac{Q^{(1)}_2}{r_2} \;+\; \frac{Q^{(1)}_3}{r_3} \;+\; \frac{k^+_2\,k^+_3}{(h+\frac{q}{r})\,r_2\,r_3}\,, \tag{5.19}$$

$$Z_2 \;=\; L_2 \;+\; \frac{K^1_+\,K^3_+}{V} \;=\; 1 \;+\; \frac{Q^{(2)}_1}{r_1} \;+\; \frac{Q^{(2)}_3}{r_3} \;+\; \frac{k^+_1\,k^+_3}{(h+\frac{q}{r})\,r_1\,r_3}\,, \tag{5.20}$$

$$Z_3 \;=\; L_3 \;+\; \frac{K^1_+\,K^2_+}{V} \;=\; 1 \;+\; \frac{Q^{(3)}_1}{r_1} \;+\; \frac{Q^{(3)}_2}{r_2} \;+\; \frac{k^+_1\,k^+_2}{(h+\frac{q}{r})\,r_1\,r_2}\,. \tag{5.21}$$

For the almost-BPS supertubes one can use the results in [37]:

$$Z_1 \;=\; 1 \;+\; \frac{Q_2^{(1)}}{r_2} \;+\; \frac{Q_3^{(1)}}{r_3} \;+\; \Big(h + \frac{q\,r}{a_2\,a_3}\Big)\,\frac{k_2^-\,k_3^-}{r_2\,r_3}\,, \tag{5.22}$$

$$Z_2 \;=\; 1 \;+\; \frac{Q_1^{(2)}}{r_1} \;+\; \frac{Q_3^{(2)}}{r_3} \;+\; \Big(h + \frac{q\,r}{a_1\,a_3}\Big)\,\frac{k_1^-\,k_3^-}{r_1\,r_3}\,, \tag{5.23}$$

$$Z_3 \;=\; 1 \;+\; \frac{Q_1^{(3)}}{r_1} \;+\; \frac{Q_2^{(3)}}{r_2} \;+\; \Big(h + \frac{q\,r}{a_1\,a_2}\Big)\,\frac{k_1^-\,k_2^-}{r_1\,r_2}\,. \tag{5.24}$$

Note that the harmonic pieces, $L_I$, are the same for both the BPS and almost-BPS systems.

The angular momentum vector, $k$, is decomposed in the usual manner:

$$k \;=\; \mu\,(d\psi + A) \;+\; \omega\,. \tag{5.25}$$

The details will not be important here but for completeness we give them in Appendix D.

### 5.2.3 The bubble equations

One defines the usual symplectic inner products for the BPS and almost-BPS charges:

$$\Gamma^+_{12} \;=\; k_1^+\,Q_2^{(1)} - k_2^+\,Q_1^{(2)}\,, \qquad \Gamma^+_{13} \;=\; k_1^+\,Q_3^{(1)} - k_3^+\,Q_1^{(3)}\,, \qquad \Gamma^+_{23} \;=\; k_2^+\,Q_3^{(2)} - k_3^+\,Q_2^{(3)}\,, \tag{5.26}$$

$$\widehat{\Gamma}_{12} \;=\; \widehat{k}_1\,Q_2^{(1)} - \widehat{k}_2\,Q_1^{(2)}\,, \qquad \widehat{\Gamma}_{13} \;=\; \widehat{k}_1\,Q_3^{(1)} - \widehat{k}_3\,Q_1^{(3)}\,, \qquad \widehat{\Gamma}_{23} \;=\; \widehat{k}_2\,Q_3^{(2)} - \widehat{k}_3\,Q_2^{(3)}\,. \tag{5.27}$$

Note that we have used the effective, local charges, $\widehat{k}_j$ in (5.27).

It was shown in [45] that supertube regularity requires the locations of the supertubes to be related to the charges via:

$$\frac{\Gamma^+_{12}}{|a_1-a_2|} \;+\; \frac{\Gamma^+_{13}}{|a_1-a_3|} \;=\; \frac{Q_1^{(2)}\,Q_1^{(3)}}{k_1^+}\Big(h + \frac{q}{a_1}\Big) \;-\; k_1^+\,, \tag{5.28}$$

$$\frac{\Gamma^+_{21}}{|a_1-a_2|} \;+\; \frac{\Gamma^+_{23}}{|a_2-a_3|} \;=\; \frac{Q_2^{(1)}\,Q_2^{(3)}}{k_2^+}\Big(h + \frac{q}{a_2}\Big) \;-\; k_2^+\,, \tag{5.29}$$

$$\frac{\Gamma^+_{31}}{|a_1-a_3|} \;+\; \frac{\Gamma^+_{32}}{|a_2-a_3|} \;=\; \frac{Q_3^{(1)}\,Q_3^{(2)}}{k_3^+}\Big(h + \frac{q}{a_3}\Big) \;-\; k_3^+\,. \tag{5.30}$$

for the BPS solutions. For the almost-BPS supertubes one must impose

$$\frac{\widehat{\Gamma}_{12}}{|a_1-a_2|} \;+\; \frac{\widehat{\Gamma}_{13}}{|a_1-a_3|} \;=\; \frac{Q_1^{(2)}\,Q_1^{(3)}}{\widehat{k}_1}\Big(h + \frac{q}{a_1}\Big) \;-\; \widehat{k}_1 \;-\; \epsilon_{123}\,Y\,, \tag{5.31}$$

$$\frac{\widehat{\Gamma}_{21}}{|a_1-a_2|} \;+\; \frac{\widehat{\Gamma}_{23}}{|a_2-a_3|} \;=\; \frac{Q_2^{(1)}\,Q_2^{(3)}}{\widehat{k}_2}\Big(h + \frac{q}{a_2}\Big) \;-\; \widehat{k}_2 \;-\; \epsilon_{213}\,Y\,, \tag{5.32}$$

$$\frac{\widehat{\Gamma}_{31}}{|a_1-a_3|} \;+\; \frac{\widehat{\Gamma}_{32}}{|a_2-a_3|} \;=\; \frac{Q_3^{(1)}\,Q_3^{(2)}}{\widehat{k}_3}\Big(h + \frac{q}{a_3}\Big) \;-\; \widehat{k}_3 \;-\; \epsilon_{312}\,Y\,, \tag{5.33}$$

where

$$Y \equiv \frac{h\,q\,k_1^-k_2^-k_3^-}{a_1a_2a_3} = \frac{h\,q\,\widehat{k}_1\widehat{k}_2\widehat{k}_3}{(q+ha_1)(q+ha_2)(q+ha_3)}\,. \tag{5.34}$$

and

$$\epsilon_{ijk} \equiv \frac{(a_i-a_j)\,(a_i-a_k)}{|a_i-a_j|\,|a_i-a_k|}\,. \tag{5.35}$$

The only difference between the two sets of equations is the term, $Y$, which vanishes in the supersymmetric limits of the solution ($h \to 0$ or $q \to 0$), and hence can be thought of as measuring the amount of supersymmetry breaking.

Our goal, in Section 5.3, will be to see how these bubble equations, and particularly the supersymmetry breaking term, can be obtained from a brane-probe calculation.

### 5.2.4 The Minkowski-space limit

If one sets $h = 0$ then the metric (5.4) becomes that of flat Minkowski space modded out by $\mathbb{Z}_q$. In this limit, the BPS and almost-BPS solutions must become the same because both solutions are necessarily BPS since the base is flat.

It is evident that the potential functions, (5.19)–(5.21) and (5.22)–(5.24), are identical for $h = 0$. The metric may then be written as

$$ds_4^2 = q\left[\frac{dr^2}{r} + r\left(\left(\frac{d\psi}{q}\right)^2 + d\theta^2 + d\phi^2 \pm \frac{2}{q}\cos\theta\,d\psi\,d\phi)\right)\right], \tag{5.36}$$

which takes a more canonical form if one sets $r = \frac{1}{4}\rho^2$. The $\pm$ sign reflects the BPS, or almost-BPS description (5.7) but this is a coordinate artifact.

There are several obvious ways of mapping the BPS description of the metric onto the almost-BPS description but one can most easily see the correct choice by looking at the magnetic fields, $B_\pm^{(I)}$, for $h = 0$. Indeed, from (5.16) one sees that the substitution

$$\psi \to -q\,\phi\,, \qquad \phi \to \frac{1}{q}\,\psi\,, \qquad k_I^+ \to \widehat{k}_I \tag{5.37}$$

maps $B_+^{(I)} \to B_-^{(I)}$. This transformation also interchanges the choice of signs in (5.36).

In Appendix D we also verify that the transformation (5.37), for $h = 0$, also maps the angular momentum vector in the BPS description to that of almost-BPS description.

## 5.3 Brane probes in almost-BPS solutions

### 5.3.1 Brane probes

We only require a relatively simple result from the brane probe analysis of [124] or the discussion of Chapter 3. We need the so-called 'radius relation' that determines the equilibrium position of a probe in a Supergravity background.

One can use the M-theory frame or one can go back to the approach of [124] and work with three-charge solutions in the IIA frame in which the three electric charges, $N_1, N_2$ and $N_3$, of the solution correspond to [5]:

$$N_1 : \text{D0} \qquad N_2 : \text{F1}\,(z) \qquad N_3 : \text{D4}\,(5678), \tag{5.38}$$

where the numbers in the parentheses refer to spatial directions wrapped by the branes and $z \equiv x^{10}$. The magnetic dipole moments of the solutions correspond to:

$$n_1 : \text{D6}\,(y5678z) \qquad n_2 : \text{NS5}\,(y5678) \qquad n_3 : \text{D2}\,(yz)\,, \tag{5.39}$$

where $y$ denotes the brane profile in the spatial base, $(x^1, \ldots, x^4)$. We will use a D2-brane probe, carrying electric D0 and F1 charges, $\widehat{Q}^{(1)}$ and $\widehat{Q}^{(2)}$, and with a D2-dipole moment, $d_3$. For the supertube worldsheet coordinates, $\zeta^\mu$, we use static gauge and allow the supertube to wind along both the $\psi$ and $\phi$ angles of the base space according to:

$$x^0 = \zeta^0\,,\; z = \zeta^1\,,\; \psi = \nu_\psi \zeta^2\,,\; \phi = \nu_\phi \zeta^2\,. \tag{5.40}$$

For such a probe, sitting along the positive $z$-axis of the base metric, the radius relation is given by:

$$\left[\widehat{Q}^{(1)} + d_3\,\mathcal{B}^{(2)}\right]\left[\widehat{Q}^{(2)} + d_3\,\mathcal{B}^{(1)}\right] \;=\; d_3^2\,\frac{Z_3}{V}\,(\nu_\psi + q\nu_\phi)^2\;, \tag{5.41}$$

where $\mathcal{B}^{(I)}$ is the pullback of the vector field, $B^{(I)}$, onto the profile of the supertube on the spatial base:

$$\mathcal{B}^{(I)} \;=\; B^{(I)}_\mu\,\frac{\partial x^\mu}{\partial \zeta_2}\,. \tag{5.42}$$

Then, using (5.16), for the BPS solutions:

$$\mathcal{B}^{(I)} \;=\; \mathcal{B}^{(I)}_+ \;=\; \frac{k^+_I}{(h + \frac{q}{r})\,r\,r_I}\left[\,\nu_\psi\,r + q\,a_I\,\nu_\phi - h\,r\,(r\cos\theta - a_I)\,\nu_\phi\,\right], \tag{5.43}$$

while for non-BPS we have

$$\mathcal{B}^{(I)} \;=\; \mathcal{B}^{(I)}_- \;=\; \frac{k^-_I}{a_I\,r_I}\left[\,a_I\,\nu_\psi - q\,r\,\nu_\phi - h\,a_I\,(r\cos\theta - a_I)\,\nu_\phi\,\right]. \tag{5.44}$$

In deriving this radius relation we have set the worldvolume field strength $\mathcal{F}_{tz} = +1$, which is the choice one makes when placing supersymmetric probes in supersymmetric solutions, and one may ask whether this choice is justified for a non-BPS probe supertube, especially because this choice does not describe the metastable supertube minima of Chapter 3. There are two ways to see that this choice correctly reproduces the almost-BPS probe supertube minima. The first, and most direct, would be to evaluate the Hamiltonian derived in Section 3.2 in an almost-BPS solution, and to find directly that the minima of this Hamiltonian have $\mathcal{F}_{tz} = +1$. While he have not done the former computation, there is a simpler, second argument that shows what the outcome must be. Remember that, unlike non-extremal solutions, almost-BPS solutions have the mass and the charge equal, and the only way a supertube action can yield a minimum with the mass equal to the charge is if its worldvolume field strength satisfies $\mathcal{F}_{tz} = +1$.

[5] For later convenience, we have permuted the labels relative to those of [124].

### 5.3.2 Probing a Supergravity solution

We now replace the third supertube in the solution of Subsection 5.2.2 by a probe: we set $k_3^{\pm} = Q_3^{(1)} = Q_3^{(2)} = 0$ and consider the action of a probe with charges $\widehat{Q}^{(1)}_{probe}$, $\widehat{Q}^{(2)}_{probe}$ and dipole charge $d_3$ at a location, $a_3$, on the $z$-axis and winding once around the $\psi$-fiber.

We then have:

$$\mathcal{B}_+^{(I)} \;=\; \frac{k_I^+}{(h+\frac{q}{a_3})\,|a_I-a_3|}\,, \qquad \mathcal{B}_-^{(I)} \;=\; \frac{k_I^-}{|a_I-a_3|}\,. \tag{5.45}$$

We know from the results of [124] that for the BPS choice the radius relation, (5.41), indeed yields the bubble equation (5.30). We therefore focus on the almost-BPS solution.

Inserting $\mathcal{B}^{(I)} = \mathcal{B}_-^{(I)}$ in (5.41) and using (5.45) one can rearrange the radius relation to give

$$\frac{1}{|a_1-a_3|}\Big[d_3\,Q_1^{(3)} \;-\; \Big(h+\frac{q}{a_3}\Big)\,k_1^-\,\widehat{Q}^{(1)}_{probe}\Big] \;+\; \frac{1}{|a_2-a_3|}\Big[d_3\,Q_2^{(3)} \;-\; \Big(h+\frac{q}{a_3}\Big)\,k_2^-\,\widehat{Q}^{(2)}_{probe}\Big] \tag{5.46}$$

$$=\; \Big(h+\frac{q}{a_3}\Big)\,\frac{\widehat{Q}^{(1)}_{probe}\,\widehat{Q}^{(2)}_{probe}}{d_3} \;-\; d_3 \;+\; \frac{q\,k_1^-\,k_2^-\,d_3}{|a_1-a_3|\,|a_2-a_3|}\,\Big(\frac{a_1\,a_2-a_3^2}{a_1\,a_2\,a_3}\Big)\,. \tag{5.47}$$

We now explicitly use the ordering (5.13) to write $|a_i-a_j| = a_i-a_j$ for $i>j$ and we use the definition (5.18) to obtain:

$$\frac{1}{|a_1-a_3|}\Big[d_3\,Q_1^{(3)} \;-\; \widehat{k}_1\,Q^{(1)}_{probe}\Big] \;+\; \frac{1}{|a_2-a_3|}\Big[d_3\,Q_2^{(3)} \;-\; \widehat{k}_2\,Q^{(2)}_{probe}\Big]$$

$$=\; \Big(h+\frac{q}{a_3}\Big)\,\frac{Q^{(1)}_{probe}\,Q^{(2)}_{probe}}{d_3} \;-\; d_3 \;-\; \frac{h\,q\,k_1^-\,k_2^-\,d_3}{a_1a_2a_3\,(h+\frac{q}{a_3})}\,, \tag{5.48}$$

where we have introduced

$$Q^{(1)}_{probe} \;\equiv\; \widehat{Q}^{(1)}_{probe} - \frac{q\,\widehat{k}_2\,d_3}{a_2a_3\,(h+\frac{q}{a_2})(h+\frac{q}{a_3})}\,, \qquad Q^{(2)}_{probe} \;\equiv\; \widehat{Q}^{(2)}_{probe} - \frac{q\,\widehat{k}_1\,d_3}{a_1a_3\,(h+\frac{q}{a_1})(h+\frac{q}{a_3})}\,. \tag{5.49}$$

This exactly matches the bubble equation (5.33) provided one makes the identifications:

$$d_3 \;=\; \widehat{k}_3 \;=\; \Big(h+\frac{q}{a_3}\Big)\,k_3^-\,, \qquad Q^{(I)}_{probe} \;=\; Q_3^{(I)}\,. \tag{5.50}$$

Hence, the action of a probe supertube that is placed at the outermost position of an almost-BPS solution that contains two other supertubes of different species can capture exactly the Supergravity information about the location of this supertube. Since all the terms in the supertube bubble equations only contain two- and three-supertube interactions, we will see in Subsection 5.3.4 that this result can be straightforwardly generalized to a probe supertube placed at the exterior position of an almost-BPS solution containing an arbitrary number of supertubes of arbitrary species.

There is another more compact way to write the formula that gives the shift from the quantized charges to the BPS parameters

$$Q^{(1)}_{probe} \;=\; \widehat{Q}^{(1)}_{probe} \;-\; \frac{q\,\widehat{k}_2\,\widehat{k}_3}{a_2\,a_3V_2V_3}\,, \qquad Q^{(2)}_{probe} \;=\; \widehat{Q}^{(2)}_{probe} \;-\; \frac{q\,\widehat{k}_1\,\widehat{k}_3}{a_1\,a_3V_1V_3}\,. \tag{5.51}$$

### 5.3.3 Interpretation of the charge shift

Given that we have matched the probe calculation to the Supergravity one by postulating the charge shift above, it is legitimate to ask whether this charge shift has any direct physical interpretation apart from the fact that it maps the probe result onto the Supergravity result. We will argue in the remaining part of this Chapter that this charge shift encodes very non-trivial properties of almost-BPS solutions.

We begin by comparing almost-BPS solutions to BPS multi-center solutions (for which there is no charge shift [124]) in the limits when the two kinds of solutions become identical. We will then explain how this charge shift solves an old puzzle about the relation between quantized charges and moduli in almost-BPS solutions

#### Mapping BPS to non-BPS solutions

There are two ways to turn an almost-BPS solution into a BPS one. The first is to set the Taub-NUT charge, $q$, to zero (and obtain black strings and supertubes extended along the $S^1$ of $\mathbb{R}^3 \times S^1$), and the second is to set the constant, $h$, in the Taub-NUT harmonic function equal to zero. In the first limit ($q = 0$), the charge shifts automatically vanish, consistent with the result of [124].

However, for $h = 0$, the shift does not vanish and this may seem a little puzzling. To understand the origin of the shift we should remember that, in the $h = 0$ limit, the BPS and the almost-BPS solutions are identical up to the coordinate transformation (5.37). Hence, a supertube wrapping the $\psi$-fiber once in the almost-BPS solution and a supertube wrapping the $\psi$-fiber once in the BPS writing of the same solution wrap different circles. Indeed, the supertube that wraps the $\psi$-fiber once in the almost-BPS solution has $(\nu_\psi, \nu_\phi) = (1, 0)$. Then the transformation (5.37) means that in the BPS writing of the solution this object is a supertube that wraps the $\phi$-fiber $\frac{1}{q}$ times, and hence it has $(\nu_\psi, \nu_\phi) = (0, \frac{1}{q})$.

Clearly two supertubes with different windings are not the same object, and the only way their radius relations can be the same is if their charges are different. To be more precise, when $h = 0$, (5.43) reduces to:

$$\mathcal{B}_+^{(I)}(\nu_\psi, \nu_\phi) \;=\; \frac{k_I^+}{q\,(a_3 - a_I)}\,[\nu_\psi\, a_3 + \nu_\phi\, q\, a_I] \;=\; \frac{k_I^+\,(\nu_\psi + q\,\nu_\phi)\,a_3}{q\,(a_3 - a_I)} \;-\; k_I^+\,\nu_\phi\,, \tag{5.52}$$

where we have used (5.13). The first term is identical for either choice of winding numbers: $(\nu_\psi, \nu_\phi) = (1, 0)$ and $(\nu_\psi, \nu_\phi) = (0, \frac{1}{q})$, and this makes sense because, for either choice, the Taub-NUT fiber is being wrapped once. However, the last term is different, which indicates that the almost-BPS supertube also wraps the Dirac string of the background magnetic flux. Hence, if the supertubes with $(\nu_\psi, \nu_\phi) = (1, 0)$ and $(\nu_\psi, \nu_\phi) = (0, \frac{1}{q})$ are to have the same radius their charges must be related by a shift. Using the charge identification $k_I^+ \to \widehat{k}_I$ in (5.37) and using (5.18) for $h = 0$, one sees that this charge shift is simply:

$$\widehat{Q}^{(1)}_{(1,0)} \;=\; \widehat{Q}^{(1)}_{(0,\frac{1}{q})} \;-\; \frac{d_3\,\widehat{k}_2}{q}\,, \qquad \widehat{Q}^{(2)}_{(1,0)} \;=\; \widehat{Q}^{(2)}_{(0,\frac{1}{q})} \;-\; \frac{d_3\,\widehat{k}_1}{q}\,. \tag{5.53}$$

which exactly matches the shift in (5.49) for $h = 0$. Hence the shift between the almost-BPS Supergravity charge and the almost-BPS quantized charge is the same as the shift from the BPS quantized charge to the almost-BPS quantized charge. This implies that the BPS quantized and Supergravity charges are the same as the almost-BPS Supergravity charge.

Another way to understand this result is to remember that one can consider a solution with a probe supertube of a certain charge wrapping a Dirac string, and take away the Dirac string by a large gauge transformation. As explained in [124], this changes the charges of the supertube. If one does this in our situation, and takes the Dirac string away from the location of the probe supertube, both the BPS and the almost-BPS supertubes will have the same charge and wrapping and will become the same object. Clearly, upon backreaction the Supergravity charges of the two will be the same. Hence, the reason why the quantized charge of the almost-BPS supertube is shifted from its Supergravity charge is because, when written as a probe in $\mathbb{R}^4$, this supertube wraps a Dirac string non-trivially.

Note that when $h = 0$ this shift involves only integers, but for a generic almost-BPS solution this shift depends also on the moduli. As we will explain in Subsection 5.4.3 this happens because almost-BPS solutions have an additional magnetic flux on the non-compact cycle extending to infinity.

**A puzzle about charges and its resolution**

Once one understands how the quantized charges of the centers of an almost-BPS solution are related to the Supergravity charge parameters one can re-examine the problem of moduli-dependence of the asymptotic charge of almost-BPS solutions. Recall that for a BPS solution in Taub-NUT the warp factors go asymptotically like

$$\begin{aligned} Z^{(1)} \;\sim\; \left[Q_2^{(1)} + Q_3^{(1)}\right]\frac{1}{r}\,, \qquad Z^{(2)} \;\sim\; \left[Q_1^{(2)} + Q_3^{(2)}\right]\frac{1}{r} \quad , \\ Z^{(3)} \;\sim\; \left[Q_1^{(3)} + Q_2^{(3)}\right]\frac{1}{r}\,, \end{aligned} \tag{5.54}$$

which confirms the fact that the asymptotic charges are simply the sum of the quantized charges of the individual component supertubes. However, for an almost-BPS solution one has

$$\begin{aligned} Z^{(1)} \;\sim\; \left[Q_2^{(1)} + Q_3^{(1)} + \tfrac{q\,\widehat{k}_2\,\widehat{k}_3}{a_2\,a_3 V_2 V_3}\right]\frac{1}{r}\,, \qquad Z^{(2)} \;\sim\; \left[Q_1^{(2)} + Q_3^{(2)} + \frac{q\,\widehat{k}_1\,\widehat{k}_3}{a_1\,a_3 V_1 V_3}\right]\frac{1}{r} \quad , \\ Z^{(3)} \;\sim\; \left[Q_1^{(3)} + Q_2^{(3)} + \tfrac{q\,\widehat{k}_1\,\widehat{k}_2}{a_1\,a_2 V_1 V_2}\right]\frac{1}{r}\,. \end{aligned} \tag{5.55}$$

This appears to imply that if one changes the moduli of a solution continuously, while keeping the charges of the centers fixed, the asymptotic charges will change continuously. If this were true, an almost-BPS solution would have non-quantized asymptotic charges for generic values of the moduli, and would only exist on certain submanifolds of the moduli space where the asymptotic charges are integer. Needless to say, this would be rather peculiar.

Our results show that this does not, in fact, happen. If one expresses the Supergravity charge in terms of quantized charges, the moduli-dependent term drops out and the asymptotics become identical to the one in (5.54). Hence, the asymptotic charges of almost-BPS solutions are also

equal to the sum of the quantized charges of the centers, and the quantization of charges does not restrict the the moduli space of supertube locations.

To see this we can make the following Gedankenexperiment: we start with a single supertube of species $I = 1$ at position $a_1$, for which the Supergravity charges are the same as the quantized charges

$$Q_1^{(2)} = \widehat{Q}_1^{(2)}\,, \qquad Q_1^{(3)} = \widehat{Q}_1^{(3)}\,. \tag{5.56}$$

We then bring in a second supertube of species $I = 2$ at position $a_2$. The Supergravity charge $Q_2^{(3)}$ of this supertubes is shifted from its quantized charge $\widehat{Q}_2^{(3)}$ because of the presence of the first supertube, while its other charge remains the same:

$$Q_2^{(1)} = \widehat{Q}_2^{(1)}\,, \qquad Q_2^{(3)} = \widehat{Q}_2^{(3)} - \frac{q\widehat{k}_1^{(1)}\widehat{k}_2^{(2)}}{a_1 a_2 V_1 V_2}\,, \tag{5.57}$$

The asymptotic charges $\widehat{\mathcal{Q}}_{12}^{(I)}$ of the resulting solution are given by the (sum of the) quantized charges, $\widehat{\mathcal{Q}}_{12}^{(1)} = \widehat{Q}_2^{(1)} = Q_2^{(1)}$, $\widehat{\mathcal{Q}}_{12}^{(2)} = \widehat{Q}_1^{(2)} = Q_1^{(2)}$ and

$$\widehat{\mathcal{Q}}_{12}^{(3)} = \widehat{Q}_1^{(3)} + \widehat{Q}_2^{(3)} = Q_1^{(3)} + Q_2^{(3)} + \frac{q\widehat{k}_1^{(1)}\widehat{k}_2^{(2)}}{a_1 a_2 V_1 V_2}\,, \tag{5.58}$$

which agrees with the coefficient of $r^{-1}$ in $Z^{(3)}$ in (5.55). After backreacting the second supertube we bring in a third supertube of species $I = 3$ at position $a_3$ whose Supergravity charges after backreaction are shifted with respect to their quantized charges

$$Q_3^{(1)} = \widehat{Q}_3^{(1)} - \frac{q\widehat{k}_2^{(2)}\widehat{k}_3^{(3)}}{a_2 a_3 V_2 V_3}\,, \qquad Q_3^{(2)} = \widehat{Q}_3^{(2)} - \frac{q\widehat{k}_1^{(1)}\widehat{k}_3^{(3)}}{a_1 a_2 V_1 V_2}\,, \tag{5.59}$$

because of the other supertubes. The asymptotic charges $\widehat{\mathcal{Q}}_{123}^{(I)}$ of the solution with all three supertubes backreacted are $\widehat{\mathcal{Q}}_{123}^{(3)} = \widehat{\mathcal{Q}}_{12}^{(3)} \sim r\ Z^{(3)}$ and

$$\widehat{\mathcal{Q}}_{123}^{(1)} = \widehat{\mathcal{Q}}_{12}^{(1)} + \widehat{Q}_3^{(1)} = Q_2^{(1)} + Q_3^{(1)} + \frac{q\widehat{k}_2^{(2)}\widehat{k}_3^{(3)}}{a_2 a_3 V_2 V_3} \sim r\ Z^{(1)}\,, \tag{5.60}$$

$$\widehat{\mathcal{Q}}_{123}^{(2)} = \widehat{\mathcal{Q}}_{12}^{(2)} + \widehat{Q}_3^{(2)} = Q_1^{(2)} + Q_3^{(2)} + \frac{q\widehat{k}_1^{(1)}\widehat{k}_3^{(3)}}{a_1 a_3 V_1 V_3} \sim r\ Z^{(2)}\,. \tag{5.61}$$

As advertised, these charges match the coefficients of $r^{-1}$ in the $Z^{(I)}$. Hence, while the shift between the quantized and Supergravity charges might have seemed surprising at first, it represents the missing ingredient necessary to relate the asymptotic charge of a multi-center solution to those of the centers.

One can also use these equations to determine the shift between the quantized and Supergravity charges for an almost-BPS black ring in Taub-NUT [39]. Although black rings have no DBI description, one can make a black ring by bringing together three supertubes with three different types of dipole charges. Since in this process both the Supergravity and the quantized charges are preserved, the shifts of the black ring charges will be the shifts of the charges of

the composing supertubes. For a Taub-NUT almost-BPS black ring with dipole charges $\widehat{k}^{(I)}$ at position $a_1$ these shifts are:

$$Q^{(I)} = \widehat{Q}^{(I)} - |\epsilon_{IJK}| \frac{q\widehat{k}^{(J)}\widehat{k}^{(K)}}{a_1^2 V_1^2}\,, \tag{5.62}$$

where capital Latin indices are not summed. Note that there are $n!$ ways of making a black ring starting with $n$ supertubes, corresponding to the different relative orderings of these supertubes, and for each ordering the charge shifts of various supertubes are different, but the sum of all these charge shifts (which gives the black ring charge shift) is always the same.

We are now ready to further use this result and the iterative procedure outlined above in order to unambiguously determine the relation of the Supergravity charge parameters and the quantized charges in a solution with an arbitrary number of centers.

### 5.3.4 Generalization to many supertubes

We can generalize the calculation in the previous Section to an almost-BPS solution containing an arbitrary number of collinear supertubes. Without loss of generality we consider a solution containing $i-1$ supertubes at positions

$$0 < a_1 < a_2 < ..... < a_{i-1}\,, \tag{5.63}$$

and we bring a probe supertube of species $I$ (wrapping the tori $T^2_J$ and $T^2_K$ in (5.1)) to the point $a_i$ on the z-axis, at the outermost position with respect to the other supertubes ($a_i > a_{i-1}$). This probe has electric charges $\widehat{Q}_i^{(J)}$, $\widehat{Q}_i^{(K)}$ and dipole charge $d_i^{(I)}$. Starting from the radius relation:

$$\left[\widehat{Q}_i^{(J)} + d_i^{(I)}\mathcal{B}_i^{(K)}\right]\left[\widehat{Q}_i^{(K)} + d_i^{(I)}\mathcal{B}_i^{(J)}\right] = (d_i^{(I)})^2 \frac{Z_i^{(I)}}{V_i} \tag{5.64}$$

with

$$\mathcal{B}_i^{(L)} = \mathcal{B}_-^{(L)}(r=a_i) = \sum_l \frac{k_l^{-(L)}}{|a_l - a_i|} = \sum_l \frac{\widehat{k}_l^{(L)}}{|a_l - a_i|\, V_l} \quad , \qquad V_i = h + \frac{q}{a_i}\,, \tag{5.65}$$

and

$$Z_i^{(I)} = Z^{(I)}(r=a_i) = 1 + \sum_j \frac{Q_j^{(I)}}{|a_i - a_j|} + |\epsilon_{IJK}| \sum_{j,k}\left(h + \frac{qa_i}{a_j a_k}\right)\frac{k_j^{-(J)}k_k^{-(K)}}{|a_i - a_j||a_i - a_k|}\,, \tag{5.66}$$

we obtain the shift of charges by matching this relation to the bubble equation for the backreacted probe center (that can be derived from the results of [37]):

$$\begin{aligned}\Big\{\sum_j \frac{1}{|a_i - a_j|}\left[d_i^{(I)}Q_j^{(I)} - \widehat{k}_j^{(J)}Q_i^{(J)}\right] + \sum_k \frac{1}{|a_i - a_k|}\left[d_i^{(I)}Q_k^{(I)} - \widehat{k}_k^{(K)}Q_i^{(K)}\right]\Big\} \\ = \frac{Q_i^{(J)}Q_i^{(K)}}{d_i^{(I)}}\left(h + \frac{q}{a_i}\right) - d_i^{(I)} - |\epsilon_{IJK}| \frac{hqd_i^{(I)}}{a_i\left(h + \frac{q}{a_i}\right)} \sum_{j,k}\epsilon_{ijk}\frac{k_j^{-(J)}k_k^{-(K)}}{a_j a_k}\,,\end{aligned} \tag{5.67}$$

where there is no summation over capital Latin indices [6]. We find that, upon identifying $d_i^{(I)} = \widehat{k}_i^{(I)} = k_i^{-(I)} V_i$, the shift between the Supergravity charge parameters of the supertube and its quantized charges are

$$Q_i^{(J)} = \widehat{Q}_i^{(J)} - |\epsilon_{JKI}| \sum_k \frac{q \widehat{k}_k^{(K)} \widehat{k}_i^{(I)}}{a_k a_i V_k V_i} \tag{5.68}$$

and similarly for $Q_i^{(K)}$, where there is no summation over capital Latin indices. In equations (5.67)–(5.68) the indices $j, k$ run over the positions of supertubes of species $J, K$ respectively.

One can now use this formula and find the charge shifts for all the centers of a certain solution, by constructing it recursively by bringing in probe supertubes. From the previous analysis it is clear that the relation between the Supergravity and the quantized charges of a given center in the interior of the solution does not change as one brings more and more supertubes at the outermost positions. Hence, the shifts of the charges of a given supertube center only depend on the locations and dipole charges of the centers that are between this supertube center and the Taub-NUT center, but not on the locations or charges of the centers at its exterior:

$$Q_i^{(J)} = \widehat{Q}_i^{(J)} - |\epsilon_{JKI}| \sum_{k<i} \frac{q \widehat{k}_k^{(K)} \widehat{k}_i^{(I)}}{a_k a_i V_k V_i}. \tag{5.69}$$

It is not hard to see that the asymptotic charge of the solution (which can be read off from the asymptotics of $Z^{(I)}$) is now the sum of the quantized charges of all the centers

$$\widehat{\mathcal{Q}}_\infty^{(I)} = \sum_j Q_j^{(I)} + |\epsilon_{IJK}| \sum_{j,k} \frac{q \widehat{k}_j^{(J)} \widehat{k}_k^{(K)}}{a_j a_k V_j V_k} = \sum_i \widehat{Q}_i^{(I)}. \tag{5.70}$$

One can also extend this calculation to describe a configuration containing an arbitrary collection of concentric supertubes and black rings, by constructing the black rings from three different species of supertubes. The general formula relating the Supergravity charge parameters to the quantized charges is

$$Q_i^{(J)} = \widehat{Q}_i^{(J)} - |\epsilon_{JKI}| \sum_{k<i} \frac{q \widehat{k}_k^{(K)} \widehat{k}_i^{(I)}}{a_k a_i V_k V_i} - |\epsilon_{JKI}| \frac{q \widehat{k}_i^{(K)} \widehat{k}_i^{(I)}}{a_i^2 V_i^2}, \tag{5.71}$$

where once again the capital Latin indices are not being summed.

## 5.4 Extracting the complete Supergravity data from supertubes

We have seen that if one considers an axially-symmetric brane configuration and brings in a brane probe along the axis from one side of the configuration then the radius relation of that

[6] Note that the terms involving $|\epsilon_{IJK}|$ in $Z^{(I)}$ and the bubble equation (5.67) differ by a factor 1/2 from the usual form (see, for example, [37]) where *there is* summation over $I, J, K$.

probe exactly reproduces the bubble equation for the charge center that would replace the brane probe in a fully backreacted Supergravity configuration. This correspondence requires the charge shifts described in Section 5.3. Since we are considering only the action of the probe, there is no immediate way in which this action could directly yield the fully backreacted bubble equations for the other centers in response to the probe. That is, given the $n$-supertube solution, the probe radius relation for the $(n+1)^{\text{st}}$ supertube yields the exact Supergravity bubble equation for that supertube. However, when backreacted, the probe supertube must introduce modifications to the bubble equations for the other supertubes and these are not given directly by the computations described above.

In contrast, the analysis of brane probes in BPS solutions [124] required no charge shifts and the bubble equations contained only two-body interactions of the form $\Gamma_{ij}|\vec{y}_i - \vec{y}_j|^{-1}$ as in (5.27)–(5.30). In that solution, the action of the probe was used to read off all the two-by-two terms between the probe and the centers, and thus derive the bubble equations for *all* the centers. However, for almost-BPS solutions the bubble equations for a certain center contain complicated three-body terms, which cannot be read off from the action describing the location of another center. However, there is still a (more complicated) way to recover the full Supergravity data from DBI actions: given a solution with $(n+1)$ supertubes one can examine all the ways of extracting one supertube and treating it is a probe in the background sourced by the others. As we will show below, this yields all the bubble equations of the solution.

### 5.4.1 Reconstructing the bubble equations from probes

For non-BPS supertubes there are three elements for the inductive modification of the bubble equations as one goes from $n$ to $(n+1)$ supertubes:

(i) Compute the charge shifts of all probe charges.

(ii) Write the left-hand sides of the bubble equations with all two-body interactions, $\Gamma_{ij}|a_i - a_j|^{-1}$.

(iii) Compute and include all the supersymmetry breaking terms, $Y$, as in (5.34) and include them with the correct relative sign on the right-hand sides of the bubble equations as in (5.31)–(5.33).

If one assembles the configuration by bringing in the charges successively along the symmetry axis from the right then the charge shifts are given by (5.68). The two-body interactions are fixed iteratively exactly as in the BPS solution. These terms are also fixed by the consistency condition that the sum of all the bubble equations must be identically zero. The new feature is that we need to specify the algorithm for (iii): We need to generalize the supersymmetry breaking terms and how they are to be included in the bubble equations. It is clear that the bubble equation for a supertube of type $I$ will have an interaction, $Y$, of the form (5.34) with every pair of supertubes of species $J, K$ where $I, J$ and $K$ are all distinct. The issue is to introduce these terms with the correct signs in each bubble equation. One can do this by making the more formal induction using all the ways of extracting one supertube and treating it is a probe. However, for simplicity, we will start by restricting our attention to configurations in which the probe is always the outermost supertube. As we will see in the next Section, the charge shifts are modified when

the probe is some other supertube in the configuration and so the discussion is a little more complicated. We will begin by completing the discussion of Subsection 5.3.4 by giving a recipe for the supersymmetry breaking terms when the probe is the outermost supertube and we will explain its derivation below.

Suppose we have an $n$-supertube system and we bring in, as a probe, a supertube of species $I$ then the bubble equations for a center of type $J$ at position $a_j$ must include an extra supersymmetry breaking term, $Y^{(J,I)}_{j,(n+1)}$, that is to be subtracted from the right-hand side. These terms are given by:

$$\begin{aligned} Y^{(J,I)}_{j,(n+1)} &= |\epsilon_{IJK}| \sum_k \frac{(a_j - a_{n+1})\,(a_j - a_k)}{|a_j - a_{n+1}||a_j - a_k|} \frac{hqd^{(I)}_{n+1}\hat{k}^{(J)}_j \hat{k}^{(K)}_k}{a_{n+1}a_j a_k V_{n+1}V_j V_k} = \\ &= -|\epsilon_{IJK}| \sum_k \frac{(a_j - a_k)}{|a_j - a_k|} \frac{hqd^{(I)}_{n+1}\hat{k}^{(J)}_j \hat{k}^{(K)}_k}{a_{n+1}a_j a_k V_{n+1}V_j V_k} \end{aligned} \tag{5.72}$$

where, for fixed $I$ and $J$, the summation over $k$ runs only over supertubes of species $K$, with $I, J, K$ all distinct. In the last equality we used that $a_{n+1} > a_j$ for $j = 1, 2, ..., n$. Thus, as we assemble the system by successively bringing supertubes from the right, for every new supertube added we have to subtract (5.72) from the right hand side of the bubble equations of the previously backreacted system.

### 5.4.2 Assembling collinear supertubes in general

The general bubble equations (5.67) for a system of $n$ collinear supertubes contain supersymmetry breaking terms, $Y$, that come with a relative sign given by by $\epsilon_{ijk}$ defined in (5.35) [7]. In the procedure discussed in Section 3, we always had $\epsilon_{ijk} = +1$ since the probe was always being placed in the outermost position of the backreacted geometry. However, if the probe is of species $I$ and located at a general position, $a_i$, then we find that its radius relation can be mapped directly onto is Supergravity bubble equation if one uses the following more general relation between Supergravity and quantized brane charges:

$$Q^{(J)}_i = \widehat{Q}^{(J)}_i - |\epsilon_{JKI}| \sum_k \frac{a_i - a_k}{|a_i - a_k|} \frac{q\widehat{k}^{(K)}_k \widehat{k}^{(I)}_i}{a_k a_i V_k V_i}\,, \tag{5.73}$$

where, once again, the capital Latin indices are not being summed and the sum over $k$ runs over supertubes of species $K$. Thus for $a_i > a_k$ the shift terms get subtracted from the quantized charge as before, but for $a_i < a_k$ the shift terms have to be added! We also find that if one uses the more general shifts in (5.73) then the radius relation exactly reproduces the correct supersymmetry breaking terms, Y, in the bubble equations.

As a result, by using (5.73), we can recreate the whole set of bubble equations of the system by the following iterative procedure. Consider a $(n+1)$-supertube system with preassigned order

$$0 < a_1 < a_2 < ..... < a_{n-1} < a_{n+1}\,. \tag{5.74}$$

[7] This $\epsilon_{ijk}$ should not be confused with the factors of $|\epsilon_{IJK}|$ that give the triple intersection number of the dipole charges.

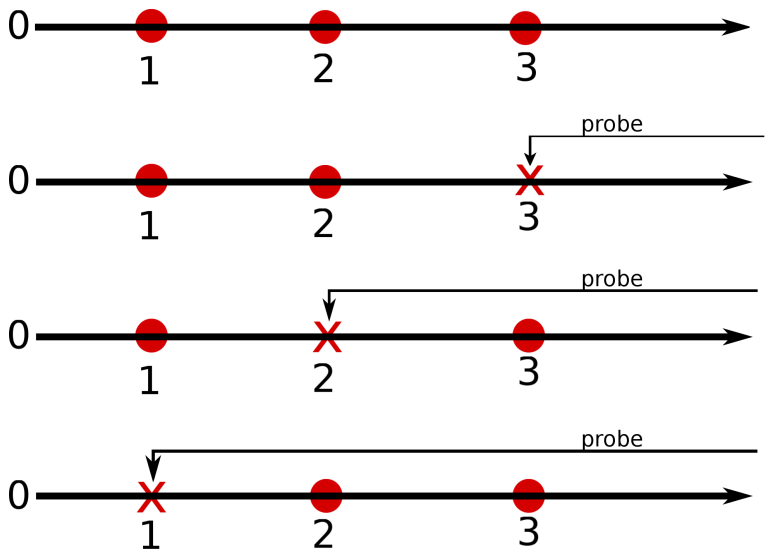


Figure 5.1: The first graph represents the three-supertube backreacted geometry while the three below represent the iterative procedure by which one removes each center of the system and treats it as a probe in the background of the remaining two Supergravity supertubes. Because supertubes cross over each other we need the formula (5.73) to generate the shift with the correct sign.

Now consider each supertube, in turn, as a probe in the Supergravity background of the remaining $n$ and imagine placing the probe in its assigned position, (5.74), to recreate the full $(n+1)$-supertube system. To be more explicit, start by taking the supertube at $a_{n+1}$ out of the Supergravity system and treat it as a probe being placed at position $a_{n+1}$. This generates the bubble equation for the center at $a_{n+1}$ as described earlier. Next, imagine the Supergravity system where the supertube at position $a_n$ has been removed and replaced by a probe placed at position $a_n$. The radius relation of this probe produces exactly the bubble equation for the center at $a_n$ provided one uses the charge shifts defined in (5.73). One can then repeat this iterative procedure (illustrated in Figure 5.1) for each of the $n+1$ centers of the system.

As we noted earlier, for a probe of species $I$, the bubble equations for the center of type $J$ will involve a supersymmetry breaking term, $Y^{(J,I)}_{j,(n+1)}$, that is a sum over all centers of species $K$ (with $I, J, K$ distinct). The importance of this general iterative procedure is that it generates all these terms in the bubble equations in exactly the correct form and yields the formula (5.72) for a general position, $a_i$, of the probe:

$$Y^{(J,I)}_{j,i} \;=\; |\epsilon_{IJK}| \sum_k \frac{(a_j - a_i)\,(a_j - a_k)}{|a_j - a_i||a_j - a_k|} \frac{hqd^{(I)}_{n+1}\hat{k}^{(J)}_j \hat{k}^{(K)}_k}{a_{n+1}a_j a_k V_{n+1} V_j V_k}\,. \tag{5.75}$$

### 5.4.3 Topology, charge shifts and backreacting probes

To understand the charge shifts and their dependence on the location of the supertubes it is important to recall the geometric structure underlying the almost-BPS Supergravity solutions.

In an appropriate duality frame [8] a solution containing multiple supertubes becomes smooth, and all the charges come from fluxes wrapping topologically non-trivial cycles. These cycles can be described in terms of $U(1)$ fibers over paths that end at the locations of the supertubes. The supertube locations are precisely where one of the $U(1)$ fibers pinches off and this, in turn, defines cycles and their intersections. The magnetic dipole charges of the supertube then correspond to cohomological fluxes through these cycles. Hence, in this particular duality frame the backreaction of a supertube corresponds to blowing up a new cycle and replacing a singular magnetic source with a cohomological flux. If one starts out with a particular Supergravity solution and makes a particular choice of homology basis, then introducing a new supertube and backreacting it will involve blowing up a new cycle and perhaps pinching off other cycles in order to achieve this. Hence, this will involve generically a reshuffling of the homology basis.

The presence of the Chern-Simons term in the electromagnetic action means that the interaction of pairs of magnetic charges can source electric charges and so the change of homology basis arising from the backreaction of a supertube can lead to shifts of electric charges. Because the magnetic charges on the compact cycles are quantized and the magnetic contributions to electric charges are determined though the intersection form, one would expect all charge shifts to be quantized. This is, indeed, precisely what one finds in all the BPS solutions: the shifts, if they are non-zero, are indeed quantized. What distinguishes the non-BPS solutions is that there is a non-vanishing, normalizable flux on a non-compact cycle that extends to infinity and this flux depends upon the Supergravity parameters and moduli. It is the interactions between the fluxes on this non-compact cycle that leads to moduli-dependence of the shifts.

One can recast this geometric picture in more physical terms through a careful examination of Dirac strings. Because a Supergravity supertube carries a magnetic charge, the supertube comes with Dirac strings attached (these are, of course, an artifact of trying to write a vector potential for a topologically non-trivial flux). A supertube wraps a $U(1)$ fiber in the background and to define its configuration properly one must specify precisely which Dirac strings are being wrapped by the supertube. This defines the dipole-dipole interaction between the probe and the background [9] and the difference between wrapping and not wrapping will appear as a shift of the electric charges that it contributes to the Supergravity solution.

If the supertubes are all collinear then one can choose all the Dirac strings to follow the axis of symmetry out to infinity. One can then set up a configuration in which an outermost probe supertube wraps the Dirac strings of all the other supertubes, and hence its charges get shifted. On the other hand the tubes at the interior of this configuration will not feel the Dirac string of the outermost supertube, and hence the relationship between their Supergravity charge and their quantized charge does not shift. In the duality frame where the multi-supertube solution is smooth, this corresponds to blowing up a homology cycle at the outer edge of the original configuration.

If one were to place the probe supertube so that it is the closest to the Taub-NUT center, its Dirac string would generically affect all the other supertubes, and would change the relation between quantized and Supergravity charges. This corresponds to blowing up a different new

[8] This can be realized by performing three generalized spectral flows on almost-BPS solutions [42].

[9] This wrapping choice determines the new homology element and its intersections with other other elements of homology.

homology element and reshuffling the homology basis. Hence, if one keeps the Supergravity charges of the backreacting supertubes fixed, as one must do in a probe approximation, bringing a supertube to a point that is closer to the center of Taub-NUT than the other supertubes will change the quantized charges of these supertubes. Thus, the resulting configuration will not have the same quantized charges on the centers as when the supertube is at the outermost location, and hence belongs to different sector of the multi-centered solutions. There are, of course, similar consequences to bringing the probe supertube to some point in the middle of the backreacted supertube centers.

One can also take a more pragmatic perspective and try to understand the charge shifts by compactifying the multi-supertube solutions to obtain a multi-center almost-BPS solution in four dimensions. The five-dimensional, smooth solutions we discuss here are singular at the supertube centers in four dimensions, but this does not impede the calculation of the conserved charges at the singularities. As explained in [202], these conserved charges differ in general from the Supergravity charge parameters by dipole-dipole position-dependent shifts similar to the ones found here, and it would be interesting to see whether one can reproduce our results using the four-dimensional KK reduction formulae of [202] (starting, for example, from equation (266) on page 55).

### 5.4.4 Quantized charges, Supergravity parameters and probes

As we have seen in the previous Section, bringing a supertube to some point in the middle of a multi-center supertube solution changes the relation between the quantized charges and the Supergravity parameters of the supertube centers at its exterior. Hence, all the probe calculations that describe supertubes at interior locations in a multi-center solution are not self-consistent, because the quantized charges of the other centers before bringing in the probe are not the same as the quantized charges with the probe inside. One can think of this as coming from the fact that all probe supertubes come with Dirac strings attached, and when these Dirac strings touch the other centers, the relation between the Supergravity and quantized charges of these centers change. Thus, the only probe supertube that one can bring without shifting everybody else's quantized charges is one that lays at the outermost position and whose Dirac string extends away from the supertubes and towards infinity.

An immediate corollary of this is that if one wants to calculate the amplitude for a supertube to tunnel to a vacuum across another center, this calculation cannot be done using the DBI action of that supertube and treating it as a probe in a fixed Supergravity background. Instead one would have to change the solution as the probe moves around, and this cannot be done off-shell. One can wonder whether there exists *any* way to compute this tunneling amplitude. Again, the correct probe for this would be a supertube *with Dirac strings attached*, such that one would change the Supergravity charges of the backreacted solution as one moves the probe around, in such a way that the quantized charges stay the same. Unfortunately, there is no known action for such a probe, so probing the interior of a multi-supertube solution with a probe supertube does not correspond to a physical process. Hence, the calculation we performed in Subsection 5.4.2, where we took the Supergravity parameters to be fixed and treated the background of $n$ supertubes merely as one would treat any other Supergravity background ignoring the details of how it might have been assembled from other supertubes, should be interpreted as a formal

calculation, which does not correspond to a physical process, but which does however reproduce the bubble equations of all the interior supertube centers. It would be clearly interesting to understand the reason for this.

It is also important to stress out that this charge shift subtlety only affects the validity of the probe calculation when the other centers are supertubes or black rings, that interact directly with the Dirac string of the probe. If the other centers are bubbled Gibbons-Hawking centers, where the geometry is smooth, the presence of a Dirac string does not change their four-dimensional charge parameters nor the fluxes wrapping the corresponding cycle in the five-dimensional solution. Hence, one can use the probe supertube action of Chapter 3 to calculate tunneling probabilities of metastable supertubes in bubbling geometries. Similarly, the description of multi-center non-BPS solutions using supergoop methods [191], being intrinsically non-gravitational, is not affected by this subtlety.

## 5.5 Discussion of the results

We have shown that a brane probe in an almost-BPS background of supertubes can capture the complete Supergravity data of the background in which the probe becomes a fully backreacted source. A similar result was established for BPS solutions in [124] but it is rather surprising that this can also be achieved for almost-BPS solutions in which the supersymmetry is broken, albeit in a rather mild manner. It is surprising because going from a probe to a backreacted Supergravity solution represents going from weak to strong coupling in the field theory on the brane and when supersymmetry is broken one would expect the parameters of this field theory to be renormalized. Our result therefore suggests that, even though supersymmetry is broken, the couplings of the field theory that govern the probe location are still protected. This does not mean that the theory is unchanged relative to its BPS counterpart: there are terms in the probe action that come from the supersymmetry breaking and these exactly reproduce the corresponding terms found in the Supergravity solution.

We suspect that the non-renormalization of the relevant parts of the probe action arises from the rather special form of the supersymmetry breaking: the probe is supersymmetric with respect to every other center in the Supergravity solution taken individually and the supersymmetry breaking arises from the fact that these supersymmetries are incompatible between multiple centers. Indeed the supersymmetry breaking terms depend on the product of the charges and dipole charges of three or more centers, and do not have the 'two-body' structure of the terms that appears in the BPS bubble equations. It would be interesting to try to extend our analysis to the other known class of non-BPS extremal multi-center solutions, the interacting non-BPS black holes [44, 203], and see if the bubble equations of these solutions are also not renormalized when one goes from weak to strong effective coupling.

One of the new features of our analysis is that the Supergravity charge parameters and the quantized charges of the supertubes need to be shifted relative to one another in order to match the Supergravity bubble equations and the probe radius relations. By taking a flat-space limit, we saw that part of this difference was related to the choice of how the supertube wraps Dirac strings, or equivalently, how the cycle is blown up after backreaction. This accounts for a quantized shift but in a Taub-NUT background the shift is no longer obviously quantized because

it depends upon moduli. Quantized shifts have also been encountered and understood in the study of black rings [204, 205, 124] but it would be very nice to understand how to extract the quantized charges, and hence the more general moduli-dependent shifts, via a pure Supergravity calculation. A good starting point may be to use the four-dimensional reduction formulas of [202] as well as a judicious accounting of the integer charge shifts caused by Dirac string, to try to reproduce the shifts we find.

Our results also suggest further interesting Supergravity calculations. For rather mysterious reasons, explicit solutions of the almost-BPS equations still elude us for non-axisymmetric configurations. Such solutions are extremely simple in the BPS system but for the almost-BPS system even the three-centered, non-axisymmetric solution is not known. The most one could get is an implicit solution in terms of integrals that one can evaluate asymptotically [202]. Finding the three-centered solution is particularly important because one can then use this solution and the methods of [37] to generate the general, non-axisymmetric, multi-centered solutions. A two-centered solution is, of course, trivially axi-symmetric and it is easy to introduce a probe in any location. It would therefore be very interesting to see if such a probe could be used to gain insight into the structure of the full Supergravity solution.

Given that our results suggest that there are non-renormalization theorems that protect the bubble equations of almost-BPS multi-center solutions, it would be extremely interesting to investigate whether almost-BPS solutions could be described in the regime of parameters where none of the centers is backreacted, using a suitable generalization of quiver Quantum Mechanics of [110]. Clearly, this generalization will have to account for the supersymmetry-breaking terms, which is highly non-trivial: these terms involve three- and four-center interactions, and at first glance no theory of strings on multiple D-branes appears capable of producing such a term. It would be very nice to understand how the charge shifts and supersymmetry breaking terms emerge from the field theory on the branes and whether the effective number of hypermultiplets may be different from the number of hypermultiplets appearing in the Lagrangian. This could be the effect of some of these hypermultiplets becoming massive and no longer contributing to the low energy dynamics. It is thus not too difficult to imagine that our results might be derivable from a field theory analysis and we intend to investigate this further in the future.

# Appendix A

# Conventions

We summarize here the conventions we use in this Thesis. We follow the conventions of [85]. See [87, 53] for more details.

### Black hole asymptotics

The mass $M$, charge $Q$ and angular momentum $J$ of a black hole in $D$ spacetime dimensions can be read off from the asymptotic expansions

$$-g_{tt} = 1 - \frac{16\pi G_N^{(D)}}{(D-2)A_{D-2}} \frac{M}{r^{D-3}} + \dots , \tag{A.1}$$

$$g_{ti} = \frac{16\pi G_N^{(D)}}{A_{D-2}} \frac{x^j J^{ji}}{r^{D-1}} + \dots , \tag{A.2}$$

$$F_{tr} = (D-3)\frac{Q}{r^{D-2}} , \tag{A.3}$$

where $r$ is the radial coordinate and $A_{D-2}$ is the area of the $(D-2)$-sphere. For $D = 4$ and the convention $G_N^{(4)} = 1$ we recover from (A.1)-(A.3) the mass, charge and angular momentum for Schwarzschild, Reissner-Nordström and Kerr as given in Section 1.1. For $D = 5$ and the convention $G_N^{(5)} = \frac{\pi}{4}$ we recover the mass and charge of the five-dimensional Reissner-Nordström black hole as given in Section 1.3.

### Planck and Newton

The Planck length in $D$ dimensions, $l_P^{(D)}$, is defined by

$$16\pi G_N^{(D)} \equiv (2\pi)^{D-3} (l_P^{(D)})^{D-2} . \tag{A.4}$$

In particular, in eleven dimensions we have

$$16\pi G_N^{(11)} \equiv (2\pi)^8 (l_P^{(11)})^9 . \tag{A.5}$$

Any lower-dimensional Newton constant can be related to the eleven-dimensional one by

$$G_N^{(D)} = \frac{G_N^{(11)}}{(2\pi)^{11-D} V_{11-D}}\,, \tag{A.6}$$

where $V_{11-D}$ is the volume of the internal compactification manifold. In particular, for $D = 5$ we get

$$G_N^{(5)} = \frac{G_N^{(11)}}{(2\pi)^6 V_6} = \frac{\pi}{4}\frac{(l_P^{(11)})^9}{V_6}\,. \tag{A.7}$$

The convention $G_N^{(5)} = \frac{\pi}{4}$ thus corresponds to fixing the size of the internal six-manifold $V_6 = (l_P^{(11)})^9$.

**Strings and branes**

We summarize the tension of fundamental strings, D$p$-branes and NS5 branes:

$$T_{\mathrm{F1}} = \frac{1}{2\pi\alpha'} \equiv \frac{1}{2\pi l_s^2}\,, \qquad T_{\mathrm{D}p} = \frac{1}{g_s(2\pi)^p l_s^{p+1}}\,, \qquad T_{\mathrm{NS5}} = \frac{1}{g_s^2(2\pi)^5 l_s^6}\,. \tag{A.8}$$

F1 strings and D4 branes correspond, respectively, to M2 branes and M5 branes wrapping the M-theory circle with radius $R_\# = l_s g_s$ and whose tension is

$$T_{\mathrm{M2}} = \frac{1}{(2\pi)^2 (l_P^{(11)})^3}\,, \qquad T_{M5} = \frac{1}{(2\pi)^5 (l_P^{(11)})^6}\,, \tag{A.9}$$

which can be verified using $l_P^{(11)} = g_s^{1/3} l_s$.

# Appendix B

# Extremal black hole microstates

## B.1 Type-IIA charge interpretations

A solution of the form presented in Section 1.4 carries eight types of charges. Six are brane charges in eleven dimensions corresponding to three types of M2 branes, wrapped on three mutually orthogonal $T^2$'s inside $T^6$ (and smeared in the other directions) and three types of M5 branes, wrapped on the dual 4-cycles inside $T^6$ and having one worldvolume direction inside the hyper-Kähler base. When this base is Gibbons-Hawking, and the M2 and M5 branes (encoded in the harmonic functions $L_I$ and $K^I$) respect the GH isometry, one can define two additional 'geometric' charges: (angular) momentum along the GH fiber $\psi$, (controlled by the harmonic function $M$), and Kaluza-Klein monopole charge (controlled by the harmonic function $V$).

| **Charge** | | | **M theory** | **IIA: M/$S_\psi$** | **IIA′: M/$S_1$** |
|---|---|---|---|---|---|
| $V$ | $\to$ | $v_i$ | KKm | D6 | KKm |
| $K^I$ | $\to$ | $k_i^1$ | M5 | D4 | NS5 |
| | | $k_i^2$ | M5 | D4 | NS5 |
| | | $k_i^3$ | M5 | D4 | D4 |
| $L_I$ | $\to$ | $\ell_{1,i}$ | M2 | D2 | F1 |
| | | $\ell_{2,i}$ | M2 | D2 | D2 |
| | | $\ell_{3,i}$ | M2 | D2 | D2 |
| $M$ | $\to$ | $m_i$ | $P_\psi$ | D0 | $P_\psi$ |

Table B.1: Interpretation in the M-Theory and two IIA frames we use of the eight charges corresponding to the eight harmonic functions $V, K^I, L_I, M$. $S_\psi$ denotes the GH circle with coordinate $\psi$, $S_1$ one of the directions of torus $T_1$ and $P_\psi$ stands for momentum along the $\psi$ circle (spacetime angular momentum).

When the GH harmonic function $V$ asymptotes to a constant, the GH space becomes multi-center Taub-NUT, which is asymptotically $\mathbb{R}^3 \times S^1$. Upon KK reduction along the $S^1$ the 11-dimensional supergravity solution becomes a four-dimensional Calabi-Yau or torus compactification of type IIA String Theory, and the eight charges of the five-dimensional geometry become

asymptotic electric and magnetic charges in four dimensions. In table B.1 we list the interpretation of the eight M-Theory charges upon the 'standard' reduction to IIA along the GH coordinate $\psi$, and in an alternative reduction, denoted by IIA$'$, over one of the torus directions.

# Appendix C

# Non-extremal black hole microstates

## C.1 Non-extremal black hole geometry

The non-extremal rotating black hole solution sourced by three M2's on $T^6$ is the Cvetic-Youm black hole. We give it in the notation of [206]. The solution depends on six parameters: a mass parameter $m$, three 'boosts' $\delta_I$ related to the charges and angular momentum parameters $a_1, a_2$. The metric is

$$ds_{11}^2 = -(H_1H_2H_3)^{-2/3}H_m(dt+k)^2 + (H_1H_2H_3)^{1/3}ds_4^2 + \sum_{I=1}^{3}\frac{(H_1H_2H_3)^{1/3}}{H_I}ds_I^2\,. \tag{C.1}$$

with

$$k = \frac{m}{f}\left[-\frac{c_1c_2c_3}{H_m}(a_1\cos^2\theta\,d\psi + a_2\sin^2\theta\,d\phi) + s_1s_2s_3(a_2\cos^2\theta\,d\psi + a_1\sin^2\theta\,d\phi)\right] \tag{C.2}$$

with $I, J, K$ all different and we write

$$c_I \equiv \cosh\delta_I\,, \qquad s_I \equiv \sinh\delta_I\,. \tag{C.3}$$

The solution is built from the functions

$$H_I = 1 + \frac{ms_I^2}{f}\,, \qquad H_m = 1 - \frac{m}{f}\,, \qquad f = \rho^2 + a_1^2\sin^2\theta + a_2^2\cos^2\theta\,. \tag{C.4}$$

The four-dimensional metric is

$$\begin{aligned} ds_4^2 &= \frac{f\rho^2}{g}d\rho^2 + f(d\theta^2 + \sin^2\theta\,d\phi^2 + \cos^2\theta\,d\psi^2) \\ &\quad + H_m^{-1}(a_1\cos^2\theta\,d\psi + a_2\sin^2\theta d\phi)^2 - (a_2\cos^2\theta\,d\psi + a_1\sin^2\theta\,d\phi)^2\,, \\ g &= (\rho^2+a_1^2)(\rho^2+a_2^2) - m\rho^2 \equiv (\rho^2-\rho_+^2)(\rho^2-\rho_-^2)\,. \end{aligned} \tag{C.5}$$

The inner and outer horizon are given by the roots of $g(\rho)$:

$$(\rho_\pm)^2 = \frac{1}{2}\left(m - a_1^2 - a_2^2 \pm \sqrt{(m-a_1^2-a_2^2)^2 - 4a_1^2a_2^2}\right)\,. \tag{C.6}$$

The ADM mass, electric charges and angular momenta of the black hole are

$$M_{ADM} = \frac{m}{2}\sum_I \cosh 2\delta_I\,, \qquad J_1 = m(a_1c_1c_2c_3 - a_2s_1s_2s_3)\,, \tag{C.7}$$

$$Q_I = \frac{m}{2}\sinh 2\delta_I\,, \qquad J_2 = -m(a_2c_1c_2c_3 - a_1s_1s_2s_3)\,, \tag{C.8}$$

where we have set $G_5 = \frac{\pi}{4}$ as discussed in appendix A of [206].

## C.2 Approximation for throat depth

We can give a good measure of the throat depth by integrating along the $z$-axis, from the outermost center $z_{MS} \equiv z_7$ up to a suitable cutoff scale $z_{\text{neck}}$:

$$L_{MS} \equiv \int_{z_{MS}}^{z_{\text{neck}}} V^{1/2}(Z_1Z_2Z_3)^{1/6}dz\,, \tag{C.9}$$

The depth of the black hole throat is the metric distance from the horizon at $\rho = \rho_+$ to the end of the throat at $\rho = \rho_{\text{neck}}$ which can be approximated by

$$\rho_{\text{neck}} = (Q_1^{BH}Q_2^{BH}Q_3^{BH})^{1/6}\,. \tag{C.10}$$

The depth of the throat is then given by integrating $\sqrt{g_{\rho\rho}}$ in the metric (C.1):

$$L_{BH} \equiv \int_{\rho_+}^{\rho_{\text{neck}}} \sqrt{g_{\rho\rho}}d\rho = \int_{\rho_+}^{\rho_{\text{neck}}} \frac{\rho\sqrt{f}}{\sqrt{g}}(H_1H_2H_3)^{1/6}d\rho\,. \tag{C.11}$$

To get a feeling for $\Delta L$, we make some approximations. First, we approximate the geometry of the non-extremal black hole by a non-rotating one, so $a_1 = a_2 = 0$. We get:

$$L_{BH} = \int_{r_+}^{r_{\text{neck}}} \frac{(H_1H_2H_3)^{1/6}}{\sqrt{1-\frac{m}{\rho^2}}}d\rho\,, \tag{C.12}$$

with $H_I = 1 + Q_I^{BH}/\rho^2$. For near-extremal black holes, this is a good approximation. We also replace the microstate geometry by the (spherically symmetric) geometry of the extremal black hole metric:

$$L_{MS} = \int_{r_{MS}}^{r_{\text{neck}}} (Z_1Z_2Z_3)^{1/6}\frac{dr}{\sqrt{r}} = \int_{\rho_{MS}}^{\rho_{\text{neck}}} (Z_1Z_2Z_3)^{1/6}d\rho\,, \tag{C.13}$$

where we performed the change of variables $r = \frac{1}{4}\rho^2$ and we have $Z_I = 1 + Q_I/\rho^2$. This is a valid approximation, since the extremal black hole geometry only differs significantly from the microstate very deep down the throat.

Second, we approximate the black hole integral by splitting it into a part where $\rho_{\text{neck}} > \rho \gg \rho_+$ and a part where $\rho_{\text{neck}} \gg \rho > \rho_+$. We choose some intermediate radius $\rho_{\text{int}} \approx \sqrt{\rho_+\rho_{\text{neck}}}$, but its exact value is of no importance.[1] With this approximation C.12 becomes:

$$L_{BH} = \rho_{\text{neck}}\int_{\rho_+}^{\rho_{\text{int}}} \frac{d\rho}{\sqrt{\rho^2-\rho_+^2}} + \int_{\rho_{\text{int}}}^{\rho_{\text{neck}}} (H_1H_2H_3)^{1/6}d\rho\,, \tag{C.14}$$

[1] In our example, we have $\rho_{\text{neck}}^2 \approx 10^6, \rho_+^2 \lesssim 10^2$ and we can choose $\rho_{\text{int}}^2 \sim 10^4$.

where we used that for the non-rotating non-extremal black hole the non-extremality parameter $m$ is just the square of the horizon radius $\rho_+$. In the same way we approximate C.13:

$$L_{MS} = \rho_{\rm neck} \int_{\rho_{MS}}^{\rho_{\rm int}} \frac{d\rho}{\rho} + \int_{\rho_{\rm int}}^{\rho_{\rm neck}} (Z_1 Z_2 Z_3)^{1/6} d\rho \,. \tag{C.15}$$

Third, we know that for the extremal and non-extremal black hole the charges are almost equal because we are working with supertube *probes*, and hence also the $Z_I = H_I$ are equal. Then the difference in depth is

$$\begin{aligned} L_{BH} - L_{MS} &= \rho_{\rm neck} \left( \int_{\rho_+}^{\rho_{\rm int}} \frac{d\rho}{\sqrt{\rho^2 - \rho_+^2}} - \int_{\rho_+}^{\rho_{\rm int}} \frac{d\rho}{r} \right) \\ &= \rho_{\rm neck} \left[ \ln \left( \frac{\rho_{\rm int} + \sqrt{\rho_{\rm int}^2 - \rho_+^2}}{\rho_+} \right) - \ln \frac{\rho_{\rm int}}{\rho_{MS}} \right] \end{aligned} \tag{C.16}$$

Since we chose $\rho_{\rm int} \gg \rho_+$, we can approximate this very well by

$$\Delta L = L_{BH} - L_{MS} = \rho_{\rm neck} \ln \left( 2 \frac{\rho_{MS}}{\rho_+} \right) . \tag{C.17}$$

We can use this result to get some idea on how the size of the supertubes and the depth of the microstates affect $\Delta L$. Consider the scaling of the supertube charges and the coordinates of the microstate centers as

$$\begin{aligned} (q_1, q_2, d_3) &\to e^{\lambda} (q_1, q_2, d_3) \,, \\ \rho_{MS} &\to e^{\mu} \rho_{MS} \,, \end{aligned} \tag{C.18}$$

Both scalings have a non-trivial effect on the size of the horizon radius of the would-be non-extremal black hole, which (neglecting rotation) is given by

$$\rho_+^2 = m = \sqrt{\frac{8\Delta M}{\frac{1}{Q_1} + \frac{1}{Q_2} + \frac{1}{Q_2}}} \,. \tag{C.19}$$

The potential $\mathcal{H}$ scales linearly with the tube charges, and in the scaling regime it also scales linearly with the coordinate size of the centers, see eq. (3.39). The same applies, of course, to the value $\Delta M$ of its metastable minimum. Hence the horizon radius, as a function of the tube charges $q^{\rm tube} \equiv (q_1, q_2, d_3)$ and the size of the microstate background $\rho_{MS}$, has the following scaling behavior:

$$\rho_+(q^{\rm tube}; \rho_{MS}) = e^{-(\lambda+\mu)/4} \rho_+(e^{\lambda} q^{\rm tube}; e^{\mu} \rho_{MS}) \,. \tag{C.20}$$

Therefore under the scalings (C.18), the difference in depths $\Delta L \equiv L_{BH} - L_{MS}$ goes as

$$\frac{\Delta L}{\rho_{\rm neck}} \to \frac{\Delta L}{\rho_{\rm neck}} - \frac{1}{4}\lambda + \frac{3}{4}\mu \,. \tag{C.21}$$

# Appendix D

# Almost BPS solutions

## D.1 Details of the angular momentum vector

The angular momentum vector, $k$, in the metric (5.1) is decomposed as in (5.25) and here we summarize the results of [45] and give the detailed expressions in our conventions. We also examine the relationship between the BPS and non-BPS descriptions for $h = 0$.

### The function $\mu$

For BPS solutions, $\mu$ is given by the standard expression in [26, 27]:

$$\mu \;=\; \tfrac{1}{6}\, V^{-2}\, C_{IJK}\, K_+^I K_+^J K_+^K \;+\; \tfrac{1}{2}\, V^{-1}\, K_+^I L_I \;+\; M_+\,, \tag{D.1}$$

where $M_+$ is harmonic function that we will take to be

$$M_+ \;=\; m_\infty^+ \;+\; \frac{m_0^+}{r} \;+\; \sum_{j=1}^{3} \frac{m_j^+}{r_j} \;+\; m_{div}^+\, r\cos\theta\,. \tag{D.2}$$

For reasons that will become apparent below, we have added an unphysical harmonic term that diverges at infinity.

For the almost-BPS system one can use the results of [37] to obtain

$$\begin{aligned} V\,\mu \;=\; & \frac{1}{2}\sum_{I=1}^{3} K_-^I (V + h(L_I - 1)) \;-\; \frac{q}{2}\sum_{\substack{i,j=1\\ j\neq i}}^{3} k_i^- Q_j^{(i)}\, \frac{r^2 - 2a_i r\cos\theta + a_i a_j}{a_i(a_i - a_j)\, r\, r_i\, r_j} \\ & +\; \frac{k_1^- k_2^- k_3^-}{r_1 r_2 r_3}\left[h^2 \;+\; \frac{q^2\, r\cos\theta}{a_1 a_2 a_3} \;+\; \frac{h\, q\,(r^2(a_1+a_2+a_3) + a_1 a_2 a_3)}{2\, a_1 a_2 a_3\, r}\right] \;+\; M_-\,, \end{aligned} \tag{D.3}$$

where $M_-$ is another harmonic function which we will take to be:

$$M_- \;=\; m_\infty^- \;+\; \frac{m_0^-}{r} \;+\; \sum_{j=1}^{3} \frac{m_j^-}{r_j} \;+\; \frac{m_{div}^-}{r^2}\,\cos\theta\,. \tag{D.4}$$

Again we have added an unphysical harmonic term but this time it diverges at the origin.

Note that regularity at the supertubes requires the following for both classes of solution:

$$m_1^{\pm} \;=\; \frac{Q_1^{(2)}\,Q_1^{(3)}}{2\,k_1^{\pm}}\,, \qquad m_2^{\pm} \;=\; \frac{Q_2^{(1)}\,Q_2^{(3)}}{2\,k_2^{\pm}}\,, \qquad m_3^{\pm} \;=\; \frac{Q_3^{(1)}\,Q_3^{(2)}}{2\,k_3^{\pm}}\,, \tag{D.5}$$

## The one-form $\omega$

Following [26, 27], for $a_i > a_j$ we define:

$$\omega_{ij} \;\equiv\; -\,\frac{(r^2\,\sin^2\theta + (r\cos\theta - a_i + r_i)(r\cos\theta - a_j - r_j))}{(a_i - a_j)\,r_i\,r_j}\,, \tag{D.6}$$

To define the BPS angular momentum vector, $\omega$, it is also convenient to introduce:

$$\Delta_1 \;\equiv\; 2\,\big(h + \frac{q}{a_1}\big)m_1^+ \;-\; \frac{\Gamma^+_{12}}{(a_2 - a_1)} \;-\; \frac{\Gamma^+_{13}}{(a_3 - a_1)} \;-\; k_1^+\,, \tag{D.7}$$

$$\Delta_2 \;\equiv\; 2\,\big(h + \frac{q}{a_2}\big)m_2^+ \;+\; \frac{\Gamma^+_{12}}{(a_2 - a_1)} \;-\; \frac{\Gamma^+_{23}}{(a_3 - a_2)} \;-\; k_2^+\,, \tag{D.8}$$

$$\Delta_3 \;\equiv\; 2\,\big(h + \frac{q}{a_3}\big)m_3^+ \;+\; \frac{\Gamma^+_{13}}{(a_3 - a_1)} \;+\; \frac{\Gamma^+_{23}}{(a_3 - a_2)} \;-\; k_3^+\,, \tag{D.9}$$

Note that the bubble equations (5.28)–(5.30) and (D.5) imply that $\Delta_j = 0$, $j = 1, 2, 3$. We will not impose these conditions here and we will not remove Dirac strings more generally.

We then find that for the BPS solution, $\omega = \omega_\phi d\phi$, with

$$\begin{aligned}\omega_\phi \;=\; & \frac{1}{2}\left(\Gamma^+_{21}\,\omega_{21} + \Gamma^+_{31}\,\omega_{31} + \Gamma^+_{32}\,\omega_{32}\right) \;+\; q\sum_{i=1}^{3}\frac{m_i^+}{a_i\,r_i}(r\,\sin^2\theta + (r\cos\theta - a_i + r_i)(\cos\theta - 1) \\ & +\; \frac{1}{2}\sum_{i=1}^{3}\Delta_i\,\frac{r\cos\theta - a_i}{r_i} \;+\; \kappa^+ \;-\; \frac{1}{2}\Big(\frac{\Gamma^+_{12}}{(a_1 - a_2)} + \frac{\Gamma^+_{13}}{(a_1 - a_3)} + \frac{\Gamma^+_{23}}{(a_2 - a_3)}\Big) \\ & +\; \Big(q\sum_{i=1}^{3}\frac{m_i^+}{a_i} - h\,m_0^+\Big)(1 - \cos\theta) - q\,m_\infty^+\cos\theta \;+\; m^+_{div}(\tfrac{1}{2}hr^2 + qr)\sin^2\theta\,,\end{aligned} \tag{D.10}$$

and where $\kappa^+$ is a constant of integration.

One may use the results of [37] to find $\omega_\phi$ for the almost-BPS solution:

$$\begin{aligned}
\omega_\phi \;=\; & -\frac{1}{2}\;\sum_{i=1}^{3}\frac{k_i^-}{a_i\,r_i}\big(h\,a_i\,(r\cos\theta-a_i)+q\,(r-a_i\cos\theta)\big)\\
& -\frac{1}{2}\sum_{\substack{i,j=1\\ j\neq i}}^{3}\frac{k_i^-Q_j^{(i)}}{a_i(a_i-a_j)\,r_i\,r_j}\big[h\,a_i\,\big(r^2-(a_i+a_j)r\cos\theta+a_ia_j\big)\\
& \qquad\qquad +q\,\big((r^2+a_ia_j\cos\theta)-r(a_i\cos2\theta+a_j)\big)\big]\\
& -\frac{k_1^-k_2^-k_3^-}{a_1a_2a_3\,r_1r_2r_3}\,\big[\,q^2\,r^2\sin^2\theta\;+\;\tfrac{1}{2}\,h\,q\,\big(r^3-(a_1+a_2+a_3)r^2\cos\theta\\
& \qquad\qquad +(a_1a_2+a_1a_3+a_2a_3)r-a_1a_2a_3\cos\theta\big)\big]\\
& -\kappa^-\;-\;\frac{m^-_{div}}{r}\sin^2\theta\;+\;m_0^-\cos\theta\;+\;\sum_{i=1}^{3}\frac{m_i^-}{r_i}(r\cos\theta-a_i)\,,
\end{aligned}\tag{D.11}$$

where $\kappa^-$ is another constant of integration.

## The Minkowski-space limit

For $h=0$ the BPS and non-BPS solutions must be the same and in Subsection 5.2.4 it was argued that this should be achieved by the coordinate change (5.37). For the angular momentum vector this means

$$\begin{aligned}
\mu_-(d\psi_-\,-\,q\,\cos\theta\,d\phi_-)\;+\;\omega_{\phi\,-}d\phi_- \;&=\; \mu_+(d\psi_+\,+\,q\,\cos\theta\,d\phi_+)\;+\;\omega_{\phi\,+}d\phi_+\\
&=\;\tilde\mu_+(-q\,d\phi_-+\cos\theta\,d\psi_-)\;+\;\frac{1}{q}\,\tilde\omega_{\phi\,+}d\psi_-
\end{aligned}\tag{D.12}$$

where the quantities with the tildes have the replacement $k_I^+\to\widehat{k}_I$. This implies that we must have (for $h=0$):

$$\mu_-\;=\;\tilde\mu_+\cos\theta\;+\;\frac{1}{q}\,\tilde\omega_{\phi\,+}\,,\qquad \omega_{\phi\,-}\;=\;\tilde\omega_{\phi\,+}\,\cos\theta\;-\;q\;\tilde\mu_+\sin^2\theta\,.\tag{D.13}$$

We have verified this by explicit computation and it works provided that one also makes the substitutions:

$$m_i^+\;\to\;\frac{a_i}{q}\,m_i^-\,,\quad m_0^+\;\to\;\frac{1}{q}\,m^-_{div}\,,\quad m^+_\infty\;\to\;\frac{1}{q}\,\kappa^-\,,\quad m^+_{div}\;\to\;\frac{1}{q}\,m^-_\infty\,,\quad \kappa^+\;\to\;m_0^-\,.\tag{D.14}$$

Thus the transformation (5.37) does indeed map the complete BPS description to the almost-BPS description. Note also that we have included the terms $m^\pm_{div}$ so as to complete this dictionary.

# List of Figures

# List of Tables

# Bibliography


[1] S. Hawking, *Particle Creation by Black Holes*, Commun.Math.Phys. **43** (1975) 199–220

[2] S. D. Mathur, *The Information paradox: A Pedagogical introduction*, Class.Quant.Grav. **26** (2009) 224001, 0909.1038

[3] A. Strominger and C. Vafa, *Microscopic origin of the Bekenstein-Hawking entropy*, Phys.Lett. **B379** (1996) 99–104, hep-th/9601029

[4] J. M. Maldacena, *The Large N limit of superconformal field theories and supergravity*, Adv.Theor.Math.Phys. **2** (1998) 231–252, hep-th/9711200

[5] E. Witten, *Anti-de Sitter space and holography*, Adv.Theor.Math.Phys. **2** (1998) 253–291, hep-th/9802150

[6] J. L. Cardy, *Operator Content of Two-Dimensional Conformally Invariant Theories*, Nucl. Phys. B **270** (1986) 186. (1986)

[7] A. Sen, *Extremal black holes and elementary string states*, Mod.Phys.Lett. **A10** (1995) 2081–2094, hep-th/9504147

[8] A. Dabholkar, *Exact counting of black hole microstates*, Phys.Rev.Lett. **94** (2005) 241301, hep-th/0409148

[9] R. M. Wald, *Black hole entropy is the Noether charge*, Phys. Rev. D **48** (1993) 3427 (1993) gr-qc/9307038

V. Iyer and R. M. Wald, *Some properties of Noether charge and a proposal for dynamical black hole entropy*, Phys.Rev. **D50** (1994) 846–864, gr-qc/9403028

[10] J. Polchinski and M. J. Strassler, *The String dual of a confining four-dimensional gauge theory*, hep-th/0003136

[11] O. Lunin and S. D. Mathur, *AdS / CFT duality and the black hole information paradox*, Nucl.Phys. **B623** (2002) 342–394, hep-th/0109154

[12] O. Lunin and S. D. Mathur, *Statistical interpretation of Bekenstein entropy for systems with a stretched horizon*, Phys.Rev.Lett. **88** (2002) 211303, hep-th/0202072

[13] O. Lunin, J. M. Maldacena and L. Maoz, *Gravity solutions for the D1-D5 system with angular momentum*, hep-th/0212210

O. Lunin and S. D. Mathur, *The Slowly rotating near extremal D1 - D5 system as a 'hot tube'*, Nucl.Phys. **B615** (2001) 285–312, hep-th/0107113

L. F. Alday, J. de Boer and I. Messamah, *The Gravitational description of coarse grained microstates*, JHEP **0612** (2006) 063, hep-th/0607222

[14] A. Donos and A. Jevicki, *Dynamics of chiral primaries in AdS(3) x S**3 x T**4*, Phys.Rev. **D73** (2006) 085010, hep-th/0512017

L. F. Alday, J. de Boer and I. Messamah, *What is the dual of a dipole?*, Nucl.Phys. **B746** (2006) 29–57, hep-th/0511246

S. Giusto, S. D. Mathur and Y. K. Srivastava, *Dynamics of supertubes*, Nucl.Phys. **B754** (2006) 233–281, hep-th/0510235

M. Taylor, *General 2 charge geometries*, JHEP **0603** (2006) 009, hep-th/0507223

K. Skenderis and M. Taylor, *Fuzzball solutions and D1-D5 microstates*, Phys.Rev.Lett. **98** (2007) 071601, hep-th/0609154

N. Iizuka and M. Shigemori, *A Note on D1-D5-J system and 5-D small black ring*, JHEP **0508** (2005) 100, hep-th/0506215

M. Boni and P. J. Silva, *Revisiting the D1/D5 system or bubbling in AdS(3)*, JHEP **0510** (2005) 070, hep-th/0506085

D. Martelli and J. F. Morales, *Bubbling AdS(3)*, JHEP **0502** (2005) 048, hep-th/0412136

Y. K. Srivastava, *Bound states of KK monopole and momentum*, hep-th/0611124

[15] V. Balasubramanian, P. Kraus and M. Shigemori, *Massless black holes and black rings as effective geometries of the D1-D5 system*, Class.Quant.Grav. **22** (2005) 4803–4838, hep-th/0508110

[16] I. Kanitscheider, K. Skenderis and M. Taylor, *Holographic anatomy of fuzzballs*, JHEP **0704** (2007) 023, hep-th/0611171

[17] A. A. Tseytlin, *Extreme dyonic black holes in string theory*, Mod.Phys.Lett. **A11** (1996) 689–714, hep-th/9601177

[18] A. A. Tseytlin, *Extremal black hole entropy from conformal string sigma model*, Nucl.Phys. **B477** (1996) 431–448, hep-th/9605091

[19] S. D. Mathur, *The Fuzzball proposal for black holes: An Elementary review*, Fortsch.Phys. **53** (2005) 793–827, hep-th/0502050

S. D. Mathur, *The Quantum structure of black holes*, Class.Quant.Grav. **23** (2006) R115, hep-th/0510180

[20] B. C. Palmer and D. Marolf, *Counting supertubes*, JHEP **0406** (2004) 028, hep-th/0403025

V. S. Rychkov, *D1-D5 black hole microstate counting from supergravity*, JHEP **0601** (2006) 063, hep-th/0512053

D. Bak, Y. Hyakutake and N. Ohta, *Phase moduli space of supertubes*, Nucl.Phys. **B696** (2004) 251–262, hep-th/0404104

D. Bak, Y. Hyakutake, S. Kim and N. Ohta, *A Geometric look on the microstates of supertubes*, Nucl.Phys. **B712** (2005) 115–138, hep-th/0407253

[21] S. Giusto, S. D. Mathur and A. Saxena, *Dual geometries for a set of 3-charge microstates*, Nucl.Phys. **B701** (2004) 357–379, hep-th/0405017

[22] S. Giusto, S. D. Mathur and A. Saxena, *3-charge geometries and their CFT duals*, Nucl.Phys. **B710** (2005) 425–463, hep-th/0406103

[23] S. Giusto and S. D. Mathur, *Geometry of D1-D5-P bound states*, Nucl.Phys. **B729** (2005) 203–220, hep-th/0409067

[24] O. Lunin, *Adding momentum to D-1 - D-5 system*, JHEP **0404** (2004) 054, hep-th/0404006

[25] I. Bena and P. Kraus, *Microstates of the D1-D5-KK system*, Phys.Rev. **D72** (2005) 025007, hep-th/0503053

[26] I. Bena and N. P. Warner, *Bubbling supertubes and foaming black holes*, Phys. Rev. **D74** (2006) 066001, hep-th/0505166

[27] P. Berglund, E. G. Gimon and T. S. Levi, *Supergravity microstates for BPS black holes and black rings*, JHEP **06** (2006) 007, hep-th/0505167

[28] A. Saxena, G. Potvin, S. Giusto and A. W. Peet, *Smooth geometries with four charges in four dimensions*, JHEP **0604** (2006) 010, hep-th/0509214

[29] I. Bena, C.-W. Wang and N. P. Warner, *The Foaming three-charge black hole*, Phys.Rev. **D75** (2007) 124026, hep-th/0604110

[30] S. Giusto, S. D. Mathur and Y. K. Srivastava, *A Microstate for the 3-charge black ring*, Nucl.Phys. **B763** (2007) 60–90, hep-th/0601193

[31] V. Balasubramanian, E. G. Gimon and T. S. Levi, *Four Dimensional Black Hole Microstates: From D-branes to Spacetime Foam*, JHEP **0801** (2008) 056, hep-th/0606118

[32] I. Bena, C.-W. Wang and N. P. Warner, *Mergers and typical black hole microstates*, JHEP **0611** (2006) 042, hep-th/0608217

[33] M. C. Cheng, *More Bubbling Solutions*, JHEP **0703** (2007) 070, hep-th/0611156

[34] J. Ford, S. Giusto and A. Saxena, *A Class of BPS time-dependent 3-charge microstates from spectral flow*, Nucl.Phys. **B790** (2008) 258–280, hep-th/0612227

[35] I. Bena, C.-W. Wang and N. P. Warner, *Plumbing the Abyss: Black ring microstates*, JHEP **0807** (2008) 019, 0706.3786

[36] K. Goldstein and S. Katmadas, *Almost BPS black holes*, JHEP **05** (2009) 058, 0812.4183

[37] I. Bena, S. Giusto, C. Ruef and N. P. Warner, *Multi-Center non-BPS Black Holes - the Solution*, JHEP **11** (2009) 032, 0908.2121

[38] I. Bena, S. Giusto, C. Ruef and N. P. Warner, *Supergravity Solutions from Floating Branes*, JHEP **03** (2010) 047, 0910.1860

[39] I. Bena, G. Dall'Agata, S. Giusto, C. Ruef and N. P. Warner, *Non-BPS Black Rings and Black Holes in Taub-NUT*, JHEP **06** (2009) 015, 0902.4526

[40] N. Bobev and C. Ruef, *The Nuts and Bolts of Einstein-Maxwell Solutions*, JHEP **01** (2010) 124, 0912.0010

[41] I. Bena, N. Bobev, S. Giusto, C. Ruef and N. P. Warner, *An Infinite-Dimensional Family of Black-Hole Microstate Geometries*, JHEP **1103** (2011) 022, 1006.3497

[42] G. Dall'Agata, S. Giusto and C. Ruef, *U-duality and non-BPS solutions*, JHEP **1102** (2011) 074, 1012.4803

[43] N. Bobev, B. Niehoff and N. P. Warner, *Hair in the Back of a Throat: Non-Supersymmetric Multi-Center Solutions from Káhler Manifolds*, JHEP **1110** (2011) 149, 1103.0520

[44] G. Bossard and C. Ruef, *Interacting non-BPS black holes*, Gen.Rel.Grav. **44** (2012) 21–66, 1106.5806

[45] O. Vasilakis and N. P. Warner, *Mind the Gap: Supersymmetry Breaking in Scaling, Microstate Geometries*, JHEP **1110** (2011) 006, 1104.2641

[46] I. Bena and N. P. Warner, *Black holes, black rings and their microstates*, Lect.Notes Phys. **755** (2008) 1–92, hep-th/0701216

[47] K. Skenderis and M. Taylor, *The fuzzball proposal for black holes*, Phys. Rept. **467** (2008) 117–171, 0804.0552

[48] V. Balasubramanian, J. de Boer, S. El-Showk and I. Messamah, *Black Holes as Effective Geometries*, Class. Quant. Grav. **25** (2008) 214004, 0811.0263

[49] I. Bena, J. de Boer, M. Shigemori and N. P. Warner, *Double, Double Supertube Bubble*, JHEP **1110** (2011) 116, 1107.2650

[50] I. Bena, S. Giusto, M. Shigemori and N. P. Warner, *Supersymmetric Solutions in Six Dimensions: A Linear Structure*, JHEP **1203** (2012) 084, 1110.2781

[51] B. E. Niehoff, O. Vasilakis and N. P. Warner, *Multi-Superthreads and Supersheets*, JHEP **1304** (2013) 046, 1203.1348

[52] O. Vasilakis, *Multi-centered Breathing Supersheets*, 1302.1241

[53] G. Gibbons and N. Warner, *Global Structure of Five-dimensional BPS Fuzzballs*, 1305.0957

[54] H. Lin, O. Lunin and J. M. Maldacena, *Bubbling AdS space and 1/2 BPS geometries*, JHEP **0410** (2004) 025, hep-th/0409174

[55] I. R. Klebanov and M. J. Strassler, *Supergravity and a confining gauge theory: Duality cascades and chi SB resolution of naked singularities*, JHEP **0008** (2000) 052, hep-th/0007191

[56] C. V. Johnson, R. C. Myers, A. W. Peet and S. F. Ross, *The Enhancon and the consistency of excision*, Phys.Rev. **D64** (2001) 106001, hep-th/0105077

[57] R. Penrose, *Structure of space-time*,

[58] P. R. Brady and J. D. Smith, *Black hole singularities: A Numerical approach*, Phys.Rev.Lett. **75** (1995) 1256–1259, gr-qc/9506067

[59] M. Dafermos, *The Interior of charged black holes and the problem of uniqueness in general relativity*, Commun.Pure Appl.Math. **58** (2005) 0445–0504, gr-qc/0307013

[60] E. Poisson and W. Israel, *Internal structure of black holes*, Phys.Rev. **D41** (1990) 1796–1809

[61] D. Marolf, *The dangers of extremes*, Gen.Rel.Grav. **42** (2010) 2337–2343, 1005.2999

[62] V. Jejjala, O. Madden, S. F. Ross and G. Titchener, *Non-supersymmetric smooth geometries and D1-D5-P bound states*, Phys.Rev. **D71** (2005) 124030, hep-th/0504181

[63] S. Giusto, S. F. Ross and A. Saxena, *Non-supersymmetric microstates of the D1-D5-KK system*, JHEP **12** (2007) 065, 0708.3845

[64] J. H. Al-Alawi and S. F. Ross, *Spectral Flow of the Non-Supersymmetric Microstates of the D1-D5-KK System*, JHEP **0910** (2009) 082, 0908.0417

[65] I. Bena, S. Giusto, C. Ruef and N. P. Warner, *A (Running) Bolt for New Reasons*, JHEP **11** (2009) 089, 0909.2559

[66] A. Almheiri, D. Marolf, J. Polchinski and J. Sully, *Black Holes: Complementarity or Firewalls?*, JHEP **1302** (2013) 062, 1207.3123

[67] S. D. Mathur, *The Information paradox and the infall problem*, Class.Quant.Grav. **28** (2011) 125010, 1012.2101

[68] S. D. Mathur and C. J. Plumberg, *Correlations in Hawking radiation and the infall problem*, JHEP **1109** (2011) 093, 1101.4899

[69] S. D. Mathur and D. Turton, *Comments on black holes I: The possibility of complementarity*, 1208.2005

[70] S. D. Mathur, *Black Holes and Beyond*, Annals Phys. **327** (2012) 2760–2793, 1205.0776

[71] S. D. Mathur, *Black holes and holography*, J.Phys.Conf.Ser. **405** (2012) 012005, 1207.5431

[72] I. Bena, M. Grana and N. Halmagyi, *On the Existence of Meta-stable Vacua in Klebanov-Strassler*, JHEP **1009** (2010) 087, 0912.3519

[73] I. Bena, G. Giecold and N. Halmagyi, *The Backreaction of Anti-M2 Branes on a Warped Stenzel Space*, JHEP **1104** (2011) 120, 1011.2195

[74] I. Bena, G. Giecold, M. Grana, N. Halmagyi and S. Massai, *On Metastable Vacua and the Warped Deformed Conifold: Analytic Results*, 1102.2403

[75] G. Giecold, E. Goi and F. Orsi, *Assessing a candidate IIA dual to metastable supersymmetry-breaking*, 1108.1789, * Temporary entry *

[76] A. Dymarsky, *On gravity dual of a metastable vacuum in Klebanov-Strassler theory*, JHEP **1105** (2011) 053, 1102.1734

[77] S. Massai, *A Comment on anti-brane singularities in warped throats*, 1202.3789

[78] J. Blaback, U. H. Danielsson, D. Junghans, T. Van Riet, T. Wrase *et al.*, *The problematic backreaction of SUSY-breaking branes*, JHEP **1108** (2011) 105, 1105.4879

[79] I. Bena, M. Grana, S. Kuperstein and S. Massai, *Anti-D3's - Singular to the Bitter End*, 1206.6369

[80] M. Cvetic, G. Gibbons, H. Lu and C. Pope, *New complete noncompact spin(7) manifolds*, Nucl.Phys. **B620** (2002) 29–54, hep-th/0103155

[81] J. Blaback, U. H. Danielsson and T. Van Riet, *Resolving anti-brane singularities through time-dependence*, JHEP **1302** (2013) 061, 1202.1132

[82] R. M. Wald, *General Relativity*. 1984

[83] S. Hawking and G. Ellis, *The Large scale structure of space-time*,

[84] J. Bekenstein, *Black holes and the second law*, Lett.Nuovo Cim. **4** (1972) 737–740

[85] J. Polchinski, *String theory. Vol. 1: An introduction to the bosonic string*. 1998

J. Polchinski, *String theory. Vol. 2: Superstring theory and beyond*. 1998

[86] K. Becker, M. Becker and J. Schwarz, *String theory and M-theory: A modern introduction*. 2007

[87] A. W. Peet, *TASI lectures on black holes in string theory*, hep-th/0008241

[88] T. Buscher, *A Symmetry of the String Background Field Equations*, Phys.Lett. **B194** (1987) 59

T. Buscher, *Path Integral Derivation of Quantum Duality in Nonlinear Sigma Models*, Phys.Lett. **B201** (1988) 466

[89] E. Bergshoeff, C. M. Hull and T. Ortin, *Duality in the type II superstring effective action*, Nucl.Phys. **B451** (1995) 547–578, hep-th/9504081

[90] R. C. Myers, *Dielectric branes*, JHEP **9912** (1999) 022, hep-th/9910053

C. V. Johnson, *D-brane primer*, hep-th/0007170

[91] T. Mohaupt, *Black holes in supergravity and string theory*, Class.Quant.Grav. **17** (2000) 3429–3482, hep-th/0004098

[92] I. Bena, S. El-Showk and B. Vercnocke, *Black holes in string theory*, Lecture Notes for the Course 'Black holes in string theory' given by Bena and El-Showk at IPHT in spring 2012 (2012)

[93] M. Guica, T. Hartman, W. Song and A. Strominger, *The Kerr/CFT Correspondence*, Phys. Rev. **D80** (2009) 124008, 0809.4266

[94] I. Bena, M. Guica and W. Song, *Un-twisting the NHEK with spectral flows*, JHEP **1303** (2013) 028, 1203.4227

[95] J. Breckenridge, R. C. Myers, A. Peet and C. Vafa, *D-branes and spinning black holes*, Phys.Lett. **B391** (1997) 93–98, hep-th/9602065

[96] D. Gaiotto, A. Strominger and X. Yin, *New connections between 4-D and 5-D black holes*, JHEP **0602** (2006) 024, hep-th/0503217

[97] D. Gaiotto, A. Strominger and X. Yin, *5D black rings and 4D black holes*, JHEP **0602** (2006) 023, hep-th/0504126

[98] H. Elvang, R. Emparan, D. Mateos and H. S. Reall, *Supersymmetric 4-D rotating black holes from 5-D black rings*, JHEP **0508** (2005) 042, hep-th/0504125

[99] I. Bena, P. Kraus and N. P. Warner, *Black rings in Taub-NUT*, Phys.Rev. **D72** (2005) 084019, hep-th/0504142

[100] K. Behrndt, G. Lopes Cardoso and S. Mahapatra, *Exploring the relation between 4-D and 5-D BPS solutions*, Nucl.Phys. **B732** (2006) 200–223, hep-th/0506251

[101] J. Ford, S. Giusto, A. Peet and A. Saxena, *Reduction without reduction: Adding KK-monopoles to five dimensional stationary axisymmetric solutions*, Class.Quant.Grav. **25** (2008) 075014, 0708.3823

[102] I. Bena and N. P. Warner, *One ring to rule them all ... and in the darkness bind them?*, Adv. Theor. Math. Phys. **9** (2005) 667–701, hep-th/0408106

[103] J. B. Gutowski and H. S. Reall, *General supersymmetric AdS(5) black holes*, JHEP **0404** (2004) 048, hep-th/0401129

[104] J. P. Gauntlett, J. B. Gutowski, C. M. Hull, S. Pakis and H. S. Reall, *All supersymmetric solutions of minimal supergravity in five- dimensions*, Class.Quant.Grav. **20** (2003) 4587–4634, hep-th/0209114

[105] J. P. Gauntlett and J. B. Gutowski, *General concentric black rings*, Phys. Rev. **D71** (2005) 045002, hep-th/0408122

[106] H. Elvang, R. Emparan, D. Mateos and H. S. Reall, *Supersymmetric black rings and three-charge supertubes*, Phys. Rev. **D71** (2005) 024033, hep-th/0408120

[107] R. Schon and S.-T. Yau, *On the Proof of the positive mass conjecture in general relativity*, Commun.Math.Phys. **65** (1979) 45–76

[108] E. Witten, *A Simple Proof of the Positive Energy Theorem*, Commun.Math.Phys. **80** (1981) 381

[109] F. Denef, *Supergravity flows and D-brane stability*, JHEP **08** (2000) 050, hep-th/0005049

[110] F. Denef, *Quantum quivers and Hall/hole halos*, JHEP **10** (2002) 023, hep-th/0206072

[111] B. Bates and F. Denef, *Exact solutions for supersymmetric stationary black hole composites*, hep-th/0304094

[112] J. P. Gauntlett, R. C. Myers and P. K. Townsend, *Black holes of D = 5 supergravity*, Class.Quant.Grav. **16** (1999) 1–21, hep-th/9810204

[113] T. Shiromizu, S. Ohashi and R. Suzuki, *A no-go on strictly stationary spacetimes in four/higher dimensions*, Phys.Rev. **D86** (2012) 064041, 1207.7250

[114] P. Breitenlohner, D. Maison and G. W. Gibbons, *Four-Dimensional Black Holes from Kaluza-Klein Theories*, Commun.Math.Phys. **120** (1988) 295

[115] F. Denef and G. W. Moore, *Split states, entropy enigmas, holes and halos*, JHEP **1111** (2011) 129, hep-th/0702146

[116] J. de Boer, S. El-Showk, I. Messamah and D. Van den Bleeken, *A Bound on the entropy of supergravity?*, JHEP **1002** (2010) 062, 0906.0011

[117] D. Mateos and P. K. Townsend, *Supertubes*, Phys. Rev. Lett. **87** (2001) 011602, hep-th/0103030

[118] D. Mateos, S. Ng and P. K. Townsend, *Tachyons, supertubes and brane / anti-brane systems*, JHEP **0203** (2002) 016, hep-th/0112054

[119] R. Emparan, D. Mateos and P. K. Townsend, *Supergravity supertubes*, JHEP **0107** (2001) 011, hep-th/0106012

[120] R. Emparan, *Born-Infeld strings tunneling to D-branes*, Phys. Lett. **B423** (1998) 71–78, hep-th/9711106

[121] J. McGreevy, L. Susskind and N. Toumbas, *Invasion of the giant gravitons from Anti-de Sitter space*, JHEP **0006** (2000) 008, hep-th/0003075

[122] J. Pawelczyk and S.-J. Rey, *Ramond-ramond flux stabilization of D-branes*, Phys.Lett. **B493** (2000) 395–401, hep-th/0007154

[123] D. Mateos, S. Ng and P. K. Townsend, *Supercurves*, Phys.Lett. **B538** (2002) 366–374, hep-th/0204062

[124] I. Bena, N. Bobev, C. Ruef and N. P. Warner, *Supertubes in Bubbling Backgrounds: Born-Infeld Meets Supergravity*, JHEP **0907** (2009) 106, 0812.2942

[125] P. Pasti, D. P. Sorokin and M. Tonin, *Covariant action for a D = 11 five-brane with the chiral field*, Phys.Lett. **B398** (1997) 41–46, hep-th/9701037

[126] I. Bena, N. Bobev, C. Ruef and N. P. Warner, *Entropy Enhancement and Black Hole Microstates*, Phys.Rev.Lett. **105** (2010) 231301, 0804.4487

[127] G. Gibbons, *Birkhoff's invariant and Thorne's Hoop Conjecture*, 0903.1580

[128] B. D. Chowdhury and A. Virmani, *Modave Lectures on Fuzzballs and Emission from the D1-D5 System*, 1001.1444

[129] B. D. Chowdhury and S. D. Mathur, *Radiation from the non-extremal fuzzball*, Class.Quant.Grav. **25** (2008) 135005, 0711.4817

[130] S. G. Avery, B. D. Chowdhury and S. D. Mathur, *Emission from the D1D5 CFT*, JHEP **10** (2009) 065, 0906.2015

[131] D. N. Page, *Average entropy of a subsystem*, Phys.Rev.Lett. **71** (1993) 1291–1294, gr-qc/9305007

[132] D. N. Page, *Black hole information*, hep-th/9305040

[133] S. D. Mathur, *What the information paradox is not*, 1108.0302

[134] S. D. Mathur, *The information paradox: conflicts and resolutions*, Pramana **79** (2012) 1059–1073, 1201.2079

[135] E. Keski-Vakkuri, G. Lifschytz, S. D. Mathur and M. E. Ortiz, *Breakdown of the semiclassical approximation at the black hole horizon*, Phys.Rev. **D51** (1995) 1764–1780, hep-th/9408039

[136] J. Polchinski, *String theory and black hole complementarity*, hep-th/9507094

[137] D. A. Lowe, J. Polchinski, L. Susskind, L. Thorlacius and J. Uglum, *Black hole complementarity versus locality*, Phys.Rev. **D52** (1995) 6997–7010, hep-th/9506138

[138] Y. Kiem, H. L. Verlinde and E. P. Verlinde, *Black hole horizons and complementarity*, Phys.Rev. **D52** (1995) 7053–7065, hep-th/9502074

[139] S. B. Giddings, *Quantization in black hole backgrounds*, Phys.Rev. **D76** (2007) 064027, hep-th/0703116

[140] S. Bose, L. Parker and Y. Peleg, *Validity of the semiclassical approximation and back reaction*, Phys.Rev. **D53** (1996) 7089–7093, gr-qc/9601035

[141] E. Keski-Vakkuri and S. D. Mathur, *Quantum gravity and turning points in the semiclassical approximation*, Phys.Rev. **D54** (1996) 7391–7406, gr-qc/9604058

[142] S. D. Mathur, *What Exactly is the Information Paradox?*, Lect.Notes Phys. **769** (2009) 3–48, 0803.2030

[143] E. Lieb and M. Ruskai, *Proof of the strong subadditivity of quantum-mechanical entropy*, J.Math.Phys. **14** (1973) 1938–1941

[144] H. Araki and E. Lieb, *Entropy inequalities*, Commun.Math.Phys. **18** (1970) 160–170

[145] S. B. Giddings and Y. Shi, *Quantum information transfer and models for black hole mechanics*, 1205.4732

[146] S. G. Avery, *Qubit Models of Black Hole Evaporation*, JHEP **1301** (2013) 176, 1109.2911

[147] S. B. Giddings, *Models for unitary black hole disintegration*, Phys.Rev. **D85** (2012) 044038, 1108.2015

[148] S. B. Giddings, *Black holes, quantum information, and unitary evolution*, Phys.Rev. **D85** (2012) 124063, 1201.1037

[149] W. Zurek, *Entropy Evaporated by a Black Hole*, Phys.Rev.Lett. **49** (1982) 1683–1686

[150] B. Czech, K. Larjo and M. Rozali, *Black Holes as Rubik's Cubes*, JHEP **1108** (2011) 143, 1106.5229

[151] M. A. Nielsen and I. L. Chuang, *Quantum Computation and Quantum Information*. Cambridge University Press, 2000

[152] S. B. Giddings and R. A. Porto, *The Gravitational S-matrix*, Phys.Rev. **D81** (2010) 025002, 0908.0004

[153] L. Susskind, *Singularities, Firewalls, and Complementarity*, 1208.3445

[154] P. Hayden and J. Preskill, *Black holes as mirrors: Quantum information in random subsystems*, JHEP **0709** (2007) 120, 0708.4025

[155] Y. Sekino and L. Susskind, *Fast Scramblers*, JHEP **0810** (2008) 065, 0808.2096

[156] S. B. Giddings, *Nonviolent nonlocality*, 1211.7070

[157] S. B. Giddings, *Nonviolent information transfer from black holes: a field theory parameterization*, 1302.2613

[158] V. Cardoso, O. J. Dias, J. L. Hovdebo and R. C. Myers, *Instability of non-supersymmetric smooth geometries*, Phys.Rev. **D73** (2006) 064031, hep-th/0512277

[159] K. A. Intriligator, N. Seiberg and D. Shih, *Dynamical SUSY breaking in meta-stable vacua*, JHEP **0604** (2006) 021, hep-th/0602239

[160] S. Kachru, J. Pearson and H. L. Verlinde, *Brane / flux annihilation and the string dual of a nonsupersymmetric field theory*, JHEP **0206** (2002) 021, hep-th/0112197

[161] M. Cvetic, G. Gibbons, H. Lu and C. Pope, *Ricci flat metrics, harmonic forms and brane resolutions*, Commun.Math.Phys. **232** (2003) 457–500, hep-th/0012011

[162] I. R. Klebanov and S. S. Pufu, *M-Branes and Metastable States*, JHEP **1108** (2011) 035, 1006.3587

[163] I. Bena and N. P. Warner, *A Harmonic family of dielectric flow solutions with maximal supersymmetry*, JHEP **0412** (2004) 021, hep-th/0406145

[164] S. D. Mathur, *Fuzzballs and the information paradox: a summary and conjectures*, 0810.4525

[165] R. Penrose, in *Battelle Rencontres*, edited by C. M. DeWitt and J. A. Wheeler (W.A. Bejamin, New York) (1968) 222

[166] J. de Boer, S. El-Showk, I. Messamah and D. Van den Bleeken, *Quantizing N=2 Multicenter Solutions*, JHEP **05** (2009) 002, 0807.4556

[167] S. Kachru, R. Kallosh, A. D. Linde, J. M. Maldacena, L. P. McAllister *et al.*, *Towards inflation in string theory*, JCAP **0310** (2003) 013, hep-th/0308055

[168] M. Cvetic and D. Youm, *General rotating five-dimensional black holes of toroidally compactified heterotic string*, Nucl.Phys. **B476** (1996) 118–132, hep-th/9603100

[169] J. Preskill, P. Schwarz, A. D. Shapere, S. Trivedi and F. Wilczek, *Limitations on the statistical description of black holes*, Mod.Phys.Lett. **A6** (1991) 2353–2362

[170] P. Kraus and F. Wilczek, *Effect of selfinteraction on charged black hole radiance*, Nucl.Phys. **B437** (1995) 231–242, hep-th/9411219

[171] S. D. Mathur, *Tunneling into fuzzball states*, Gen.Rel.Grav. **42** (2010) 113–118, 0805.3716

[172] B. D. Chowdhury and S. D. Mathur, *Fractional Brane State in the Early Universe*, Class.Quant.Grav. **24** (2007) 2689–2720, hep-th/0611330

[173] S. D. Mathur, *What can the information paradox tell us about the early Universe?*, Int.J.Mod.Phys. **D21** (2012) 1241002, 1205.3140

[174] S. Mathur and D. Turton, *Private communication*, to appear (2013)

[175] L. Susskind, L. Thorlacius and J. Uglum, *The Stretched horizon and black hole complementarity*, Phys.Rev. **D48** (1993) 3743–3761, hep-th/9306069

[176] S. Mathur, H. Bruntt, C. Catala, O. Benomar, G. Davies *et al.*, *Study of HD 169392A observed by CoRoT and HARPS*, 1209.5696

[177] E. Verlinde and H. Verlinde, *Black Hole Entanglement and Quantum Error Correction*, 1211.6913

[178] K. Papadodimas and S. Raju, *An Infalling Observer in AdS/CFT*, 1211.6767

[179] Y. Nomura, J. Varela and S. J. Weinberg, *Complementarity Endures: No Firewall for an Infalling Observer*, JHEP **1303** (2013) 059, 1207.6626

Y. Nomura, J. Varela and S. J. Weinberg, *Black Holes, Information, and Hilbert Space for Quantum Gravity*, 1210.6348

Y. Nomura and J. Varela, *A Note on (No) Firewalls: The Entropy Argument*, 1211.7033

Y. Nomura, J. Varela and S. J. Weinberg, *Low Energy Description of Quantum Gravity and Complementarity*, 1304.0448

[180] M. Schlosshauer, *Decoherence, the measurement problem, and interpretations of quantum mechanics*, Rev.Mod.Phys. **76** (2004) 1267–1305, quant-ph/0312059

[181] L. Susskind and L. Thorlacius, *Gedanken experiments involving black holes*, Phys.Rev. **D49** (1994) 966–974, hep-th/9308100

[182] S. G. Avery, B. D. Chowdhury and S. D. Mathur, *Excitations in the deformed D1D5 CFT*, JHEP **06** (2010) 032, 1003.2746

[183] W. G. Unruh and R. M. Wald, *What happens when an accelerating observer detects a Rindler particle*, Phys.Rev. **D29** (1984) 1047–1056

[184] M. Van Raamsdonk, *Comments on quantum gravity and entanglement*, 0907.2939

[185] M. Van Raamsdonk, *Building up spacetime with quantum entanglement*, Gen.Rel.Grav. **42** (2010) 2323–2329, 1005.3035

[186] W. Israel, *Thermo field dynamics of black holes*, Phys.Lett. **A57** (1976) 107–110

[187] J. M. Maldacena, *Eternal black holes in anti-de Sitter*, JHEP **0304** (2003) 021, hep-th/0106112

[188] J. M. Maldacena and A. Strominger, *Black hole grey body factors and d-brane spectroscopy*, Phys.Rev. **D55** (1997) 861–870, hep-th/9609026

[189] I. Bena, G. Giecold, M. Grana and N. Halmagyi, *On The Inflaton Potential From Antibranes in Warped Throats*, 1011.2626

[190] I. Bena, G. Giecold, M. Grana, N. Halmagyi and S. Massai, *The backreaction of anti-D3 branes on the Klebanov-Strassler geometry*, 1106.6165, * Temporary entry *

[191] D. Anninos, T. Anous, F. Denef, G. Konstantinidis and E. Shaghoulian, *Supergoop Dynamics*, JHEP **1303** (2013) 081, 1205.1060

[192] S. G. Avery and B. D. Chowdhury, *Firewalls in AdS/CFT*, 1302.5428

[193] A. Almheiri, D. Marolf, J. Polchinski, D. Stanford and J. Sully, *An Apologia for Firewalls*, 1304.6483

[194] S. Mathur and D. Turton, *Private communication*, (2013)

[195] J. Manschot, B. Pioline and A. Sen, *Wall Crossing from Boltzmann Black Hole Halos*, JHEP **1107** (2011) 059, 1011.1258

[196] J. P. Gauntlett and J. B. Gutowski, *Concentric black rings*, Phys.Rev. **D71** (2005) 025013, hep-th/0408010

[197] I. Bena, B. D. Chowdhury, J. de Boer, S. El-Showk and M. Shigemori, *Moulting Black Holes*, JHEP **1203** (2012) 094, 1108.0411

[198] I. Bena, M. Berkooz, J. de Boer, S. El-Showk and D. Van den Bleeken, *Scaling BPS Solutions and pure-Higgs States*, JHEP **1211** (2012) 171, 1205.5023

[199] S.-J. Lee, Z.-L. Wang and P. Yi, *Quiver Invariants from Intrinsic Higgs States*, JHEP **1207** (2012) 169, 1205.6511

[200] J. Manschot, B. Pioline and A. Sen, *From Black Holes to Quivers*, JHEP **1211** (2012) 023, 1207.2230

[201] R. Emparan and G. T. Horowitz, *Microstates of a Neutral Black Hole in M Theory*, Phys.Rev.Lett. **97** (2006) 141601, hep-th/0607023

[202] G. Bossard, *Octonionic black holes*, JHEP **1205** (2012) 113, 1203.0530

[203] G. Bossard and S. Katmadas, *Duality covariant non-BPS first order systems*, JHEP **1209** (2012) 100, 1205.5461

[204] B. de Wit and S. Katmadas, *Near-Horizon Analysis of D=5 BPS Black Holes and Rings*, JHEP **1002** (2010) 056, 0910.4907

[205] K. Hanaki, K. Ohashi and Y. Tachikawa, *Comments on charges and near-horizon data of black rings*, JHEP **0712** (2007) 057, 0704.1819

[206] B. D. Chowdhury and B. Vercnocke, *New instability of non-extremal black holes: spitting out supertubes*, JHEP **1202** (2012) 116, 1110.5641